Unveiling the antifungal resistance mechanisms of the emergent fungal pathogen *Candida parapsilosis*

Joana Alexandra Vilarinho Branco

Dissertação de candidatura ao grau de Doutor em Biomedicina, apresentada à Faculdade de Medicina da Universidade do Porto

Programa Doutoral em Biomedicina

Os trabalhos experimentais realizados na presente dissertação decorreram no Serviço e Laboratório de Microbiologia da Faculdade de Medicina da Universidade do Porto, Portugal.

Orientação

Professor Doutor Acácio Agostinho Gonçalves Rodrigues

Doutora Isabel Alexandra Marcos Miranda

Júri da Prova de Doutoramento em Biomedicina

Presidente

Doutor Alberto Manuel Barros da Silva, Professor Catedrático da Faculdade de Medicina da Universidade do Porto

Vogais

Doutor Miguel Nobre Parreira Cacho Teixeira, Professor Associado com Agregação do Instituto de Bioengenharia e Biociências, do Instituto Superior Técnico, da Universidade de Lisboa.

Doutora Teresa Maria Fonseca de Oliveira Gonçalves, Professora Associada com Agregação da Faculdade de Medicina da Universidade de Coimbra.

Doutora Cândida Manuela Ferreira Abreu, Professora Auxiliar Convidada da Faculdade de Medicina da Universidade do Porto.

Doutor Acácio Agostinho Gonçalves Rodrigues, Professor Catedrático da Faculdade de Medicina da Universidade do Porto.

Doutor Luís Filipe Duarte Reino Cobrado, Professor Auxiliar da Faculdade de Medicina da Universidade do Porto.

Doutora Carmen Maria Lisboa da Silva, Professora Auxiliar da Faculdade de Medicina da Universidade do Porto.

Artigo 48, Paragrafo 31: "A Faculdade não responde pelas doutrinas expendidas na Dissertação." (Regulamento da Faculdade de Medicina da Universidade do Porto/Decreto-Lei nº 19337, 29 de Dezembro de 1931).

Acknowledgments

Agradeço ao meu orientador, Professor Doutor Acácio Agostinho Gonçalves Rodrigues, Diretor do Serviço e Laboratório de Microbiologia, pela oportunidade e orientação na realização deste projeto.

À minha orientadora, Professora Doutora Isabel Marcos Miranda, Investigadora no Departamento de Cirurgia e Fisiologia, gostaria de agradecer a excelente orientação e todo o apoio pessoal e profissional durante todos estes anos. Obrigada por teres feito parte da minha caminhada. Levo-te para a vida!

A todos que contribuíram para a realização dos trabalhos, o meu mais profundo e sincero agradecimento.

Aos colaboradores que estão ou passaram pelo Serviço e Laboratório de Microbiologia, gostaria de agradecer pela amizade e companheirismo durante todos estes anos.

À minha família, obrigada por me terem dado a força para percorrer este caminho.
Aos meus amados pais, obrigada por me incentivaram a fazer mais e melhor!

List of Publications

Fazem parte integrante desta dissertação os seguintes trabalhos publicados, ou em vias de publicação:

I. **J. Branco**, I. M. Miranda and A. G. Rodrigues. "*Candida parapsilosis* virulence and antifungal resistance mechanisms: a comprehensive review of key determinants". *Journal of Fungi* (2023) 9 (1): 80. DOI: 10.3390/jof9010080

II. **J. Branco**, C. Martins-Cruz, T. Gonçalves, I. M. Miranda and A. G. Rodrigues. "Antifungal susceptibility profile characterization of *Candida parapsilosis* species complex: a Portuguese analysis". (Submitted)

III. **J. Branco**, Adam P. Ryan, A. Silva, G. Butler, I. M. Miranda and A. G. Rodrigues. Clinical azole cross-resistance in *Candida parapsilosis* is related to a novel *MRR1* gain-of-function mutation. *Clinical Microbiology Infection* (2022) 28 (12): 1655.e5-e1655.e8. DOI: 10.1016/j.cmi.2022.08.014

IV. **J. Branco**, C. Martins-Cruz, L. Rodrigues, R. M. Silva, N. Araújo-Gomes, T. Gonçalves, I. M. Miranda and A. G. Rodrigues. The transcription factor *NDT80* is a repressor of *Candida parapsilosis* virulence attributes. *Virulence* (2021) 12 (1): 601-14. DOI: 10.1080/21505594.2021.1878743

List of Abbreviations

AmB Amphotericin B

ATCC American Type Culture Collection

CGD Candida Genome Database

CLSI Clinical and Laboratory Standards Institute

CNV Copy Number Variation

CV Crystal Violet

DAPI 4',6-diamidino-2-phenylindole

ECM Extracellular Matrix

EPA Epithelial adhesion

FCS Fetal Calf Serum

FLC Fluconazole

FMUP Faculdade de Medicina da Universidade do Porto

GO Gene Ontology

HSP Heat Shock Protein

Hwp Hyphal wall protein

ICU Intensive Care Unit

IGV Integrative Genomics Viewer

ISDA Infectious Diseases Society of America

LIP Lipases

MIC Minimal Inhibitory Concentration

MOI Multiplicity of Infection

MOPS 3-(N-Morpholino) propane sulfonic acid

MSE Middle Sporulation Element

NACs non-albicans *Candida* species

ORF Open Reading Frame

PBS Phosphate Buffer Saline

PSC Posaconazole

RT-qPCR Real Time-quantitative Polymerase Chain Reaction

SAP Secreted Aspartyl Protease

SNP Single Nucleotide Polymorphism

SRA Short Read Archive

UTI Urinary Tract Infection

VRC Voriconazole

WGA Wheat Germ Agglutinin

List of Figures and Tables

Chapter III

Contents

Introduction

Candida and human disease

Fungi can cause a diversity of health disorders in humans, ranging from allergic syndromes and mucocutaneous infections to invasive diseases that seriously threaten life. It is estimated that fungal diseases annually affect over a billion people and cause 1.5 million deaths worldwide (1). Invasive fungal infections caused by *Candida* species are widely associated with high rates of severe illness and may be responsible for as many as 30% of all deaths from fungal disease. In the United States, the health cost attributable to prolonged hospitalizations resulting from candidaemia is estimated at USD 46,684 per patient (2).

Candidosis is a broad term that refers to cutaneous, mucosal, and deep-seated organ infections caused by opportunistic pathogens of the *Candida* genus (3). *Candida* spp. are commensal yeasts commonly found in the human gastrointestinal tract, mucous membranes, and skin. Disruption of the gastrointestinal and cutaneous barriers following shock, localized infections, or the replacement of an intravascular catheter can all promote invasive candidosis, which is widely recognized as a major cause of morbidity and mortality. The patient populations most at risk are the elderly, premature newborns, and those with compromised immune systems due to HIV, chemotherapy, or transplant-necessitated immunosuppression therapy (4). Invasive candidosis is a disorder that can potentially affect any organ. Each distinct *Candida* species exhibits its own unique characteristics in terms of its invasive potential, virulence, and antifungal susceptibility pattern (3).

The distribution of *Candida* species varies geographically, with notable differences between hospital centers. The underlying condition of the patient and whether they have experienced previous antifungal therapy both have an effect on the distribution and frequency of *Candida* spp. (5). While *Candida albicans* is the most common pathogen associated with nosocomial invasive candidosis worldwide, an increasing number of infections by non-albicans *Candida* species (NACs) have also been reported in recent years, including *Candida glabrata*, *Candida parapsilosis*, *Candida tropicalis*, *Candida krusei* and *Candida auris*, among others (6). Of these, *C. glabrata* predominates in Northern European countries and in the United States, but *C. parapsilosis* and/or *C. tropicalis* are more prevalent in India, Pakistan, Latin America, and Mediterranean countries (3).

Candida parapsilosis

Since its discovery in 1928, *C. parapsilosis* has undergone several changes in phylogenetic classification. Initially isolated from the stool of a patient with diarrhea in Puerto Rico, the species was first classified as *Monilia parapsilosis* (i.e., a species of the *Monilia* genus, incapable of fermenting maltose) to distinguish it from *Monilia psilosis*, which is today known as *C. albicans* (7). In 1932, it was renamed *Candida parapsilosis*. In 2005, Tavanti *et al*. (8) confirmed, through multilocus sequence typing, the existence of a *C. parapsilosis* complex comprising three distinct species: *Candida parapsilosis sensu stricto*, *Candida orthopsilosis,* and *Candida metapsilosis*. In this paper, we focus on *Candida parapsilosis*.

C. parapsilosis is widely distributed in nature and is often isolated from a variety of non-human sources, such as domestic animals, insects, soil, and marine environments (9). This yeast successfully colonizes the human skin and mucosal membranes as a commensal microorganism, wherein the hands of healthcare professionals are recognized as a major vector for *C. parapsilosis* nosocomial acquisition (10-12). In addition, the selective ability of *C. parapsilosis* to grow in hyperalimentation solutions promotes the infection risk by this pathogen (13). *C. parapsilosis* represents a high risk for immunocompromised individuals, such as HIV sufferers and surgical patients, particularly those subjected to gastrointestinal track surgery. Also at high risk are patients requiring prolonged use of a central venous catheter or other indwelling devices, due to the innate ability of *C. parapsilosis* to adhere to prosthetic surfaces and implanted medical devices. In such cases, biofilm formation typically begins soon after attachment. When the structure is mature, it greatly decreases the ability of antifungals to reach cells, with potentially life-threatening consequences in the host (14-16). Because *C. parapsilosis* is responsible for one-third of neonatal *Candida* infections, with a mortality rate of approximately 10%, low-birth-weight neonates are at especially high risk (17).

The distribution of *C. parapsilosis* recovered from patients with bloodstream infections in various studies conducted in different geographical areas shows that its relative dominance differs according to region (5). It is the second most common *Candida* isolate in Latin America countries, such as Argentina, Peru and Brazil. In Venezuela and Colombia, *C. parapsilosis* even outranks *C. albicans* infections (5, 18, 19). The incidence of *C. parapsilosis* infections in Europe is region-dependent; in Southern European hospitals (Portugal, Spain, Italy, and Greece) it is the second most isolated species (20-23),], and in central and northern countries of Europe the incidence of *C. parapsilosis* ranks third, after that of *C. albicans* and *C. glabrata* (24-26). A different prevalence was also reported in North American countries, Canada and USA, where *C. parapsilosis* ranks second and third, respectively (27-30). According to studies of bloodstream

fungal infections in Asia (China and Japan), *C. parapsilosis* is commonly found after *C. albicans* (31, 32), while in India it ranks third (33). A similar incidence of infection was observed in Australia (34).

The two cryptic *psilosis* species, *Candida orthopsilosis* and *Candida metapsilosis*, are also opportunistic pathogens, associated with local and systemic diseases. As with *C. parapsilosis*, their frequency and distribution reportedly differ in distinct geographical areas (35, 36).

C. parapsilosis is a diploid pathogen, with eight chromosome pairs and an estimated genome size of 13.1 Mb. From the 5837 ORFs identified in this species, only 107 (1.83%) have actually been characterized (37). Its genome is highly conserved; compared to other *Candida* spp., it exhibits a remarkably low level of heterozygosity with just one single nucleotide polymorphism (SNP) per 15,553 bases, more than 70 times less than the corresponding number in the closely related *Lodderomyces elongisporus* (38).

The yeast cells of *C. parapsilosis* display an oval, round, or cylindrical shape, and their colony phenotypes have been identified as crepe, concentric, smooth, or crater (Figure 1) (13, 39). Unlike *C. albicans*, *C. parapsilosis* does not form true hyphae; it only exists as yeast or in pseudohyphal forms. Form and colony phenotypes are intimately linked; cells exhibiting crepe and concentric phenotypes are almost entirely pseudohyphal, whereas those with smooth and crater phenotypes are mostly yeast-like (39).
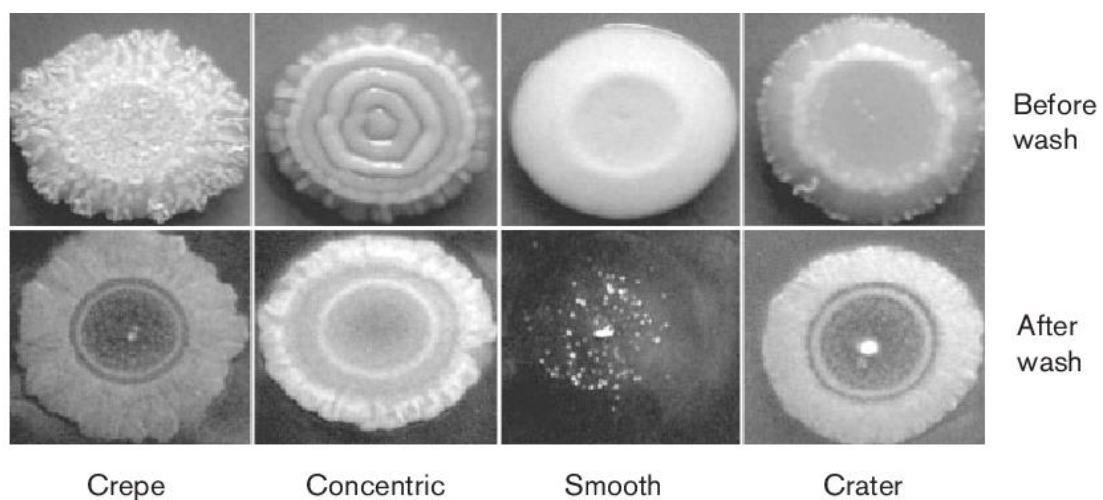
Figure 1. Examples of colonies phenotypes described in *C. parapsilosis*. Colonies were photographed before and after washing with water, to observe the amount of invasion in the agar. Adapted from Laffey and Butler (39).

Virulence attributes

Similarly to other microorganisms, *Candida* species have developed several specific and effective strategies to enhance their pathogenicity. The virulence of *C. parapsilosis* is mainly attributed to its intrinsic ability to adhere to the abiotic surfaces of medical devices and prosthetic materials, and to the host's mucosal epithelium. This ability is crucial for biofilm formation and consequently damage to the host (15, 40).

Researchers have found that the ability to colonize upon mucosal surfaces or inert materials varies among *Candida* species (41). An unusually high intraspecies variation in terms of adhesion ability has also been identified among clinical isolates of *C. parapsilosis*, compared with other *Candida* species. A correlation between the site of isolation and the rate of adhesion has also been reported, as *C. parapsilosis* mucocutaneous isolates demonstrate higher adhesiveness (41).

Cell Adhesion

Adhesion is an important, multifactorial process that is mediated by the characteristics of fungal and host (biotic or abiotic) cells, including cell surface hydrophobicity, cell wall composition, and growth conditions (42). Initially, the adhesion of the yeast cells is highly dependent upon hydrophobic interactions between the microorganism and host surfaces. Cell surface hydrophobicity is strongly correlated with adhesion to both polystyrene/polyetherurethane surfaces and to epithelial cells. *Candida* species generally exhibit a high degree of cell surface hydrophobicity (43).

In adhesion, the key trigger interaction is promoted by specific cell wall proteins, namely adhesins. This process promotes the attachment of the fungal cells to other microorganisms, the host's epithelium, and abiotic surfaces (40). Among *Candida* spp., several adhesin families are involved in adherence. Important adhesin families include: (i) the hyphal wall protein (Hwp) family, which includes five proteins, namely, Hwp1, Hwp2, Rbt1, Eap1, and Ywp1, that play a role in *C. albicans* biofilm formation (42, 44); (ii) the adhesins of the *EPA* (epithelial adhesion) family in *C. glabrata*, comprising 23 genes, of which *EPA1*, *EPA6*, and *EPA7* are described as the most important for the adhesion process in this species (42, 44, 45); and iii) the Als-like (agglutinin-like sequence) family encoding large-cell-surface glycoproteins involved in *Candida* adhesion, including *C. albicans*, *C. parapsilosis*, *C. tropicalis*, *C. dubliniensis*, *C. lusitaniae*, and *C. guilliermondii* (42, 44). Among the eight Als members described in *C. albicans*, Als3 has the most profound impact on biofilm formation; its deletion causes a severe biofilm formation defect (46).

C. parapsilosis, five Als proteins are present on the surface of the pseudohyphae, and the ortholog CaAls7 has been described as a determinant for adhesion to host epithelial cells (47, 48). Other adhesion proteins and non-protein factors with similar properties, such as Eap1, Iff4, Mp65, Ecm33, Utr2, Int1, and Mnt1, have also been identified in *Candida* species; however, these have not been widely studied to date (49).

Secretion of Hydrolytic Enzymes

*Candid*a species can produce and secrete several hydrolytic enzymes, including secreted aspartyl proteases (SAPs), lipases (LIPs) and phospholipases. The activity of these enzymes is closely linked with *Candida*'s pathogenicity, such adhesion, cell damage, and the invasion of host tissues (40).

The production of SAPs by *Candida* cells aims to degrade structural and immunological defense proteins in the host, facilitating invasion and colonization of the host tissue. Compared to *C. albicans*, *C. parapsilosis* expresses less SAP activity (50). To date, three aspartyl protease-encoding genes (*SAPP1* to *SAPP3*) have been identified in *C. parapsilosis*, with a wide variability in expression among different isolates (51). Isolates from body surfaces, such as skin or vaginal mucosa, are more invasive than those recovered from systemic infections or from environmental surfaces, due to the production of such enzymes (52).

In addition to SAPs, enzymes categorized as lipases catalyze both the hydrolysis and synthesis of triacylglycerols. Of the four secreted-lipase-encoding genes identified in the *C. parapsilosis* genome, only two (*LIP1* and *LIP2*) have been confirmed as able to encode functionally active proteins. Although the production of LIPs varies greatly among *C. parapsilosis* isolates, ranging from 36% to 80%, their role in enhanced pathogenicity has been confirmed (53). The putative roles played by LIPs in a successful host invasion include the digestion of lipids for nutrient acquisition, the enhancement of adhesion and biofilm formation, and the suppression of immune response, among others (54, 55).

Other hydrolytic enzymes have also been described, including secreted phospholipases, which hydrolyze phospholipids and fatty acids, thereby exposing host receptors and facilitating adhesion; however, these are still poorly understood in *C. parapsilosis* (56).

Biofilm Formation

Biofilms have been described as an organized community, comprising of a dense network of microbial cells embedded in an extracellular matrix (ECM) of polymers (13). Biofilm formation

is a potent virulence attribute of several *Candida* species. Biofilm formation during infection has been linked to higher mortality rates in cases involving such species when compared with isolates incapable of forming biofilm (57). Biofilm development is a well-regulated process comprising three sequential stages (Figure 2): an early phase, involving the entire adhesion process of the cells, as described above; an intermediated phase, and, finally, a maturation/dispersion phase (40). In the intermediate phase, following initial fungal adhesion, yeast cells undergo a morphology transition from yeast to filamentous or pseudohyphal forms, forming a mixed population with multilayer formation (Figure 2). Afterwards, biofilm maturation begins through the production and secretion of a polysaccharide-rich extracellular matrix, formed by polysaccharides, proteins, lipids, and nucleic acids, which provides structural and functional stability to the biofilm (40, 58).
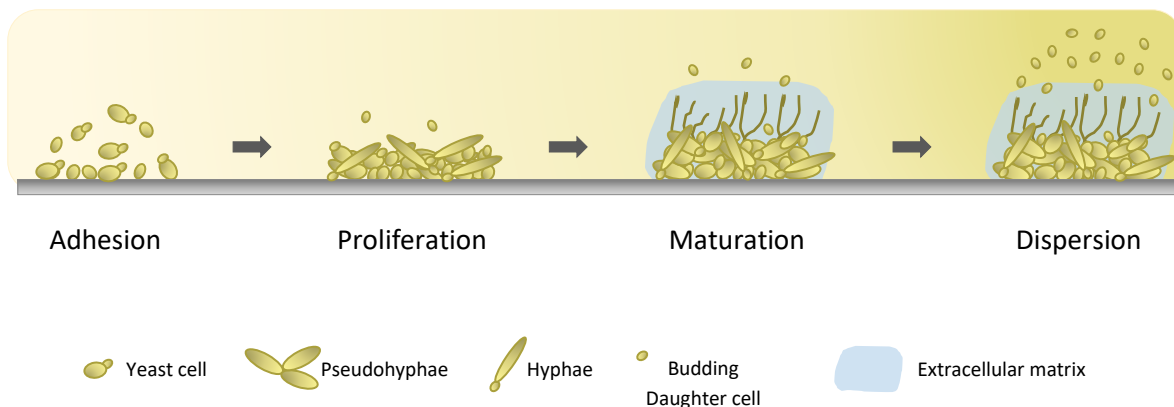
Figure 2. Illustration of biofilm formation cycle in *Candida* spp. Biofilm development consists of three stages: an early phase, in which cells adhere to biotic or abiotic surfaces; an intermediate phase, involving cell proliferation and formation of a mixed population; and, finally, a maturation/dispersion phase, characterized by the production of the extracellular matrix and the massive dispersion of cells. The detachment and dispersion of daughter cells occurs in all stages of biofilm development.

The biofilm's architecture, morphology, and thickness also vary widely among *Candida* species and between strains (58). These features are influenced by several host and *Candida*-derived variables, including: i) physiological conditions, such as pH and oxygen concentration; ii) fluid flow at the infection site, which influences nutrient exchange and impacts the biofilm´s structural integrity; iii) available nutrients in the growth media, including sugars, lipids, and serum; and iv) the material on which the biofilm grows (those typically used in medical devices include silicone, latex, and polyurethane, among others) and v) community microbial

interactions, either fungal-fungal or fungal-bacterial, which modulate the ability of *Candida* to form biofilm and also represent a promising topic for future research (58-60).

C. parapsilosis biofilm growth is especially common in patients fitted with a central venous catheter who receive total parenteral nutrition (61, 62). The biofilm structure of *C. parapsilosis* exhibits high variability among clinical isolates. Because *C. parapsilosis* does not form true hyphae, its biofilm is composed of aggregated blastoconidia and pseudohyphae that occupy a volume lower than that of other *Candida* species (63, 64). In addition, the extracellular matrix of *C. parapsilosis* biofilm is mainly composed of carbohydrates and low levels of protein (63).

The ability to form biofilms is closely related to its virulence potential, because only limited penetration of substances is possible through the biofilm matrix, resulting in a greatly decreased susceptibility to antimicrobial agents (65, 66). The development of the biofilm also serves to counter the host immune response by inhibiting macrophage phagocytosis and antibody activity (65).

The process of biofilm development involves a massive cell detachment during the final maturation phase, with consequent dispersion that promotes the colonization of new locations and surfaces (40). However, Uppuluri *et al.* (67) found that dispersion was not confined to the maturation phase and occurs continuously during the biofilm development process. A more robust biofilm is produced by dispersed cells compared with the biofilm formed by initial planktonic mother cells such that the virulence potential increases over generations. All of these findings represent matters of serious clinical concern, not only for the treatment of patient infections but also in terms of public health (66).

The complexity of all stages of biofilm formation, involving such phenomena as the control of adhesion, morphology changes, and ECM production, among others, requires an extensive and complex regulatory network (68). The biofilm formation regulatory process has been extensively studied in *C. albicans*; however, as with other characteristics, such knowledge cannot be simply transposed to other *Candida* species. For example, the four transcription factors *BRG1*, *TEC1*, *ROB1*, and *FLO8* are all involved in the biofilm regulatory network of *C. albicans* but play no role in *C. parapsilosis* biofilm regulation (68, 69). Conversely, *CZF1*, *UME6*, *GZF3*, and *CPH2* have been highlighted as key contributors to biofilm formation in *C. parapsilosis*, but these genes play a negligible role in this process in *C. albicans*. However, other genes required for biofilm development, such as *ACE2*, *BCR1*, and *EFG1*, have been found to perform a similar function in both species (68, 70).

Antifungals and Resistance Mechanisms

Despite ongoing research efforts concerning new therapeutic compounds and treatment strategies, only a limited number of options of antifungal drugs are available for the treatment of candidosis (71). Currently, the arsenal of systemic antifungals available for clinical use consists of only three major drug classes: polyenes, echinocandins and azoles (72).

Polyenes

Amphotericin B (AmB) is the most used member of the class of polyenes, being clinically used for more than 55 years (72). Its potent fungicidal activity is derived from its interaction with the ergosterol of fungal cells by binding to the lipid bilayer, forming pores in the cell membrane and facilitating the leakage of intracellular components, such as potassium ions (K^+), into the extracellular medium (Figure 3) (73). Consequently, this interaction results in a drastic change in cell permeability, ultimately leading to cell lysis. This antifungal has low solubility and is highly toxic to the host cell due to the close structural relationship between ergosterol and cholesterol, the mammalian membrane sterol. This limits its use in long-term antifungal therapy (74). However, less toxic, lipid-based polyene formulations have now been developed, including liposomal amphotericin B (LAmB), which has become the first-line treatment for various types of invasive fungal infections (75).

The development of fungal resistance to polyenes is rare. Most of *Candida* spp., including *C. albicans*, *C. glabrata*, and *C. parapsilosis*, are generally considered to be susceptible to AmB, with surveillance studies reporting an AmB susceptibility rate close to 100% (76). Recently, a global pooled prevalence meta-analysis estimated *C. parapsilosis* AmB-resistance at 1.3% (77). Emerging AmB resistance has been reported in species, such as *C. auris* (78). The resistance mechanisms of this class are less well understood than those of echinocandins and azoles; nevertheless, several hypotheses have been forwarded to explain resistance, as illustrated in Figure 3. These include: i) sterol composition modulation through depletion or replacement of ergosterol triggered by mutations in genes involved in the ergosterol biosynthesis pathway, specifically in *ERG1* to *ERG4*, *ERG6*, and *ERG11* (79-81), and ii) enhanced defense against oxidative damage to break down the reactive oxygen species (ROS) that are produced under AmB exposure, either by means of catalase activity and/or by the molecular chaperones of the heat shock protein (HSP) family, namely, Hsp90 and Hsp70 (82-84).
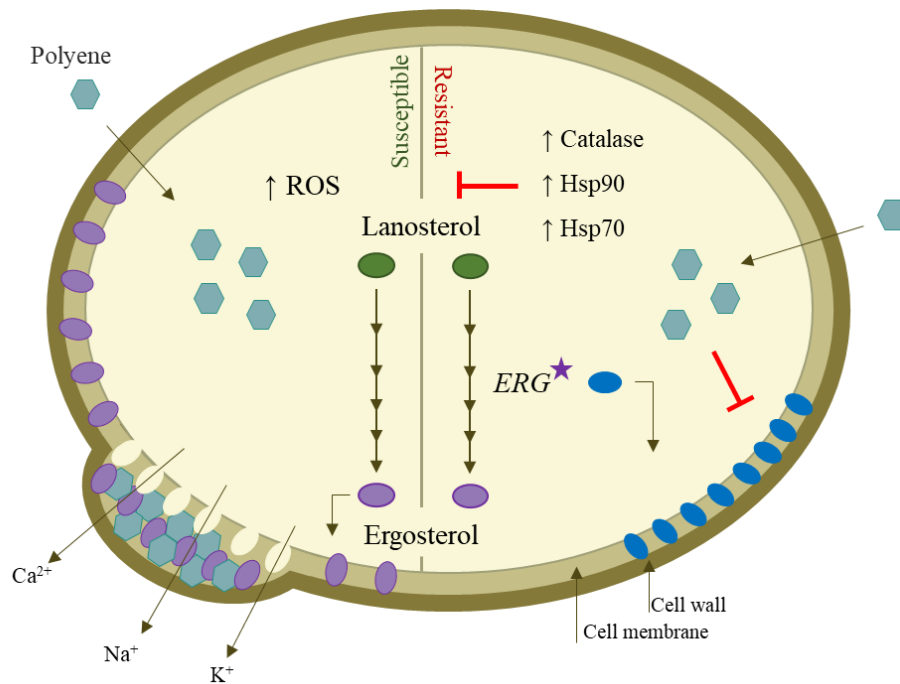
Figure 3. Mechanism of action of polyenes against *Candida* spp. and mechanisms underlying drug resistance. Polyenes act by forming polyene/ergosterol aggregates, destabilizing the fungal membrane by promoting membrane permeabilization and dysfunction. The action of polyenes can be overcome through mutations in ergosterol biosynthesis genes responsible for altered sterol composition and by the activation of stress response pathways, such as catalase and Hsp. Red T-shaped bars indicate inhibition. Star icon indicates gene mutation.

Echinocandins

Echinocandins, i.e., caspofungin, micafungin, and anidulafungin, are the newest class of antifungal drugs available for the treatment of invasive fungal infections and offer an excellent safety profile combined with high fungicidal activity (85, 86). They noncompetitively inhibit (1,3)-β-D-glucan synthase, which is responsible for biosynthesis of 1,3-β-D-glucan, a crucial structural component of fungal cell walls (87, 88). Specifically, echinocandins target the catalytic subunits Fks1 of β-D-glucan synthase, encoded by *FKS1* and *FKS2* genes, leading to the disruption of cell wall glucan, osmotic instability, cell lysis, and death for most species (Figure 4) (89, 90). Although their antifungal spectrum is limited, echinocandins are fungicidal against most *Candida* spp., including azole-resistant strains and biofilm (91, 92). However, as the use of these drugs has expanded, reports of resistance to echinocandin treatment among *Candida* spp. have increased (92). In particular, *C. parapsilosis* tends to be associated with increased *in vitro* minimum inhibitory concentrations (MICs) of echinocandin (93, 94), raising concerns that such drugs may facilitated the development of high levels of resistance (95-97).

Decreased echinocandin susceptibility can occur via two main mechanisms (Figure 4): i) an adaptive stress response mechanism, involving a compensatory increase in the synthesis of chitin (an essential cell wall component) that is mediated, for example, via the activation of calcineurin (Ca^{2+}) signaling pathway. The activation of this pathway is initially signaled by the Hsp90 chaperone, a key regulator of cellular stress response, and thus confers protection against the antifungal agent (98-100); and ii) acquired or intrinsic mutations in genes encoding the *FKS1* and *FKS2*, characterized by amino acid substitutions in specific regions clustered around two highly conserved regions (termed hot spots 1 and 2) of Fksp, which is generally correlated with increased resistance to such drugs (94, 101, 102). Acquired mutations have been reported for *C. albicans*, *C. tropicalis*, *C. krusei*, and *C. glabrata* (101, 103) but not ye t for *C. parapsilosis* (95, 104). In *C. parapsilosis,* naturally occurring *FKS1* mutations in the hot spot 1 region were found to be responsible for the intrinsic reduced susceptibility of this species to echinocandins (105).
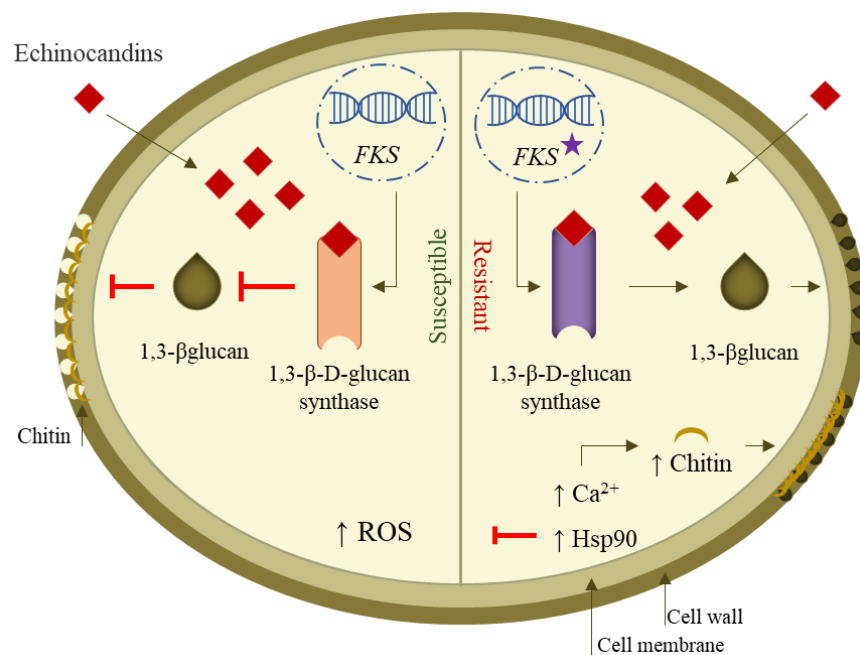
Figure 4. Mechanism of action of echinocandins against *Candida* spp. and mechanisms underlying drug resistance. Echinocandins act as noncompetitive inhibitors of (1,3)-β-D-glucan synthase, encoded by *FKS* genes, causing a depletion of the 1,3-β-glucan in the cell wall. Echinocandin resistance in *Candida* is associated with mutations in *FKS* genes and the activation of cell wall stress response mediator pathways, such as Hsp90 and calcineurin (Ca^{2+}), increasing the chitin content. Red T-shaped bars indicate inhibition. Star icon indicates gene mutation.

Azoles

Azoles represent the largest class of antifungal agents in clinical use due to their broad spectrum of activity, favorable safety profile, and bioavailability (72). The clinically approved azoles include fluconazole (FLC), voriconazole (VRC), posaconazole (PSC), itraconazole and isavuconazole. Azoles exhibit mainly fungistatic activity against *Candida* (106). Due to differences between the membranes of fungal and human cells (mainly composed of cholesterol), the use of azoles does not interfere with human body cells during treatment. They bind to and inhibit the activity of the enzyme lanosterol 14α-demethylase (encoded by the *ERG11* gene in yeasts), which is a key enzyme in the ergosterol biosynthetic pathway (Figure 5) (107-109). Ergosterol is an important component of fungal cell membranes (110). The interruption of its synthesis enables accumulation of a toxic 14α-methyl sterol, which impairs the membrane integrity and also the function of some membrane-bound proteins (such as those involved in cell wall synthesis), with consequences in terms of cell growth (107, 110, 111).

The emergence of azole resistance in *Candida* species represents a major challenge to treatment (112-115). *Candida* spp. azole resistance has been linked to different molecular mechanisms that include (Figure 5): i) mutations in the gene encoding the azole target enzyme lanosterol 14α-demethylase (*ERG11*), with resulting overexpression, and reduced azole binding, which also results in the reduction or loss of affinity with azoles, preventing azoles binding; ii) alterations in the ergosterol biosynthetic pathway, caused by loss-of-function point mutations in *ERG3*, leading to a depletion of ergosterol and to the accumulation of 14α-methyl fecosterol, which is less damaging to cell membranes, thus enabling continued growth in the presence of azoles; and iii) the upregulation of multidrug efflux pumps *CDR1* and *CDR2* (*Candida* drug resistance) and *MDR1* (multidrug resistance) genes that transport the drug out of the cells (116, 117). The analysis of serial isolates from individual patients has revealed that acquired azole resistance commonly relies on multiple and often-combined molecular mechanisms (118).

Similarly to *C. albicans*, *C. parapsilosis* harbors several genes that have been found to be involved in resistance development. For example, Mrr1p (multidrug resistance regulator 1) is a zinc cluster transcription factor that controls *MDR1* expression (119). Several authors have demonstrated that gain-of-function mutations in the *MRR1* gene, which render the transcription factor constitutively active, are responsible for the upregulation of the *MDR1* efflux pump and thus play a central role in the development of drug resistance (120-123). The hyperactivation of the Tac1 (transcriptional activator of *CDR* genes 1) transcription factor is also conferred by gain-of-function mutations that consequently promote the overexpression of *CDR1* and *CDR2* genes (124, 125).
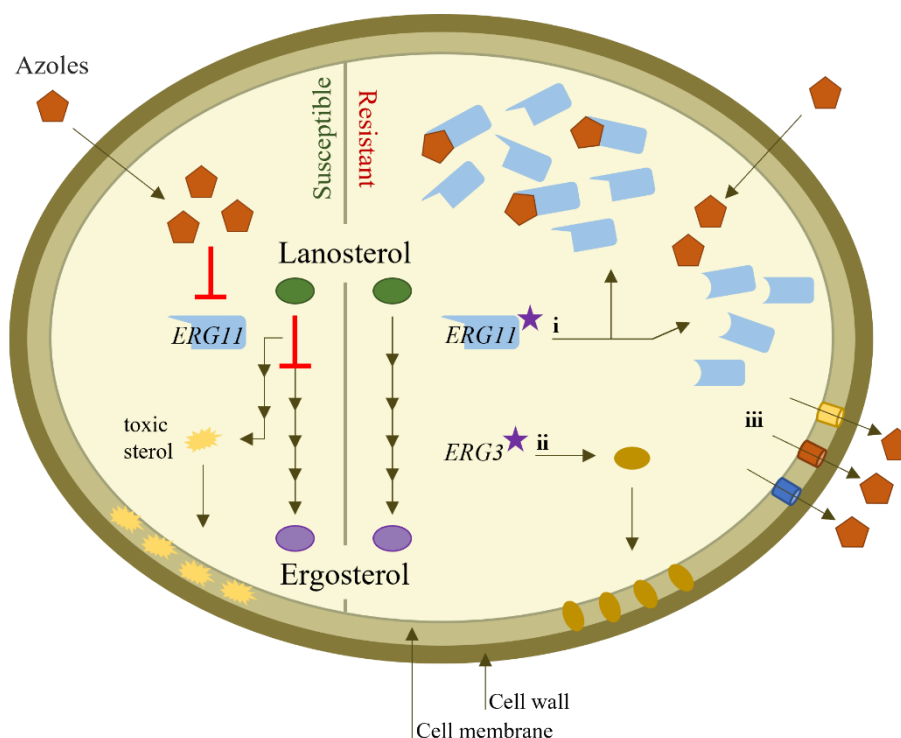
Figure 5. Mechanism of action of azoles against *Candida* spp. and mechanisms underlying drug resistance. Azoles target and inhibit the enzyme lanosterol 14α-demethylase, encoded by the *ERG11* gene, leading to the accumulation of toxic sterol. Azole resistance involves: **(i)** point mutations in the *ERG11* gene, which can be responsible for its overexpression and/or the inhibition of enzyme lanosterol 14α-demethylase, due to the decrease in azole–target binding affinity; **(ii)** mutations in *ERG* genes involved in the ergosterol biosynthesis pathway, particularly in *ERG3*; and **(iii)** increased efflux of the azole drugs from the fungal cell through the overexpression of multidrug efflux pumps. Red T-shaped bars indicate inhibition. Star icon indicates gene mutation.

Upc2 (Sterol uptake control protein 2), another member of the zinc cluster transcription factor family, is a key regulator of ergosterol metabolism that controls the expression of the azole target *ERG11* gene (126-128). Gain-of-function mutations in *UPC2* lead to the increased *ERG11* expression, contributing to fluconazole resistance in this species (129-131). As with *UPC2*, the transcription factor Ndt80 also modulates the expression of several ergosterol metabolism genes (128, 132). Moreover, Chen *et al*. (2004) demonstrated the involvement of this regulatory factor in azole tolerance by controlling the expression of the *CDR1* gene in *C. albicans* (133).

Alterations in the ergosterol biosynthetic pathway, including mutations in *ERG11* gene or its overexpression, have also been linked to azole resistance (134). The amino acid Y132F substitution in *ERG11* is frequently reported among *Candida* spp., including *C. parapsilosis* (112, 135-138). The persistence of *C. parapsilosis* isolates harboring the Y132F mutation in clinical settings has been associated with outbreaks of infections in hospitals, with fatal consequences (114, 115, 139).

Summarization

Candida parapsilosis is a predominant species within NACs that is responsible for invasive candidosis in low-birth-weight neonates, transplant recipients, critical-care patients and those receiving parenteral nutrition. The high prevalence of *C. parapsilosis* is also promoted by its well-documented ability to persist and thrive in the hospital environments for long periods. Its remarkable ability to adhere to abiotic surfaces, such as catheters, and to form biofilms constitutes a gateway to systemic colonization. The extensive use of antifungals, both prophylactically and therapeutically, is also recognized as a major cause of worldwide antifungal resistance in this pathogen.

In light of the above, there can be no doubt that further comprehensive research efforts addressing the epidemiology, pathogenic attributes, antimicrobial susceptibility profile, and genetic resistance mechanisms of *Candida parapsilosis* will contribute to improved treatments and prevention of infections, leading to improved patient outcomes and lower burdens upon healthcare systems.

Aims

This investigation has four main goals:

1. To carry out the characterization of the susceptibility profile, of the most commonly used antifungal in clinical practice, azoles, in a large set of *C. parapsilosis* clinical strains.

2. To elucidate the molecular mechanisms responsible for azole resistance, through the expression profile of the resistance-associated genes (*MDR1, CDR1, ERG11*) displayed by *C. parapsilosis* fluconazole resistant strains.

3. The characterization of the acquired resistance mechanisms by three consecutive *C. parapsilosis* isolates, obtained during prolonged fluconazole treatment.

4. To explore the role of Ndt80 in *C. parapsilosis* morphogenesis, adhesion and biofilm formation, triggering relevant pathogenic attributes.

Such goals were addressed according to the chapters that follow.

Chapter I

Candida parapsilosis species complex antifungal susceptibility profile and resistance characterization

Background

Surveillance programs of healthcare-associated pathogens are essential sources of information necessary for those developing preventive measures and policies. The continuous monitoring of pathogens incidence and its respective antimicrobial susceptibility patterns are also crucial to elucidate about species distribution trends, track the emergence of resistance, monitor changes in underlying conditions and predisposing risk factors, as well as to assess trends in antifungal treatment regiments and outcomes (27).

C. parapsilosis is an important pathogen worldwide and was previously reported as an important agent associated to healthcare acquired infections in Portugal, being second after *C. albicans*, resulting in 12% of crude mortality rate. The incidence of *C. orthopsilosis* and *C. metapsilosis* were also evaluated, revealing a growing incidence (20, 140, 141).

In this chapter, we characterize the antifungal susceptibility pattern to FCL, VRC and PSC of a collection of *C. parapsilosis* complex clinical strains; in addition, we explore the molecular mechanisms involved in *C. parapsilosis* fluconazole resistance, by evaluating the *CDR1*, *MDR1* and *ERG11* gene expressions. Moreover, the coding sequences of the previous genes and their transcription regulators *TAC1*, *MRR1* and *UPC2* were scanned for the presence of single nucleotide polymorphisms (SNPs).

Material and Methods

Candida parapsilosis strains

All the strains of *Candida parapsilosis* complex (*n* = 281) assessed in this study were made available from the fungal collection of the Microbiology Laboratory of the Faculty of Medicine of the University of Porto (n = 210) and from the Clinical Yeast Collection of the University of Coimbra (CYCUC) (n = 71). They had been previously isolated from patients admitted at Centro Hospitalar e Universitário de São João, Porto, Portugal, and Hospital dos Covões, Coimbra, Portugal, isolated from several sources - respiratory tract, urine, central venous catheter, blood, and skin - during years 2013 to 2016.

Until testing, all strains were stored in YPD broth medium (1% Bacto Yeast Extract, 2% Bacto Peptone, 2% D-(+)-Glucose) with 40% glycerol at −80°C. For each experiment, the microorganisms were sub-cultured twice on the recommended medium to assess the purity of the culture and its viability.

Species complex differentiation

C. parapsilosis strains were initially identified by VITEK 2 YST cards from bioMérieux (Marcy l'Etoile, France). To differentiate strains among *Candida parapsilosis* complex, the analysis of the restriction fragment length polymorphism (RFLP) analysis of the *SADH* gene was carried out as described by Tavanti *et al.* (8). Briefly, the amplification of the *SADH* gene fragment (716 bp) was performed followed by *BanI* restriction pattern analysis.

Antifungal susceptibility testing

C. parapsilosis, C. orthopsilosis and *C. metapsilosis* strains were characterized regarding the antifungal susceptibility profile to the azole drug, namely, FLC (Pfizer, New York, NY, USA), VRC (Pfizer) and PSC (Schering-Plough, Kenilworth, NJ, USA) accordingly to the broth dilution method of Clinical and Laboratory Standards Institute (CLSI) M27 protocol guidelines (142). *C. parapsilosis* minimal inhibitory concentration (MIC) was registered after 48 h and the susceptibility breakpoints for FLC and VRC were those described in CLSI M60-Ed2 (143). For FLC, the susceptibility MIC was ≤ 2 µg mL^{-1}, the MIC for susceptible-dose dependent (SDD) was 4 µg mL^{-1}, and the MIC for resistance was ≥ 8 µg mL^{-1}. For VRC, the susceptibility MIC was ≤ 0.12 µg

mL^{-1}, the MIC for intermediate (I) was 0.25 to 0.5 µg mL^{-1} and the MIC for resistance was ≥ 1 µg mL^{-1}.

For the cryptic species, *C. orthopsilosis* and *C. metapsilosis*, epidemiological cutoff values (ECVs) were also registered after 48 h and analyzed as recommended by CLSI M59-Ed3 (144). For *C. orthopsilosis*, fluconazole and voriconazole ECV of ≤ 2 µg mL^{-1} and ≤ 0.125 µg mL^{-1} were considered as a wild type (WT) phenotype, respectively. For *C. metapsilosis*, fluconazole and voriconazole ECV of ≤ 4 µg mL^{-1} and ≤ 0.06 µg mL^{-1} were considered as a wild type phenotype, respectively.

For PSC, all *C. parapsilosis* complex strains were considered as a wild type phenotype in case of an ECV ≤ 0.25 µg mL^{-1} and a non-wild type (non-WT) whenever > 0.25 µg mL^{-1}, accordingly with CLSI M59-Ed3 (144).

Candida parapsilosis ATCC 22019 type strain was used for quality control, as recommended.

Real time-quantitative PCR

In *C. parapsilosis* fluconazole resistant strains molecular mechanisms were investigated via *CDR1* (CPAR2_405290)*, MDR1* (CPAR2_301760) and *ERG11* (CPAR2_303740) gene expressions (Table 1), quantified by RT-qPCR, as described by Branco *et al.* (128) with adaptations. Briefly, yeast cells of each strain were collected after growing in YPD broth medium at 30ºC until reaching an OD_{600} ranging between 0.6 and 0.8. Afterwards, total RNA was extracted with RNeasy Plus Mini Kit (Qiagen), being the concentration and quality controls measured using Nanodrop equipment (Eppendorf). The RNA samples, with A_{260}/A_{280} ratios ranging from 1.8 to 2.2 and no signs of degradation after electrophoresis, were used. First-strand cDNA was synthesized using the SensiFAST cDNA Synthesis Kit (Bioline), following the manufacturer´s instructions. cDNA was used in three replicates per strain for each gene expression experiment, performed with the SensiFAST SYBR Hi-ROX Kit (Bioline), 3-step cycling, according to the manufacturer's instructions. RT-qPCR was carried out in a StepOnePlus™ Real-Time PCR System. The constitutively *ACT1* gene signal was used as a reference for normalizing the relative expression levels of analyzed genes, detailed in Table 1. StepOnePlus™ Software v2.3 8 (Applied Biosystems) was used to determine the dissociation curve and threshold cycle (Ct). The $2^{-\Delta\Delta CT}$ method was used to calculate changes in gene expression among clinical strains.

Table 1. Primers used in chapter I

Primer name	Primer sequence (5` to 3`)
RT-qPCR	
CpACT1_F2	TTGATGAAGATTTTGTCCGAA
CpACT1_R2	GATGATTGTGATGAGGTTTGC
CpCDR1_F	TCAGAGGTGTTTCAGGTGGT
CpCDR1_R	GGCAATCAATGGTGTGGTAT
CpMDR1_F1	CATCCCCATTGCTATTGTTG
CpMDR1_R1	CACCTGAAGTTGTCGTTGC
CpERG11_F2	GACCGCATTGACTACCGAT
CpERG11_R2	ACGCCACTTTTCTGTTTCTTC
Gene Amplification/Sequencing	
CpERG11_F1	GCTACTAACTTTCCCTACCTTCG
CpERG11_R1	GTGAGTCAACAAAGAAGACAATC
CpUPC2_F1	GGTAAACCATCCTCAGAGTGAGA
CpUPC2_F	ATTGGAGTGTGGGTATCTTCAT
CpUPC2_F2	CACAATCAGGGCAGCAGCAG
CpUPC2_R1	CCCATTGAGCATATTATCCAGC
CpMRR1_up_F	CTACTGATATGCCTGACGCCAC
CpMRR1_down_R	GCTTTCTTGTTTTCAATAAGAGAGA
CpMRR1_F2 A	CCCTTTCTTCCGCAGATTTC
CpMRR1_F2 B	CCTTACTTGAACGAAATGGAG
CpMRR_F3	GAAGATGGCGATGAT
CpMRR1_R2 A	CGTTGTAAAGATGGCGTGGT
CpMDR1_F2	GCAACAAAACCCCATCTCA
CpMDR1_R2	GCACGAAAGGGTCAAAGG
CpMDR1_F3	TTTGGAACTTGCCCTTGTC
CpCDR1_F4	ATAACCCATTTCCAACTTTT
CpCDR1_R4	CTGAGCACATACGGCATC
CpCDR1_F	TCAGAGGTGTTTCAGGTGGT
CpCDR1_F2	CGGTTTTTCTTTTATTGGCTCA
CpCDR1_F3	ACTCGTCATTCCAAAGGTCG
CpTAC1_F	GGTCAATAGGCGAAGGAAA
CpTAC1_R	CAAAATGGTTATCAAATGTCAA
CpTAC1_F1	TCGTGATGGAGTTGGTCG

Gene sequencing

Candida parapsilosis fluconazole resistant strains overexpressing the *CDR1, MDR1* and *ERG11* genes were submitted to an analysis of its encoding sequences. The transcription factors *TAC1* (CPAR2_303510), *MRR1* (CPAR2_807270) and *UPC2* (CPAR2_207280) were also sequenced. All above-mentioned genes were amplified by PCR using the primers listed in Table 1. For genomic DNA extraction, DNeasy Plant Mini Kit (Qiagen) was used as the manufacturer's

instructions. PCR products were amplified using NZYProof DNA polymerase (NZYTech) and sequenced in a company, with sanger sequencing methodology. The sequences were analyzed using DNA Sequence Assembler v4 (2013), Heracle BioSoft and compared to the reference strain *C. parapsilosis* CDC317.

Results

Candida parapsilosis complex differentiation

The entire collection, a total of 281 strains identified within *C. parapsilosis* complex, was tested for *SADH* gene restriction profile. As described by Tavanti *et al*. (8), *C. parapsilosis* contains one *BanI* restriction site at position 196, *C. orthopsilosis* has no restriction site, while *C. metapsilosis* possesses three *BanI* restriction sites at 96, 469, and 529 positions. The amplified fragments of *C. orthopsilosis*, were sequenced to exclude a point mutation in the restriction site of *C. parapsilosis*. We identified 88.97% (*n* = 250) as *Candida parapsilosis sensu stricto*, 4.98% (*n* = 14) as *Candida orthopsilosis* and 6.05% (*n* = 17) as *C. metapsilosis* (Figure 6).

■*Candida parapsilosis sensu stricto* ■*Candida orthopsilosis* ■*Candida metapsilosis*
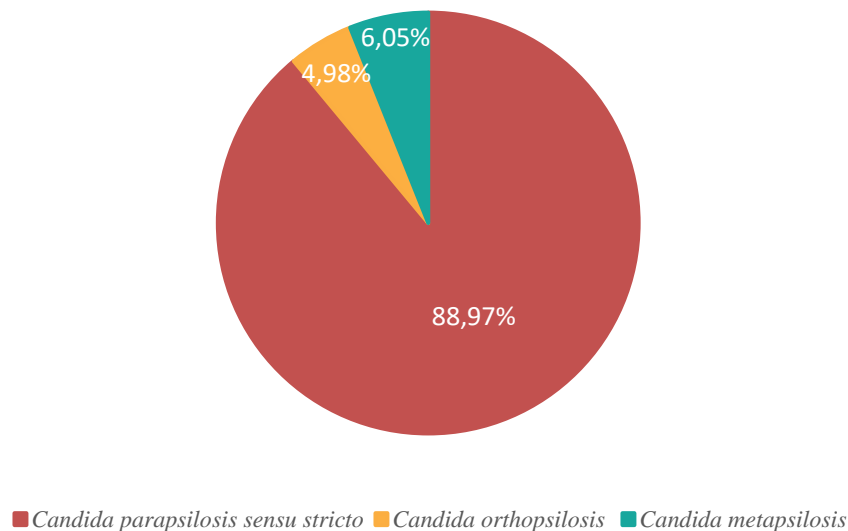
Figure 6. Prevalence of *C. parapsilosis* complex isolates belonging to the Microbiology Laboratory of the Faculty of Medicine of the University of Porto and the Clinical Yeast Collection of the University of Coimbra collection.

Azoles susceptibility profile

Azole susceptibility testing was performed in accordance with CLSI guidelines (Suppl. Table S1). We characterized 83.2% of *C. parapsilosis* as susceptible to FLC and 86% as susceptible to VRC (Figure 7). Susceptible-dose dependent (SDD) strains to FLC and with an intermediate (I) phenotype to VRC was found to be 6.40% and 10.8%, respectively; a resistant phenotype to FLC and VRC was detected in 10.4% and 3.2%, respectively. All strains VRC resistant were also

resistant to FLC. Relatively to PSC, 98.8% of *C. parapsilosis* strains correspond to a wild type phenotype and 1.2% to a non-wild type profile.

From the fourteen *C. orthopsilosis* strains, thirteen correspond to a wild type phenotype to FLC and VRC; one strain (Co14) exhibits a non-wild type phenotype to FLC (32 µg mL^{-1}) and VRC (0.25 µg mL^{-1}) (Suppl. Table S2).

In the case of *C. metapsilosis* strains we found an ECV of ≤ 4 µg mL^{-1} to FLC and ≤ 0.06 µg mL^{-1} to VRC, corresponding to a wild type phenotype. An exception was observed in strain Cm09 that corresponded to a non-wild type phenotype, since the VRC ECV was 0.125 µg mL^{-1} (Suppl. Table S3).

All *C. orthopsilosis* and *C. metapsilosis* strains exhibited a wild type phenotype to PSC.
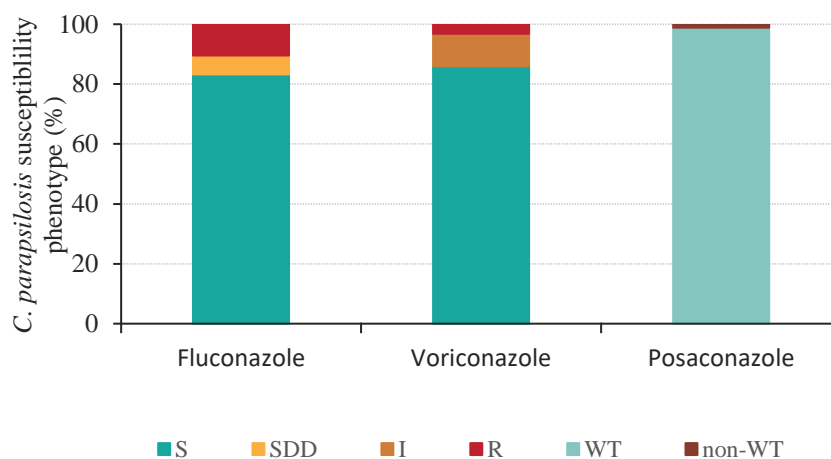
Figure 7. Antifungal susceptibility phenotype of *C. parapsilosis* strains. Abbreviations: S, Susceptible; SDD, Susceptible-dose dependent; I, Intermediate; R, Resistant; WT, wild type; non-WT, non-Wild Type.

Expression of *CDR1*, *MDR1* and *ERG11* in *C. parapsilosis* fluconazole resistant strains

The expression of genes *CDR1, MDR1 and ERG11* was quantified by RT-qPCR in the twenty-six *C. parapsilosis* FLC resistant strains (Figure 8, Suppl. Table S4). The analysis was performed by comparison to the relative expression average of eight *C. parapsilosis* strains,
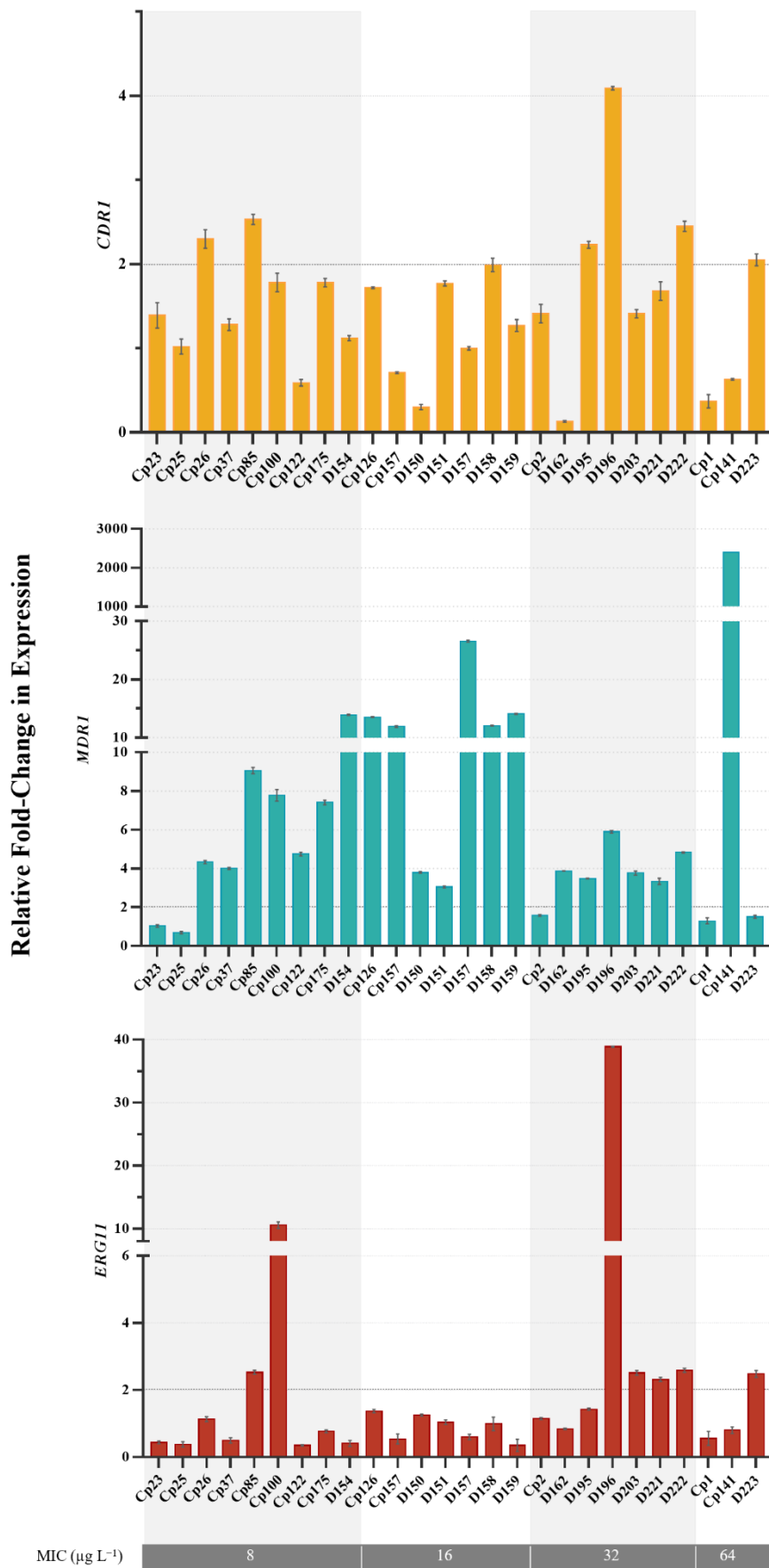
Figure 8. Gene expression associated with *C. parapsilosis* fluconazole resistance. Relative expression

levels of *CDR1*, *MDR1* and *ERG11* genes in *C. parapsilosis* fluconazole resistant strains. The experiences were performed in triplicate and compared with an average of eight *C. parapsilosis* susceptible/wild type strains. We assumed 2-fold as an increase in gene expression. The represented values are the mean value ± standard error. Strains were grouped according to their MIC to FLC.

randomly selected from the collection, displaying FLC and VRC susceptible and PSC wild-type phenotypes. We defined overexpression as a 2-fold increase in gene expression.

Resistance to FLC emerged mainly due to an increase in the capacity of fungal cells to expel fluconazole from the inside of the cell to the extracellular environment. This was achieved mostly by the upregulation of *MDR1* gene (21/26), whose expression in these strains vary from 3 to 2393-fold increase comparatively to the control group. Concomitantly with *MDR1* expression, *CDR1* gene was also overexpressed in 7 of the 26 strains assessed, exhibiting relatively low values compared to *MDR1* gene expressions, ranging from 2 up to 4-fold increase comparatively to the control group.

Together with azole extrusion, *ERG11* overexpression was clearly a mechanism of FLC response in 2 of the strains, Cp100 and D196, displaying an up regulation of 10,5 and 39-fold respectively. Mild levels of *ERG11* gene expression, around 2-fold increase were also detected in other 5 strains (Cp85, D203, D221, D222, D223). Interestingly, in 4 of the 26 strains, expression of the screened genes was not different from the one of the control group suggesting that the mechanism associated with FLC resistance does not involve *ERG11* overexpression or efflux pumps activity.

Simultaneous *MDR1*, *CDR1* and *ERG11* overexpression were observed in three isolates (Cp85, D222 and D223).

Sequencing of overexpressed genes and their corresponding transcription factors

In the *C. parapsilosis* fluconazole resistant strains with *CDR1*, *MDR1* and *ERG11* genes overexpressed, we searched for single-nucleotide polymorphisms (SNPs) within its encoding sequences and in its respective regulators *TAC1*, *MRR1* and *UPC2*.

Among the seven strains overexpressing *CDR1* gene we did not detect any nucleotide alteration. The same happened for its transcription factor Tac1p, excepting strain D158, in which a heterozygous L877P (T2630C) substitution was found.

In the twenty-one *MDR1*-overexpressing strains, mutations leading to amino acid substitutions in Mdr1p were detected in six strains: amino acid substitution I396V (A1186G) in

strains D154 and D162; heterozygous I396V (A1186G) alteration in strains D150, D151, D158 and D159. In the *MRR1* nucleotide sequence, it was found the homozygous amino acid substitutions R405K (G1214A) and G604R (G1810A) in strains Cp37 and Cp141, respectively. A heterozygous D615G (A1844G) alteration was detected in the strains D150, D151 and D154. In the remaining sixteen strains, no gene nucleotide alterations were found.

Since Erg11p is the fluconazole target, all fluconazole resistant strains (n = 26) were screened for polymorphisms in this gene. Among the 19 resistant strains which did not have Erg11p overexpressed, we found the Y132F amino acid substitution in heterozygosity in four cases. Other SNP G1193T leading to R398I amino acid alteration were found in 9 of such resistant strains. We did not identify any alteration in *ERG11* gene sequence in the other six *C. parapsilosis* resistant strains overexpressing this gene.

Among seven cases exhibiting *ERG11* gene overexpression, strains Cp100, D196 and D223 did not reveal any alteration in its encoding sequence; the Y132F heterozygous alteration was detected in strains, Cp85, D221 and D222; the R398I substitution was detected in strain D203. The Erg11p transcription factor, *UPC2* was also analyzed in the seven resistant strains overexpressing the fluconazole target and no alteration was found in their nucleotide sequences.

Table 2. Amino acid mutations identified in *C. parapsilosis* fluconazole resistant strains

Strain	MIC (µg mL^{-1}) | Phenotype[a]			Amino acid Mutations					
	Fluconazole	Voriconazole	Posaconazole	Cdr1p	Tac1p	Mdr1p	Mrr1p	Erg11p	Upc2p
Cp23	8 | R	0.5 | I	0.12 | WT	*		*		ND	
Cp25	8 | R	0.5 | I	0.12 | WT	*		*		ND	
Cp26	8 | R	0.5 | I	0.12 | WT	**ND**	ND	**ND**	ND	ND	
Cp37	8 | R	0.25 | I	0.12 | WT	*		**ND**	R405K	ND	
Cp85	8 | R	0.5 | I	0.25 | WT	**ND**	ND	**ND**	ND	**Y132F°**	ND
Cp100	8 | R	0.0015 | S	0.03 | WT	*		**ND**	ND	**ND**	ND
Cp122	8 | R	0.03 | S	0.125 | WT	*		**ND**	ND	R398I	
Cp175	8 | R	0.25 | I	0.125 | WT	*		**ND**	ND	Y132F°	
D154	8 | R	0.25 | I	0.12| WT	*		**I396V**	D615G°	R398I	
Cp126	16 | R	0.03 | S	0.125 | WT	*		**ND**	ND	R398I	
Cp157	16 | R	1 | R	0,06 | WT	*		**ND**	ND	Y132F°	
D150	16 | R	0.5 | I	0.06| WT	*		**I396V°**	D615G°	R398I	
D151	16 | R	0.25 | I	0.06| WT	*		**I396V°**	D615G°	R398I	
D157	16 | R	0.06 | S	0.06 | WT	*		**ND**	ND	R398I	
D158	16 | R	0.06 | S	0.06 | WT	**ND**	L877P°	**I396V°**	ND	R398I	
D159	16 | R	0.03 | S	0.06 | WT	*		**I396V°**	ND	R398I	
Cp2	32 | R	1 | R	0,06 | WT	*		*		Y132F°	
D162	32 | R	0.0015 | S	0.03 | WT	*		**I396V**	ND	R398I	
D195	32 | R	2 | R	0,06 | WT	**ND**	ND	**ND**	ND	ND	
D196	32 | R	1 | R	0,06 | WT	**ND**	ND	**ND**	ND	**ND**	ND
D203	32 | R	0.06 | S	0,06 | WT	*		**ND**	ND	**R398I**	ND
D221	32 | R	1 | R	0,06 | WT	*		**ND**	ND	**Y132F°**	ND
D222	32 | R	0.5 | I	0,03 | WT	**ND**	ND	**ND**	ND	**Y132F°**	ND
Cp1	64 | R	4 | R	0,12 | WT	*		*		Y132F°	
Cp141	64 | R	1 | R	0,25 | WT	*		**ND**	G604R	ND	
D223	64 | R	2 | R	0,06 | WT	**ND**	ND	*		**ND**	ND

[a] S, Susceptible; I, Intermediate; R, Resistant; WT, wild type.
ND, Not Detected mutation.
*Not overexpressed gene. Overexpressed genes are marked in bold.
°Mutations detected in heterozygosity.

Discussion

Since 2005, when Tavanti *et al*. (8) confirmed a *C. parapsilosis* complex of three distinct species, namely *C. parapsilosis sensu stricto*, *C. orthopsilosis* and *C. metapsilosis*, several studies reported its distinct prevalence rates, virulence potential and *in vitro* antifungal susceptibility profiles (35, 145).

While the global prevalence of *C. parapsilosis sensu stricto* ranks within the complex, the incidence of *C. orthopsilosis* and *C. metapsilosis* can vary in different geographical regions (30, 53, 146). The higher prevalence in the hospital environment of *C. parapsilosis* could be linked to the expression of distinct virulence attributes, with comparison to *C. orthopsilosis* and *C. metapsilosis* (35).

In 2009, an incidence of 2.3% and 2.9% of *C. orthopsilosis* and *C. metapsilosis*, respectively, were reported, while *C. parapsilosis* accounted for 91.4% of the total *C. parapsilosis* complex isolates in Portugal (141). Interestingly, in 2014 a decrease in the prevalence of *C. parapsilosis* (89.09%) and an increase of the cryptic species, *C. orthopsilosis* (7.27%) and *C. metapsilosis* (3.64%) was observed (20). Interestingly, in the present study, using a set of unrelated strains that had been recovered at 2 distinct university hospitals, between years 2013-2016, we found 88.97% of *C. parapsilosis*, 4.98% of *C. orthopsilosis* and 6.05% of *C. metapsilosis*. While such values might suggest a growing trend of *C. orthopsilosis* and *C. metapsilosis* in proportion to *C. parapsilosis*, such conclusion cannot be taken once these strains belong to a collection and no epidemiological study was carried out.

Similarly to our results, Guo *et al*. (147), in a fifteen-year retrospective study conducted in Eastern China, described a distribution of *C. parapsilosis* and *C. orthopsilosis* of 86.3% and 5.5%, respectively; a higher incidence of 8.1% of *C. metapsilosis* was observed. In a six-year multicenter study from Iran, a higher percentage of *C. parapsilosis* (94.5%) and a similar value of *C. orthopsilosis* (5.3 %) was reported, in comparison to our study. Surprisingly, C. *metapsilosis* comprised only 0.17% of all *C. parapsilosis* species complex isolates in such study (145).

The antifungal susceptibility profile of *C. parapsilosis* complex has been increasingly studied, as the incidence of the *psilosis* complex prevalence has raised continuously. Worldwide, the azole susceptible phenotype of *C. parapsilosis* isolates remains high (89.1–91.6%) (148). However, azole resistance has progressively increased over time, with geographic variations. Recent studies reported rates of *C. parapsilosis* FLC resistant or susceptible-dose dependent phenotypes of 15% in Europe and 3.6% in North America (148). In a multicenter study in China, a rate of 6% of *C. parapsilosis* complex isolates were found to be resistant/non-wild type to

azoles (32). Another study from Eastern China describes *C. orthopsilosis* and *C. metapsilosis* bloodstream isolates to be wild type to azole drugs (of about 92.3 – 100% to FLC and VRC) (147).

According to our results, the susceptible phenotype or wild type remains the most prevalent phenotype ranging from 83.2% for FLC to 98.80% for PSC among *C. parapsilosis*. The highest values of resistance were found in case of FLC (10.4%) and VRC (3.2%). However, these susceptibility profiles are not directly comparable with those described in the 2014 study (20), since meanwhile azole breakpoints were changed. Interestingly, VRC resistance was found in 3.2% of the *C. parapsilosis* strains, while no resistance was registered in 2014.

The majority (80,8%) of the *C. parapsilosis* fluconazole resistant strains exhibit *MDR1* overexpression, what makes it the most prevalent azole mechanism among our strain collection. We detected several point mutations in *MDR1* (I396V, in homo- and heterozygosity) and *MRR1* (R405K and G604R, in homozygosity; D615G in heterozygosity) genes, which possibly are responsible for the Mdr1 overexpression. Also, the Tac1p mutation L877P was also observed in heterozygosity in strain D158. However, it is crucial to confirm whether such mutations are, in fact, connected with resistance to fluconazole using molecular approaches.

In the last decade several studies aimed to unveil the molecular mechanisms involved in *C. parapsilosis* azole resistance. Berkow *et al*. (125) demonstrated that overexpression of *CDR1* and *MDR1* drug transporters can contribute directly to azole resistance of *C. parapsilosis* through activating mutations in the genes encoding their respective transcriptional factors. Grossman *et al*. 2015 (149), using *C. parapsilosis* isolates from a U.S. surveillance system demonstrated that *ERG11* mutations are a frequent cause of fluconazole resistance in this species and that *MRR1* mutations could also be involved. They also detected R405K mutation in Mrr1p, however an association with fluconazole resistance was not establish since this alteration is present in susceptible, SDD and resistant isolates.

In the present study, in strains with *MDR1* gene activation, we analysed whether *CDR1* and *ERG11* genes were overexpressed simultaneous in three isolates. *ERG11* upregulation was detected in seven *C. parapsilosis* strains, which displayed also efflux pump gene overexpression (*MDR1* and/or *CDR1*). We identified Y132F, in heterozygosity, and R398I mutations in the fluconazole resistant strains overexpressing *ERG11*. Y132F is the most described mutation in *ERG11* gene and it is only detected in resistant isolates, being directly involved it in ergosterol biosynthesis alterations. R398I mutation, assumed to be a compensatory mutation, is not considered to cause azole resistance on its own (112, 148).

It has been widely considered that single *ERG11* overexpression, by itself, is an uncommon resistance mechanism among *C. parapsilosis* isolates; it is usually the detection of a combination

of distinct molecular mechanisms, involving sterol and efflux pump gene alterations that confers such a resistant profile (35, 148).

Chapter II

Candida parapsilosis clinical azole cross-resistance

Background

Urinary tract infection (UTI) by *Candida* spp. is a common healthcare infection associated with increased mortality, especially in patients admitted to intensive care units (ICUs) often suffering from other severe comorbidities (150). In the ICU setting, the mortality rate of patients with candiduria is three times higher versus patients without candiduria (151). Infections caused by these opportunistic pathogens have increased during the last decades due to, among others, the common use of urinary catheters and other medical indwelling devices, long-term prophylactic use of antifungals, and broad-spectrum antibiotics regimens (152, 153). The severity of such manifestations varies from asymptomatic candiduria to clinical sepsis. In many patients UTIs can be asymptomatic, with no recommendation for antifungal therapy. However in risk groups treatment is strongly indicated, namely very low birth weight infants, patients undergoing urinary tract invasive procedures, immunocompromised patients, and elderly patients (152, 154, 155).

Candida species are responsible for ~10-15% of UTIs in tertiary care hospitals and specialized medical centers (156). *C. albicans* is the most common causative species, accounting for 50 to 70% of total *Candida* isolates, followed by *C. glabrata*, *C. tropicalis* and *C. parapsilosis* (155, 157). *C. parapsilosis* is estimated to be responsible for 1 to 7% of *Candida* UTIs, especially among neonates, and is often associated with systemic infection (157).

Azoles are the most widely used drugs for the treatment of fungal UTIs, within a reduced number of antifungal options (158). According to Infectious Diseases Society of America (IDSA) guidelines, fluconazole is strongly recommended for the treatment of UTIs caused by fluconazole-susceptible pathogens, since it achieves a high active concentration in urine and has a somewhat reduced hepatotoxicity activity (86, 154). Although with benefits to patient's outcome, the widespread use of azoles in clinical and in the environment (e.g., in agriculture or veterinary), have contributed to the emergence of *Candida* spp. resistant isolates, including *C. parapsilosis* (148). The persistence of these isolates in clinical settings has been associated with hospital-associated outbreaks, often with fatal outcomes (115).

In this chapter we describe a case of *in vivo* acquisition of cross azole resistance by *C. parapsilosis*, based upon the analysis of three consecutive isolates obtained following prolonged fluconazole treatment of a patient diagnosed with candiduria.

Material and Methods

Clinical isolates

A 41-year-old male patient, with a previous medical history of a single kidney and a pyelo-ureteral junction syndrome at the right, and with a double J ureteral catheter, was diagnosed with candiduria caused by *C. parapsilosis.* During fluconazole treatment (three cycles of 200 mg daily, orally, each cycle for 14 days, followed by a 10-day pause) a set of three consecutive isolates (Isolates CPS-A, -B, and -C) were obtained from routine urine cultures (Figure 9). Meanwhile, endoscopic replacement of double J ureteral catheter was performed during the antifungal treatment. Data regarding underlying diseases and treatment was collected and made available anonymously to the lab team. Until testing, all isolates were maintained at −80°C in YPD medium (1% Bacto Yeast Extract, 2% Bacto Peptone, 2% D-(+)-Glucose) with 40% glycerol. This study was carried out under CHUSJ Ethical Approval nº348/18.
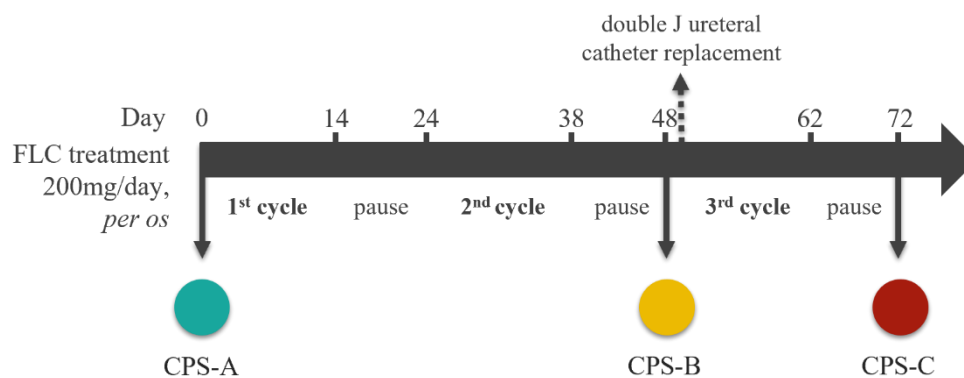
Figure 9. Schematic representation of *in vivo* antifungal resistance acquisition. Along fluconazole treatment the patient (with a J ureteral catheter) was diagnosed with candiduria by *C. parapsilosis* and treated with fluconazole (three cycles of 200 mg daily, orally, for 14 days, each followed by a 10 day pause). Along this period, 3 consecutive isolates were collected (Isolate CPS-A, -B and -C). Replacement of the double J ureteral catheter was performed at the beginning of the third cycle.

Identification, DNA Extraction and Genome sequencing

C. parapsilosis sensu stricto isolates were initially identified by matrix-assisted laser desorption/ionization-time of flight mass spectrometry (VITEK MS, BioMerieux). Afterwards, whole genome sequencing of all isolates was performed. *C. parapsilosis* CPS-A, CPS-B, and CPS-C were grown on YPD agar (2% Bacto Agar) at 30°C. Single colonies were inoculated into liquid

cultures of 15 mL YPD broth and grown at 30°C overnight with 200 rpm shaking. Then, DNA purification using the phenol-chloroform protocol was performed as described by Dymond (159).

Genomic DNA libraries

Genomic DNA libraries were prepared following the manufacturer's instruction for the Illumina® DNA Prep kit (Cat. 20018704) and Illumina® Nextera DNA CD Indexes (Cat. 20018707) using 500 ng DNA per sample. Library yield was quantified using the Qubit® 3.0 fluorometer and the dsDNA HS Assay kit (Invitrogen). Size distribution and integrity of libraries were measured using an Agilent Bioanalyzer; 5 µl of 4 nM dilutions of each quantified library was pooled and prepared following the manufacturer's instructions into a 24 sample multiplex reaction. This was sequenced using a NextSeq 500 Illumina sequencing machine using the NextSeq 500/550 Mid Output Kit v2.5 for 300 Cycles (Cat. 20024905). Samples were sequenced using a 2 x 150 bp paired-end format. Base call files were converted to FASTQ format for downstream analysis. Reads for other isolates were obtained from BioProject Numbers PRJNA563885, PRJNA326748, PRJEB1831, PRJNA361149 and PRJNA57912.

Variant Calling

Paired-end Illumina reads for each strain were trimmed using Skewer (v. 0.2.2) retaining reads with mean qualities of 30 and a minimum length of 35 (160). Reads were aligned to the reference *C. parapsilosis* CDC317 assembly using BWA mem (v. 0.7.17-r1188) (161). Output BAM files were sorted and duplicate reads were marked using Samtools Sort (v.1.10) and Picard Tools MarkDuplicates (v. 2.21.6) respectively (162, 163). Variants for each strain were called in GVCF format, and combined and genotyped using the Genome Analysis Tool Kit (GATK v. 4.2.0.0) components HaplotypeCaller, CombineGVCFs and GenotypeGVCFs (164). GATK (v. 4.2.0.0) VariantFiltration was used to retain variants with a minimum read depth of 15 and minimum genotype quality of 40. Clusters of 5 SNPs in 100 bp windows were removed. A custom script (https://github.com/CMOTsean/milt_variant_filtration) was used to remove variants flanked by long mono/di-nucleotide repeats as well as heterozygous alleles with a depth ratio of below 0.25 or above 0. 75 (165). Potentially deleterious SNP variants were identified using SIFT (166). Initially, individual variant files for each isolate were generated

and splited into heterozygous and homozygous variants using BCFTools (1.10.2) (162). Variants that were common to all three isolates (CPS-A, CPS-B, and CPS-C) were removed using BCFTools isec. Filtered variants were merged using BCFTools concat. Three hundred and twenty-four variants were identified in CPS-B and CPS-C compared to CPS-A, with 70 shared between the two isolates. This includes 59 Single Nucleotide Polymorphisms (SNPs) that are unique to CPS-B, 113 unique to CPS-C, with 63 that are common to both isolates. In addition, 36 indels are unique to CPS-B, 46 in CPS-C, with 7 shared.

A SIFT prediction database for *Candida parapsilosis* was generated as described in Bergin *et al.* (165) using the SIFT4g algorithm and Uniref90 protein database (166). SIFT analysis identified 24 SNPs that are likely to be deleterious with high confidence, 2 SNPs resulting in premature stop codons, and a further 14 with low confidence. Identified SNPs that were predicted to be deleterious were then manually viewed using the Integrative Genomics Viewer (IGV) (167) and were removed if they fell in regions with poor assembly. 23 SNPs remained. Genes with variants predicted to have deleterious functions were collated and inspected using the Candida Genome Database batch download tool (37).

SNP Tree Generation

GATK (v. 4.2.0.0) SelectVariants was used to select SNPs and to remove indels from the filtered VCF. SNPs were concatenated and heterozygous alleles were resolved using 1000 random haplotypes generated by Random Repeated Haplotype Sampling (168). SNP trees were constructed from each concatenation of random haplotypes using RAxML under GTRGAMMA model with a random seed of "12345" (169). The tree with the highest maximum likelihood was selected and the remaining 999 were used to generate bootstrap values.

Coverage Analysis

Coverage statistics were derived using BEDTools (170). Modal average coverage per chromosome per sample was derived using bedtools genomecov. Mean coverage per 1 kb window per chromosome per sample, and mean coverage per gene were derived using bedtools coverage. Gene copy number in each sample was calculated by dividing the average coverage of the gene by the modal coverage of the relevant chromosome. This was multiplied by two to account for diploidy. Genes with copy number >3 or <1 were retained (Suppl. Table S5). Data availability: Raw reads were uploaded to the Short Read

Archive (SRA) under accession numbers SAMN28778594, SAMN28778595, SAMN28778596.

Antifungal susceptibility testing

The MIC of FLC, VRC and PSC was determined for all the isolates, according to the M27 document of the CLSI (142). The MIC of each antifungal was registered after 48 h and the susceptibility breakpoints for FLC and VRC were those described in CLSI M60 supplement (143). For PSC, a wild type phenotype was considered for (ECV ≤0.25 μg mL^{-1} and a non-wild type for >0.25 μg mL^{-1} according to the CLSI M59 supplement (144). *Candida parapsilosis* ATCC 22019 type strain was used for quality control, as recommended.

Editing *MRR1*

The *MRR1* disruption cassette was constructed by cloning two flanking sites of *MRR1* in pCD8 (Figure 10 A) using MRR1_F1/MRR1_R1 and MRR1_F2/MRR1_R2 pair primers (Table 3), containing recognition sites for *KpnI - ApaI* and *SacII - SacI*, respectively, generating the plasmid pJB2. The *SAT1* flipper cassette methodology was used to disrupt the *C. parapsilosis MRR1* gene in the parental susceptible strain (isolate CPS-A) (171). By electroporation, pJB2 was introduced in the *MRR1* locus of isolate CPS-A (128). Since *C. parapsilosis* is a diploid organism, two rounds of integration/excision of *MRR1* deletion cassette were required to knockout the *MRR1* gene in the isolate CPS-A, generating afterwards the *mrr1ΔΔ* clone (JB24) (Figure 10 B).

Site direct mutagenesis, using MRR1_SDM2_F1 and MRR1_SDM2_R1 pair primers (Table 3), was carried out in the pJB9 vector (122) (GenBank accession number KT160017), generating pJB11 integration cassette, containing the G1810A nucleotide substitution in the *MRR1*.The same methodology described above was used to introduce pJB11 in the *mrr1ΔΔ* clone. The genomic integration of pJB11 in the *MRR1* allele was confirmed by PCR (Figure 10 B) and the new clone was named JB25. After *SAT1* recycling, the *MRR1*$_{RI}$ strain was generated.

Candida parapsilosis transformation

The introduction of the constructed cassettes into *C. parapsilosis* cells was performed by electroporation, as described previously (171). Briefly, an overnight yeast cell culture was diluted at an initial OD$_{600}$ of 0.2, in 50 mL of YPD broth medium, and incubated at 30°C until an

Table 3. Primers used in chapter II

Primer name	Primer sequence (5` to 3`)
Construction of deletion cassette	
MRR1_F1	GGGGGTACCCTACTGATATGCCTGACGCCAC
MRR1_R1	GGGGGGCCCTCTCTCTTATTGAAAACAAGAAAGC
MRR1_F2	CCGCGGTAACTTAGCGAATAGAAAATATGGT
MRR1_R2	GGGGAGCTCTCTCTCTTATTGAAAACAAGAAAGC
Site-directed mutagenesis	
MRR1SDM2_F1	GATAAGAGAAAGAATCATCTTAGGAGAAAGATTTGGCAAGTC
MRR1SDM2_R1	GACTTGCCAAATCTTTCTCCTAAGATGATTCTTTCTCTTATC
PCR Confirmation	
MRR1_UP3_F	GAAAACAAGTAATCAAAACACGGGG
MRR1_down2_R	TCCAACCCCCCCCTTTACAGAC
FLP_R	TTTATGATGGAATGAATGGGATG
MRR1_F4	CGGCATCTCGCAGCAACAA
MRR1_R3	GGTCTCCATTTCGTTCAAGT
RT-qPCR	
CpACT1_F2	TTGATGAAGATTTTGTCCGAA
CpACT1_R2	GATGATTGTGATGAGGTTTGC
CpMRR1_F	ACAATGGTCTGAGCAATGAA
CpMRR1_R	GGCAATACTGGTGATGGAA
CpMDR1_F1	CATCCCCATTGCTATTGTTG
CpMDR1_R1	CACCTGAAGTTGTCGTTGC
CpCDR1_F	TCAGAGGTGTTTCAGGTGGT
CpCDR1_R	GGCAATCAATGGTGTGGTAT
CpERG11_F2	GACCGCATTGACTACCGAT
CpERG11_R2	ACGCCACTTTTCTGTTTCTTC
CPAR2_304370_F	TTTACATTGCCCTCACGG
CPAR2_304370_R	GCCTCTTCCATCCTCTTTTG

OD$_{600}$ of 2.0 was reached. After being pelleted, yeasts were re-suspended in 10 mL of Tris-EDTA buffer (10 mM Tris-HCl, 1 mM EDTA, pH 7.5) containing 10 mM dithiothreitol, and incubated at 30°C for 1 h with agitation (100 rpm). Afterwards, yeast cells were washed twice with 40 mL of cold water, once with 10 mL 1 M sorbitol, and finally re-suspended in 125 µL of the last solution.

Posteriorly, 50 µL aliquots of the competent cells were mixed with approximately 1 µg of purified *KpnI - SacI* cassette and transferred to a 1-mm electroporation cuvette. Electroporation shock occurred at 1.25 kV, in a Gene Pulser X-cell Electroporater (Bio-Rad); immediately after, 950 µL of YPD containing 1 M sorbitol was added to the mixture and incubated at 30°C for 4 h

with agitation. Yeast cells were then collected and plated on YPD supplemented with nourseothricin at a final concentration of 200 µg mL^{-1}. Transformants were collected after 48 h.
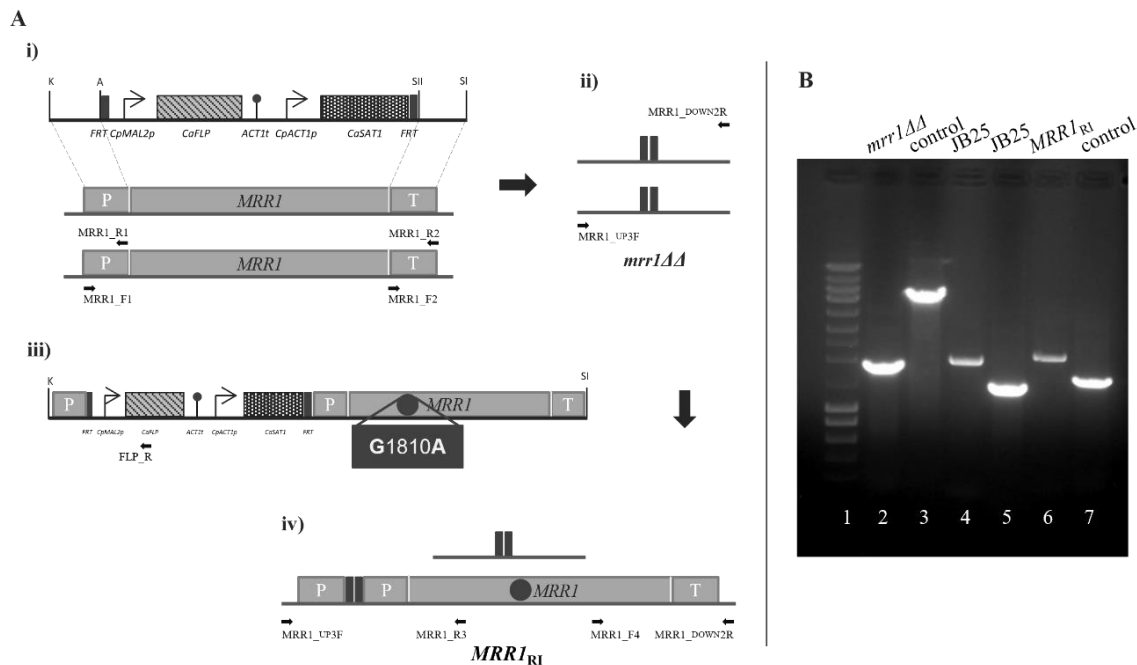
Figure 10. Steps involving the introduction of mutated *MRR1* transcription factor gene in the susceptible isolate CPS-A. Knockout of *MRR1* gene, followed by reintegration of *MRR1* harboring G1810A mutation in isolate CPS-A was performed using *SAT1* flipper cassette. A *MRR1* deletion cassette was constructed (**A**, i), which after two rounds of genomic integration in *MRR1 loci* of isolate CPS-A and recycling generated the *mrr1ΔΔ* clone (JB24) (**A**, ii). Confirmation was carried out by PCR, using primers MRR1_up3F and MRR1_down2R amplifying a 1.6 kb fragment (**B**, lane 2). Isolate CPS-A was used as control, amplifying a 5 kb fragment (**B**, lane 3). *MRR1* cassette, harboring G1810A mutation (pJB11), (**A**, iii) integration in the *mrr1ΔΔ* clone was confirmed using the primers MRR1_up3F and FLP_R amplifying a 1.9 kb fragment (**B**, lane 4; JB25) and MRR1_F4 and MRR1_down2R originating a 1.3 kb PCR product (**B**, lane 5; JB25). Successful recycling of the integration cassette (**A**, iv) and the generation of *MRR1*RI clone (JB26) was confirmed using MRR1_up3F and MRR1_R3 primers which amplified a 2 kb fragment, (**B**, lane 6, *MRR1*RI). In the control strain (Isolate CPS-A) was amplified a 1.5 kb fragment (**B**, lane 7). K – *KpnI*; A - *ApaI*; SII – *SacII*; SI – *SacI*, restriction enzymes. P – Promoter; T – Terminator. Lane 1 - Molecular size marker (NZYDNA Ladder III).

Real-time - quantitative PCR

MRR1, *MDR1, ERG11,* and *CDR1B* (CPAR2_304370) expression was quantified by RT-qPCR, as described by Branco *et al*. (122) with adaptations. Briefly, yeast cells of each isolate were collected after growing in YPD medium at 30ºC until reaching a log-phase, OD$_{600}$ ranging between 0.6 and 0.8. Total RNA was extracted with RNeasy Plus Mini Kit (Qiagen), and the

concentration and quality controls were measured using Nanodrop equipment (Eppendorf). RNA samples, with A_{260}/A_{280} ratios ranging from 1.8 to 2.2 and no signs of degradation after electrophoresis, were used. First-strand cDNA was synthesized using the SensiFAST cDNA Synthesis Kit (Bioline), following the manufacturer´s instructions. cDNA was used in three replicates per strain for each gene expression experiment, performed with the SensiFAST SYBR Hi-ROX Kit (Bioline), 3-step cycling, according to the manufacturer's instructions. RT-qPCR was carried out in a PikoReal Real-Time PCR System instrument (Thermo Scientific). The signal obtained for each gene, detailed in Table 3, was normalized with the *ACT1* gene. Data obtained were analyzed with REST software.

Results

Azole resistance acquisition during fluconazole treatment

The analysis of the sequential isolates obtained from the patient diagnosed with candiduria under FLC treatment revealed that azole resistance was acquired during infection. The initial isolate, CPS-A, is susceptible to FLC, VRC, and PSC. The second isolate, CPS-B, obtained after two cycles of FLC treatment, has a susceptible-dose dependent phenotype, while the final isolate, CPS-C, is resistant to FLC and VRC (Figure 9, Table 4). All three isolates are susceptible to PSC.

Table 4. MIC value and susceptibility phenotype of *Candida parapsilosis* strains

Strain	MIC (µg/mL) | Phenotype[a]		
	Fluconazole	Voriconazole	Posaconazole
CPS-A	1 | S	0.03 | S	0.25 | WT
CPS-B	4 | SDD	0.06 | S	0.06 | WT
CPS-C	64 | R	1 | R	0.125 | WT
mrr1ΔΔ	1 | S	0.03 | S	0.03 | WT
MRR1$_{RI}$	32 | R	1 | R	0.03 | WT

[a] S, Susceptible; SDD, Susceptible-dose dependent; R, Resistant; WT, wild type.

Analysis of isolate relationship

To characterize the relations of the three isolates (CPS-A, CPS-B, and CPS-C), genomic DNA was extracted and the genomes were sequenced. Phylogenetic analysis of the sequences in combination with unrelated *C. parapsilosis* isolates, as described by Zhai *et al.* (172), revealed that the three isolates are very similar (Figure 11). There are very few differences between the genomes suggesting all three are very closely related, and highly likely descendent from the same parent isolate.
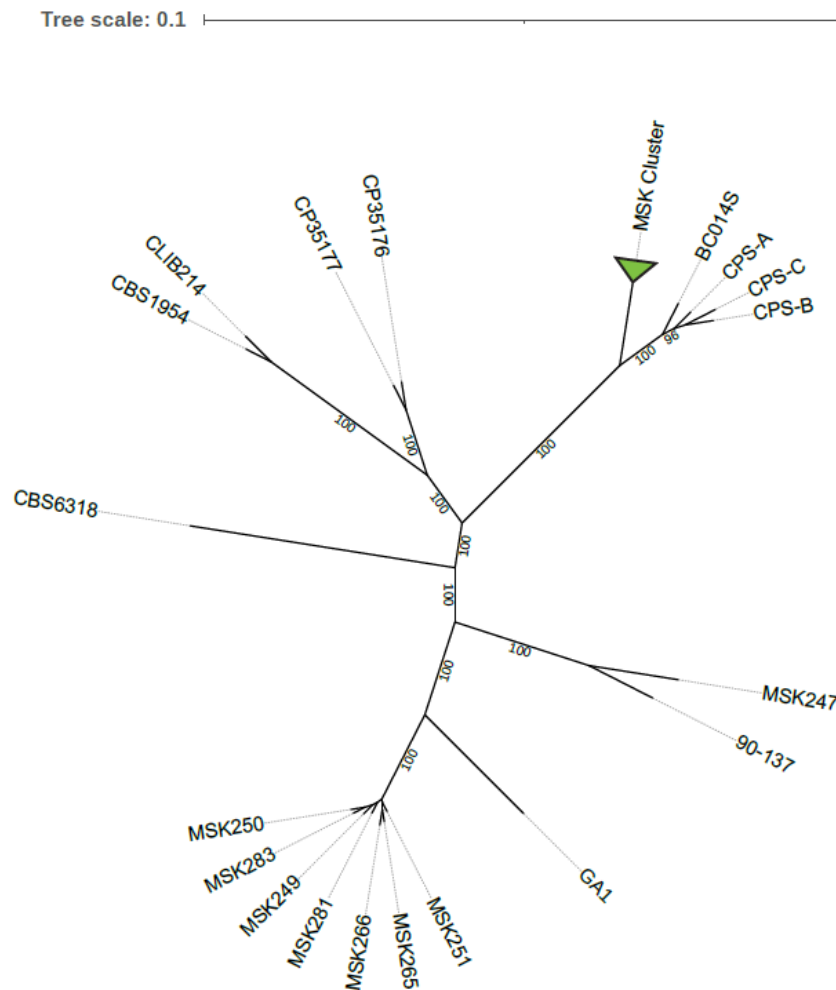
Figure 11. Isolates CPS-A, CPS-B and CPS-C relationship. Unrooted SNP-based phylogeny of 41 *Candida parapsilosis* isolates. The "MSK Cluster" represents 23 closely related isolates described in Zhai *et al*. (172). Bootstraps above 90% are indicated. *C. parapsilosis* CPS-A, -B and -C are closely related and are separated from their closest relative (*C. parapsilosis* BC014S) (33) supported by a bootstrap of 96%.

Identification of genomic changes among isolates

To identify variants that are likely to result in the observed azole-resistant phenotypes, variants that are present in isolates CPS-B and CPS-C and not in CPS-A were identified as described in Materials and Methods. SIFT analysis identified 23 variants that are likely to result in deleterious phenotypes. Four variants in 4 genes are present in both CPS-B and CPS-C (see Suppl. Table S5). All three are heterozygous variants (present in one allele only). Four additional heterozygous variants are unique to CPS-C, and one are unique to CPS-B. None of these are predicted to result in azole resistance (Suppl. Table S5). Fourteen homozygous variants were identified, 6 unique to CPS-B and 8 unique to CPS-C. One of the homozygous variants in CPS-C

results in a nucleotide substitution, from guanine to adenine in the 1810 position (G1810A), leading to a change from glycine to arginine (G604R) in the Mrr1p polypeptide chain (CPAR2_807270).

We note that one homozygous variant in CPS-C results in a Q1554P substitution in CPAR2_804030, an ortholog of 1,3-β-glucan synthase gene *FKS2*. This is heterozygous in CPS-A and CPS-B. Null variants of *FKS2* have been implicated with increased echinocandin resistance in other fungal species (173). None of the other homozygous variants in CPS-C or CPS-B are predicted to affect drug resistance.

G1810A mutation in the *MRR1* gene is a gain-of-function mutation

To determine whether the G1810A nucleotide substitution in the *MRR1* gene represents a gain-of-function mutation responsible for fluconazole and voriconazole resistance, the *MRR1* gene was deleted in the susceptible isolate CPS-A and the mutated version was reintegrated, *mrr1ΔΔ* and *MRR1*$_{RI}$ transformants, respectively (Figure 10). These lasts two transformants were assessed for susceptibility to azoles. As predicted, deletion of the *MRR1* gene in isolate CPS-A did not change its susceptibility profile. In contrast, the G1810A nucleotide mutation provides an increased the MIC of FLC and VRC to 32 and 1 µg mL^{-1}, respectively, to the *MRR1*$_{RI}$ clone, indicating a resistant phenotype to these two azole drugs (Table 4). The sensitivity to PSC did not change.

Identification of increased copy number of *CDR* gene

Since no obvious SNPs or indels that could explain reduced susceptibility in *C. parapsilosis* CPS-B, we searched for changes in gene or chromosome copy number. No chromosome level aneuploidies were identified. Eighty-four genes had a copy number >3 or <1 with respect to the reference genome (Suppl. Table S6). Most of these (64 genes) lie in large segmental amplification of ~120 kb on chromosome 1, which is present in both CSP-B and CSP-C (Suppl. Table S6). Most of the other copy number variations (CNVs) are shared with CSP-A. However, CPAR2_304370 has approximately 15 copies in CPS-B compared to 4 copies found in CPS-A and CPS-C. CPAR2_304370 is a member of the ABC superfamily of multidrug transporters represented by *CDR1* in *C. albicans* (174) and recently named *CDR1B* in *C. parapsilosis* (175). Increased copy number of CPAR2_304370 may result in increased expression, and therefore increased efflux of fluconazole.

Gene expression profile

To determine how the *MRR1* GOF mutation (G1810A) results in increased azole resistance, we measured expression of *MRR1* and its target, *MDR1*. In CPS-C, expression of *MRR1* and *MDR1* genes are up-regulated 35-fold and 260-fold, respectively, compared to the gene expression level in the initial isolate, CPS-A (Figure 12). The importance of the G1810A GOF mutation in determining resistance was corroborated by first deleting mrr1 in CPS-A (*mrr1ΔΔ*) and then introducing the GOF mutation (*MRR1*$_{RI}$ strain). Introducing the mutated *MRR1* gene in the *mrr1ΔΔ* clone (*MRR1*$_{RI}$ strain) results in an up-regulation of *MDR1* and *MRR1* gene expression by approximately 220-fold and 30-fold respectively (Figure 12).

Expression of *MRR1* and *MDR1* in isolate CPS-B is identical to the susceptible isolate CPS-A. However, the increase in the copy number of *CDR1B* in CPS-B is correlated with an increase in expression of approximately 9,5-fold of *CDR1B* in comparison to isolate CPS-A (Figure 12). Notably, expression of *CDR1B* (CPAR2_304370) is also increased (10.5-fold) in the CPS-C isolate, independently from the gene copy number. In the *MRR1*$_{RI}$ strain, CPAR2_304370 expression is 3.5-fold upregulated in comparison to isolate CPS-A and 3-fold overexpressed relatively to *mrr1ΔΔ* strain (Figure 12).
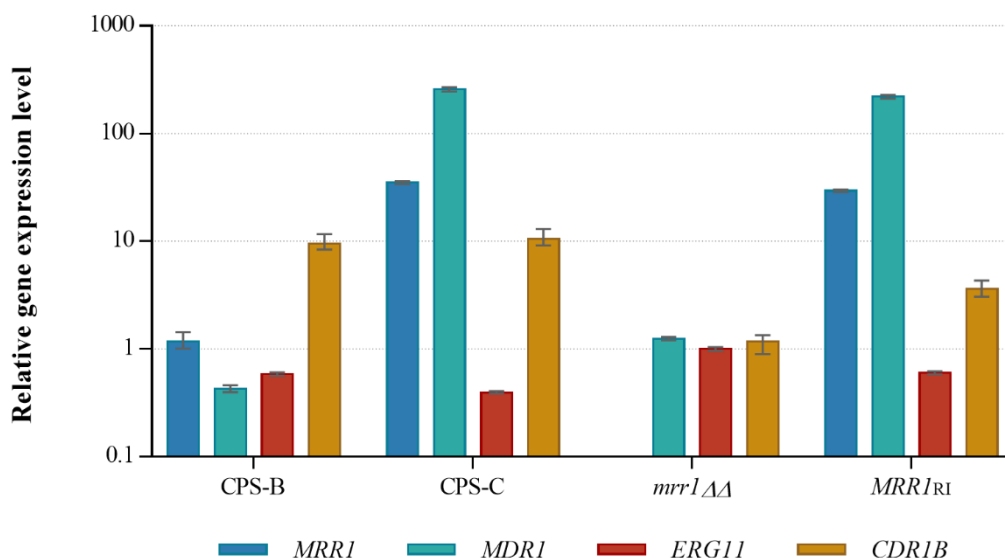
Figure 12. Gene expression associated with *C. parapsilosis* resistance. Relative expression levels of *MRR1*, *MDR1*, *ERG11* and *CDR1B* in isolates CPS-B and CPS-C, and in the transformants, *mrr1ΔΔ* and *MRR1*$_{RI}$ strains, comparatively to isolate CPS-A. *ACT1* was used as a normalizer gene. Expression level values represent the mean value ± standard error.

Expression of *ERG11* decreased about 40% and 60% in isolates CPS-B and CPS-C, respectively, in comparison to the initial isolate CPS-A. A similar reduction (40%) in *ERG11* gene expression was detected in *MRR1*$_{RI}$ strain. Interestingly, *ERG11* expression was not significantly different between isolates CPS-B and CPS-C.

Discussion

The emergence of *C. parapsilosis* as one prevalent fungal pathogen raise questions about the mechanisms underlying antifungal resistance. As indicated by surveillance studies, a growing number of *C. parapsilosis* clinical isolates display antifungal resistance (149). So far, and in parallel with *C. albicans*, the major mechanisms identified among *C. parapsilosis* azole resistant isolates are linked to alterations in ergosterol biosynthesis (Erg11) or upregulation of multidrug transporters (Mdr1 and Cdr1) (51). The most common SNP with demonstrated impact upon fluconazole susceptibility in *C. parapsilosis* is the *ERG11* Y132F mutation (112, 149). This mutation is also associated with decreased susceptibility to azoles in other pathogenic species, like *C. albicans*, *C. tropicalis* and *C. auris* (135-137). Upregulation of *ERG11* expression has also been described as a strategy to overcome fluconazole effect in clinical resistant isolates of *C. parapsilosis* (125). According to Berkow *et al.* (125), eight of thirty-five (22.8%) fluconazole resistant *C. parapsilosis* isolates showed up-regulation of *ERG11* by 2-fold to 11-fold. Conversely, our results show a reduction of *ERG11* gene following prolonged fluconazole exposure. In a previous study using an *in vitro* induction assay with a clinical isolate daily exposed to a fluconazole plasma concentration for 60 days, a similar result was found (174). We hypothesized that a decrease of *ERG11* gene expression is a direct consequence of the ergosterol reduction metabolism in response to azole stress.

In *C. parapsilosis*, the efficient efflux of azole drugs can result from the upregulation of transporter pumps encoded by *MDR1* and *CDR1.* The increased expression levels of these multidrug transporters can occur by gain-of-function mutations, either in the nucleotide sequence of these transporters or in the transcriptional factors *MRR1* and *TAC1* (122, 125, 149, 176). However, the impact on azole resistance of the majority of the *MDR1* and *MRR1* gene mutations identified remains yet unclear. Hereby, we show that azole resistance exhibited by isolate CPS-C following FLC exposure results from the GOF mutation (G604R) in the Mrr1p, upregulating expression of the transcription factor and consequently its effector, *MDR1* efflux pump.

Similar to MFS transporters, *CDR1* efflux pumps can be overexpressed triggered by GOF mutations (125). We did not identify any alteration in the sequence of *TAC1* or *CDR1*. However, a significant copy number variation of the ABC transporter *CDR1* member, CPAR2_304370 gene was detected in isolate CPS-B, a susceptible-dose dependent profile to FLC. The increased copy number correlates with overexpression. Genome modifications can occur during the adaptation of fungal cells to antifungal stress, ranging from a single gene alteration to chromosome rearrangement events (177). In *C. albicans*, changes in copy number of *ERG11, MRR1* and *TAC1*

impacts the fluconazole resistance (178, 179).In addition, CNVs potentiate the emergence of drug resistant point mutations (178).

Independently from increased copy number, we also observed overexpression of *CDR1B* (CPAR2_304370) in the resistant isolate CPS-C. Interestingly, introducing the GOF *MRR1* allele (*MRR1*$_{RI}$ clone) also increased *CDR1B* gene expression approximately 4-fold. This strongly suggests that expression of *CDR1B* gene is regulated by *MRR1* transcription factor as recently suggested by Doorley *et al.* (175). Interestingly, the ABC transporter *CDR1* expression in *C. lusitaniae,* named CLUG_03113, was also shown to be regulated by GOF mutation in *MRR1* (180).

Our results clearly demonstrate that expression of *CDR1* impacts on azole susceptibility of *C. parapsilosis*, and that expression can be altered either by a GOF mutation in Mrr1 (CSP-C), or by increased copy number (CSP-B).

Chapter III

Impact of Ndt80 in *Candida parapsilosis* virulence

Background

Besides its ability to grow and persist in the hospital environment surfaces, *C. parapsilosis* stands out for its capacity to adhere to the abiotic surface of implanted devices, later involving biofilm formation (13, 16, 181). In fact, adhesion and formation of biofilm are intimately related with *C. parapsilosis* virulence and are critical for its involvement in hospital outbreaks (9).

To identify putative *C. parapsilosis* biofilm regulators, more than 100 transcription factors were knocked-out and mutants were assessed for biofilm formation ability by Holland *et al.* (68). Previously identified as biofilm regulators in *C. albicans*, Bcr1, Efg1 and Ace2 were also directly implicated in biofilm development in *C. parapsilosis* (68, 69, 182-184), together with the transcription factor Gzf3, whose involvement in biofilm formation seems to be restricted to *C. parapsilosis* (68). In this large-scale screen of *C. parapsilosis* biofilm defective mutants, *NDT80* was firstly pointed as a putative biofilm regulator, in analogy with *C. albicans* biofilm regulation network. However, in the case of *C. parapsilosis, NDT80* role was undisclosed due to marked growth defects exhibited by *ndt80* mutant (68). In *C. albicans*, Ndt80 was first described as a key modulator of azole drug sensitivity, being involved in the control of ergosterol biosynthesis (185) and activation of the efflux pump Cdr1 (186).

The FMUP team identified *C. parapsilosis* Ndt80 ortholog to be a transcription factor upregulated following azole resistance acquisition (174). Later, we showed that *ndt80* mutant exhibits increased susceptibility to azoles and that, together with Upc2 transcription factor, also regulates the expression of various genes of ergosterol biosynthetic pathway, namely *ERG25*, *ERG6*, *ERG2*, *ERG3* and *ERG4* (128).

In this chapter, we address the role of Ndt80 in *C. parapsilosis* in virulence attribute expression, namely morphogenesis, adhesion and biofilm formation. Additionally, we explore the morphological phenotypes, its constitutive filamentous growth and the adhesion profile resulting from *NDT80* knockout, as well as its interaction with host immune system by assessing macrophage mediated response.

Material and Methods

Culture conditions

Yeast strains used in this study were routinely grown in YPD broth medium (1% yeast extract, 2% bacto peptone, 2% glucose) at 30°C with agitation (180 rpm) or on YPD agar plates, following addition of 2% of agar. To recycle the *SAT1* flipper cassette, transformants were incubated in YPM medium (1% yeast extract, 2% peptone, 2% maltose) overnight, with agitation (180 rpm); afterward, approximately 100 cells were plated on YPD plates supplemented with nourseothricin at final concentration of 20 µg mL^{-1}. All *C. parapsilosis* strains were stored in YPD broth with 40% glycerol, at − 80°C.

RAW 264.7 murine macrophages were obtained from the European Collection of Cell Cultures and maintained in DMEM (Sigma-Aldrich) with 10% non-inactivated Fetal Calf Serum (FCS), 10 mM HEPES, 12 mM sodium bicarbonate and 11 mg mL^{-1} sodium pyruvate at 37°C in a humidified atmosphere with 5% CO2. The culture medium was changed every 2 days, until ~70% of cell confluence was reached. RAW 264.7 cells were resuspended in RPMI 1640 medium (Sigma-Aldrich) supplemented with 10% inactivated FCS, 23.8 mM sodium bicarbonate and 50 mM glucose for the experimental assays (initiated until the cells 15th generation).

Plasmid construction

To knockout *NDT80* gene in *C. parapsilosis* BC014S (wild-type strain) (174), the pNG4 disruption cassette described by Branco *et al*. (128) was used. Briefly, a 478 bp upstream and 460 bp downstream sequences of *NDT80* gene were amplified using CpNDT80up_F and CpNDT80up_R primers (containing recognition sites for *KpnI* and *ApaI*) and CpNDT80down_F and CpNDT80down_R primers (containing recognition sites for *SacII* and *SacI*), respectively, and cloned into the flanking sites of pCD8 plasmid (171). After restriction with *KpnI* and *SacI*, pNG4 disruption cassette was introduced into the native locus of *NDT80* gene of *C. parapsilosis* BC014S. All primer sequences are listed in Table 5.

C. parapsilosis transformation

Transformation of wild-type strain was performed by electroporation as described by Ding *et al*. (171). Briefly, an overnight cell culture was diluted in 50 mL of YPD broth medium for an initial OD$_{600}$ of 0.2 and incubated at 30°C until reaching approximately OD$_{600}$ of 2.0. After being

Table 5. Primers used in chapter III

Primer name	Primer sequence (5` to 3`)
Construction of deletion cassette	
CpNDT80up_F	GGGGGTACCGGCAATTTTGATTTTTGGGTTC
CpNDT80up_R	GGGGGGCCCGAGGCACCACCAGCAGTAGAGT
CpNDT80down_F	TCCCCGCGGGATGGGAGAAAAAACTGAACCTTG
CpNDT80down_R	CGAGCTCAGATGGCATTGTAGTCAGTAGCATC
PCR Confirmation	
CpNDT80gen_F	GCCTTTTACATCTATCGAAGTCAAACTTG
FLP_R	TTTATGATGGAATGAATGGGATG
RT-qPCR	
CpACT1_F1	TGCTCCAGAAGAACACCCA
CpACT1_R1	CACCTGAATCCAAAACAATACCAGT
CpBCR1_F	TCGCCACCACTACTCG
CpBCR1_R	AAAGGATAATGTTGCTGTGA
CpEFG1_F	GAGCGGAGCAGCAGTT
CpEFG1_R	GAAGCATAAGGTTGTTGGG
CpACE2_F	AACAACAACAACAACCCC
CpACE2_R	ACATCTAAATCCTGCAATCC
CpUME6_F	CTTTTCCCCCGTCTGTA
CpUME6_R	TGCAATGTTTTCTGTTCACT
CpMKC1_F	TCAGAGAATCCAGAACAAAA
CpMKC1_R	ATCCAACAGACCACACG
CpCZF1_F	CCAACAACAAAACTCCAAC
CpCZF1_R	TCTCGACTCACAACATCTCT
CpGZF3_F	GATACATTCAAAGCAGCAAA
CpGZF3_R	GTGGTTATCTTCAGTTCCG
CpCPH2_F	TCCAAAGTGACAAAGCC
CpCPH2_R	GCAATTCTCAAAGCAGG
CpRHR2_F	TTTGTTTGACTGTGACGG
CpRHR2_R	TACGGCATCCATGAGAAG
CpALS3_F	CGCACCAGCAAACTCATCAA
CpALS3_R	CCAATGAACTCGGGGGAAAT
CpALS7_F1	CTTCTGTTGTTGTGTCATCCCTG
CpALS7_R1	CACCATCTGTTGAGCCTGTAG
NDT80_F3	CAAAGGGCGGTATGAATGGTA
NDT80_R3	TGGTGTGGATGGTGTGGA
CpCW41_F	TGACGACGACGATGAACGCG
CpCW41_R	TGGTGATGAGCGGGGATA
CpSTP3_F	TCCGCCACGATAAAGCCA
CpSTP3_R	GAATCACCCAGACCACCG
CpOCH1_F	AATGCGATGCCCTTGTTGC
CpOCH1_R	TTGCTTGCCCACTCGTCA

pelleted, yeast cells were resuspended in 10 mL of Tris-EDTA buffer (10 mM Tris-HCl, 1 mM EDTA, pH 7.5) containing 10 mM dithiothreitol and incubated at 30°C for 1 h with agitation (100 rpm). Yeast cells were washed twice with 40 mL of cold water plus once with 10 mL 1 M Sorbitol and, subsequently resuspended in 125 µL of this solution. Approximately 1 µg of purified *KpnI-SacI* fragment of pNG4 was added to 50 µL of competent cells. The cell mixture was then transferred to a 1 mm electroporation cuvette. Electroporation shock was performed at 1.25 kV, using a Gene Pulser X-cell Electroporator (Bio-Rad). Afterward, 950 µL of YPD containing 1 M sorbitol was immediately added; the mixture was incubated at 30°C for 4 h with agitation; afterward 100 µL were plated on YPD agar supplemented with nourseothricin at final concentration of 200 µg mL^{-1}. Transformants were obtained after 24 h of incubation at 30°C.

Adhesion assay

Yeast adhesion was quantified by flow cytometry, as described by Silva-Dias *et al*. (187). Briefly, yeasts were grown overnight at 30°C in Sabouraud broth medium, with agitation (180 rpm); the culture was centrifuged at 10,000 *g* for 5 min and washed twice with phosphate buffer saline (PBS) (Sigma-Aldrich). A yeast suspension was standardized to 2×10^6 cells mL^{-1} in the same buffer and mixed with 2×10^7 microspheres mL^{-1} of 1 µm uncoated carboxylated highly green fluorescent polystyrene microspheres (Molecular Probes). This mixture was incubated at room temperature for 30 min at 150 rpm. The suspensions were vortexed, and 50,000 events were analyzed using a FACS Calibur flow cytometer (BD Biosciences). Cell adhesion results are expressed as the percentage of cells with microspheres attached, representative of at least three independent experiments, performed in triplicate.

Biofilm formation assays

After overnight growth at 37°C with agitation (180 rpm) in Sabouraud broth medium, yeast cells were collected by centrifugation at 10,000 *g* for 5 min, washed once with PBS and standardized to obtain a suspension of 1×10^6 yeast cells mL^{-1} in RPMI-1640 medium supplemented with L-glutamine and buffered with MOPS acid (Sigma-Aldrich). One mL of such cell suspension was placed in each of a 12-well polystyrene microplate and incubated for 24 and 48 h at 37°C. Following incubation, total biomass was quantified by Crystal Violet (CV) assay, as previously described by Silva-Dias *et al*. (41). Biofilm mass was calculated from at least three independent experiments, performed in triplicate. For dry mass assessment, *C. parapsilosis*

strains were set up as previously described, except the standardization of the cell suspension, which was diluted to an OD_{600} of 1; afterward, 5 mL were distributed in each well of a 6-well polystyrene plate. After 24 and 48 h of incubation at 37°C, adherent biofilms were washed with PBS, scrapped from the bottom of the wells, and vacuum filtered, as described by Holland, *et al*. (68). The average of the total biomass was calculated by subtracting the initial weight of the filter to the final weight, determined from three independent experiments, performed in triplicate.

Microscopic imaging

Colony phenotypes were observed and photographed under 20× magnification using a Stereo zoom S9i (Leica Microsystems) dissection microscope, after growth on YPD agar at 30°C, for 72 h. Images of yeast cell morphology were taken with a Zeiss Axioplan microscope, coupled with an AxioVision image acquisition system (Zeiss), after staining with Calcofluor White (Sigma-Aldrich) and mounting on glass slides. Yeast cells were photographed under 1000× magnification, oil immersion.

RNA extraction, cDNA synthesis and RT-qPCR

RNA was extracted as described by Kohrer and Domdey (188). Concentration and quality of RNA samples were measured using a Nanodrop equipment (Eppendorf). Only samples yielding A_{280}/A_{260} ratios ranging from 1.6 to 2.2 and showing no signs of degradation, after electrophoresis, were used in subsequent analyses. From 100 ng of total RNA, the first-strand cDNA was synthesized using the SensiFAST cDNA Synthesis Kit (Bioline) according to the manufacturer´s instructions. The resulting cDNA was stored at −20°C prior to use for real-time quantitative polymerase chain reaction (RT-qPCR). The genes analyzed were the followed: *NDT80* (CPAR2_213640), *OCH1* (CPAR2_404930), *ALS3* (CPAR2_404770), *ALS7* (CPAR2_404800), *GZF3* (CPAR2_800210), *ALS7* (CPAR2_404800), *BCR1* (CPAR2_205990), *EFG1* (CPAR2_701620), and the orthologues of *Candida albicans STP3* (CPAR2_200390), *CWH41* (CPAR2_501400), *STP3* (CPAR2_200390), *MKC1* (CPAR2_800090), *CPH2* (CPAR2_603440), *RHR2* (CPAR2_503990), *ACE2* (CPAR2_204370), *CPH2* (CPAR2_603440), *UME6* (CPAR2_803820) and *CZF1* (CPAR2_501290). For each real-time quantitative PCR, five replicates per strain were analyzed. All primers used are detailed in Table 5. PCRs were performed using the SensiFAST SYBR Hi-ROX Kit (Bioline) 3-step cycling, according to the manufacturer's instructions, in a PikoReal Real-Time PCR System

instrument (Thermo Scientific). *ACT1* gene expression was used to normalize the signal obtained for each gene. Data obtained were analyzed with REST software.

Bioinformatic analysis

Sequences from *C. parapsilosis* CDC317 open reading frames (ORFs) plus 1000 bp upstream and downstream (version s01-m03-r14, from 7 February 2016) were downloaded from the Candida Genome Database (CGD, http://candidagenome.org/). To identify putative Ndt80-regulated genes, a search for the MSE consensus motif (gNCRCAAAY) was performed in the promoter regions (1000 bp upstream the start codon). The resulting ORFs containing MSE sequences were grouped according to Gene Ontology (GO) terms using the CGD Gene Ontology Slim Mapper with the default parameters.

Macrophage-yeast interaction assays

Macrophage-yeast interaction assays were carried out as previously described (189). Briefly, RAW 264.7 macrophage cells were platted in 96-, in 12-well (with 16 mm glass coverslips) or in μ-slide 8 well plates, and incubated for 18 h at 37°C, under a 5% CO2 atmosphere. After this incubation period, yeast cells were added to the macrophages at an MOI (Multiplicity of Infection) of 1:1.

Immunofluorescence and microscopic analysis

Macrophages grown in coverslips were incubated with *C. parapsilosis* as described below. At the end of each incubation period (10 min, 30 min, 1 h 30 min, 3 h), coverslips were washed twice with ice-cold PBS and fixed with 4% paraformaldehyde in PBS for 15 min at room temperature. After 3 washing steps with PBS, cell membranes were stained with WGA, for 10 min, protected from light. Macrophages were treated with a blocking solution of 10% bovine serum albumin in PBS for 30 min at 37°C. Cells were then incubated overnight, at room temperature, with the primary rabbit polyclonal antibody against Candida (GTX40096; GeneTex), diluted (1:200) in blocking solution. Coverslips were washed and incubated for 2 h at room temperature with the AlexaFluor 488 donkey anti-rabbit IgG secondary antibody (A21206; Invitrogen). Finally, after a washing step, macrophage cells were incubated with DAPI 0.02% for 10 min at room temperature. Cells were subsequently washed and the coverslips were mounted in glass slides with DAKO

mounting medium and kept at −20°C until observation under confocal or fluorescence microscopy. Digital images were captured using a Carl Zeiss LSM 710 Confocal Microscope, using Plan-ApoChromat 40x/ 63x/1.4 oil objectives; Zen Blue and FiJi software's were used to analyze the images.

Yeast and macrophage viability assays

The yeast cell viability following interaction with RAW 264.7 macrophage cells was assessed by a colony forming unit (CFU) assay. After 30 min and 3 h of coincubation, supernatants were collected and plated on YPD agar, to count non-internalized or non-adhered yeast cells. The remaining adhered RAW 264.7 macrophages were scraped and lysed with 0.5% Triton X-100. This cell suspension, representing the amount of yeast cells internalized was plated on YPD agar, using serial dilutions. Following 3 days of incubation, at 30°C, the number of yeast colonies per mL was calculated. For macrophage viability assay, after 30 min and 3 h of co-incubation, viable, and death macrophage cells were calculated using a hemocytometer, after staining with Trypan Blue (T8154; Sigma-Aldrich).

Live cell imaging assays

For live cell imaging assays, culture media without phenol-red was used and macrophage cell membranes were stained with Wheat Germ Agglutinin, Tetramethylrhodamine conjugate (WGA, W849; Molecular Probes). Image acquisitions were conducted during at least 45 min, using a confocal Cell Observer Spinning Disk microscope (Zeiss), equipped with an LCI PlanNeofluar 63x/1.3 glycerol objective; Zen Blue software was used to analyze the time-lapse videos obtained.

Statistical analysis

Statistical analysis of results of adhesion, biofilm and infection assays was performed using one-way ANOVA followed by a Dunnett post hoc test. Differences were considered statistically significant for a p-value <0.05. Significant differences were marked with an asterisk character (*), in which *p < 0.05, **p < 0.01, ***p < 0.001. All results are presented as mean ± standard deviation, of at least three independent experiments.

Results

Deleting *NDT80* transcription factor gene triggers morphogenesis

To gain insight into the role of Ndt80 in *C. parapsilosis* virulence attribute expression, two independent lineages lacking one (*ndt80Δ* – NG2 strain) or both (*ndt80ΔΔ* – EF16 strain) copies of *NDT80* were generated from *C. parapsilosis* strain BC014S (wild-type strain) (174). Deletion was carried out using a gene specific disruption cassette (pNG4) based on the recyclable nourseothricin-resistant marker as previously described (171). The introduction of pNG4 into the*NDT80* locus of the wild-type strain, generated NG1 clone, which after cassette recycling, resulted in the NG2 strain. To delete the second copy of *NDT80* gene, a second round of integration/recycling were performed, generating EF15 and EF16 clones, respectively. Gene knockout was confirmed by PCR (Figure 13 A and B). Deletion of *NDT80* had a major effect
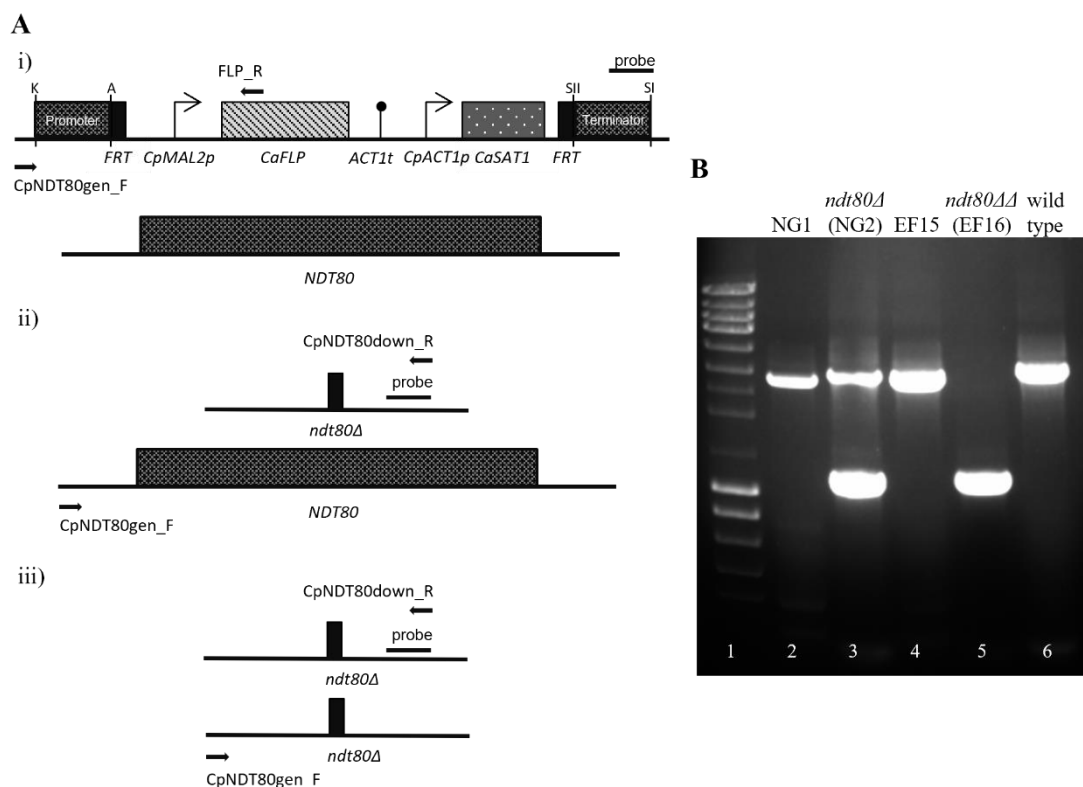
Figure 13. Deletion of *NDT80* transcription factor gene in *C. parapsilosis*. Gene knockout was confirmed by PCR. Genomic integration of NDT80 disruption cassette in the wild type strain was confirmed using the following pairs of primers CpNDT80gen_F and FLP_R (**A**, i), which amplified a 2.9 kb fragment (**B**, NG1 strain, lane 2). The recycling of the disruption cassette was confirmed using primers CpNDT80gen_F and CpNDT80down_R (**A**, ii), originating a 3.1 kb (second copy of NDT80 gene) and 1.2 kb PCR products (disruption of the first copy) (**B**, NG2 strain, lane 3). Disruption of the second allele in strain NG2 was

confirmed following the same strategy, using the primers: CpNDT80gen_F and FLP_R (**A**, i), which amplified a 2.9 kb fragment that corresponds to the second integration of NDT80 disruption cassette (**B**, EF15 strain, lane 4) and CpNDT80gen_F and CpNDT80down_R (**A**, iii), amplifying a 1.2 kb PCR product, indicating a successful recycling of the cassette (**B**, EF16 strain, lane 5). Wild type strain was used as PCR control of CpNDT80gen_F and CpNDT80down_R pair primers, amplifying a 3.1 kb fragment (**B**, lane 6). Lane 1 represents the molecular size marker (NZYDNA Ladder III, NZYTech).

upon colony and yeast cell morphology (Figure 14 A and B). The parental strain and the *ndt80Δ* haploid mutant grow as smooth-white and creaky-opaque colonies, respectively, whereas colonies from *ndt80ΔΔ* diploid mutant display a crepe phenotype. Wild-type and haploid cells are yeast-shaped cells; in contrast, the *ndt80ΔΔ* cell population is mostly composed of elongated cells and pseudohyphae.

A

wild type	*ndt80Δ*	*ndt80ΔΔ*

B

Figure 14. *NDT80* deletion triggers morphogenesis changes in *C. parapsilosis*. (A) Colony morphology of wild type, *ndt80Δ* and *ndt80ΔΔ* strains. Yeasts were grown at 30ºC for 2 days and colonies photographed under 20× magnification. Smooth colonies were found in wild type strain; *ndt80Δ* mutant displays creaky-opaque colonies, while only crepe phenotype colonies were observed in the *ndt80ΔΔ* mutant strain. **(B)** Cell morphology of wild type, *ndt80Δ* and *ndt80ΔΔ* strains. Staining of wild type and *ndt80Δ* cells with calcofluor white revealed a cell population mainly composed by yeasts; in contrast, *ndt80ΔΔ* mutant shows a mixture of elongated cells and pseudohyphae. Cells were visualized under fluorescence microscopy and photographed under 1000× magnification, oil immersion.

Deleting *NDT80* promotes adhesion and biofilm formation ability

The yeast to pseudohyphae transition was observed along with the formation of fungal cell aggregates, typical of enhanced cell to cell adhesion. The *ndt80Δ* and *ndt80ΔΔ* mutants flocculate in liquid medium, suggesting that Ndt80 negatively impairs the cell-cell adhesion process (Figure 15 A). The ability of *C. parapsilosis* to adhere to polystyrene microspheres, representative of abiotic surfaces, was quantified using a flow cytometric adhesion assay, as described previously (187). Compared to wild-type, manipulated strains displayed a significant increase of about 2-fold in adhesion ability (Figure 15 B). Filamentous growth and adhesion displayed by *ndt80ΔΔ* mutant are two known promoters of biofilm formation. We assessed wild-type and mutant strains regarding the ability to form biofilm, using two independent methods, Cristal Violet (CV) staining (41) and dry weight (68). *C. parapsilosis* lacking one or both copies of *NDT80* gene exhibits enhanced capacity to form biofilm compared to wild-type strain (Figure 15 C and D). Differences were statistically significant when using both methodologies. Nevertheless, comparatively to *ndt80Δ* mutant, *ndt80ΔΔ* mutant produced lower biofilm biomass, a result statistically significant when using CV staining for biofilm quantification.
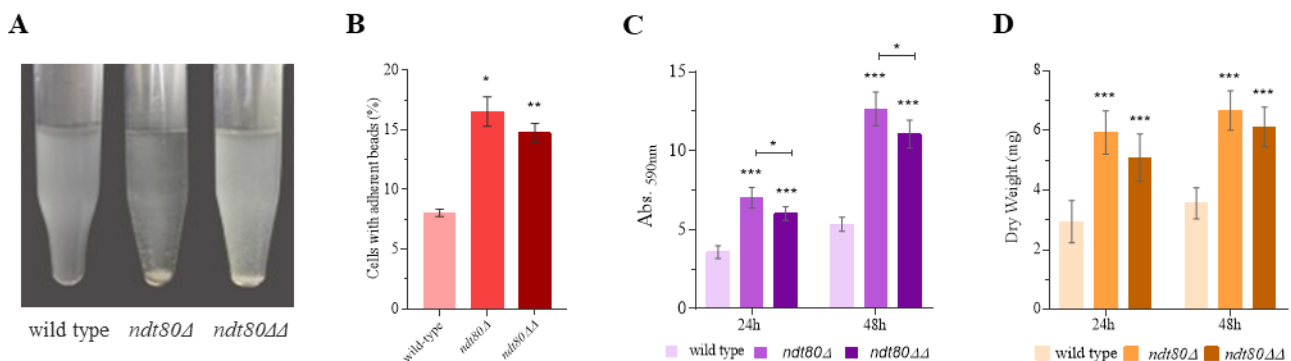
Figure 15. Deletion of *NDT80* increases adherence and biofilm formation ability. (A) Images of wild type, *ndt80Δ* and *ndt80ΔΔ* strains grown in liquid media; the mutants strains exhibit a strong flocculation (cell-cell adhesion) phenotype. **(B)** Percentage of yeast cells with adherent beads. *ndt80Δ* and *ndt8ΔΔ* mutants exhibited significantly higher adhesion ability than wild type. The ability to form biofilm was quantified by **(C)** Cristal Violet (CV) staining and **(D)** dry weight, following 24 and 48 h of growth; in both assays, a significant increase of biofilm formation by *ndt80Δ* and *ndt8ΔΔ* mutants compared to the parental strain was observed. CV staining revealed a statistical decrease in biofilm formation between *ndt80Δ* and *ndt8ΔΔ* mutants, at both time points. *p<0.05, **p<0.01 and ***p<0.001 wild type vs *ndt80Δ* and *ndt8ΔΔ* mutants, or both groups.

Ndt80 regulates the expression of adhesion-,morphology- and biofilm-related genes

A set of transcription factor genes, namely Czf1, Ume6, Gzf3, Cph2, Efg1, Bcr1, Ace2, additional regulators like Stp3, Cwh41, Och1, Rhr2, one protein kinase (Mkc1)and also adhesins Als-like (Als7, Als3), were identified by several authors (15, 47, 68) as regulators of morphology transition, and as effectors in adhesion and biofilm formation by *C. parapsilosis*. In an attempt to identified Ndt80 targets involved in triggering virulence factors, we quantified the expression of the above-mentioned genes by RT-qPCR (Figure 16, Suppl. Table S7). Relatively to adhesin-like genes, the expression of *ALS7* in *ndt80Δ* and *ndt80ΔΔ* mutants was upregulated 210- and 180-fold, respectively, compared to wild-type. In contrast, *ALS3* gene expression was not changed significantly among the studied mutant strains. The expression of *UME6* was upregulated, approximately, 5-fold in the *ndt80Δ* haploid mutant and a 13-fold in the *ndt80ΔΔ* diploid mutant, compared to the wildtype. *MKC1* expression was also upregulated 2.8-fold and 36-fold in haploid and diploid mutants, respectively, comparatively to the wild-type. *CPH2* gene exhibited a 1.2-fold upregulation in *ndt80Δ* mutant and of approximately 4-fold increased expression in *ndt80ΔΔ* mutant, in comparison to the wild-type. *ACE2, CWH41* and *OCH1* genes displayed similar expression values of approximately 3-fold, 2-fold, and 1.2-fold, respectively, in the haploid and diploid mutants. *BCR1* gene was 1.5 and 1.7-fold upregulated in *ndt80Δ* and *ndt80ΔΔ* mutants in comparison to wild-type. The expression of *STP3* was increased approximately 1.8-fold in *ndt80Δ* mutant but remained unchanged in *ndt80ΔΔ* mutant. In contrast, *EFG1, GZF3* and *RHR2* were downregulated in *ndt80ΔΔ* mutant comparatively to the wild-type; *ndt80Δ* mutant exhibited a slight upregulation of expression of such genes (of about 1.1-, 1.4-, and 2.6- fold, respectively). *CZF1* gene was progressively downregulated following sequential *NDT80* gene copy deletion, by approximately 30% and 70%, respectively. As expected, no *NDT80* transcript was observed in the null strain. Interestingly, the expression of *NDT80* in *ndt80Δ* mutant was 1.6-fold up-regulated. Since *NDT80* gene has in its promoter region the MSE binding sequence, we could hypothesize that to cope with one copy gene deletion, Ndt80 up-regulates itself expression, as described in *S. cerevisiae* and *A. nidulans* (190, 191).
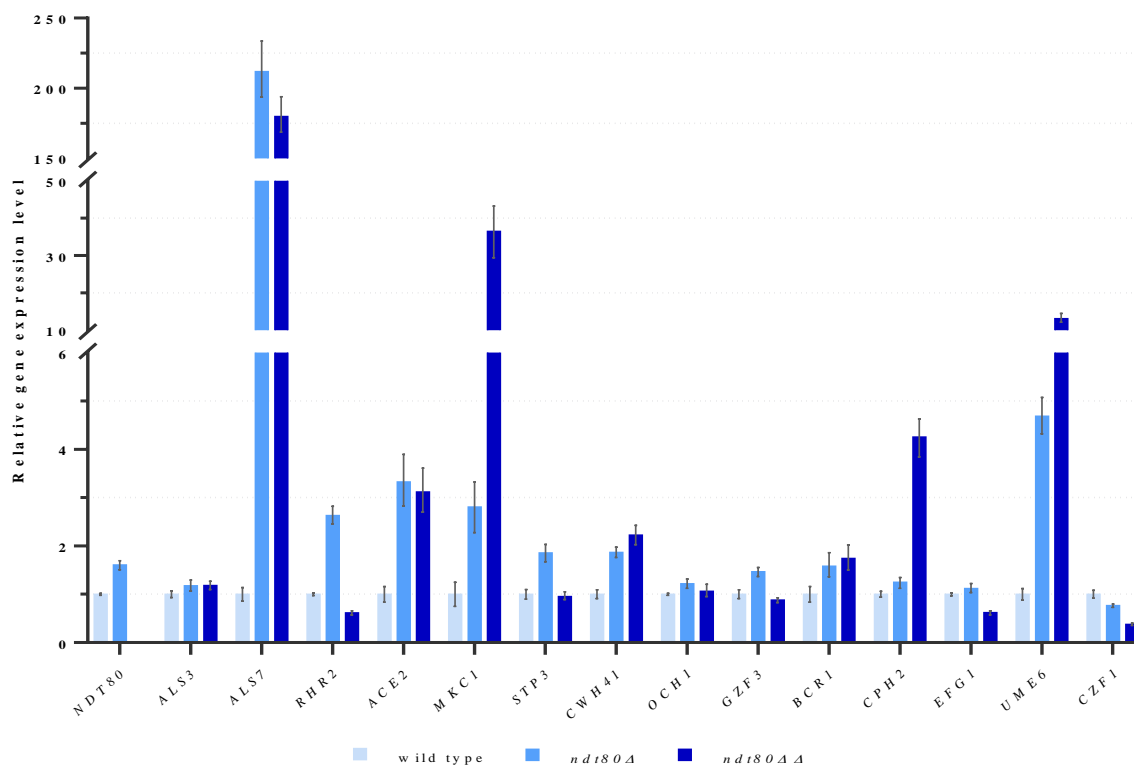
Figure 16. Putative targets of Ndt80 transcription factor. Relative expression levels of *NDT80*, *ALS7*, *ALS3*, *CZF1*, *UME6*, *GZF3*, *CPH2*, *EFG1*, *BCR1*, *ACE2*, *STP3*, *CWH41*, *OCH1*, *RHR2* and *MKC1* genes in *ndt80Δ* and *ndt8ΔΔ* strains compared with wild type strain. *ACT1* was used as a normalizer gene. Expression values represent the mean value and ± standard deviation of five independent experiments.

Identification of putative *NDT80*-regulated genes

Ndt80 was found to bind to the middle sporulation element (MSE) (5'-CACAAA-3') in the target gene promoter region (192) of *C. albicans* and *S. cerevisiae* ORFeomes (69, 185). The putative colony transition, adhesion- and biofilm-related genes mentioned above were analyzed for the presence of MSE motifs using the NCBI blast tool. As some of the promoter regions bound by biofilm regulators are larger than the normal (69, 192), the considered sequence was approximately 1 kb upstream of the start codon. All genes assessed for their expression (Figure 16) contain putative MSE recognition sites, being identified in promoter regions. Considering such findings, we further expanded the search for MSE consensus sequences in the complete *C. parapsilosis* ORFeome. This analysis allowed the retrieval of 417 ORFs containing MSE motifs in their promoters. These were mapped to GO terms and grouped according to Biological Process, Molecular Function or Cellular Component (Figure 17). Results showed that most ORFs with MSE elements (with over 10% and excluding the unknowns) belong to cell transport regulation,

74

organelle organization, response to stress/chemical and RNA metabolic processes. Also, these ORFs are mostly related with enzymes with hydrolase or transferase activity which in addition to the cytoplasm and nucleus, many are located in cell membranes and mitochondria (Figure 17).
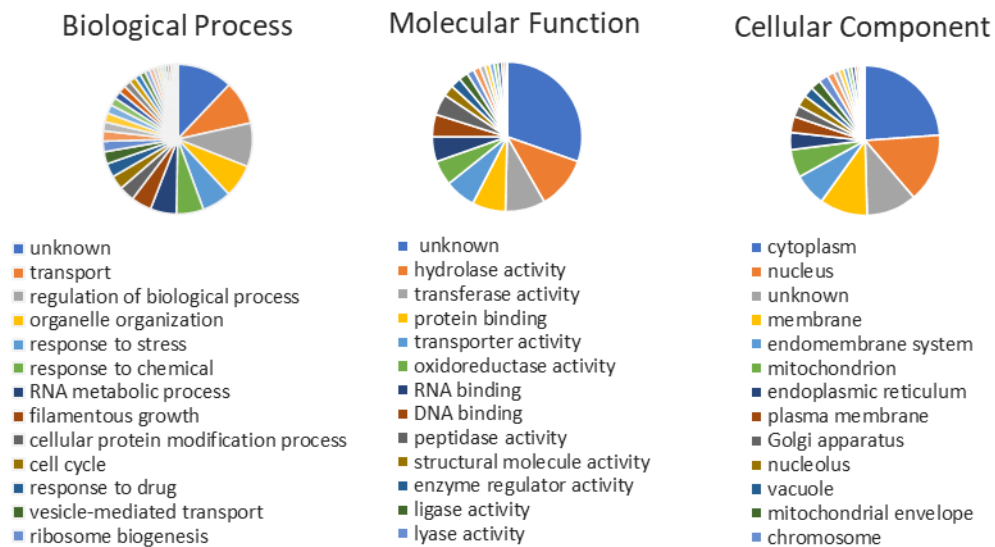
Figure 17. GO analysis of Candida parapsilosis genes putatively regulated by the Ndt80 transcription factor. ORFs containing MSE elements are grouped according to Biological Process, Molecular Function and Cellular Component.

C. parapsilosis strains lacking *NDT80* are more resistant to macrophage attack and impair macrophage viability

The capacity of fungal cells to resist to macrophage mediated killing contributes to its pathogenicity (15, 51, 193). We conducted a phagocytic assay using the murine macrophage cell line RAW264.7 in order to determine the impact resulting from *NDT80* deletion upon phagocytic cells response. The interaction between macrophages and *C. parapsilosis* cells begins as early as 10 min (Figure 18 A). However, while *C. parapsilosis* wild-type cells hardly interact, at the same time point a higher number of *ndt80ΔΔ* cells are attached to macrophages with clear signs of internalization, as indicated by the tridimensional green staining fading (Figure 18 A); the *ndt80Δ* cells showed a intermediate behavior. Clearly, mutant strains exhibited a more effective adherence and internalization profile soon after 27 min of coculturing (Movie S1), while this
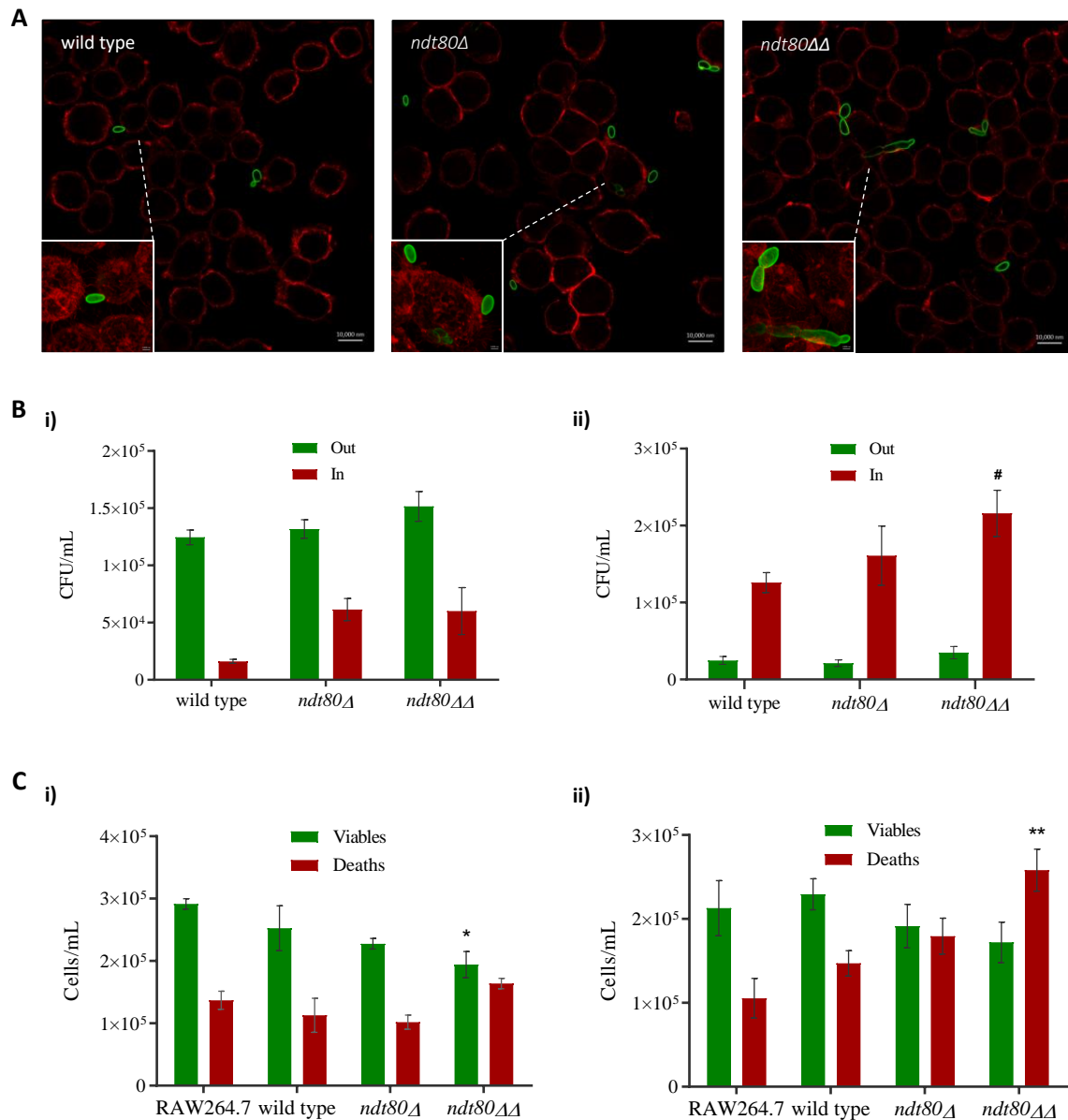
Figure 18. Interaction of *C. parapsilosis NDT80* deletion strains with RAW264.7 macrophage cells. (A) Representative confocal microscopy images of RAW264.7 macrophages and wild type, *ndt80Δ* and *ndt80ΔΔ* strains after 10 min of interaction at MOI of 1:1; scale bar represents 10 μm. Cells are distinguished through their different fluorescence staining with WGA (red macrophages) and Alexa Fluor 488 labelled anti-Candida antibody (green yeasts). Small boxes correspond to fluorescent projection details, highlighting mutant yeasts more adherent and internalized by macrophages ("tridimensional" images with fading green staining as indicator of phagocytosis and inclusion inside macrophages), when compared with wild type. **(B)** Viable *C. parapsilosis* counts after i) 30 min and ii) 3 h interaction with macrophages at MOI of 1:1. Viable counts were performed using a CFU assay of co-culture supernatants (yeasts not internalized or adherent) and of lysed macrophage cells (phagocyted/internalized yeasts). **(C)** Viable and dead macrophage counts after i) 30 min and ii) 3 h interaction with C. parapsilosis strains at MOI of 1:1. Macrophage counts were performed after Trypan Blue exclusion test of cell viability. *p<0.05 and **p<0.01 wild type or RAW264.7 macrophages control groups.

process is more delayed for the wild-type macrophage interaction; after 30 min of interaction, most of the *C. parapsilosis* cells were still outside of the macrophages, adherent or not (Figure 18 B, i). Following 3 h of interaction, wild-type and both mutant strains were mostly internalized; notably, the number of *ndt80ΔΔ* mutant cells inside macrophages was statistically higher versus the two other cell types (Figure 18 B, ii). Macrophage viability decreased along the assay (Figure 18 C, i and ii). Macrophage challenge with *ndt80ΔΔ* mutant cells, caused a significant reduction of the number of viable macrophages soon after 30 min (Figure 18 C, i). Following 3 h of coculture, an increase of lysed macrophages was observed with all the strains assessed; however, this result was statistically significant in the case of *ndt80ΔΔ* strain (Figure 18 C, ii).

Discussion

While molecular mechanisms are well characterized in *C. albicans*, several studies addressing the regulatory networks of non-*albicans* species, like *C. glabrata* and *C. parapsilosis*, reveal a significant difference in the evolutionary adaptation of such yeasts to the human host (68, 194). Although the available knowledge regarding the expression of *C. parapsilosis* virulence attributes is still somewhat limited, this species displays many biological features that are presumed to be directly related to its environmental colonization and pathogenicity, such as enhanced adherence and biofilm development on abiotic surfaces.

Adhesion, morphogenetic variations and biofilm formation are virulence attributes clearly depicted for *C. albicans* (195, 196) and are intimately related to each other. Filamentous growth is closely related to the expression of surface proteins, such as Als1, Als3 and the hyphal-specific protein, Hwp1. In turn, these proteins play relevant roles in cell-cell and cell-surface adhesion and are required for biofilm formation as contact mediators that promote further biomass accumulation and enhance biofilm resilience (197, 198). Ndt80 was identified as one of the many regulators of filamentous growth by binding to promoters of genes encoding cell wall components (e.g. *ALS3* and *HWP1*), being required for their normal expression (199). Thus, deletion of *NDT80* reduces *C. albicans* virulence *in vivo*, by blocking yeast to hyphal transition, as well as the expression of genes involved in the filamentous transcriptional program (199).

Surprisingly, and opposing to what was described for *C. albicans*, the disruption of *C. parapsilosis NDT80* gene triggers two noticeable phenotypic changes: morphogenesis in a spontaneous and constitutive manner (Figure 14), and prompted adhesion, both cell to cell and to abiotic surfaces, but also to murine macrophages (Figure 15 and Figure 18, respectively). Despite the scarce knowledge on *C. parapsilosis* adhesion mediators, we demonstrated that *ndt80* mutants adhesion is conferred by *ALS7* (CPAR2_404800), whose expression is extraordinary increased. This adhesin was previously identified as a mediator of *C. parapsilosis* adhesion to human buccal epithelial cells (47). Although only 0.5% of the ORFs related with cell adhesion contain putative recognition sites for Ndt80, *ALS7* and *ALS3* are included in this group.

According to our findings Ndt80 can have a dual role in yeast to pseudohyphae transition: on one hand, by impairing the expression of *UME6* and *CPH2*, described as inducers of yeast to pseudohyphae transition (68); on the other hand, by acting as an activator of Czf1 and Efg1 (68, 192), two known transcription factors regulating phenotypic switching and filamentous growth in *C. albicans*. Other genes like *OCH1*, the orthologs of *C. albicans CWH41* and *STP3* are also involved in *C. parapsilosis* phenotypic switching, as positive and negative regulators, respectively (51, 200). We found that Ndt80 has no impact upon the expression of *OCH1* and the ortholog of

C. albicans STP3; interestingly, the ortholog *C. albicans CWH41* expression doubles in *ndt80ΔΔ* mutant, suggesting that this gene could be a target for Ndt80, which putatively represses the expression of this pseudohyphae formation factor.

Ndt80 is also part of a network of six transcription factors (Bcr1, Efg1, Tec1, Rob1, Bgr1, and Ndt80) responsible for the regulation of *C. albicans* biofilm development (69). In this species, *NDT80* deletion significantly compromises biofilm formation either *in vitro* or *in vivo* models (69). Conversely, we found that deletion of *C. parapsilosis NDT80* gene promotes biofilm growth *in vitro*, suggesting that this transcription factor is acting as a repressor of genes involved in such process. Other biofilm regulators, acting as repressors and activators in a circuit system were already previously identified in *C. albicans* and *C. parapsilosis* (68). Efg1, Bcr1, and Ace2 play similar roles regarding biofilm development in both species, while Cph2, Czf1, Gzf3, and Ume6 have major roles just in *C. parapsilosis* (68). In *C. parapsilosis*, deletion of *CZF1, GZF3, UME6,* and *CPH2* was associated with a reduced biofilm formation ability. Although Ndt80 was not identified as a component of *C. parapsilosis* regulatory network due to the inherent growth defects (68), we analyzed the promoter sequences of all the biofilm transcription factors described by Holland *et al*. (68) for the presence of Ndt80 MSE motifs and identified putative recognition sites in all of the genes tested. The gene expression profile analysis of *ndt80ΔΔ* mutant revealed an approximately 36-fold, 13-fold, 4-fold and 3-fold upregulation of *MKC1, UME6, CPH2* and *ACE2*, respectively, while other genes also described to be required for biofilm formation, such as *GZF3* and *CZF1*, were demonstrated to be downregulated. These findings strongly suggest the role of Ndt80 as a negative regulator of *MKC1, UME6, CPH2* and *ACE2* expression and as an activator of *GZF3* and *CZF1* expression. Thus, in Ndt80 absence, and despite *GZF3* and *CZF1* genes exhibiting a reduced expression, the upregulation of *MKC1, UME6, CPH2* and *ACE2* genes occurs and biofilm development is promoted (Figure 16). *RHR2* was also considered to be involved in biofilm development by *C. parapsilosis*, as its expression was increased during biofilm formation (68). Nevertheless, in *ndt80ΔΔ* mutant characterized by enhanced biofilm production, *RHR2* gene is downregulated probably denoting the lack of Ndt80 regulation as an activator.

The virulence-related phenotypes exhibited by *ndt80ΔΔ* mutant led us to explore its interaction with immune system cells. The ability to switch from yeast to a filamentous form is a key factor that allows successful phagocytosis evasion of *C. albicans* (201). In the case of *C. parapsilosis*, several studies have elucidated distinct virulence traits of this species that could modulate the mechanism by which phagocytosis and the immune response proceed (202-204). We found, in our *in vitro* infection assays a prompter interaction of both mutants with the macrophage cells in comparison to the wild-type strain. This finding is also in accordance with results obtained with the adhesion assays to abiotic surfaces and to other yeast cells.

Toth *et al*. (193) using other host cell models (J774.1 murine macrophage cell line and human peripheral blood mononuclear cells) described that the length of *C. parapsilosis* pseudohyphae did not correlate with the engulfment time. In our assays, after 3 h of coculturing, only the *ndt80ΔΔ* mutant induced a significantly increase of macrophage killing with concomitant higher yeast viability, while neither the wildtype nor the *ndt80Δ* mutant promoted significant damage of the macrophage cells. These results show that the phenotype prompted by *NDT80* knockout results in a more virulent *C. parapsilosis* strains, more resistant to macrophage attack, associated with a decrease of macrophage cytoplasmic membrane integrity and a concomitant increase of macrophage cell death. Virulence attributes are not exclusively related to the constitutive pseudohyphal form; notably, the promoted expression of *ALS7* and *MKC1* transcripts (factors essential to cell wall integrity and remodeling) (48, 205) provides a strong evidence of alterations of cell wall concerning composition and architecture in the *ndt80ΔΔ* mutant, with impact upon adhesion and recognition by immune system cells (206).

In fungi, *NDT80*-like genes recognize the conserved DNA-binding domain motif, MSE, through an Ig fold. As other members of the Ig-fold family of transcription factors, such as p53 or NFAR from mammals, *NDT80*-like genes share a similar regulation mechanism (207). However, the number and attributable functions of *NDT80*-like genes are divergent among fungal species and even within species (191). These disparities range from *NDT80* absence, as seen in *Schizosaccharomyces pombe*, to a family of six members, as seen in *Fusarium oxysporum*. While in *Saccharomyces cerevisiae, NDT80* single gene functions as a master regulator of meiosis process and sporulation (208), in other fungal species possessing several paralogous of *NDT80*-like genes the unraveling of its function and regulation mechanism is laborious and far from being obtained. NdtA and XprG are two of the Ndt80-like proteins in the filamentous fungal species *Aspergillus nidulans*. The former has a high homology with Ndt80 and like in *S. cerevisiae*, it is crucial for sexual reproduction. The later, under carbon starvation, regulates positively fungal response by controlling its extracellular proteases, mycotoxin, and penicillin expression, which could result in autolysis, hyphal fragmentation and ultimately in cell death (209). *Neurospora crassa* possesses three Ndt80-like proteins, Vib-1, Ncu04729 and Fsd-1. Vib1, closely related to XprG, is an activator of extracellular protease production and is also associated with apoptosis (210); Fsd1 (more similar to NdtA) together with Vib-1, is involved in the female sexual structure formation, but no one is required for meiosis. So far, NCU04729 gene deletion has no effect upon phenotype, which impairs the understanding of its function. In the CTG clade, *C. albicans* has three *NDT80*-like DNA-binding domain genes, *NDT80, RON1* and *REP1* (211). These Ndt80-like transcription factors seem to be functionally independent from each other. Rep1 was found to be a regulator of the drug efflux pump *MDR1* and is required for yeast growth on

presence of N-acetylglucosamine (GlcNAc) and galactose. Ron1 is associated with GlcNAc regulation signaling.

Conclusions

Chapter I

***Candida parapsilosis* species complex antifungal susceptibility profile and resistance characterization**

- *C. parapsilosis* remains the main etiologic agent among the *psilosis* complex. However, a decreasing trend in *C. parapsilosis* and *C. orthopsilosis*, in favor of higher values of prevalence of *C. metapsilosis* was observed, comparatively to last studies conducted at FMUP lab.

- Although susceptible/WT profiles to azoles remain the most prevalent phenotypes, our results demonstrate an increase of azole resistance/non-WT within the *psilosis* complex, in accordance with an emergent antifungal resistance problem described worldwide.

- Mdr1p efflux pumps are the major mechanism activated in *C. parapsilosis* FLC resistant strains. Cdr1 efflux pumps and *ERG11* gene also were involved in FLC resistance. Several mutations were identified in these genes and in its respective regulators, with a putative function.

- This study provides relevant data, regarding *C. parapsilosis* antifungal susceptibility profile and resistance mechanisms, resulting in a better understanding of its behavior, which may help the clinicians to adapt the therapeutic approach when confronted with infections by such pathogen.

Chapter II

***Candida parapsilosis* clinical azole cross-resistance**

- This is the first study to characterize an *in vivo* acquisition of resistance during a prolonged FLC treatment of a patient infected by *C. parapsilosis*.

- The continuous exposure to FLC resulted in either increased copy number of the *CDR1B* gene or in a GOF (G604R amino acid substitution) mutation in *MRR1* gene. Ultimately, both mechanisms result in increased expression of *CDR1B*. In addition, the GOF mutation in *MRR1* also results in up-regulation of *MDR1*.

- Our results strongly suggest that *MRR1* regulates the expression of *CDR1B* and that

expression of *CDR1B* independently of *MDR1* negatively impairs the susceptibility to azoles*.*

Chapter III

Impact of Ndt80 in *Candida parapsilosis* virulence

- The disruption of *C. parapsilosis NDT80* gene triggers a substantial spontaneous and constitutive colony and cell morphologies changes.

- Morphogenetic alterations prompted adhesion in mutants, both cell to cell and to abiotic surfaces, as also to murine macrophages. Likewise, enhanced capacity to form biofilm was observed in the *C. parapsilosis* mutants*,* lacking one or both copies of *NDT80* gene.

- Interestingly, we identified several transcription factors like, Ume6, Cph2, Cwh41, Ace2, Bcr1, protein kinase Mkc1 and adhesin Als7 to be under Ndt80 negative regulation, partially explaining the phenotypes displayed by the *ndt80ΔΔ* mutant.

- Furthermore, *ndt80ΔΔ* pseudohyphae form mutant induced a significant killing of the macrophage cells, becoming deleterious to such cells after phagocytosis.

- Unexpectedly, our findings provide the first evidence for a direct role of Ndt80 as a repressor of *C. parapsilosis* virulence attributes, diverging from its homolog in the close related fungal pathogen *C. albicans*.

Future Perspectives

Antifungal resistance is an emergent public health global concern, making the study of new putative targets an area of high medical interest. The exploration of the complex network of antifungal stress response in *C. parapsilosis,* and other fungal pathogens, will certainly help in the development of additional fungal-selective molecules, that could disrupt these pathways.

The future research will involve studies uncovering the role of point mutations in the azole associated genes in *C. parapsilosis*, using the gene editing toll, CRISPR/Cas. Due to time limitations, we could not confirm the involvement of these mutations in azole resistance, since the percentage of positive mutants using the *SAT1* flipper methodology is very low and time consumable. Also, the expression of *CDR1B* gene, the new target of *MRR1* GOF mutation, should be evaluated in fluconazole resistant strains of our collection.

The molecular mechanisms involved in *C. parapsilosis* PSC non-WT phenotype usually involve the ergosterol biosynthetic pathway adaptation, accordingly, we consider important to study the strains with such phenotype among our collection. The molecular study of the two non-WT strains of *C. orthopsilosis* and *C. metapsilosis* would be also a great opportunity to unveil the mechanisms involved in such phenotypes.

References

1.   Bongomin F, Gago S, Oladele RO, Denning DW. 2017. Global and Multi-National Prevalence of Fungal Diseases-Estimate Precision. J Fungi (Basel) 3.
2.   Strollo S, Lionakis MS, Adjemian J, Steiner CA, Prevots DR. 2016. Epidemiology of Hospitalizations Associated with Invasive Candidiasis, United States, 2002-2012(1). Emerg Infect Dis 23:7-13.
3.   Pappas PG, Lionakis MS, Arendrup MC, Ostrosky-Zeichner L, Kullberg BJ. 2018. Invasive candidiasis. Nat Rev Dis Primers 4:18026.
4.   McCarty TP, White CM, Pappas PG. 2021. Candidemia and Invasive Candidiasis. Infect Dis Clin North Am 35:389-413.
5.   Guinea J. 2014. Global trends in the distribution of Candida species causing candidemia. Clin Microbiol Infect 20 Suppl 6:5-10.
6.   Koehler P, Stecher M, Cornely OA, Koehler D, Vehreschild M, Bohlius J, Wisplinghoff H, Vehreschild JJ. 2019. Morbidity and mortality of candidaemia in Europe: an epidemiologic meta-analysis. Clin Microbiol Infect 25:1200-1212.
7.   Ashford BK. 1928. Certain conditions of the gastrointestinal tract in Puerto Rico and their relation to tropical sprue. American Journal of Tropical Medicine and Hygiene 8:507-538.
8.   Tavanti A, Davidson AD, Gow NA, Maiden MC, Odds FC. 2005. Candida orthopsilosis and Candida metapsilosis spp. nov. to replace Candida parapsilosis groups II and III. J Clin Microbiol 43:284-92.
9.   van Asbeck EC, Clemons KV, Stevens DA. 2009. Candida parapsilosis: a review of its epidemiology, pathogenesis, clinical aspects, typing and antimicrobial susceptibility. Crit Rev Microbiol 35:283-309.
10.   Bonassoli LA, Bertoli M, Svidzinski TI. 2005. High frequency of Candida parapsilosis on the hands of healthy hosts. J Hosp Infect 59:159-62.
11.   van Asbeck EC, Huang YC, Markham AN, Clemons KV, Stevens DA. 2007. Candida parapsilosis fungemia in neonates: genotyping results suggest healthcare workers hands as source, and review of published studies. Mycopathologia 164:287-93.
12.   Levin AS, Costa SF, Mussi NS, Basso M, Sinto SI, Machado C, Geiger DC, Villares MC, Schreiber AZ, Barone AA, Branchini ML. 1998. Candida parapsilosis fungemia associated with implantable and semi-implantable central venous catheters and the hands of healthcare workers. Diagn Microbiol Infect Dis 30:243-9.
13.   Trofa D, Gacser A, Nosanchuk JD. 2008. Candida parapsilosis, an emerging fungal pathogen. Clin Microbiol Rev 21:606-25.
14.   Ramage G, Martinez JP, Lopez-Ribot JL. 2006. Candida biofilms on implanted biomaterials: a clinically significant problem. FEMS Yeast Res 6:979-86.
15.   Nemeth T, Toth A, Szenzenstein J, Horvath P, Nosanchuk JD, Grozer Z, Toth R, Papp C, Hamari Z, Vagvolgyi C, Gacser A. 2013. Characterization of virulence properties in the C. parapsilosis sensu lato species. PLoS One 8:e68704.
16.   Cuellar-Cruz M, Lopez-Romero E, Villagomez-Castro JC, Ruiz-Baca E. 2012. Candida species: new insights into biofilm formation. Future Microbiology 7:755-771.
17.   Pammi M, Holland L, Butler G, Gacser A, Bliss JM. 2013. Candida parapsilosis is a Significant Neonatal Pathogen: A Systematic Review and Meta-Analysis. The Pediatric infectious disease journal 32:e206-e216.
18.   Nucci M, Queiroz-Telles F, Alvarado-Matute T, Tiraboschi IN, Cortes J, Zurita J, Guzman-Blanco M, Santolaya ME, Thompson L, Sifuentes-Osornio J, Echevarria JI, Colombo AL, on behalf of the Latin American Invasive Mycosis N. 2013. Epidemiology of Candidemia in Latin America: A Laboratory-Based Survey. PLoS ONE 8:e59373.
19.   Rodriguez L, Bustamante B, Huaroto L, Agurto C, Illescas R, Ramirez R, Diaz A, Hidalgo J. 2017. A multi-centric Study of Candida bloodstream infection in Lima-Callao, Peru: Species distribution, antifungal resistance and clinical outcomes. PLoS One 12:e0175172.

20.   Faria-Ramos I, Neves-Maia J, Ricardo E, Santos-Antunes J, Silva AT, Costa-de-Oliveira S, Canton E, Rodrigues AG, Pina-Vaz C. 2014. Species distribution and in vitro antifungal susceptibility profiles of yeast isolates from invasive infections during a Portuguese multicenter survey. Eur J Clin Microbiol Infect Dis 33:2241-7.

21.   Guinea J, Zaragoza Ó, Escribano P, Martín-Mazuelos E, Pemán J, Sánchez-Reus F, Cuenca-Estrella M. 2014. Molecular Identification and Antifungal Susceptibility of Yeast Isolates Causing Fungemia Collected in a Population-Based Study in Spain in 2010 and 2011. Antimicrobial Agents and Chemotherapy 58:1529-1537.

22.   Tedeschi S, Tumietto F, Giannella M, Bartoletti M, Cristini F, Cioni G, Ambretti S, Carretto E, Sambri V, Sarti M, Viale P, Emilia Romagna Candida N. 2016. Epidemiology and outcome of candidemia in internal medicine wards: A regional study in Italy. Eur J Intern Med 34:39-44.

23.   Vogiatzi L, Ilia S, Sideri G, Vagelakoudi E, Vassilopoulou M, Sdougka M, Briassoulis G, Papadatos I, Kalabalikis P, Sianidou L, Roilides E. 2013. Invasive candidiasis in pediatric intensive care in Greece: a nationwide study. Intensive Care Med 39:2188-95.

24.   Arendrup MC, Bruun B, Christensen JJ, Fuursted K, Johansen HK, Kjældgaard P, Knudsen JD, Kristensen L, Møller J, Nielsen L, Rosenvinge FS, Røder B, Schønheyder HC, Thomsen MK, Truberg K. 2011. National Surveillance of Fungemia in Denmark (2004 to 2009). Journal of Clinical Microbiology 49:325-334.

25.   Ericsson J, Chryssanthou E, Klingspor L, Johansson AG, Ljungman P, Svensson E, Sjolin J. 2013. Candidaemia in Sweden: a nationwide prospective observational survey. Clin Microbiol Infect 19:E218-21.

26.   Chalmers C, Gaur S, Chew J, Wright T, Kumar A, Mathur S, Wan WY, Gould IM, Leanord A, Bal AM. 2011. Epidemiology and management of candidaemia--a retrospective, multicentre study in five hospitals in the UK. Mycoses 54:e795-800.

27.   Toda M, Williams SR, Berkow EL, Farley MM, Harrison LH, Bonner L, Marceaux KM, Hollick R, Zhang AY, Schaffner W, Lockhart SR, Jackson BR, Vallabhaneni S. 2019. Population-Based Active Surveillance for Culture-Confirmed Candidemia - Four Sites, United States, 2012-2016. MMWR Surveill Summ 68:1-15.

28.   Ting JY, Roberts A, Synnes A, Canning R, Bodani J, Monterossa L, Shah PS, Canadian Neonatal Network I. 2018. Invasive Fungal Infections in Neonates in Canada: Epidemiology and Outcomes. Pediatr Infect Dis J 37:1154-1159.

29.   Tsay SV, Mu Y, Williams S, Epson E, Nadle J, Bamberg WM, Barter DM, Johnston HL, Farley MM, Harb S, Thomas S, Bonner LA, Harrison LH, Hollick R, Marceaux K, Mody RK, Pattee B, Shrum Davis S, Phipps EC, Tesini BL, Gellert AB, Zhang AY, Schaffner W, Hillis S, Ndi D, Graber CR, Jackson BR, Chiller T, Magill S, Vallabhaneni S. 2020. Burden of Candidemia in the United States, 2017. Clin Infect Dis 71:e449-e453.

30.   Pfaller MA, Diekema DJ, Turnidge JD, Castanheira M, Jones RN. 2019. Twenty Years of the SENTRY Antifungal Surveillance Program: Results for Candida Species From 1997-2016. Open Forum Infect Dis 6:S79-S94.

31.   Kakeya H, Yamada K, Kaneko Y, Yanagihara K, Tateda K, Maesaki S, Takesue Y, Tomono K, Kadota JI, Kaku M, Miyazaki Y, Kamei K, Shibuya K, Niki Y, Yoshida M, Sei Y. 2018. [National Trends in the Distribution of Candida Species Causing Candidemia in Japan from 2003 to 2014]. Med Mycol J 59:E19-E22.

32.   Xiao M, Chen SC, Kong F, Xu XL, Yan L, Kong HS, Fan X, Hou X, Cheng JW, Zhou ML, Li Y, Yu SY, Huang JJ, Zhang G, Yang Y, Zhang JJ, Duan SM, Kang W, Wang H, Xu YC. 2020. Distribution and Antifungal Susceptibility of Candida Species Causing Candidemia in China: An Update From the CHIF-NET Study. J Infect Dis 221:S139-S147.

33.   Rajni E, Chaudhary P, Garg VK, Sharma R, Malik M. 2022. A complete clinico-epidemiological and microbiological profile of candidemia cases in a tertiary-care hospital in Western India. Antimicrob Steward Healthc Epidemiol 2:e37.

34. Chapman B, Slavin M, Marriott D, Halliday C, Kidd S, Arthur I, Bak N, Heath CH, Kennedy K, Morrissey CO, Sorrell TC, van Hal S, Keighley C, Goeman E, Underwood N, Hajkowicz K, Hofmeyr A, Leung M, Macesic N, Botes J, Blyth C, Cooley L, George CR, Kalukottege P, Kesson A, McMullan B, Baird R, Robson J, Korman TM, Pendle S, Weeks K, Liu E, Cheong E, Chen S, Australian, New Zealand Mycoses Interest G. 2017. Changing epidemiology of candidaemia in Australia. J Antimicrob Chemother 72:1103-1108.

35. Neji S, Hadrich I, Trabelsi H, Abbes S, Cheikhrouhou F, Sellami H, Makni F, Ayadi A. 2017. Virulence factors, antifungal susceptibility and molecular mechanisms of azole resistance among Candida parapsilosis complex isolates recovered from clinical specimens. J Biomed Sci 24:67.

36. Németh TM GA, Nosanchuk JD. 2018. Candida psilosis complex. *In* Elsevier SD, CA (ed), In Reference module in life sciences doi:10.1016/b978-0-12-809633-8.20709-7.

37. Skrzypek MS, Binkley J, Binkley G, Miyasato SR, Simison M, Sherlock G. 2017. The Candida Genome Database (CGD): incorporation of Assembly 22, systematic identifiers and visualization of high throughput sequencing data. Nucleic Acids Res 45:D592-D596.

38. Butler G, Rasmussen MD, Lin MF, Santos MA, Sakthikumar S, Munro CA, Rheinbay E, Grabherr M, Forche A, Reedy JL, Agrafioti I, Arnaud MB, Bates S, Brown AJ, Brunke S, Costanzo MC, Fitzpatrick DA, de Groot PW, Harris D, Hoyer LL, Hube B, Klis FM, Kodira C, Lennard N, Logue ME, Martin R, Neiman AM, Nikolaou E, Quail MA, Quinn J, Santos MC, Schmitzberger FF, Sherlock G, Shah P, Silverstein KA, Skrzypek MS, Soll D, Staggs R, Stansfield I, Stumpf MP, Sudbery PE, Srikantha T, Zeng Q, Berman J, Berriman M, Heitman J, Gow NA, Lorenz MC, Birren BW, Kellis M, et al. 2009. Evolution of pathogenicity and sexual reproduction in eight Candida genomes. Nature 459:657-62.

39. Laffey SF, Butler G. 2005. Phenotype switching affects biofilm formation by Candida parapsilosis. Microbiology (Reading) 151:1073-1081.

40. Cavalheiro M, Teixeira MC. 2018. Candida Biofilms: Threats, Challenges, and Promising Strategies. Front Med (Lausanne) 5:28.

41. Silva-Dias A, Miranda IM, Branco J, Monteiro-Soares M, Pina-Vaz C, Rodrigues AG. 2015. Adhesion, biofilm formation, cell surface hydrophobicity, and antifungal planktonic susceptibility: relationship among Candida spp. Frontiers in Microbiology 6.

42. Silva S, Negri M, Henriques M, Oliveira R, Williams DW, Azeredo J. 2011. Adherence and biofilm formation of non-Candida albicans Candida species. Trends Microbiol 19:241-7.

43. Chandra J, Patel JD, Li J, Zhou G, Mukherjee PK, McCormick TS, Anderson JM, Ghannoum MA. 2005. Modification of surface properties of biomaterials influences the ability of Candida albicans to form biofilms. Appl Environ Microbiol 71:8795-801.

44. de Groot PW, Bader O, de Boer AD, Weig M, Chauhan N. 2013. Adhesins in human fungal pathogens: glue with plenty of stick. Eukaryot Cell 12:470-81.

45. Modrzewska B, Kurnatowski P. 2015. Adherence of Candida sp. to host tissues and cells as one of its pathogenicity features. Ann Parasitol 61:3-9.

46. Nobile CJ, Andes DR, Nett JE, Smith FJ, Yue F, Phan QT, Edwards JE, Filler SG, Mitchell AP. 2006. Critical role of Bcr1-dependent adhesins in C. albicans biofilm formation in vitro and in vivo. PLoS Pathog 2:e63.

47. Bertini A, Zoppo M, Lombardi L, Rizzato C, De Carolis E, Vella A, Torelli R, Sanguinetti M, Tavanti A. 2016. Targeted gene disruption in Candida parapsilosis demonstrates a role for CPAR2_404800 in adhesion to a biotic surface and in a murine model of ascending urinary tract infection. Virulence 7:85-97.

48. Neale MN, Glass KA, Longley SJ, Kim DJ, Laforce-Nesbitt SS, Wortzel JD, Shaw SK, Bliss JM. 2018. Role of the Inducible Adhesin CpAls7 in Binding of Candida parapsilosis to the Extracellular Matrix under Fluid Shear. Infect Immun 86.

49. Czechowicz P, Nowicka J, Gosciniak G. 2022. Virulence Factors of Candida spp. and Host Immune Response Important in the Pathogenesis of Vulvovaginal Candidiasis. Int J Mol Sci 23.

50. Ruchel R, Boning B, Borg M. 1986. Characterization of a secretory proteinase of Candida parapsilosis and evidence for the absence of the enzyme during infection in vitro. Infect Immun 53:411-9.

51. Toth R, Nosek J, Mora-Montes HM, Gabaldon T, Bliss JM, Nosanchuk JD, Turner SA, Butler G, Vagvolgyi C, Gacser A. 2019. Candida parapsilosis: from Genes to the Bedside. Clin Microbiol Rev 32.

52. Dagdeviren M, Cerikcioglu N, Karavus M. 2005. Acid proteinase, phospholipase and adherence properties of Candida parapsilosis strains isolated from clinical specimens of hospitalised patients. Mycoses 48:321-6.

53. Tosun I, Akyuz Z, Guler NC, Gulmez D, Bayramoglu G, Kaklikkaya N, Arikan-Akdagli S, Aydin F. 2013. Distribution, virulence attributes and antifungal susceptibility patterns of Candida parapsilosis complex strains isolated from clinical samples. Med Mycol 51:483-92.

54. Gacser A, Trofa D, Schafer W, Nosanchuk JD. 2007. Targeted gene deletion in Candida parapsilosis demonstrates the role of secreted lipase in virulence. J Clin Invest 117:3049-58.

55. Trofa D, Agovino M, Stehr F, Schafer W, Rykunov D, Fiser A, Hamari Z, Nosanchuk JD, Gacser A. 2009. Acetylsalicylic acid (aspirin) reduces damage to reconstituted human tissues infected with Candida species by inhibiting extracellular fungal lipases. Microbes Infect 11:1131-9.

56. Ghannoum MA. 2000. Potential role of phospholipases in virulence and fungal pathogenesis. Clin Microbiol Rev 13:122-43, table of contents.

57. Mukherjee PK, Chandra J. 2004. Candida biofilm resistance. Drug Resist Updat 7:301-9.

58. Chandra J, Mukherjee PK. 2015. Candida Biofilms: Development, Architecture, and Resistance. Microbiol Spectr 3.

59. Douglas LJ. 2003. Candida biofilms and their role in infection. Trends Microbiol 11:30-6.

60. Estivill D, Arias A, Torres-Lana A, Carrillo-Munoz AJ, Arevalo MP. 2011. Biofilm formation by five species of Candida on three clinical materials. J Microbiol Methods 86:238-42.

61. Shin JH, Kee SJ, Shin MG, Kim SH, Shin DH, Lee SK, Suh SP, Ryang DW. 2002. Biofilm production by isolates of Candida species recovered from nonneutropenic patients: comparison of bloodstream isolates with isolates from other sources. J Clin Microbiol 40:1244-8.

62. Branchini ML, Pfaller MA, Rhine-Chalberg J, Frempong T, Isenberg HD. 1994. Genotypic variation and slime production among blood and catheter isolates of Candida parapsilosis. J Clin Microbiol 32:452-6.

63. Silva S, Henriques M, Martins A, Oliveira R, Williams D, Azeredo J. 2009. Biofilms of non-Candida albicans Candida species: quantification, structure and matrix composition. Med Mycol 47:681-9.

64. Kuhn DM, Chandra J, Mukherjee PK, Ghannoum MA. 2002. Comparison of biofilms formed by Candida albicans and Candida parapsilosis on bioprosthetic surfaces. Infect Immun 70:878-88.

65. Mitchell KF, Zarnowski R, Sanchez H, Edward JA, Reinicke EL, Nett JE, Mitchell AP, Andes DR. 2015. Community participation in biofilm matrix assembly and function. Proc Natl Acad Sci U S A 112:4092-7.

66. Silva S, Rodrigues CF, Araujo D, Rodrigues ME, Henriques M. 2017. Candida Species Biofilms' Antifungal Resistance. J Fungi (Basel) 3.

67. Uppuluri P, Chaturvedi AK, Srinivasan A, Banerjee M, Ramasubramaniam AK, Kohler JR, Kadosh D, Lopez-Ribot JL. 2010. Dispersion as an important step in the Candida albicans biofilm developmental cycle. PLoS Pathog 6:e1000828.

68. Holland LM, Schroder MS, Turner SA, Taff H, Andes D, Grozer Z, Gacser A, Ames L, Haynes K, Higgins DG, Butler G. 2014. Comparative phenotypic analysis of the major fungal pathogens Candida parapsilosis and Candida albicans. PLoS Pathog 10:e1004365.

69. Nobile CJ, Fox EP, Nett JE, Sorrells TR, Mitrovich QM, Hernday AD, Tuch BB, Andes DR, Johnson AD. 2012. A recently evolved transcriptional network controls biofilm development in Candida albicans. Cell 148:126-38.

70. Ding C, Vidanes GM, Maguire SL, Guida A, Synnott JM, Andes DR, Butler G. 2011. Conserved and divergent roles of Bcr1 and CFEM proteins in Candida parapsilosis and Candida albicans. PLoS One 6:e28151.

71. Denning DW, Hope WW. Therapy for fungal diseases: opportunities and priorities. Trends in Microbiology 18:195-204.

72. Ben-Ami R, Kontoyiannis DP. 2021. Resistance to Antifungal Drugs. Infect Dis Clin North Am 35:279-311.

73. Carolus H, Pierson S, Lagrou K, Van Dijck P. 2020. Amphotericin B and Other Polyenes-Discovery, Clinical Use, Mode of Action and Drug Resistance. J Fungi (Basel) 6.

74. Fanos V, Cataldi L. 2000. Amphotericin B-induced nephrotoxicity: a review. J Chemother 12:463-70.

75. Groll AH, Rijnders BJA, Walsh TJ, Adler-Moore J, Lewis RE, Bruggemann RJM. 2019. Clinical Pharmacokinetics, Pharmacodynamics, Safety and Efficacy of Liposomal Amphotericin B. Clin Infect Dis 68:S260-S274.

76. Lockhart SR, Iqbal N, Cleveland AA, Farley MM, Harrison LH, Bolden CB, Baughman W, Stein B, Hollick R, Park BJ, Chiller T. 2012. Species identification and antifungal susceptibility testing of Candida bloodstream isolates from population-based surveillance studies in two U.S. cities from 2008 to 2011. J Clin Microbiol 50:3435-42.

77. Yamin D, Akanmu MH, Al Mutair A, Alhumaid S, Rabaan AA, Hajissa K. 2022. Global Prevalence of Antifungal-Resistant Candida parapsilosis: A Systematic Review and Meta-Analysis. Trop Med Infect Dis 7.

78. Chowdhary A, Prakash A, Sharma C, Kordalewska M, Kumar A, Sarma S, Tarai B, Singh A, Upadhyaya G, Upadhyay S, Yadav P, Singh PK, Khillan V, Sachdeva N, Perlin DS, Meis JF. 2018. A multicentre study of antifungal susceptibility patterns among 350 Candida auris isolates (2009-17) in India: role of the ERG11 and FKS1 genes in azole and echinocandin resistance. J Antimicrob Chemother 73:891-899.

79. Martel CM, Parker JE, Bader O, Weig M, Gross U, Warrilow AG, Kelly DE, Kelly SL. 2010. A clinical isolate of Candida albicans with mutations in ERG11 (encoding sterol 14alpha-demethylase) and ERG5 (encoding C22 desaturase) is cross resistant to azoles and amphotericin B. Antimicrob Agents Chemother 54:3578-83.

80. Young LY, Hull CM, Heitman J. 2003. Disruption of ergosterol biosynthesis confers resistance to amphotericin B in Candida lusitaniae. Antimicrob Agents Chemother 47:2717-24.

81. Perlin DS. 2015. Echinocandin Resistance in Candida. Clin Infect Dis 61 Suppl 6:S612-7.

82. Sokol-Anderson M, Sligh JE, Jr., Elberg S, Brajtburg J, Kobayashi GS, Medoff G. 1988. Role of cell defense against oxidative damage in the resistance of Candida albicans to the killing effect of amphotericin B. Antimicrob Agents Chemother 32:702-5.

83. Kristanc L, Bozic B, Jokhadar SZ, Dolenc MS, Gomiscek G. 2019. The pore-forming action of polyenes: From model membranes to living organisms. Biochim Biophys Acta Biomembr 1861:418-430.

84. Cowen LE, Lindquist S. 2005. Hsp90 potentiates the rapid evolution of new traits: drug resistance in diverse fungi. Science 309:2185-9.

85. Denning DW. Echinocandin antifungal drugs. The Lancet 362:1142-1151.

86. Pappas PG, Kauffman CA, Andes DR, Clancy CJ, Marr KA, Ostrosky-Zeichner L, Reboli AC, Schuster MG, Vazquez JA, Walsh TJ, Zaoutis TE, Sobel JD. 2016. Clinical Practice Guideline for the Management of Candidiasis: 2016 Update by the Infectious Diseases Society of America. Clin Infect Dis 62:e1-50.

87. Chen SA, Slavin M, Sorrell T. 2011. Echinocandin Antifungal Drugs in Fungal Infections. Drugs 71:11-41.

88. Beyda ND, Lewis RE, Garey KW. 2012. Echinocandin Resistance in Candida Species: Mechanisms of Reduced Susceptibility and Therapeutic Approaches. Annals of Pharmacotherapy 46:1086-1096.

89. Pfaller MA, Diekema DJ, Andes D, Arendrup MC, Brown SD, Lockhart SR, Motyl M, Perlin DS. Clinical breakpoints for the echinocandins and Candida revisited: Integration of molecular, clinical, and microbiological data to arrive at species-specific interpretive criteria. Drug Resistance Updates 14:164-176.

90. Douglas CM, D'Ippolito JA, Shei GJ, Meinz M, Onishi J, Marrinan JA, Li W, Abruzzo GK, Flattery A, Bartizal K, Mitchell A, Kurtz MB. 1997. Identification of the FKS1 gene of Candida albicans as the essential target of 1,3-beta-D-glucan synthase inhibitors. Antimicrobial Agents and Chemotherapy 41:2471-9.

91. Bachmann SP, VandeWalle K, Ramage G, Patterson TF, Wickes BL, Graybill JR, López-Ribot JL. 2002. In Vitro Activity of Caspofungin against Candida albicans Biofilms. Antimicrobial Agents and Chemotherapy 46:3591-3596.

92. Perlin DS. 2011. Current perspectives on echinocandin class drugs. Future Microbiology 6:441-457.

93. Ostrosky-Zeichner L, Rex JH, Pappas PG, Hamill RJ, Larsen RA, Horowitz HW, Powderly WG, Hyslop N, Kauffman CA, Cleary J, Mangino JE, Lee J. 2003. Antifungal Susceptibility Survey of 2,000 Bloodstream Candida Isolates in the United States. Antimicrobial Agents and Chemotherapy 47:3149-3154.

94. Perlin DS. Resistance to echinocandin-class antifungal drugs. Drug Resistance Updates 10:121-130.

95. Garcia-Effron G, Canton E, Pemán J, Dilger A, Romá E, Perlin DS. 2012. Epidemiology and echinocandin susceptibility of Candida parapsilosis sensu lato species isolated from bloodstream infections at a Spanish university hospital. Journal of Antimicrobial Chemotherapy 67:2739-2748.

96. Siopi M, Papadopoulos A, Spiliopoulou A, Paliogianni F, Abou-Chakra N, Arendrup MC, Damoulari C, Tsioulos G, Giannitsioti E, Frantzeskaki F, Tsangaris I, Pournaras S, Meletiadis J. 2022. Pan-Echinocandin Resistant C. parapsilosis Harboring an F652S Fks1 Alteration in a Patient with Prolonged Echinocandin Therapy. J Fungi (Basel) 8.

97. Ning Y, Xiao M, Perlin DS, Zhao Y, Lu M, Li Y, Luo Z, Dai R, Li S, Xu J, Liu L, He H, Liu Y, Li F, Guo Y, Chen Z, Xu Y, Sun T, Zhang L. 2023. Decreased echinocandin susceptibility in Candida parapsilosis causing candidemia and emergence of a pan-echinocandin resistant case in China. Emerg Microbes Infect 12:2153086.

98. Singh SD, Robbins N, Zaas AK, Schell WA, Perfect JR, Cowen LE. 2009. Hsp90 governs echinocandin resistance in the pathogenic yeast Candida albicans via calcineurin. PLoS Pathog 5:e1000532.

99. Munro CA, Selvaggini S, de Bruijn I, Walker L, Lenardon MD, Gerssen B, Milne S, Brown AJ, Gow NA. 2007. The PKC, HOG and Ca2+ signalling pathways co-ordinately regulate chitin synthesis in Candida albicans. Mol Microbiol 63:1399-413.

100. Lee KK, Maccallum DM, Jacobsen MD, Walker LA, Odds FC, Gow NA, Munro CA. 2012. Elevated cell wall chitin in Candida albicans confers echinocandin resistance in vivo. Antimicrob Agents Chemother 56:208-17.

101. Park S, Kelly R, Kahn JN, Robles J, Hsu M-J, Register E, Li W, Vyas V, Fan H, Abruzzo G, Flattery A, Gill C, Chrebet G, Parent SA, Kurtz M, Teppler H, Douglas CM, Perlin DS. 2005. Specific Substitutions in the Echinocandin Target Fks1p Account for Reduced Susceptibility of Rare Laboratory and Clinical Candida sp. Isolates. Antimicrobial Agents and Chemotherapy 49:3264-3273.

102. Katiyar S, Pfaller M, Edlind T. 2006. Candida albicans and Candida glabrata Clinical Isolates Exhibiting Reduced Echinocandin Susceptibility. Antimicrobial Agents and Chemotherapy 50:2892-2894.

103.   Garcia-Effron G, Kontoyiannis DP, Lewis RE, Perlin DS. 2008. Caspofungin-Resistant Candida tropicalis Strains Causing Breakthrough Fungemia in Patients at High Risk for Hematologic Malignancies. Antimicrobial Agents and Chemotherapy 52:4181-4183.

104.   Pfaller MA, Messer SA, Woosley LN, Jones RN, Castanheira M. 2013. Echinocandin and Triazole Antifungal Susceptibility Profiles for Clinical Opportunistic Yeast and Mold Isolates Collected from 2010 to 2011: Application of New CLSI Clinical Breakpoints and Epidemiological Cutoff Values for Characterization of Geographic and Temporal Trends of Antifungal Resistance. Journal of Clinical Microbiology 51:2571-2581.

105.   Garcia-Effron G, Katiyar SK, Park S, Edlind TD, Perlin DS. 2008. A Naturally Occurring Proline-to-Alanine Amino Acid Change in Fks1p in Candida parapsilosis, Candida orthopsilosis, and Candida metapsilosis Accounts for Reduced Echinocandin Susceptibility. Antimicrobial Agents and Chemotherapy 52:2305-2312.

106.   Robbins N, Caplan T, Cowen LE. 2017. Molecular Evolution of Antifungal Drug Resistance. Annu Rev Microbiol 71:753-775.

107.   Odds FC, Brown AJP, Gow NAR. Antifungal agents: mechanisms of action. Trends in Microbiology 11:272-279.

108.   Cowen LE, Sanglard D, Howard SJ, Rogers PD, Perlin DS. 2014. Mechanisms of Antifungal Drug Resistance. Cold Spring Harbor Perspectives in Medicine doi:10.1101/cshperspect.a019752.

109.   Xiao L, Madison V, Chau AS, Loebenberg D, Palermo RE, McNicholas PM. 2004. Three-Dimensional Models of Wild-Type and Mutated Forms of Cytochrome P450 14α-Sterol Demethylases from Aspergillus fumigatus and Candida albicans Provide Insights into Posaconazole Binding. Antimicrobial Agents and Chemotherapy 48:568-574.

110.   Akins RA. 2005. An update on antifungal targets and mechanisms of resistance in Candida albicans. Medical Mycology 43:285-318.

111.   Xie JL, Polvi EJ, Shekhar-Guturja T, Cowen LE. 2014. Elucidating drug resistance in human fungal pathogens. Future Microbiology 9:523-542.

112.   Magobo RE, Lockhart SR, Govender NP. 2020. Fluconazole-resistant Candida parapsilosis strains with a Y132F substitution in the ERG11 gene causing invasive infections in a neonatal unit, South Africa. Mycoses 63:471-477.

113.   Branco J, Ryan AP, Silva AP, Butler G, Miranda IM, Rodrigues AG. 2022. Clinical azole cross-resistance in Candida parapsilosis is related to a novel MRR1 gain-of-function mutation. Clin Microbiol Infect doi:10.1016/j.cmi.2022.08.014.

114.   Martini C, Torelli R, de Groot T, De Carolis E, Morandotti GA, De Angelis G, Posteraro B, Meis JF, Sanguinetti M. 2020. Prevalence and Clonal Distribution of Azole-Resistant Candida parapsilosis Isolates Causing Bloodstream Infections in a Large Italian Hospital. Front Cell Infect Microbiol 10:232.

115.   Fekkar A, Blaize M, Bougle A, Normand AC, Raoelina A, Kornblum D, Kamus L, Piarroux R, Imbert S. 2021. Hospital outbreak of fluconazole-resistant Candida parapsilosis: arguments for clonal transmission and long-term persistence. Antimicrob Agents Chemother doi:10.1128/AAC.02036-20.

116.   Sanglard D, Odds FC. Resistance of Candida species to antifungal agents: molecular mechanisms and clinical consequences. The Lancet Infectious Diseases 2:73-85.

117.   Pfaller MA. Antifungal Drug Resistance: Mechanisms, Epidemiology, and Consequences for Treatment. The American Journal of Medicine 125:S3-S13.

118.   Morio F, Pagniez F, Besse M, Gay-andrieu F, Miegeville M, Le Pape P. Deciphering azole resistance mechanisms with a focus on transcription factor-encoding genes TAC1, MRR1 and UPC2 in a set of fluconazole-resistant clinical isolates of Candida albicans. International Journal of Antimicrobial Agents 42:410-415.

119.   Morschhäuser J, Barker KS, Liu TT, Blaß-Warmuth J, Homayouni R, Rogers PD. 2007. The Transcription Factor Mrr1p Controls Expression of the *MDR1* Efflux

Pump and Mediates Multidrug Resistance in *Candida albicans*. PLoS Pathog 3:e164.

120. Dunkel N, Blaß J, Rogers PD, Morschhäuser J. 2008. Mutations in the multi-drug resistance regulator MRR1, followed by loss of heterozygosity, are the main cause of MDR1 overexpression in fluconazole-resistant Candida albicans strains. Molecular Microbiology 69:827-840.

121. Schubert S, Rogers PD, Morschhäuser J. 2008. Gain-of-Function Mutations in the Transcription Factor MRR1 Are Responsible for Overexpression of the MDR1 Efflux Pump in Fluconazole-Resistant Candida dubliniensis Strains. Antimicrobial Agents and Chemotherapy 52:4274-4280.

122. Branco J, Silva AP, Silva RM, Silva-Dias A, Pina-Vaz C, Butler G, Rodrigues AG, Miranda IM. 2015. Fluconazole and Voriconazole Resistance in Candida parapsilosis Is Conferred by Gain-of-Function Mutations in MRR1 Transcription Factor Gene. Antimicrob Agents Chemother 59:6629-33.

123. Papp C, Bohner F, Kocsis K, Varga M, Szekeres A, Bodai L, Willis JR, Gabaldon T, Toth R, Nosanchuk JD, Vagvolgyi C, Gacser A. 2020. Triazole Evolution of Candida parapsilosis Results in Cross-Resistance to Other Antifungal Drugs, Influences Stress Responses, and Alters Virulence in an Antifungal Drug-Dependent Manner. mSphere 5.

124. Coste AT, Karababa M, Ischer F, Bille J, Sanglard D. 2004. TAC1, transcriptional activator of CDR genes, is a new transcription factor involved in the regulation of Candida albicans ABC transporters CDR1 and CDR2. Eukaryot Cell 3:1639-52.

125. Berkow EL, Manigaba K, Parker JE, Barker KS, Kelly SL, Rogers PD. 2015. Multidrug Transporters and Alterations in Sterol Biosynthesis Contribute to Azole Antifungal Resistance in Candida parapsilosis. Antimicrob Agents Chemother 59:5942-50.

126. Silver PM, Oliver BG, White TC. 2004. Role of Candida albicans Transcription Factor Upc2p in Drug Resistance and Sterol Metabolism. Eukaryotic Cell 3:1391-1397.

127. Schubert S, Barker KS, Znaidi S, Schneider S, Dierolf F, Dunkel N, Aïd M, Boucher G, Rogers PD, Raymond M, Morschhäuser J. 2011. Regulation of Efflux Pump Expression and Drug Resistance by the Transcription Factors Mrr1, Upc2, and Cap1 in Candida albicans. Antimicrobial Agents and Chemotherapy 55:2212-2223.

128. Branco J, Ola M, Silva RM, Fonseca E, Gomes NC, Martins-Cruz C, Silva AP, Silva-Dias A, Pina-Vaz C, Erraught C, Brennan L, Rodrigues AG, Butler G, Miranda IM. 2017. Impact of ERG3 mutations and expression of ergosterol genes controlled by UPC2 and NDT80 in Candida parapsilosis azole resistance. Clin Microbiol Infect 23:575 e1-575 e8.

129. Heilmann CJ, Schneider S, Barker KS, Rogers PD, Morschhäuser J. 2010. An A643T Mutation in the Transcription Factor Upc2p Causes Constitutive ERG11 Upregulation and Increased Fluconazole Resistance in Candida albicans. Antimicrobial Agents and Chemotherapy 54:353-359.

130. Flowers SA, Barker KS, Berkow EL, Toner G, Chadwick SG, Gygax SE, Morschhäuser J, Rogers PD. 2012. Gain-of-Function Mutations in UPC2 Are a Frequent Cause of ERG11 Upregulation in Azole-Resistant Clinical Isolates of Candida albicans. Eukaryotic Cell 11:1289-1299.

131. Dunkel N, Liu TT, Barker KS, Homayouni R, Morschhäuser J, Rogers PD. 2008. A Gain-of-Function Mutation in the Transcription Factor Upc2p Causes Upregulation of Ergosterol Biosynthesis Genes and Increased Fluconazole Resistance in a Clinical Candida albicans Isolate. Eukaryotic Cell 7:1180-1190.

132. Sellam A, Tebbji F, Nantel A. 2009. Role of Ndt80p in Sterol Metabolism Regulation and Azole Resistance in Candida albicans. Eukaryotic Cell 8:1174-1183.

133. Chen C-G, Yang Y-L, Shih H-I, Su C-L, Lo H-J. 2004. CaNdt80 Is Involved in Drug Resistance in Candida albicans by Regulating CDR1. Antimicrobial Agents and Chemotherapy 48:4505-4512.

134. Pristov KE, Ghannoum MA. 2019. Resistance of Candida to azoles and echinocandins worldwide. Clin Microbiol Infect 25:792-798.

135. Morio F, Loge C, Besse B, Hennequin C, Le Pape P. 2010. Screening for amino acid substitutions in the Candida albicans Erg11 protein of azole-susceptible and azole-resistant clinical isolates: new substitutions and a review of the literature. Diagn Microbiol Infect Dis 66:373-84.

136. Vandeputte P, Larcher G, Berges T, Renier G, Chabasse D, Bouchara JP. 2005. Mechanisms of azole resistance in a clinical isolate of Candida tropicalis. Antimicrob Agents Chemother 49:4608-15.

137. Healey KR, Kordalewska M, Jimenez Ortigosa C, Singh A, Berrio I, Chowdhary A, Perlin DS. 2018. Limited ERG11 Mutations Identified in Isolates of Candida auris Directly Contribute to Reduced Azole Susceptibility. Antimicrob Agents Chemother 62.

138. Singh A, Singh PK, de Groot T, Kumar A, Mathur P, Tarai B, Sachdeva N, Upadhyaya G, Sarma S, Meis JF, Chowdhary A. 2019. Emergence of clonal fluconazole-resistant Candida parapsilosis clinical isolates in a multicentre laboratory-based surveillance study in India. J Antimicrob Chemother 74:1260-1268.

139. Arastehfar A, Daneshnia F, Hilmioglu-Polat S, Fang W, Yasar M, Polat F, Metin DY, Rigole P, Coenye T, Ilkit M, Pan W, Liao W, Hagen F, Kostrzewa M, Perlin DS, Lass-Florl C, Boekhout T. 2020. First Report of Candidemia Clonal Outbreak Caused by Emerging Fluconazole-Resistant Candida parapsilosis Isolates Harboring Y132F and/or Y132F+K143R in Turkey. Antimicrob Agents Chemother 64.

140. Costa-de-Oliveira S, Pina-Vaz C, Mendonca D, Goncalves Rodrigues A. 2008. A first Portuguese epidemiological survey of fungaemia in a university hospital. Eur J Clin Microbiol Infect Dis 27:365-74.

141. Silva AP, Miranda IM, Lisboa C, Pina-Vaz C, Rodrigues AG. 2009. Prevalence, distribution, and antifungal susceptibility profiles of Candida parapsilosis, C. orthopsilosis, and C. metapsilosis in a tertiary care hospital. J Clin Microbiol 47:2392-7.

142. CLSI. 2017. Reference Method for Broth Dilution Antifungal Susceptibility Testing of Yeasts, 4th ed. CLSI standard M27. Wayne, PA: Clinical Laboratory Standards Institute.

143. CLSI. 2020. Performance Standards for Antifungal Susceptibility Testing of Yeasts, 2nd ed. CLSI supplement M60. Wayne, PA: Clinical Laboratory Standards Institute.

144. CLSI. 2020. Epidemiological Cutoff Values for Antifungal Susceptibility Testing, 3rd ed. CLSI supplement M59. Wayne, PA: Clinical Laboratory Standards Institute.

145. Arastehfar A, Khodavaisy S, Daneshnia F, Najafzadeh MJ, Mahmoudi S, Charsizadeh A, Salehi MR, Zarrinfar H, Raeisabadi A, Dolatabadi S, Zare Shahrabadi Z, Zomorodian K, Pan W, Hagen F, Boekhout T. 2019. Molecular Identification, Genotypic Diversity, Antifungal Susceptibility, and Clinical Outcomes of Infections Caused by Clinically Underrated Yeasts, Candida orthopsilosis, and Candida metapsilosis: An Iranian Multicenter Study (2014-2019). Front Cell Infect Microbiol 9:264.

146. Canton E, Peman J, Quindos G, Eraso E, Miranda-Zapico I, Alvarez M, Merino P, Campos-Herrero I, Marco F, de la Pedrosa EG, Yague G, Guna R, Rubio C, Miranda C, Pazos C, Velasco D, Group FS. 2011. Prospective multicenter study of the epidemiology, molecular identification, and antifungal susceptibility of Candida parapsilosis, Candida orthopsilosis, and Candida metapsilosis isolated from patients with candidemia. Antimicrob Agents Chemother 55:5590-6.

147. Guo J, Zhang M, Qiao D, Shen H, Wang L, Wang D, Li L, Liu Y, Lu H, Wang C, Ding H, Zhou S, Zhou W, Wei Y, Zhang H, Xi W, Zheng Y, Wang Y, Tang R, Zeng L, Xu H, Wu W. 2021. Prevalence and Antifungal Susceptibility of Candida parapsilosis Species Complex in Eastern China: A 15-Year Retrospective Study by ECIFIG. Front Microbiol 12:644000.

148. Castanheira M, Deshpande LM, Messer SA, Rhomberg PR, Pfaller MA. 2020. Analysis of global antifungal surveillance results reveals predominance of Erg11 Y132F alteration

among azole-resistant Candida parapsilosis and Candida tropicalis and country-specific isolate dissemination. Int J Antimicrob Agents 55:105799.

149. Grossman NT, Pham CD, Cleveland AA, Lockhart SR. 2015. Molecular mechanisms of fluconazole resistance in Candida parapsilosis isolates from a U.S. surveillance system. Antimicrob Agents Chemother 59:1030-7.

150. Fisher JF. 2011. Candida urinary tract infections--epidemiology, pathogenesis, diagnosis, and treatment: executive summary. Clin Infect Dis 52 Suppl 6:S429-32.

151. Alvarez-Lerma F, Nolla-Salas J, Leon C, Palomar M, Jorda R, Carrasco N, Bobillo F, Group ES. 2003. Candiduria in critically ill patients admitted to intensive care medical units. Intensive Care Med 29:1069-76.

152. Kauffman CA. 2014. Diagnosis and management of fungal urinary tract infection. Infect Dis Clin North Am 28:61-74.

153. Padawer D, Pastukh N, Nitzan O, Labay K, Aharon I, Brodsky D, Glyatman T, Peretz A. 2015. Catheter-associated candiduria: Risk factors, medical interventions, and antifungal susceptibility. Am J Infect Control 43:e19-22.

154. Odabasi Z, Mert A. 2020. Candida urinary tract infections in adults. World J Urol 38:2699-2707.

155. Gajdacs M, Doczi I, Abrok M, Lazar A, Burian K. 2019. Epidemiology of candiduria and Candida urinary tract infections in inpatients and outpatients: results from a 10-year retrospective survey. Cent European J Urol 72:209-214.

156. Sobel JD, Fisher JF, Kauffman CA, Newman CA. 2011. Candida urinary tract infections--epidemiology. Clin Infect Dis 52 Suppl 6:S433-6.

157. Kauffman CA. 2005. Candiduria. Clin Infect Dis 41 Suppl 6:S371-6.

158. Chen SC, Playford EG, Sorrell TC. 2010. Antifungal therapy in invasive fungal infections. Curr Opin Pharmacol 10:522-30.

159. Dymond JS. 2013. Preparation of genomic DNA from Saccharomyces cerevisiae. Methods Enzymol 529:153-60.

160. Jiang H, Lei R, Ding SW, Zhu S. 2014. Skewer: a fast and accurate adapter trimmer for next-generation sequencing paired-end reads. BMC Bioinformatics 15:182.

161. Li H, Durbin R. 2009. Fast and accurate short read alignment with Burrows-Wheeler transform. Bioinformatics 25:1754-60.

162. Danecek P, Bonfield JK, Liddle J, Marshall J, Ohan V, Pollard MO, Whitwham A, Keane T, McCarthy SA, Davies RM, Li H. 2021. Twelve years of SAMtools and BCFtools. Gigascience 10.

163. Institue B. 2019. Picard toolkit. Broad Institute, GitHub repository.

164. Auwera GAVd OCB. 2020. Genomics in the Cloud. 1st Edition ed: O'Reilly Media, Inc.

165. Bergin SA ZF, Ryan AP, Müller CA, Nieduszynski CA, Zhai B, Rolling T, Hohl TM, Morio F, Scully J, Wolfe KH, Butler G. 2021. Resistance to miltefosine results from amplification of the RTA3 floppase or inactivation of flippases in Candida parapsilosis. bioRxiv doi: 10.1101/2021.12.16.473093.

166. Vaser R, Adusumalli S, Leng SN, Sikic M, Ng PC. 2016. SIFT missense predictions for genomes. Nat Protoc 11:1-9.

167. Robinson JT, Thorvaldsdottir H, Winckler W, Guttman M, Lander ES, Getz G, Mesirov JP. 2011. Integrative genomics viewer. Nat Biotechnol 29:24-6.

168. Lischer HE, Excoffier L, Heckel G. 2014. Ignoring heterozygous sites biases phylogenomic estimates of divergence times: implications for the evolutionary history of microtus voles. Mol Biol Evol 31:817-31.

169. Stamatakis A. 2014. RAxML version 8: a tool for phylogenetic analysis and post-analysis of large phylogenies. Bioinformatics 30:1312-3.

170. Quinlan AR, Hall IM. 2010. BEDTools: a flexible suite of utilities for comparing genomic features. Bioinformatics 26:841-2.

171. Ding C, Butler G. 2007. Development of a gene knockout system in Candida parapsilosis reveals a conserved role for BCR1 in biofilm formation. Eukaryot Cell 6:1310-9.

172. Zhai B, Ola M, Rolling T, Tosini NL, Joshowitz S, Littmann ER, Amoretti LA, Fontana E, Wright RJ, Miranda E, Veelken CA, Morjaria SM, Peled JU, van den Brink MRM, Babady NE, Butler G, Taur Y, Hohl TM. 2020. High-resolution mycobiota analysis reveals dynamic intestinal translocation preceding invasive candidiasis. Nat Med 26:59-64.

173. Katiyar SK, Alastruey-Izquierdo A, Healey KR, Johnson ME, Perlin DS, Edlind TD. 2012. Fks1 and Fks2 are functionally redundant but differentially regulated in Candida glabrata: implications for echinocandin resistance. Antimicrob Agents Chemother 56:6304-9.

174. Silva AP, Miranda IM, Guida A, Synnott J, Rocha R, Silva R, Amorim A, Pina-Vaz C, Butler G, Rodrigues AG. 2011. Transcriptional profiling of azole-resistant Candida parapsilosis strains. Antimicrob Agents Chemother 55:3546-56.

175. Doorley LA, Rybak JM, Berkow EL, Zhang Q, Morschhauser J, Rogers PD. 2022. Candida parapsilosis Mdr1B and Cdr1B Are Drivers of Mrr1-Mediated Clinical Fluconazole Resistance. Antimicrob Agents Chemother 66:e0028922.

176. Zhang L, Xiao M, Watts MR, Wang H, Fan X, Kong F, Xu YC. 2015. Development of fluconazole resistance in a series of Candida parapsilosis isolates from a persistent candidemia patient with prolonged antifungal therapy. BMC Infect Dis 15:340.

177. Coste A, Selmecki A, Forche A, Diogo D, Bougnoux ME, d'Enfert C, Berman J, Sanglard D. 2007. Genotypic evolution of azole resistance mechanisms in sequential Candida albicans isolates. Eukaryot Cell 6:1889-904.

178. Todd RT, Selmecki A. 2020. Expandable and reversible copy number amplification drives rapid adaptation to antifungal drugs. Elife 9.

179. Selmecki A, Gerami-Nejad M, Paulson C, Forche A, Berman J. 2008. An isochromosome confers drug resistance in vivo by amplification of two genes, ERG11 and TAC1. Mol Microbiol 68:624-41.

180. Borgeat V, Brandalise D, Grenouillet F, Sanglard D. 2021. Participation of the ABC Transporter CDR1 in Azole Resistance of Candida lusitaniae. J Fungi (Basel) 7.

181. Pfaller MA, Diekema DJ. 2007. Epidemiology of invasive candidiasis: a persistent public health problem. Clin Microbiol Rev 20:133-63.

182. Pannanusorn S, Ramirez-Zavala B, Lunsdorf H, Agerberth B, Morschhauser J, Romling U. 2014. Characterization of biofilm formation and the role of BCR1 in clinical isolates of Candida parapsilosis. Eukaryot Cell 13:438-51.

183. Ramage G, VandeWalle K, Lopez-Ribot JL, Wickes BL. 2002. The filamentation pathway controlled by the Efg1 regulator protein is required for normal biofilm formation and development in Candida albicans. Fems Microbiology Letters 214:95-100.

184. Finkel JS, Xu W, Huang D, Hill EM, Desai JV, Woolford CA, Nett JE, Taff H, Norice CT, Andes DR, Lanni F, Mitchell AP. 2012. Portrait of Candida albicans adherence regulators. PLoS Pathog 8:e1002525.

185. Sellam A, Tebbji F, Nantel A. 2009. Role of Ndt80p in sterol metabolism regulation and azole resistance in Candida albicans. Eukaryot Cell 8:1174-83.

186. Chen CG, Yang YL, Shih HI, Su CL, Lo HJ. 2004. CaNdt80 is involved in drug resistance in Candida albicans by regulating CDR1. Antimicrobial Agents and Chemotherapy 48:4505-4512.

187. Silva-Dias A, Miranda IM, Rocha R, Monteiro-Soares M, Salvador A, Rodrigues AG, Pina-Vaz C. 2012. A novel flow cytometric protocol for assessment of yeast cell adhesion. Cytometry A 81:265-70.

188. Kohrer K, Domdey H. 1991. Preparation of high molecular weight RNA. Methods Enzymol 194:398-405.

189. Almeida MC, Antunes D, Silva BMA, Rodrigues L, Mota M, Borges O, Fernandes C, Goncalves T. 2019. Early Interaction of Alternaria infectoria Conidia with Macrophages. Mycopathologia 184:383-392.

190. Pak J, Segall J. 2002. Regulation of the premiddle and middle phases of expression of the NDT80 gene during sporulation of Saccharomyces cerevisiae. Mol Cell Biol 22:6417-29.

191. Katz ME, Cooper S. 2015. Extreme Diversity in the Regulation of Ndt80-Like Transcription Factors in Fungi. G3 (Bethesda) 5:2783-92.

192. Connolly LA, Riccombeni A, Grozer Z, Holland LM, Lynch DB, Andes DR, Gacser A, Butler G. 2013. The APSES transcription factor Efg1 is a global regulator that controls morphogenesis and biofilm formation in Candida parapsilosis. Molecular Microbiology 90:36-53.

193. Toth R, Toth A, Papp C, Jankovics F, Vagvolgyi C, Alonso MF, Bain JM, Erwig LP, Gacser A. 2014. Kinetic studies of Candida parapsilosis phagocytosis by macrophages and detection of intracellular survival mechanisms. Front Microbiol 5:633.

194. Galocha M, Pais P, Cavalheiro M, Pereira D, Viana R, Teixeira MC. 2019. Divergent Approaches to Virulence in C. albicans and C. glabrata: Two Sides of the Same Coin. Int J Mol Sci 20.

195. Naglik JR, Challacombe SJ, Hube B. 2003. Candida albicans secreted aspartyl proteinases in virulence and pathogenesis. Microbiol Mol Biol Rev 67:400-28, table of contents.

196. Polke M, Hube B, Jacobsen ID. 2015. Candida survival strategies. Adv Appl Microbiol 91:139-235.

197. Nobile CJ, Schneider HA, Nett JE, Sheppard DC, Filler SG, Andes DR, Mitchell AP. 2008. Complementary adhesin function in C. albicans biofilm formation. Curr Biol 18:1017-24.

198. Fox EP, Nobile CJ. 2012. A sticky situation: untangling the transcriptional network controlling biofilm development in Candida albicans. Transcription 3:315-22.

199. Sellam A, Askew C, Epp E, Tebbji F, Mullick A, Whiteway M, Nantel A. 2010. Role of transcription factor CaNdt80p in cell separation, hyphal growth, and virulence in Candida albicans. Eukaryot Cell 9:634-44.

200. Toth R, Cabral V, Thuer E, Bohner F, Nemeth T, Papp C, Nimrichter L, Molnar G, Vagvolgyi C, Gabaldon T, Nosanchuk JD, Gacser A. 2018. Investigation of Candida parapsilosis virulence regulatory factors during host-pathogen interaction. Sci Rep 8:1346.

201. Tavanti A, Campa D, Bertozzi A, Pardini G, Naglik JR, Barale R, Senesi S. 2006. Candida albicans isolates with different genomic backgrounds display a differential response to macrophage infection. Microbes Infect 8:791-800.

202. Toth A, Zajta E, Csonka K, Vagvolgyi C, Netea MG, Gacser A. 2017. Specific pathways mediating inflammasome activation by Candida parapsilosis. Sci Rep 7:43129.

203. Singh DK, Nemeth T, Papp A, Toth R, Lukacsi S, Heidingsfeld O, Dostal J, Vagvolgyi C, Bajtay Z, Jozsi M, Gacser A. 2019. Functional Characterization of Secreted Aspartyl Proteases in Candida parapsilosis. mSphere 4.

204. Bliss JM. 2015. Candida parapsilosis: an emerging pathogen developing its own identity. Virulence 6:109-11.

205. Navarro-Garcia F, Alonso-Monge R, Rico H, Pla J, Sentandreu R, Nombela C. 1998. A role for the MAP kinase gene MKC1 in cell wall construction and morphological transitions in Candida albicans. Microbiology (Reading) 144 (Pt 2):411-424.

206. Chen T, Jackson JW, Tams RN, Davis SE, Sparer TE, Reynolds TB. 2019. Exposure of Candida albicans beta (1,3)-glucan is promoted by activation of the Cek1 pathway. PLoS Genet 15:e1007892.

207. Fingerman IM, Sutphen K, Montano SP, Georgiadis MM, Vershon AK. 2004. Characterization of critical interactions between Ndt80 and MSE DNA defining a novel family of Ig-fold transcription factors. Nucleic Acids Res 32:2947-56.

208. Chen X, Gaglione R, Leong T, Bednor L, de Los Santos T, Luk E, Airola M, Hollingsworth NM. 2018. Mek1 coordinates meiotic progression with DNA break repair by directly

phosphorylating and inhibiting the yeast pachytene exit regulator Ndt80. PLoS Genet 14:e1007832.

209. Katz ME, Braunberger K, Yi G, Cooper S, Nonhebel HM, Gondro C. 2013. A p53-like transcription factor similar to Ndt80 controls the response to nutrient stress in the filamentous fungus, Aspergillus nidulans. F1000Res 2:72.

210. Hutchison EA, Glass NL. 2010. Meiotic regulators Ndt80 and ime2 have different roles in Saccharomyces and Neurospora. Genetics 185:1271-82.

211. Min K, Biermann A, Hogan DA, Konopka JB. 2018. Genetic Analysis of NDT80 Family Transcription Factors in Candida albicans Using New CRISPR-Cas9 Approaches. mSphere 3.

Abstract

Candida parapsilosis is the second most common *Candida* isolated in Asia, Southern European and Latin American countries, linked to healthcare-associated invasive infections. This pathogen is part of the *psilosis* complex, also including *C. orthopsilosis* and *C. metapsilosis. C. parapsilosis* infection is particularly relevant among low-birth neonates, immunocompromised individuals and patients requiring prolonged use of a central venous catheter or other indwelling devices, mostly due to its notorious capacity to adhere and develop biofilm at the surface of medical indwelling devices. Despite its notorious prevalence, its biology is far from being explored as it happens in *C. albicans.* Molecular mechanistic pathways are followed differently by these two species, namely in virulence, regulatory and antifungal drug resistance. Therefore it is remarkably important the continuous search for species-specific features.

The four main goals of this investigation involved: (1) the characterization of the antifungal susceptibility profile of *C. parapsilosis* complex clinical strains against the major class of antifungal drugs commonly used in clinical practice, azoles, (2) the elucidation of the *C. parapsilosis* molecular mechanisms responsible for fluconazole resistance; (3) the molecular characterization of *in vivo* acquisition of azole resistance through the study of three consecutive *C. parapsilosis* isolates, obtained during prolonged fluconazole treatment of a patient diagnosed with candiduria and (4) the assessment of the role of Ndt80 transcription factor in *C. parapsilosis* morphogenesis, adhesion and biofilm formation.

Concerning the first objective, the analysis and characterization of the susceptibility profile to azoles drugs, namely fluconazole (FLC), voriconazole (VRC) and posaconazole (PSC), was conducted among a collection of *C. parapsilosis* complex strains. Our results confirm that *C. parapsilosis* remains the main etiologic agent among the *psilosis* complex. The antifungal susceptibility patterns reveal the emergence of azole strains within the *psilosis* complex. Within the second aim, we observed that Mdr1 efflux pumps overexpression was the major mechanism involved in *C. parapsilosis* FLC resistance. The involvement of *CDR1* efflux pumps and *ERG11* gene also impacts the FLC resistance. We identified several mutations in the coding sequences of the last genes and their regulators, which could possibly be involved in the decreased susceptibility profile to azoles. These studies provide relevant data, regarding *C. parapsilosis* antifungal susceptibility profile and resistance mechanisms, benefiting a more comprehensive understanding of its behavior, which may help the clinicians to adapt the therapeutic approach whenever treating such infections.

Regarding the third objective, a set of three consecutive *C. parapsilosis* isolates (CPS-A, CPS-B, CPS-C) recovered from urine samples of a patient, exhibiting a switch of susceptibility phenotype from susceptible to resistant following prolonged FLC exposure, were comprehensively characterized regarding the molecular mechanisms underlying azole

resistance acquisition. The initial isolate CPS-A was susceptible to all three azoles tested (FLC, VRC and PSC); isolate CPS-B, collected after the 2nd cycle of treatment, displayed a susceptible-dose dependent (SDD) phenotype to FLC, while isolate CPS-C, recovered after the 3rd cycle, exhibited a cross-resistance profile to FLC and VRC. Whole-genome sequencing (WGS) revealed a putative resistance mechanism in isolate CPS-C, associated with a G1810A nucleotide substitution, leading to an aminoacidic change G604R in the Mrr1 transcription factor. Introducing this mutation into the susceptible CPS-A isolate results in resistant phenotype to FLC and VRC, as well as the upregulation of *MRR1* and *MDR1* genes. Interestingly, the SDD phenotype exhibited by isolate CPS-B is associated with an increased copy number of the *CDR1B* gene. Expression of *CDR1B* is increased in both isolates CPS-B and CPS-C, and in the CPS-A strain expressing the *MRR1* gene harboring the gain-of-function (GOF) mutation. Our results characterize the *in vivo* azole cross-resistance acquisition in *C. parapsilosis* due to a G1810A (G604R) GOF mutation resulting in *MRR1* hyperactivation and consequently, *MDR1* efflux pump overexpression. We also associated amplification of *CDR1B* gene with decreased FLC susceptibility and showed that it is a putative target of the *MRR1* GOF mutation.

The fourth objective was clarify the function of Ndt80 transcription factor in *C. parapsilosis* virulence attributes. By knocking out *NDT80* gene, or even just one single copy of the gene, we observed substantial morphogenetic alterations and changes in adhesion and biofilm growth profiles. Both *ndt80Δ* and *ndt80ΔΔ* mutants changed colony and cell morphologies from smooth, yeast-shaped to crepe and pseudohyphal elongated forms, exhibiting promoted adherence to polystyrene microspheres and notably, forming a higher amount of biofilm compared to the wild type strain. Interestingly, we identified transcription factors Ume6, Cph2, Cwh41, Ace2, Bcr1, protein kinase Mkc1 and adhesin Als7 to be under Ndt80 negative regulation, partially explaining the phenotypes displayed by the *ndt80ΔΔ* mutant. Furthermore, *ndt80ΔΔ* pseudohyphae adhered more rapidly and were more resistant to murine macrophage attack, becoming deleterious to such cells after phagocytosis. Unexpectedly, these findings provide the first evidence for a direct role of Ndt80 as a repressor of *C. parapsilosis* virulence attributes, showing a functional divergence from its homolog in the close related fungal pathogen *C. albicans*.

In summary, the study highlighted the molecular mechanisms involved in *C. parapsilosis* azole resistance, as well as the importance of the continuous study of the regulatory mechanisms in this emergent species, given the occurrence of divergent processes relatively to *C. albicans*.

Resumo

Candida parapsilosis é a segunda espécie de *Candida* mais frequentemente isolada em várias regiões da Ásia, do sul da Europa e nos países da América Latina, estando associada a infeções invasivas associadas a cuidados de saúde. Este agente patogénico integra o grupo *psilosis*, que incluiu as espécies *C. orthopsilosis* e *C. metapsilosis*. A incidência de *C. parapsilosis* é particularmente preocupante em recém-nascidos prematuros, indivíduos imuno-comprometidos e doentes que necessitem do uso prolongado de cateteres venosos centrais ou outros dispositivos médicos implantados, uma vez que apresenta uma notória capacidade de aderir e desenvolver biofilme na superfície destes dispositivos. Apesar da sua prevalência crescente, os aspetos relacionados com a sua biologia estão longe de ser conhecidos, como acontece com *C. albicans*. Os mecanismos moleculares subjacentes a determinadas características, tais como a virulência, a regulação e a resistência a antifúngicos, diferem entre estas espécies, tornando essencial a procura contínua de informação sobre as particularidades desta espécie.

Os principais objetivos desta investigação envolveram: (1) a caracterização do perfil de suscetibilidade antifúngica de estirpes clínicas do grupo *C. parapsilosis* à principal classe de antifúngicos utilizados na prática clínica, os azoles; (2) a elucidação dos mecanismos moleculares associados à resistência ao fluconazole (FLC); (3) o estudo e caracterização dos mecanismos de resistência ao FLC em três isolados clínicos de *C. parapsilosis*, obtidos sequencialmente durante o tratamento prolongado com FLC, num doente diagnosticado com candidúria e (4) o impacto do fator de transcrição Ndt80 na morfogénese, adesão e formação de biofilme de *C. parapsilosis*.

Relativamente aos primeiros objetivos, foi realizada uma análise e caracterização dos perfis de suscetibilidade a compostos azólicos, nomeadamente ao FLC, voriconazole (VRC) e posaconazole (PSC), numa coleção de estirpes clínicas do grupo de *C. parapsilosis*. Os resultados confirmam que *C. parapsilosis* mantem-se como o principal agente etiológico do grupo *psilosis*. No entanto, a percentagem de *C. metapsilosis* aparentemente duplicou, comparativamente a estudos anteriores desenvolvidos no Laboratório de Microbiologia da FMUP. Os perfis de suscetibilidade aos antifúngicos revelaram o aumento de estirpes não suscetíveis no grupo *psilosis*, caracterizadas maioritariamente pela sobre expressão das bombas de efluxo Mdr1; que se destacou como sendo o principal mecanismo subjacente à resistência ao FLC em *C. parapsilosis*, embora tenha sido detetado concomitantemente o envolvimento das bombas de efluxo *CDR1* e do gene *ERG11* na resistência ao FLC. Foram identificadas várias mutações nas sequências codificantes destes genes e dos seus reguladores, que possivelmente estarão envolvidas na diminuição do perfil de suscetibilidade aos azoles. Este estudo fornece dados clinicamente relevantes, particularmente sobre a suscetibilidade antifúngica e mecanismos de

resistência de *C. parapsilosis*, possibilitando aos clínicos adaptarem a abordagem e estratégia terapêutica no tratamento das infeções por estes agentes patogénicos.

Relativamente ao terceiro objetivo do trabalho, três isolados de *C. parapsilosis* (CPS-A, CPS-B, CPS-C) - recuperados de amostras consecutivas de urina do mesmo doente - apresentaram alteração de perfil de suscetibilidade, de suscetível para resistente após exposição prolongada ao FLC, foram caracterizados os mecanismos moleculares subjacentes à aquisição de resistência. O isolado inicial CPS-A, apresentou um perfil suscetível aos três azoles testados (FLC; VRC, PSC); o isolado CPS-B, recuperado após o segundo ciclo de tratamento, apresentou um fenótipo suscetível dose-dependente (SDD) ao FLC, enquanto o isolado CPS-C, recuperado após o terceiro ciclo, exibiu um perfil de resistência cruzada ao FLC e VRC. A sequenciação do genoma revelou um possível mecanismo de resistência no isolado CPS-C associado à substituição nucleotídica G1810A, levando a uma alteração aminoacídica (G604R) no fator de transcrição Mrr1. A introdução desta mutação no isolado suscetível CPS-A resultou na alteração do fenótipo de suscetibilidade para resistente ao FLC e VRC, bem como no aumento da expressão dos genes *MRR1* e *MDR1*. Curiosamente, o fenótipo SDD exibido pelo isolado CPS-B foi associado ao aumento do número de cópias do gene *CDR1B*. A expressão do *CDR1B* encontra-se aumentada nos isolados CPS-B e CPS-C, assim como no mutante da estirpe CPS-A que expressa a mutação de ganho-de-função (GOF) no gene *MRR1*. Estes resultados confirmam que a aquisição de resistência cruzada aos azoles *in vivo* em *C. parapsilosis* foi devida à mutação GOF G1810A (G604R), que induziu a hiperatividade do fator de transcrição Mrr1p, levando à sobre expressão das bombas de efluxo *MDR1*. A amplificação do gene *CDR1B* foi também associada à diminuição da suscetibilidade ao FLC tendo sido identificado como um alvo da mutação GOF do gene *MRR1*.

O quarto objetivo incidiu no esclarecimento da função do fator de transcrição Ndt80 nos atributos de virulência de *C. parapsilosis*. Ao eliminar o gene *NDT80*, total ou parcialmente, surgiram alterações morfogénicas, nos perfis de adesão e na produção de biofilme. Nos mutantes *ndt80Δ* e *ndt80ΔΔ* ocorreram alterações da morfologia das colónias e das células, de lisas e leveduriformes, para as formas crepe e pseudo-hifas alongadas. Este tipo celular revelou ser mais aderente entre si (célula-célula) e às microesferas de poliestireno (superfície abiótica), formando uma maior quantidade de biofilme, comparativamente à estirpe selvagem. Curiosamente, foram identificados os fatores de transcrição Ume6, Cph2, Cwh41, Ace2, Bcr1, a proteína quinase Mkc1 e a adesina Als7, sob regulação negativa do Ndt80, explicando parcialmente os fenótipos exibidos pelo mutante *ndt80ΔΔ*. Na interação com macrófagos murinos, as pseudohifas do mutante *ndt80ΔΔ* aderiram rapidamente a este tipo de células, tendo contribuído para a sua morte após fagocitose. Os nossos resultados fornecem a primeira

evidência acerca do papel do Ndt80 como repressor de atributos de virulência de *C. parapsilosis*, demonstrando uma divergência funcional com o seu homólogo em *C. albicans*.

Em resumo, o estudo permitiu evidenciar os mecanismos moleculares envolvidos na resistência de *C. parapsilosis* aos antifúngicos azólicos, assim como a importância do estudo dos mecanismos de regulação nesta espécie emergente, dada a divergência relativamente a *C. albicans*.

Supplementary Material

Chapter I

Table S1. MIC value and susceptibility phenotype of *C. parapsilosis* strains.

Table S2. MIC value and susceptibility phenotype of *C. orthopsilosis* strains.

Table S3. MIC value and susceptibility phenotype of *C. metapsilosis* strains.

Table S4. Relative fold-change expressions in the twenty-six *C. parapsilosis* fluconazole-resistant strains.

Chapter II

Table S5. Deleterious phenotypes based on SIFT analysis.

Table S6. Gene copy number variation.

Chapter III

Table S7. Relative gene expression level in the *ndt80Δ* and *ndt8ΔΔ* strains.

Movie S1. Live cell imaging time lapse videos. (Digital version only) Time lapse videos were produced using a confocal Cell Observer Spinning Disk microscope and Zen Blue software (Zeiss). Using the micrographs taken every 1 min over a time period of 45 min. Shorter videos were afterwards generated, highlighting the earlier time point interactions between RAW 264.7 macrophage cells and *Candida parapsilosis* cells: **A)** wild type strain, with adhesion beginning at 27 min; **B)** *ndt80Δ* mutant strain, with adhesion and internalization beginning at 14 min, and **C)** *ndt80ΔΔ* mutant strain, with interactions beginning at 9 min. Short time lapse videos are representative of different sets of independent experiments; macrophages are stained red (Wheat Germ Agglutinin (WGA), Tetramethylrhodamine conjugate - W849; Molecular Probes); scale bars represents 10 μm.

Table S1. MIC value and susceptibility phenotype of *C. parapsilosis* strains

	MIC (µg mL^{-1}) | Phenotype[a]					
Strain	Fluconazole		Voriconazole		Posaconazole	
Cp1	**64**	**R**	**4**	**R**	0,12	WT
Cp2	**32**	**R**	**1**	**R**	0,06	WT
Cp3	**4**	**SDD**	**0,5**	**I**	0,25	WT
Cp4	1	S	0,03	S	0,25	WT
Cp5	1	S	0,03	S	0,25	WT
Cp6	1	S	0,03	S	0,25	WT
Cp7	0,5	S	0,03	S	0,25	WT
Cp8	1	S	**0,25**	**I**	0,25	WT
Cp9	1	S	0,03	S	0,5	WT
Cp11	2	S	0,03	S	0,12	WT
Cp12	1	S	0,03	S	0,12	WT
Cp13	2	S	0,06	S	0,12	WT
Cp14	1	S	0,03	S	0,12	WT
Cp15	0,5	S	0,03	S	0,12	WT
Cp16	1	S	0,12	S	0,5	WT
Cp17	0,5	S	0,03	S	0,25	WT
Cp18	0,5	S	0,03	S	0,25	WT
Cp19	0,5	S	0,015	S	0,25	WT
Cp20	1	S	0,03	S	0,5	WT
Cp22	2	S	0,12	S	0,25	WT
Cp23	**8**	**R**	**0,5**	**I**	0,12	WT
Cp24	2	S	0,12	S	0,5	WT
Cp25	**8**	**R**	**0,5**	**I**	0,12	WT
Cp26	**8**	**R**	**0,5**	**I**	0,06	WT
Cp27	1	S	0,03	S	0,25	WT
Cp28	1	S	0,06	S	0,25	WT
Cp29	1	S	0,03	S	0,25	WT
Cp31	0,5	S	0,03	S	0,25	WT
Cp32	1	S	0,03	S	0,5	WT
Cp33	1	S	0,03	S	0,25	WT
Cp34	2	S	0,12	S	0,5	WT
Cp35	0,5	S	0,03	S	0,25	WT
Cp36	1	S	0,03	S	0,25	WT
Cp37	**8**	**R**	**0,25**	**I**	0,12	WT
Cp38	1	S	0,015	S	0,25	WT
Cp39	0,5	S	0,03	S	0,25	WT
Cp40	1	S	0,03	S	0,25	WT
Cp41	**4**	**SDD**	**0,25**	**I**	0,25	WT
Cp42	**4**	**SDD**	**0,25**	**I**	**0,5**	**non-WT**
Cp43	**4**	**SDD**	**0,25**	**I**	0,25	WT
Cp44	2	S	0,06	S	0,25	WT
Cp46	2	S	0,06	S	0,25	WT
Cp47	2	S	0,12	S	0,25	WT

Cp48	2	S	0,06	S	0,25	WT
Cp49	1	S	0,03	S	0,25	WT
Cp50	2	S	0,06	S	0,25	WT
Cp51	2	S	0,03	S	0,25	WT
Cp52	2	S	0,03	S	0,25	WT
Cp53	1	S	0,03	S	0,25	WT
Cp54	1	S	0,03	S	0,25	WT
Cp55	1	S	0,03	S	0,25	WT
Cp56	2	S	0,06	S	0,25	WT
Cp57	2	S	0,03	S	0,25	WT
Cp58	1	S	0,03	S	0,25	WT
Cp59	2	S	0,12	S	0,25	WT
Cp60	2	S	0,03	S	0,25	WT
Cp62	1	S	0,03	S	0,25	WT
Cp63	1	S	0,03	S	0,25	WT
Cp64	1	S	**0,25**	**I**	0,25	WT
Cp65	1	S	0,03	S	0,25	WT
Cp66	2	S	0,06	S	0,25	WT
Cp67	2	S	0,03	S	0,25	WT
Cp68	2	S	0,03	S	0,25	WT
Cp69	2	S	0,03	S	0,25	WT
Cp70	0,5	S	0,12	S	0,25	WT
Cp71	1	S	**0,25**	**I**	0,25	WT
Cp72	2	S	0,06	S	0,25	WT
Cp73	2	S	0,06	S	0,25	WT
Cp74	0,5	S	0,015	S	0,25	WT
Cp75	1	S	0,015	S	0,25	WT
Cp76	1	S	0,015	S	0,12	WT
Cp77	2	S	0,03	S	0,25	WT
Cp78	0,5	S	0,006	S	0,25	WT
Cp84	**4**	**SDD**	**0,5**	**I**	0,25	WT
Cp85	8	R	**0,5**	**I**	0,25	WT
Cp86	2	S	**0,5**	**I**	0,25	WT
Cp87	2	S	**0,5**	**I**	0,25	WT
Cp88	2	S	**0,5**	**I**	**0,5**	**non-WT**
Cp89	2	S	0,125	S	0,5	WT
Cp90	1	S	0,125	S	**1**	**non-WT**
Cp92	1	S	0,006	S	0,5	WT
Cp95	0,5	S	0,015	S	0,03	WT
Cp98	0,5	S	0,015	S	0,03	WT
Cp99	1	S	0,015	S	0,03	WT
Cp100	**8**	**R**	0,015	S	0,03	WT
Cp101	1	S	0,015	S	0,03	WT
Cp102	1	S	0,015	S	0,03	WT
Cp103	1	S	0,015	S	0,03	WT
Cp104	**4**	**SDD**	0,06	S	0,06	WT
Cp105	1	S	0,015	S	0,03	WT
Cp106	2	S	0,015	S	0,03	WT

Cp108	1	S	0,03	S	0,06	WT
Cp109	0,5	S	0,015	S	0,03	WT
Cp110	1	S	0,015	S	0,06	WT
Cp111	1	S	0,015	S	0,06	WT
Cp112	1	S	0,015	S	0,06	WT
Cp113	0,5	S	0,015	S	0,06	WT
Cp114	1	S	0,015	S	0,06	WT
Cp115	0,5	S	0,015	S	0,06	WT
Cp116	1	S	0,015	S	0,06	WT
Cp118	1	S	0,015	S	0,06	WT
Cp119	1	S	0,015	S	0,06	WT
Cp120	1	S	0,015	S	0,06	WT
Cp121	0,125	S	<0,016	S	0,06	WT
Cp122	**8**	**R**	0,03	S	0,125	WT
Cp123	2	S	0,03	S	0,125	WT
Cp124	2	S	0,015	S	0,125	WT
Cp125	1	S	0,015	S	0,125	WT
Cp126	**16**	**R**	0,03	S	0,125	WT
Cp127	0,5	S	<0,015	S	0,06	WT
Cp129	2	S	0,03	S	0,125	WT
Cp130	2	S	0,03	S	0,125	WT
Cp131	2	S	0,03	S	0,125	WT
Cp132	2	S	0,03	S	0,06	WT
Cp133	1	S	0,03	S	0,125	WT
Cp134	1	S	0,06	S	0,125	WT
Cp135	1	S	0,06	S	0,125	WT
Cp136	1	S	0,03	S	0,125	WT
Cp137	1	S	0,03	S	0,125	WT
Cp138	**4**	**SDD**	**0,25**	**I**	0,125	WT
Cp139	**4**	**SDD**	**0,25**	**I**	0,06	WT
Cp140	1	S	0,03	S	0,06	WT
Cp141	**64**	**R**	**1**	**R**	0,25	WT
Cp142	2	S	0,06	S	0,125	WT
Cp144	2	S	0,03	S	0,06	WT
Cp145	2	S	0,03	S	0,06	WT
Cp146	2	S	0,03	S	0,06	WT
Cp147	2	S	0,03	S	0,06	WT
Cp148	2	S	0,03	S	0,06	WT
Cp149	1	S	0,03	S	0,25	WT
Cp150	1	S	0,03	S	0,125	WT
Cp151	1	S	0,03	S	0,25	WT
Cp152	1	S	0,03	S	0,25	WT
Cp153	**4**	**SDD**	0,125	S	0,25	WT
Cp154	0,25	S	0,015	S	0,125	WT
Cp155	1	S	0,06	S	0,25	WT
Cp156	1	S	0,03	S	0,25	WT
Cp157	**16**	**R**	**1**	**R**	0,06	WT
Cp158	0,25	S	0,015	S	0,03	WT

Cp159	0,5	S	0,03	S	0,125	WT
Cp160	1	S	0,03	S	0,125	WT
Cp161	1	S	0,03	S	0,25	WT
Cp162	1	S	0,03	S	0,125	WT
Cp163	1	S	0,06	S	0,125	WT
Cp164	2	S	0,06	S	0,125	WT
Cp165	2	S	0,06	S	0,06	WT
Cp166	1	S	0,03	S	0,03	WT
Cp167	0,5	S	0,015	S	0,03	WT
Cp168	1	S	0,03	S	0,03	WT
Cp169	1	S	0,03	S	0,125	WT
Cp170	**4**	**SDD**	0,125	S	0,25	WT
Cp171	1	S	0,06	S	0,125	WT
Cp172	1	S	0,03	S	0,125	WT
Cp173	1	S	0,03	S	0,125	WT
Cp174	0,5	S	0,015	S	0,125	WT
Cp175	**8**	**R**	**0,25**	**I**	0,125	WT
Cp176	2	S	0,06	S	0,125	WT
Cp177	2	S	0,125	S	0,125	WT
Cp178	1	S	0,125	S	0,125	WT
Cp179	1	S	0,03	S	0,06	WT
Cp180	1	S	0,03	S	0,125	WT
D140	1	S	0,06	S	0,06	WT
D141	1	S	0,015	S	0,03	WT
D143	0,5	S	0,03	S	0,03	WT
D144	0,5	S	0,03	S	0,06	WT
D145	1	S	0,03	S	0,03	WT
D146	0,5	S	0,06	S	0,06	WT
D147	1	S	0,03	S	<0,03	WT
D148	1	S	0,03	S	0,03	WT
D149	2	S	0,12	S	0,06	WT
D150	**16**	**R**	**0,5**	**I**	0,06	WT
D151	**16**	**R**	**0,25**	**I**	0,06	WT
D152	2	S	0,06	S	0,06	WT
D153	0,5	S	0,03	S	0,06	WT
D154	**8**	**R**	**0,25**	**I**	0,12	WT
D155	2	S	0,06	S	0,06	WT
D156	2	S	0,12	S	0,12	WT
D157	**16**	**R**	0,06	S	0,06	WT
D158	**16**	**R**	0,06	S	0,06	WT
D159	**16**	**R**	0,03	S	0,06	WT
D161	2	S	0,03	S	0,06	WT
D162	**32**	**R**	0,015	S	0,03	WT
D163	2	S	0,015	S	0,06	WT
D164	0,5	S	0,015	S	<0,03	WT
D165	2	S	0,06	S	0,12	WT
D166	1	S	0,06	S	0,12	WT
D167	1	S	0,03	S	0,12	WT

D168	1	S	0,03	S	0,12	WT
D169	**4**	**SDD**	0,12	S	0,06	WT
D171	0,5	S	0,03	S	0,12	WT
D172	0,5	S	0,015	S	0,12	WT
D173	1	S	0,06	S	0,12	WT
D174	1	S	0,06	S	0,12	WT
D175	1	S	0,06	S	0,06	WT
D176	1	S	0,06	S	0,12	WT
D177	2	S	0,06	S	0,12	WT
D178	1	S	0,06	S	0,12	WT
D180	2	S	0,06	S	0,12	WT
D181	1	S	0,06	S	0,06	WT
D182	1	S	0,06	S	0,03	WT
D183	1	S	0,06	S	0,03	WT
D184	1	S	0,06	S	0,06	WT
D185	1	S	0,03	S	0,06	WT
D186	1	S	0,06	S	0,03	WT
D187	2	S	0,06	S	0,06	WT
D188	1	S	0,06	S	0,03	WT
D189	1	S	0,12	S	0,06	WT
D190	1	S	0,06	S	0,06	WT
D191	1	S	0,06	S	0,06	WT
D192	1	S	0,06	S	0,03	WT
D193	1	S	0,06	S	0,03	WT
D194	0,5	S	0,06	S	0,03	WT
D195	**32**	**R**	**2**	**R**	0,06	WT
D196	**32**	**R**	**1**	**R**	0,06	WT
D197	1	S	0,06	S	0,06	WT
D198	**4**	**SDD**	0,12	S	0,06	WT
D199	2	S	0,06	S	0,06	WT
D201	1	S	0,03	S	0,06	WT
D202	2	S	0,06	S	0,06	WT
D203	**32**	**R**	0,06	S	0,06	WT
D204	1	S	0,06	S	0,06	WT
D205	0,5	S	0,015	S	<0,06	WT
D206	1	S	0,06	S	0,12	WT
D207	1	S	0,06	S	0,12	WT
D208	**4**	**SDD**	0,06	S	0,06	WT
D209	1	S	0,06	S	0,06	WT
D210	1	S	0,06	S	0,12	WT
D212	1	S	**0,5**	**I**	0,06	WT
D213	**4**	**SDD**	**0,25**	**I**	0,06	WT
D214	2	S	**0,25**	**I**	0,06	WT
D215	**4**	**SDD**	**0,25**	**I**	0,06	WT
D216	1	S	0,12	S	0,06	WT
D217	1	S	0,12	S	0,06	WT
D218	2	S	0,12	S	0,06	WT
D219	1	S	0,12	S	0,06	WT

D221	**32**	**R**	**1**	**R**	0,06	WT
D222	**32**	**R**	**0,5**	**I**	0,03	WT
D223	**64**	**R**	**2**	**R**	0,06	WT
D224	1	S	0,06	S	0,06	WT
D225	1	S	0,06	S	0,06	WT
D226	1	S	0,03	S	0,06	WT
D227	1	S	0,03	S	0,06	WT
D228	2	S	0,03	S	0,12	WT
D229	1	S	0,03	S	0,12	WT
D230	1	S	0,03	S	0,12	WT
D231	**2**	**SDD**	0,12	S	0,5	WT
D232	1	S	0,03	S	0,12	WT
D235	2	S	0,06	S	0,06	WT
D236	2	S	0,06	S	0,12	WT
D237	2	S	0,12	S	0,06	WT

[a] S, Susceptible; SDD, Susceptible-dose dependent; I, Intermetiate R, Resistant;
WT, wild type; non-WT, non-wild type.

Table S2. MIC value and susceptibility phenotype of *C. orthopsilosis* strains

MIC (µg mL^{-1}) | Phenotype[a]					
Strain	Fluconazole		Voriconazole		Posaconazole	
CO1	2	WT	0,015	WT	0,125	WT
CO2	2	WT	0,015	WT	0,125	WT
CO3	1	WT	0,015	WT	0,06	WT
CO4	1	WT	0,06	WT	0,03	WT
CO5	1	WT	0,06	WT	0,03	WT
CO6	1	WT	0,06	WT	0,03	WT
CO7	1	WT	0,015	WT	0,125	WT
CO8	1	WT	0,06	WT	0,125	WT
CO9	1	WT	0,06	WT	0,125	WT
CO10	1	WT	0,03	WT	0,125	WT
CO11	0,5	WT	0,015	WT	<0,03	WT
CO12	0,25	WT	0,015	WT	0,03	WT
CO13	0,25	WT	0,015	WT	0,03	WT
CO14	**32**	**non-WT**	**0,25**	**non-WT**	0,125	WT

[a] WT, wild type; non-WT, non-wild type.

Table S3. MIC value and susceptibility phenotype of *C. metapsilosis* strains

MIC (µg mL^{-1}) | Phenotype[a]					
Strain	Fluconazole		Voriconazole		Posaconazole	
CM01	1	WT	0,03	WT	0,03	WT
CM02	1	WT	0,06	WT	0,03	WT
CM03	1	WT	0,03	WT	0,03	WT
CM04	1	WT	0,06	WT	0,03	WT
CM05	1	WT	0,06	WT	0,03	WT
CM06	1	WT	0,06	WT	0,03	WT
CM07	2	WT	0,06	WT	0,06	WT
CM08	2	WT	0,06	WT	0,125	WT
CM09	2	WT	**0,125**	**non-WT**	0,25	WT
CM10	1	WT	0,03	WT	0,06	WT
CM11	1	WT	0,03	WT	0,03	WT
CM12	1	WT	0,03	WT	0,06	WT
CM13	1	WT	0,03	WT	0,06	WT
CM14	1	WT	0,03	WT	0,06	WT
CM15	1	WT	0,03	WT	0,06	WT
CM16	1	WT	0,03	WT	0,03	WT
CM17	4	WT	0,03	WT	0,03	WT

[a] WT, wild type; non-WT, non-wild type.

Table S4. Relative fold-change expressions in the twenty-six *C. parapsilosis* fluconazole-resistant strains

FLC MIC (µg mL^{-1})	Strain	CDR1	MDR1	ERG11
8	Cp23	1,39	1,04	0,44
	Cp25	1,02	0,69	0,38
	Cp26	**2,3**	**4,33**	1,13
	Cp37	1,28	**4,01**	0,5
	Cp85	**2,53**	**9,06**	**2,53**
	Cp100	1,78	**7,78**	**10,54**
	Cp122	0,59	**4,75**	0,35
	Cp175	1,78	**7,41**	0,77
	D154	1,12	**13,94**	0,41
16	Cp126	1,72	**13,54**	1,37
	Cp157	0,71	**11,91**	0,54
	D150	0,3	**3,8**	1,25
	D151	1,77	**3,05**	1,04
	D157	1	**26,58**	0,6
	D158	**1,99**	**12,07**	0,99
	D159	1,27	**14,1**	0,35
32	Cp2	1,41	1,58	1,15
	D162	0,13	**3,88**	0,84
	D195	**2,23**	**3,48**	1,83
	D196	**4,09**	**5,9**	38,88
	D203	1,41	**3,77**	**2,51**
	D221	1,68	**3,34**	**2,32**
	D222	**2,45**	**4,83**	**2,59**
64	Cp1	0,37	1,3	0,56
	Cp141	0,63	**2392,74**	0,8
	D223	**2,05**	1,51	**2,48**

Overexpression was defined as 2-fold increase, marked at bold.

117

Table S5. Deleterious phenotypes based on SIFT analysis – part I

CPS-B	CPS-C	GENE_NAME	CHROM	POS	REF_ALLELE	ALT_ALLELE	TRANSCRIPT_ID	GENE_ID	GENE_NAME	REGION	VARIANT_TYPE
1	0	CPAR2_200100	cpar_Chr_2	14397	G	A	CPAR2_200100_mRNA	CPAR2_200100	CPAR2_200100	CDS	NONSYNONYMOUS
1	1	CPAR2_602540	cpar_Chr_6	599142	T	C	CPAR2_602540_mRNA	CPAR2_602540	CPAR2_602540	CDS	NONSYNONYMOUS
0	1	CPAR2_207980	cpar_Chr_2	1714457	G	C	CPAR2_207980_mRNA	CPAR2_207980	CPAR2_207980	CDS	NONSYNONYMOUS
0	1	CPAR2_702680	cpar_Chr_7	573233	G	T	CPAR2_702680_mRNA	CPAR2_702680	CPAR2_702680	CDS	NONSYNONYMOUS
1	1	CPAR2_602590	cpar_Chr_6	614660	C	T	CPAR2_602590_mRNA	CPAR2_602590	CPAR2_602590	CDS	NONSYNONYMOUS
1	1	CPAR2_602980	cpar_Chr_6	700123	C	T	CPAR2_602980_mRNA	CPAR2_602980	CPAR2_602980	CDS	NONSYNONYMOUS
0	1	CPAR2_405310	cpar_Chr_4	768461	C	T	CPAR2_405310_mRNA	CPAR2_405310	CPAR2_405310	CDS	NONSYNONYMOUS
0	1	CPAR2_204320	cpar_Chr_2	877224	C	A	CPAR2_204320_mRNA	CPAR2_204320	CPAR2_204320	CDS	NONSYNONYMOUS
1	0	CPAR2_100300	cpar_Chr_1	48995	C	G	CPAR2_100300_mRNA	CPAR2_100300	CPAR2_100300	CDS	NONSYNONYMOUS
1	0	CPAR2_209000	cpar_Chr_2	1934977	G	A	CPAR2_209000_mRNA	CPAR2_209000	CPAR2_209000	CDS	NONSYNONYMOUS
0	1	CPAR2_209250	cpar_Chr_2	1985443	G	A	CPAR2_209250_mRNA	CPAR2_209250	CPAR2_209250	CDS	NONSYNONYMOUS
1	0	CPAR2_209310	cpar_Chr_2	1994973	A	T	CPAR2_209310_mRNA	CPAR2_209310	CPAR2_209310	CDS	NONSYNONYMOUS
1	0	CPAR2_209840	cpar_Chr_2	2114188	C	T	CPAR2_209840_mRNA	CPAR2_209840	CPAR2_209840	CDS	NONSYNONYMOUS
0	1	CPAR2_212030	cpar_Chr_2	2595908	G	C	CPAR2_212030_mRNA	CPAR2_212030	CPAR2_212030	CDS	NONSYNONYMOUS

part I - continued

HOM/HET	REF_AMINO	ALT_AMINO	AMINO_POS	SIFT_SCORE	SIFT_MEDIAN	NUM_SEQS	dbSNP	SIFT_PREDICTION	Standard Name	Standard Name Ortholog | Best Hit
HOM	P	S	208	0,03	2,8	17	novel	DELETERIOUS	NA	POP3
HET	I	T	325	0,01	2,66	13	novel	DELETERIOUS	NA	Uncharacterised
HOM	S	C	1189	0	3,06	12	novel	DELETERIOUS	NA	GIN1
HET	A	S	147	0	2,77	17	novel	DELETERIOUS	NA	NBP2
HET	G	E	196	0	2,74	19	novel	DELETERIOUS	NA	PTK2
HET	S	L	20	0,01	3,08	13	novel	DELETERIOUS	NA	SEC8
HET	R	K	86	0,04	2,97	399	novel	DELETERIOUS	NA	RPS19A
HET	N	K	1608	0	2,56	35	novel	DELETERIOUS	NA	STT4
HET	G	R	151	0	2,81	72	novel	DELETERIOUS	TNA1	TNA1
HOM	L	F	319	0	3,34	11	novel	DELETERIOUS	NA	NA
HOM	G	E	95	0	2,65	334	novel	DELETERIOUS	NA	COQ5
HOM	S	R	558	0	3,05	25	novel	DELETERIOUS	NA	DCK1
HOM	S	L	130	0	3,41	6	novel	DELETERIOUS	NA	TES4
HOM	E	Q	146	0,03	3,03	10	novel	DELETERIOUS	NA	MTF1

part I - continued

Ortholog | Best Hit Species	Feature
C. albicans	Ortholog(s) have ribonuclease MRP activity, ribonuclease P activity and role in intronic box C/D RNA processing, nuclear-transcribed mRNA catabolic process, endonucleolytic cleavage-dependent decay, rRNA processing, tRNA processing
NA	Has domain(s) with predicted zinc ion binding activity
C. albicans	Ortholog(s) have role in DNA repair, DNA replication, DNA replication checkpoint signaling, chromatin silencing at telomere and maintenance of DNA repeat elements, more
C. albicans	Ortholog(s) have protein-macromolecule adaptor activity, role in inactivation of MAPK activity, negative regulation of MAPK cascade and cytoplasm localization
C. albicans	Ortholog(s) have protein kinase activity, role in G1/S transition of mitotic cell cycle, cellular ion homeostasis, putrescine transport, spermidine transport, spermine transport and cytoplasm, nucleus, plasma membrane localization
C. albicans	Ortholog(s) have role in Golgi inheritance, Golgi to plasma membrane transport, ascospore-type prospore membrane formation, endocytosis, endoplasmic reticulum inheritance, exocytosis
C. albicans	Ortholog(s) have structural constituent of ribosome activity, role in rRNA export from nucleus, ribosomal small subunit biogenesis and cytosolic small ribosomal subunit localization
C. albicans	Ortholog(s) have 1-phosphatidylinositol 4-kinase activity, cytoskeletal protein-membrane anchor activity
C. albicans	Ortholog(s) have carboxylic acid transmembrane transporter activity and role in carboxylic acid transport, quinolinic acid transmembrane transport
C. albicans	Ortholog of C. albicans SC5314 : C1_06970C_A, C. dubliniensis CD36 : Cd36_06520, Candida tenuis NRRL Y-1498 : CANTEDRAFT_120265 and Debaryomyces hansenii CBS767 : DEHA2F24728g
C. albicans	Ortholog(s) have 2-hexaprenyl-6-methoxy-1,4-benzoquinone methyltransferase activity, role in aerobic respiration, ubiquinone biosynthetic process and mitochondrial matrix, mitochondrion localization
C. albicans	Ortholog(s) have role in autophagy of mitochondrion, intracellular signal transduction and mitochondrion, plasma membrane localization
C. albicans	Has domain(s) with predicted acyl-CoA hydrolase activity and role in acyl-CoA metabolic process
C. albicans	Ortholog(s) have mitochondrial transcription factor activity

part I - continued

Ortholog	Best Hit Feature

Putative RNase MRP and nuclear RNase P component; decreased repressed by prostaglandins; Spider biofilm induced

NA

Protein involved in regulation of DNA-damage-induced filamentous growth; putative component of DNA replication checkpoint; ortholog of S. cerevisiae Mrc1p, an S-phase checkpoint protein; Hap43p-induced gene

Protein containing an SH3 domain; involved in vacuolar fusion in hyphae; mutants form multiple germ tubes; Spider biofilm induced

Putative protein kinase of polyamine import; mutation confers hypersensitivity to high concentrations of tunicamycin; YPD flow model biofilm induced; rat catheter and Spider biofilm induced

Predicted subunit of the exocyst complex, involved in exocytosis; localizes to a crescent on the surface of the hyphal tip

Putative ribosomal protein S19; protein level decreases in stationary phase cultures; Spider biofilm repressed

Putative phosphatidylinositol-4-kinase

Putative nicotinic acid transporter; detected at germ tube plasma membrane by mass spectrometry; transcript induced upon phagocytosis by macrophage; rat catheter biofilm induced

NA

Putative methyltransferase of ubiquinone biosynthesis; regulated by Gcn4; repressed by amino acid starvation (3-AT), Hap43; induced upon adherence to polystyrene; Spider biofilm repressed

Putative guanine nucleotide exchange factor; required for embedded filamentous growth; activates Rac1; has a DOCKER domain; similar to adjacent DCK2 and to S. cerevisiae Ylr422wp; regulated by Nrg1; Spider biofilm induced

Ortholog of C. dubliniensis CD36 : Cd36_20380, C. parapsilosis CDC317 : CPAR2_209840, Candida tropicalis MYA-3404 : CTRG_01513 and Candida albicans WO-1 : CAWG_04340

Putative mitochondrial RNA polymerase specificity factor; possibly an essential gene, disruptants not obtained by UAU1 method

Table S5. Deleterious phenotypes based on SIFT analysis – part II

CPS-B	CPS-C	GENE_NAME	CHROM	POS	REF_ALLELE	ALT_ALLELE	TRANSCRIPT_ID	GENE_ID	GENE_NAME	REGION	VARIANT_TYPE
0	1	CPAR2_402300	cpar_Chr_3	507455	G	T	CPAR2_402300_mRNA	CPAR2_402300	CPAR2_402300	CDS	NONSYNONYMOUS
1	0	CPAR2_704300	cpar_Chr_7	940606	G	A	CPAR2_704300_mRNA	CPAR2_704300	CPAR2_704300	CDS	NONSYNONYMOUS
0	1	CPAR2_803770	cpar_Chr_8	836074	T	C	CPAR2_803770_mRNA	CPAR2_803770	CPAR2_803770	CDS	NONSYNONYMOUS
1	1	CPAR2_601970	cpar_Chr_6	470646	G	T	CPAR2_601970_mRNA	CPAR2_601970	CPAR2_601970	CDS	NONSYNONYMOUS
0	1	CPAR2_804030	cpar_Chr_8	898967	T	G	CPAR2_804030_mRNA	CPAR2_804030	CPAR2_804030	CDS	NONSYNONYMOUS
0	1	CPAR2_804640	cpar_Chr_8	1031472	T	A	CPAR2_804640_mRNA	CPAR2_804640	CPAR2_804640	CDS	NONSYNONYMOUS
0	1	CPAR2_807270	cpar_Chr_8	1678868	G	A	CPAR2_807270_mRNA	CPAR2_807270	CPAR2_807270	CDS	NONSYNONYMOUS
1	0	CPAR2_209780	cpar_Chr_2	2098759	G	T	CPAR2_209780_mRNA	CPAR2_209780	CPAR2_209780	CDS	STOP-GAIN
0	1	CPAR2_303750	cpar_Chr_3	1313750	A	T	CPAR2_303750_mRNA	CPAR2_303750	CPAR2_303750	CDS	STOP-GAIN

part II - continued

HOM/HET	REF_AMINO	ALT_AMINO	AMINO_POS	SIFT_SCORE	SIFT_MEDIAN	NUM_SEQS	dbSNP	SIFT_PREDICTION	Standard Name	Standard Name Ortholog | Best Hit
HOM	P	T	120	0	3,12	9	novel	DELETERIOUS	NA	NA
HOM	P	S	223	0,01	2,66	34	novel	DELETERIOUS	NA	CYR1
HOM	Y	H	326	0	2,61	294	novel	DELETERIOUS	NA	COQ1
HET	A	E	174	0	2,62	54	novel	DELETERIOUS	NA	LIP1
HOM	Q	P	1554	0	2,92	398	novel	DELETERIOUS	NA	FKS2
HOM	N	Y	923	0,04	2,94	26	novel	DELETERIOUS	NA	CLA4
HOM	G	R	604	0,01	3,33	9	novel	DELETERIOUS	MRR1	MRR1
HOM	S	*	85	NA	NA	NA	novel	NA	NA	CNT
HET	L	*	429	NA	NA	NA	novel	NA	NA	HMS1

part II - continued

Ortholog | Best Hit Species	Feature
C. albicans	Ortholog of C. albicans SC5314 : C4_00050W_A, C. dubliniensis CD36 : Cd36_40110, C. auris B8441 : B9J08_003539 and Candida tenuis NRRL Y-1498 : CANTEDRAFT_94507
C. albicans	Ortholog(s) have adenylate cyclase activity, manganese ion binding activity. In C. albicans: class III adenylyl cyclase; mutant lacks cAMP; involved in regulation of filamentation, phenotypic switching and mating; mutant hyphal growth defect rescued by exogenous cAMP; downstream of Ras1p and CO2 signaling
C. albicans	Ortholog(s) have di-trans,poly-cis-decaprenylcistransferase activity, trans-hexaprenyltranstransferase activity and role in farnesyl diphosphate biosynthetic process, mevalonate pathway, ubiquinone biosynthetic process
C. albicans	Has domain(s) with predicted triglyceride lipase activity and role in lipid catabolic process
C. albicans	Has domain(s) with predicted 1,3-beta-D-glucan synthase activity, role in (1->3)-beta-D-glucan biosynthetic process and 1,3-beta-D-glucan synthase complex localization
C. albicans	Ortholog(s) have enzyme binding, kinase activity, protein serine/threonine kinase activity
C. albicans	Regulator of MDR1 transcription; expression increased in fluconazole and voriconazole resistant strains
C. albicans	Ortholog(s) have nucleoside transmembrane transporter activity and role in nucleoside transport, uridine transport
C. albicans	Has domain(s) with predicted protein dimerization activity

part II - continued

Ortholog | Best Hit Feature
NA
Class III adenylyl cyclase; mutant lacks cAMP; involved in regulation of filamentation, phenotypic switching and mating; mutant hyphal growth defect rescued by exogenous cAMP; downstream of Ras1p and CO2 signaling
Ortholog(s) have di-trans,poly-cis-decaprenylcistransferase activity, trans-hexaprenyltranstransferase activity and role in farnesyl diphosphate biosynthetic process, mevalonate pathway, ubiquinone biosynthetic process
Secreted lipase, member of a lipase gene family whose members are expressed differentially in response to carbon source and during infection; may have a role in nutrition and/or in creating an acidic microenvironment
Protein similar to beta-1,3-glucan synthase; 16 predicted membrane-spanning regions; transcript regulated by Nrg1; very low gene expression in yeast-form and hyphal cells
Ste20p family Ser/Thr kinase required for wild-type filamentous growth, organ colonization and virulence in mouse systemic infection; role in chlamydospore formation; functional homolog of S. cerevisiae Cla4p; mutant caspofungin sensitive
Putative Zn(II)2Cys6 transcription factor; regulator of MDR1 transcription; gain-of-function mutations cause upregulation of MDR1 (a plasma membrane multidrug efflux pump) and multidrug resistance; Hap43-induced
CNT family H(+)/nucleoside symporter; transports adenosine, uridine, inosine, guanosine, tubercidin; variant alleles for high/low-affinity isoforms; S or G at residue 328 affects specificity; Spider, flow model biofilm induced
hLh domain Myc-type transcript factor; required for morphogenesis induced by elevated temperature or Hsp90 compromise; acts downstream of Pcl1; Spider biofilm induced

NA, non applicable.

Table S6. Gene copy number variation

Gene	CPS-A	CPS-B	CPS-C
CPAR2_103140	0,295318182	0,303490099	0,35004497
CPAR2_108130	2,637681818	4,720990099	4,553136095
CPAR2_108860	2,161045455	4,267861386	4,050698225
CPAR2_108870	2,236988636	4,573217822	4,186224852
CPAR2_108880	2,169659091	4,521217822	4,255704142
CPAR2_108890	1,997522727	4,350227723	4,266307692
CPAR2_108900	2,034693182	4,313960396	4,185491124
CPAR2_108910	2,133772727	4,29439604	3,894863905
CPAR2_108915	2,037590909	4,501821782	4,109337278
CPAR2_108920	2,233147727	4,456940594	4,656485207
CPAR2_108930	2,040806818	3,924366337	3,875218935
CPAR2_108940	2,062863636	4,108247525	4,072378698
CPAR2_108950	2,102386364	3,993811881	3,994852071
CPAR2_108960	1,891522727	4,03249505	3,844840237
CPAR2_108970	1,959	3,985475248	3,965005917
CPAR2_108980	2,047431818	4,129633663	4,059384615
CPAR2_108990	1,901261364	3,903782178	4,099467456
CPAR2_109000	2,066306818	3,940851485	4,055656805
CPAR2_109010	1,980545455	4,056009901	3,80356213
CPAR2_109020	2,317465909	4,335178218	4,357372781
CPAR2_109030	2,134761364	4,374366337	4,298497041
CPAR2_109040	2,221738636	4,132227723	4,095254438
CPAR2_109050	2,116488636	4,538188119	4,369100592
CPAR2_109060	2,022193182	6,141633663	6,014579882
CPAR2_109070	1,997386364	5,962415842	6,022911243
CPAR2_109080	1,995284091	6,040356436	5,991609467
CPAR2_109090	2,118136364	5,70780198	5,840568047
CPAR2_109100	1,802465909	3,686653465	3,737147929
CPAR2_109110	2,193715909	5,783089109	5,59139645
CPAR2_109120	1,925431818	5,589405941	5,638698225
CPAR2_109130	1,966386364	6,002138614	5,841408284
CPAR2_109140	2,168613636	6,236910891	6,56035503
CPAR2_109150	1,987909091	5,65339604	5,984023669
CPAR2_109160	2,179011364	6,103108911	6,026449704
CPAR2_109170	2,106261364	6,273217822	6,064248521
CPAR2_109180	1,964670455	5,90829703	5,964295858
CPAR2_109190	1,923011364	5,717752475	5,832733728
CPAR2_109200	2,083818182	6,12719802	6,435775148
CPAR2_109210	2,054795455	6,102376238	6,134650888
CPAR2_109220	2,069068182	5,884980198	5,985443787
CPAR2_109230	1,947977273	5,662673267	5,735668639
CPAR2_109240	2,013943182	5,811376238	6,180733728
CPAR2_109250	2,013215909	5,714712871	5,980331361
CPAR2_109260	1,926568182	5,446089109	5,687100592
CPAR2_109270	2,127590909	6,068168317	6,15295858
CPAR2_109280	2,047454545	5,871514851	6,197526627

CPAR2_109290	1,860420455	5,503851485	5,969739645
CPAR2_109300	2,133556818	5,661019802	6,176710059
CPAR2_109310	1,921261364	5,402247525	5,86947929
CPAR2_109320	2,087568182	5,66870297	6,026035503
CPAR2_109330	1,997147727	5,532811881	5,885988166
CPAR2_109340	2,294602273	6,26290099	6,422118343
CPAR2_109350	2,013238636	6,122584158	6,106343195
CPAR2_109360	2,231511364	6,185148515	6,292449704
CPAR2_109370	2,087238636	5,786267327	6,165005917
CPAR2_109380	2,341352273	6,083207921	6,439976331
CPAR2_109390	2,756488636	5,545	5,731005917
CPAR2_109400	2,308875	4,51150495	4,441230769
CPAR2_109410	1,989045455	3,817267327	3,945550296
CPAR2_109420	2,135193182	3,75639604	3,975905325
CPAR2_109430	2,050886364	3,96629703	3,780343195
CPAR2_109440	1,916090909	3,687871287	3,975218935
CPAR2_109450	2,012693182	3,808346535	3,931242604
CPAR2_109460	2,09375	4,017861386	4,379751479
CPAR2_200520	3,352906977	3,019540816	3,028409639
CPAR2_200890	0,97624186	1,162918367	0,974304819
CPAR2_201160	3,572418605	3,344765306	3,462409639
CPAR2_209690	3,484988372	3,829469388	3,660180723
CPAR2_210110	2,945023256	3,054897959	2,793036145
CPAR2_300110	3,690372881	3,982646154	2,979450292
CPAR2_300120	2,98959322	3,074769231	2,457695906
CPAR2_300610	3,106971751	2,741784615	2,638444444
CPAR2_301450	3,669706215	3,751446154	3,517380117
CPAR2_304370	**4,410606742**	**14,80300971**	**4,369005988**
CPAR2_402040	3,584438202	3,069747573	3,550407186
CPAR2_600440	0,332830168	0,418278469	0,361001156
CPAR2_601730	0,692731844	0,638742584	0,706195376
CPAR2_601740	0,123306145	0,126608612	0,121427746
CPAR2_703720	2,90560452	2,982924623	3,101592814
CPAR2_803040	0,412871264	0,392752764	0,471167273
CPAR2_805410	0,45004023	0,483484422	0,45073697
CPAR2_806420	0,939958621	1,012492462	1,039008485
CPAR2_806620	3,136528736	2,71721608	3,141442424

Table S7. Relative gene expression level in the *ndt80Δ* and *ndt8ΔΔ* strains

Gene	*ndt80Δ*	*ndt80ΔΔ*
NDT80	1,605	
ALS3	1,174	1,179
ALS7	211,85	179,95
RHR2	2,627	0,614
ACE2	3,322	3,118
MKC1	2,803	36,495
STP3	1,853	0,953
CWH41	1,867	2,226
OCH1	1,215	1,06
GZF3	1,467	0,878
BCR1	1,578	1,74
CPH2	1,246	4,251
EFG1	1,121	0,62
UME6	4,683	13,104
CZF1	0,763	0,378

Publications

Paper I

Candida parapsilosis virulence and antifungal resistance mechanisms: a comprehensive review of key determinants

Journal of
Fungi

Review

Candida parapsilosis Virulence and Antifungal Resistance Mechanisms: A Comprehensive Review of Key Determinants

Joana Branco [1,2,*], Isabel M. Miranda [3,†] and Acácio G. Rodrigues [1,2,†]

1 Division of Microbiology, Department of Pathology, Faculty of Medicine, University of Porto, 4200-319 Porto, Portugal
2 Center for Health Technology and Services Research—CINTESIS@RISE, Faculty of Medicine, University of Porto, 4200-450 Porto, Portugal
3 Cardiovascular Research & Development Centre—UnIC@RISE, Faculty of Medicine, University of Porto, 4200-450 Porto, Portugal
* Correspondence: joanabranco@med.up.pt; Tel./Fax: +351-225513662
† These authors contributed equally to this work.

Abstract: Candida parapsilosis is the second most common Candida species isolated in Asia, Southern Europe, and Latin America and is often involved in invasive infections that seriously impact human health. This pathogen is part of the psilosis complex, which also includes Candida orthopsilosis and Candida metapsilosis. C. parapsilosis infections are particularly prevalent among neonates with low birth weights, individuals who are immunocompromised, and patients who require prolonged use of a central venous catheter or other indwelling devices, whose surfaces C. parapsilosis exhibits an enhanced capacity to adhere to and form biofilms. Despite this well-acknowledged prevalence, the biology of C. parapsilosis has not been as extensively explored as that of Candida albicans. In this paper, we describe the molecular mechanistic pathways of virulence in C. parapsilosis and show how they differ from those of C. albicans. We also describe the mode of action of antifungal drugs used for the treatment of Candida infections, namely, polyenes, echinocandins, and azoles, as well as the resistance mechanisms developed by C. parapsilosis to overcome them. Finally, we stress the importance of the ongoing search for species-specific features that may aid the development of effective control strategies and thus reduce the burden on patients and healthcare costs.

Keywords: fungal infections; *Candida* spp.; *Candida parapsilosis*; virulence attributes; polyenes; echinocandins; azoles; antifungal resistance; biofilm formation; healthcare-related infections

1. *Candida* and Human Disease

Fungi can cause a diversity of health disorders in humans, ranging from allergic syndromes and mucocutaneous infections to invasive diseases that seriously threaten life. It is estimated that fungal diseases annually affect over a billion people and cause 1.5 million deaths worldwide [1]. Invasive fungal infections caused by *Candida* species are widely associated with high rates of severe illness and may be responsible for as many as 30% of all deaths from fungal disease. In the United States, the health cost attributable to prolonged hospitalizations resulting from candidaemia is estimated at USD 46,684 per patient [2].

Candidosis is a broad term that refers to cutaneous, mucosal, and deep-seated organ infections caused by opportunistic pathogens of the *Candida* genus [3]. *Candida* spp. are commensal yeasts commonly found in the human gastrointestinal tract, mucous membranes, and skin. Disruption of the gastrointestinal and cutaneous barriers following shock, localized infections, or the replacement of an intravascular catheter can all promote invasive candidosis, which is widely recognized as a major cause of morbidity and mortality. The patient populations most at risk are the elderly, premature newborns, and those with

compromised immune systems due to HIV, chemotherapy, or transplant-necessitated immunosuppression therapy [4]. Invasive candidosis is a disorder that can potentially affect any organ. Each distinct *Candida* species exhibits its own unique characteristics in terms of its invasive potential, virulence, and antifungal susceptibility pattern [3].

The distribution of *Candida* species varies geographically, with notable differences between hospital centers. The underlying condition of the patient and whether they have experienced previous antifungal therapy both have an effect on the distribution and frequency of *Candida* spp. [5]. While *C. albicans* is the most common pathogen associated with nosocomial invasive candidosis worldwide, an increasing number of infections by non-albicans *Candida* species (NACs) have also been reported in recent years, including *Candida glabrata, Candida parapsilosis, Candida tropicalis, Candida krusei*, and *Candida auris*, among others [6]. Of these, *C. glabrata* predominates in Northern European countries and in the United States, but *C. parapsilosis* and/or *C. tropicalis* are more prevalent in India, Pakistan, Latin America, and Mediterranean countries [3].

2. Candida parapsilosis

Since its discovery in 1928, *C. parapsilosis* has undergone several changes in phylogenetic classification. Initially isolated from the stool of a patient with diarrhea in Puerto Rico, the species was first classified as *Monilia parapsilosis* (i.e., a species of the *Monilia* genus, incapable of fermenting maltose) to distinguish it from *Monilia psilosis*, which is today known as *C. albicans* [7]. In 1932, it was renamed *Candida parapsilosis*. In 2005, Tavanti et al. [8] confirmed, through multilocus sequence typing, the existence of a *C. parapsilosis* complex comprising three distinct species: *Candida parapsilosis sensu stricto, Candida orthopsilosis*, and *Candida metapsilosis*. In this paper, we focus on *Candida parapsilosis*.

C. parapsilosis is widely distributed in nature and is often isolated from a variety of non-human sources, such as domestic animals, insects, soil, and marine environments [9]. This yeast successfully colonizes the human skin and mucosal membranes as a commensal microorganism, wherein the hands of healthcare professionals are recognized as a major vector for *C. parapsilosis* nosocomial acquisition [10–12]. In addition, the selective ability of *C. parapsilosis* to grow in hyperalimentation solutions promotes the infection risk by this pathogen [13]. *C. parapsilosis* represents a high risk for immunocompromised individuals, such as HIV sufferers and surgical patients, particularly those subjected to gastrointestinal track surgery. Additionally, patients requiring prolonged use of a central venous catheter or other indwelling devices are at high risk, due to the innate ability of *C. parapsilosis* to adhere to prosthetic surfaces and implanted medical devices. In such cases, biofilm formation typically begins soon after attachment. When the structure is mature, it greatly decreases the ability of antifungals to reach cells, with potentially life-threatening consequences in the host [14–16]. Because *C. parapsilosis* is responsible for one-third of neonatal *Candida* infections, with a mortality rate of approximately 10%, low-birth-weight neonates are at especially high risk [17].

The distribution of *C. parapsilosis* recovered from patients with bloodstream infections in various studies conducted in different geographical areas shows that its relative dominance differs according to region [5]. It is the second most common *Candida* isolate in Latin America countries, such as Argentina, Peru and Brazil. In Venezuela and Colombia, *C. parapsilosis* even outranks *C. albicans* infections [5,18,19]. The incidence of *C. parapsilosis* infections in Europe is region-dependent; in Southern European hospitals (Portugal, Spain, Italy, and Greece) it is the second most isolated species [20–23], and in central and northern countries of Europe the incidence of *C. parapsilosis* ranks third, after that of *C. albicans* and *C. glabrata* [24–26]. A different prevalence was also reported in North American countries, Canada and USA, where *C. parapsilosis* ranks second and third, respectively [27–30]. According to studies of bloodstream fungal infections in Asia (China and Japan), *C. parapsilosis* is commonly found after *C. albicans* [31,32], while in India it ranks third [33]. A similar incidence of infection was observed in Australia [34].

The two cryptic *psilosis* species, *Candida orthopsilosis* and *Candida metapsilosis*, are also opportunistic pathogens, associated with local and systemic diseases. As with *C. parapsilosis*, their frequency and distribution reportedly differ in distinct geographical areas [35,36].

C. parapsilosis is a diploid pathogen, with eight chromosome pairs and an estimated genome size of 13.1 Mb. From the 5837 ORFs identified in this species, only 107 (1.83%) have actually been characterized [37]. Its genome is highly conserved; compared to other *Candida* spp., it exhibits a remarkably low level of heterozygosity with just one single nucleotide polymorphism (SNP) per 15,553 bases, more than 70 times less than the corresponding number in the closely related *Lodderomyces elongisporus* [38].

The yeast cells of *C. parapsilosis* display an oval, round, or cylindrical shape, and their colony phenotypes have been identified as crepe, concentric, smooth, or crater [13,39]. Unlike *C. albicans*, *C. parapsilosis* does not form true hyphae; it only exists as yeast or in pseudohyphal forms. Form and colony phenotypes are intimately linked; cells exhibiting crepe and concentric phenotypes are almost entirely pseudohyphal, whereas those with smooth and crater phenotypes are mostly yeast-like [39].

3. Virulence Attributes

Similarly to other microorganisms, *Candida* species have developed several specific and effective strategies to enhance their pathogenicity. The virulence of *C. parapsilosis* is mainly attributed to its intrinsic ability to adhere to the abiotic surfaces of medical devices and prosthetic materials, and to the host's mucosal epithelium. This ability is crucial for biofilm formation and consequently damage to the host [15,40].

Researchers have found that the ability to colonize upon mucosal surfaces or inert materials varies among *Candida* species [41]. An unusually high intraspecies variation in terms of adhesion ability has also been identified among clinical isolates of *C. parapsilosis*, compared with other *Candida* species. A correlation between the site of isolation and the rate of adhesion has also been reported, as *C. parapsilosis* mucocutaneous isolates demonstrate higher adhesiveness [41].

3.1. Cell Adhesion

Adhesion is an important, multifactorial process that is mediated by the characteristics of fungal and host (biotic or abiotic) cells, including cell surface hydrophobicity, cell wall composition, and growth conditions [42]. Initially, the adhesion of the yeast cells is highly dependent upon hydrophobic interactions between the microorganism and host surfaces. Cell surface hydrophobicity is strongly correlated with adhesion to both polystyrene/polyetherurethane surfaces and to epithelial cells. *Candida* species generally exhibit a high degree of cell surface hydrophobicity [43].

In adhesion, the key trigger interaction is promoted by specific cell wall proteins, namely adhesins. This process promotes the attachment of the fungal cells to other microorganisms, the host's epithelium, and abiotic surfaces [40]. Among *Candida* spp., several adhesin families are involved in adherence. Important adhesin families include: (i) the hyphal wall protein (Hwp) family, which includes five proteins, namely, Hwp1, Hwp2, Rbt1, Eap1, and Ywp1, that play a role in *C. albicans* biofilm formation [42,44]; (ii) the adhesins of the *EPA* (epithelial adhesion) family in *C. glabrata*, comprising 23 genes, of which *EPA1*, *EPA6*, and *EPA7* are described as the most important for the adhesion process in this species [42,44,45]; and (iii) the Als-like (agglutinin-like sequence) family encoding large-cell-surface glycoproteins involved in *Candida* adhesion, including *C. albicans*, *C. parapsilosis*, *C. tropicalis*, *C. dubliniensis*, *C. lusitaniae*, and *C. guilliermondii* [42,44]. Among the eight Als members described in *C. albicans*, Als3 has the most profound impact on biofilm formation; its deletion causes a severe biofilm formation defect [46]. In *C. parapsilosis*, five Als proteins are present on the surface of the pseudohyphae, and the ortholog CaAls7 has been described as a determinant for adhesion to host epithelial cells [47,48]. Other adhesion proteins and non-protein factors with similar properties, such as Eap1, Iff4, Mp65, Ecm33,

Utr2, Int1, and Mnt1, have also been identified in *Candida* species; however, these have not been widely studied to date [49].

3.2. Secretion of Hydrolytic Enzymes

Candida species can produce and secrete several hydrolytic enzymes, including secreted aspartyl proteases (SAPs), lipases (LIPs), and phospholipases. The activity of these enzymes is closely linked with *Candida*'s pathogenicity, such adhesion, cell damage, and the invasion of host tissues [40].

The production of SAPs by *Candida* cells aims to degrade structural and immunological defense proteins in the host, facilitating the invasion and colonization of the host tissue. Compared to *C. albicans*, *C. parapsilosis* expresses less SAP activity [50]. To date, three aspartyl protease-encoding genes (*SAPP1* to *SAPP3*) have been identified in *C. parapsilosis*, with a wide variability in expression among different isolates [51]. Isolates from body surfaces, such as skin or vaginal mucosa, are more invasive than those recovered from systemic infections or from environmental surfaces, due to the production of such enzymes [52].

In addition to SAPs, enzymes categorized as lipases catalyze both the hydrolysis and synthesis of triacylglycerols. Of the four secreted-lipase-encoding genes identified in the *C. parapsilosis* genome, only two (*LIP1* and *LIP2*) have been confirmed as able to encode functionally active proteins. Although the production of LIPs varies greatly among *C. parapsilosis* isolates, ranging from 36% to 80%, their role in enhanced pathogenicity has been confirmed [53]. The putative roles played by LIPs in a successful host invasion include the digestion of lipids for nutrient acquisition, the enhancement of adhesion and biofilm formation, and the suppression of immune response, among others [54,55].

Other hydrolytic enzymes have also been described, including secreted phospholipases, which hydrolyze phospholipids and fatty acids, thereby exposing host receptors and facilitating adhesion; however, these are still poorly understood in *C. parapsilosis* [56].

3.3. Biofilm Formation

Biofilms have been described as an organized community, comprising a dense network of microbial cells embedded in an extracellular matrix (ECM) of polymers [13]. Biofilm formation is a potent virulence attribute of several *Candida* species. Biofilm formation during infection has been linked to higher mortality rates in cases involving such species when compared with isolates incapable of forming biofilm [57]. Biofilm development is a well-regulated process comprising three sequential stages (Figure 1): an early phase, involving the entire adhesion process of the cells, as described above; an intermediated phase, and, finally, a maturation/dispersion phase [40]. In the intermediate phase, following initial fungal adhesion, yeast cells undergo a morphology transition from yeast to filamentous or pseudohyphal forms, forming a mixed population with a multilayer formation (Figure 1). Afterwards, biofilm maturation begins through the production and secretion of a polysaccharide-rich extracellular matrix, formed by polysaccharides, proteins, lipids, and nucleic acids, which provides structural and functional stability to the biofilm [40,58].

The biofilm's architecture, morphology, and thickness also vary widely among *Candida* species and between strains [58]. These features are influenced by several host and *Candida*-derived variables, including: (i) physiological conditions, such as pH and oxygen concentration; (ii) fluid flow at the infection site, which influences nutrient exchange and impacts the biofilm's structural integrity; (iii) available nutrients in the growth media, including sugars, lipids, and serum; and (iv) the material on which the biofilm grows (those typically used in medical devices include silicone, latex, and polyurethane, among others); and (v) community microbial interactions, either fungal–fungal or fungal–bacterial, which modulate the ability of *Candida* to form biofilm and also represent a promising topic for future research [58–60].

Figure 1. Illustration of biofilm formation cycle in *Candida* spp. Biofilm development consists of three stages: an early phase, in which cells adhere to biotic or abiotic surfaces; an intermediate phase, involving cell proliferation and the formation of a mixed population; and, finally, a maturation/dispersion phase, characterized by the production of the extracellular matrix and the massive dispersion of cells. The detachment and dispersion of daughter cells occurs in all stages of biofilm development.

C. parapsilosis biofilm growth is especially common in patients fitted with a central venous catheter who receive total parenteral nutrition [61,62]. The biofilm structure of *C. parapsilosis* exhibits high variability among clinical isolates. Because *C. parapsilosis* does not form true hyphae, its biofilm is composed of aggregated blastoconidia and pseudohyphae that occupy a volume lower than that of other *Candida* species [63,64]. In addition, the extracellular matrix of *C. parapsilosis* biofilm is mainly composed of carbohydrates and low levels of protein [63].

The ability to form biofilms is closely related to its virulence potential, because only limited penetration of substances is possible through the biofilm matrix, resulting in a greatly decreased susceptibility to antimicrobial agents [65,66]. The development of the biofilm also serves to counter the host immune response by inhibiting macrophage phagocytosis and antibody activity [65].

The process of biofilm development involves a massive cell detachment during the final maturation phase, with consequent dispersion that promotes the colonization of new locations and surfaces [40]. However, Uppuluri et al. [67] found that dispersion was not confined to the maturation phase and occurs continuously during the biofilm development process. A more robust biofilm is produced by dispersed cells compared with the biofilm formed by initial planktonic mother cells such that the virulence potential increases over generations. All of these findings represent matters of serious clinical concern, not only for the treatment of patient infections but also in terms of public health [66].

The complexity of all stages of biofilm formation, involving such phenomena as the control of adhesion, morphology changes, and ECM production, among others, requires an extensive and complex regulatory network [68]. The biofilm formation regulatory process has been extensively studied in *C. albicans*; however, as with other characteristics, such knowledge cannot be simply transposed to other *Candida* species. For example, the four transcription factors *BRG1*, *TEC1*, *ROB1*, and *FLO8* are all involved in the biofilm regulatory network of *C. albicans* but play no role in the biofilm regulation of *C. parapsilosis* [68,69]. Conversely, *CZF1*, *UME6*, *GZF3*, and *CPH2* have been highlighted as key contributors to biofilm formation in *C. parapsilosis*, but these genes play a negligible role in this process in *C. albicans*. One recent report identified the direct role of Ndt80 as a repressor of *C. parapsilosis* virulence attributes, thereby diverging functionally from its homolog in the closely related fungal pathogen *C. albicans* [70]. However, other genes required for biofilm development, such as *ACE2*, *BCR1*, and *EFG1*, have been found to perform a similar function in both species [68,71].

4. Antifungals and Resistance Mechanisms

Despite ongoing research efforts concerning new therapeutic compounds and treatment strategies, only a limited number of options of antifungal drugs are available for the treatment of candidosis [72]. Currently, the arsenal of systemic antifungals available for clinical use consists of only three major drug classes: polyenes, echinocandins, and azoles [73].

4.1. Polyenes

Amphotericin B (AmB) is the most used member of the class of polyenes, being clinically used for more than 55 years [73]. Its potent fungicidal activity is derived from its interaction with the ergosterol of fungal cells by binding to the lipid bilayer, forming pores in the cell membrane and facilitating the leakage of intracellular components, such as potassium ions (K^+), into the extracellular medium (Figure 2A) [74]. Consequently, this interaction results in a drastic change in cell permeability, ultimately leading to cell lysis. This antifungal has low solubility and is highly toxic to the host cell due to the close structural relationship between ergosterol and cholesterol, the mammalian membrane sterol. This limits its use in long-term antifungal therapy [75]. However, less toxic, lipid-based polyene formulations have now been developed, including liposomal amphotericin B (LAmB), which has become the first-line treatment for various types of invasive fungal infections [76].

The development of fungal resistance to polyenes is rare. Most *Candida* spp., including *C. albicans*, *C. glabrata*, and *C. parapsilosis*, are generally considered to be susceptible to AmB, with surveillance studies reporting an AmB susceptibility rate close to 100% [77]. Recently, a global pooled prevalence meta-analysis estimated *C. parapsilosis* AmB-resistance at 1.3% [78]. Emerging AmB resistance has been reported in species, such as *C. auris* [79]. The resistance mechanisms of this class are less well understood than those of echinocandins and azoles; nevertheless, several hypotheses have been forwarded to explain resistance, as illustrated in Figure 2A. These include: (i) sterol composition modulation through the depletion or replacement of ergosterol triggered by mutations in genes involved in the ergosterol biosynthesis pathway, specifically in *ERG1* to *ERG4*, *ERG6*, and *ERG11* [80–82]; (ii) enhanced defense against oxidative damage to break down the reactive oxygen species (ROS) that are produced under AmB exposure, either by means of catalase activity and/or by the molecular chaperones of the heat shock protein (HSP) family, namely, Hsp90 and Hsp70 [83–85].

4.2. Echinocandins

Echinocandins, i.e., caspofungin, micafungin, and anidulafungin, are the newest class of antifungal drugs available for the treatment of invasive fungal infections and offer an excellent safety profile combined with high fungicidal activity [86,87]. They noncompetitively inhibit (1,3)-β-D-glucan synthase, which is responsible for the biosynthesis of 1,3-β-D-glucan, a crucial structural component of fungal cell walls [88,89]. Specifically, echinocandins target the catalytic subunits *FKS1* of β-D-glucan synthase, encoded by *FKS1* and *FKS2* genes, leading to the disruption of cell wall glucan, osmotic instability, cell lysis, and death for most species (Figure 2B) [90,91]. Although their antifungal spectrum is limited, echinocandins are fungicidal against most *Candida* spp., including azole-resistant strains and biofilm [92,93]. However, as the use of these drugs has expanded, reports of resistance to echinocandin treatments among *Candida* spp. have increased [93]. In particular, *C. parapsilosis* tends to be associated with increased in vitro minimum inhibitory concentrations (MICs) of echinocandin [94,95], raising concerns that such drugs may facilitated the development of high levels of resistance [96–98].
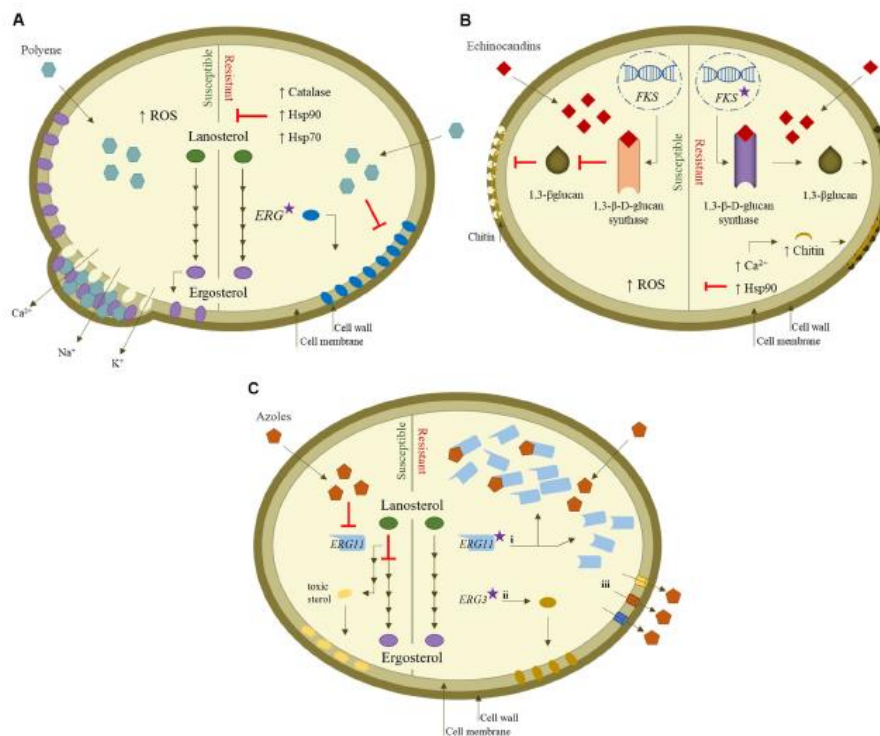
Figure 2. Mechanism of action of antifungals against *Candida* spp. and mechanisms underlying drug resistance. (**A**) Polyenes act by forming polyene/ergosterol aggregates, destabilizing the fungal membrane. The action of polyenes can be overcome through mutations in ergosterol biosynthesis genes responsible for altered sterol composition and by the activation of stress response pathways, such as catalase and Hsp. (**B**) Echinocandins act as noncompetitive inhibitors of (1,3)-β-D-glucan synthase, encoded by *FKS* genes, causing a depletion of the 1,3-β-glucan in the cell wall. Echinocandin resistance in *Candida* is associated with mutations in *FKS* genes and the activation of cell wall stress response mediator pathways, such as Hsp90 and calcineurin (Ca^{2+}), increasing the chitin content. (**C**) Azoles target and inhibit the enzyme lanosterol 14α-demethylase, encoded by the *ERG11* gene, leading to the accumulation of toxic sterol. Azole resistance involves: (i) point mutations in the *ERG11* gene, which can be responsible for its overexpression and/or the inhibition of enzyme lanosterol 14α-demethylase, due to the decrease in azole–target binding affinity; (ii) mutations in *ERG* genes involved in the ergosterol biosynthesis pathway, particularly in *ERG3*; and (iii) increased efflux of the azole drugs from the fungal cell through the overexpression of multidrug efflux pumps. Red T-shaped bars indicate inhibition. Star icon indicates gene mutation.

Decreased echinocandin susceptibility can occur via two main mechanisms (Figure 2B): (i) an adaptive stress response mechanism, involving a compensatory increase in the synthesis of chitin (an essential cell wall component) that is mediated, for example, via the activation of the calcineurin (Ca^{2+}) signaling pathway. The activation of this pathway is initially signaled by the Hsp90 chaperone, a key regulator of cellular stress response, and thus

confers protection against the antifungal agent [99–101]; (ii) acquired or intrinsic mutations in genes encoding *FKS1* and *FKS2*, characterized by amino acid substitutions in specific regions clustered around two highly conserved regions (termed hot spots 1 and 2) of *Fksp*, which is generally correlated with increased resistance to such drugs [95,102,103]. Acquired mutations have been reported for *C. albicans*, *C. tropicalis*, *C. krusei*, and *C. glabrata* [102,104] but not yet for *C. parapsilosis* [96,105]. In *C. parapsilosis*, naturally occurring *FKS1* mutations in the hot spot 1 region were found to be responsible for the intrinsic reduced susceptibility of this species to echinocandins [106].

4.3. Azoles

Azoles represent the largest class of antifungal agents in clinical use due to their broad spectrum of activity, favorable safety profile, and bioavailability [73]. The clinically approved azoles include fluconazole (FLC), voriconazole (VRC), posaconazole (PSC), itraconazole, and isavuconazole. Azoles exhibit mainly fungistatic activity against *Candida* [107]. Due to differences between the membranes of fungal and human cells (mainly composed of cholesterol), the use of azoles does not interfere with human body cells during treatment. They bind to and inhibit the activity of the enzyme lanosterol 14α-demethylase (encoded by the *ERG11* gene in yeasts), which is a key enzyme in the ergosterol biosynthetic pathway (Figure 2C) [108–110]. Ergosterol is an important component of fungal cell membranes [111]. The interruption of its synthesis enables the accumulation of a toxic 14α-methyl sterol, which impairs the membrane integrity and also the function of some membrane-bound proteins (such as those involved in cell wall synthesis), with consequences in terms of cell growth [108,111,112].

The emergence of azole resistance in *Candida* species represents a major challenge to treatment [113–116]. *Candida* spp. azole resistance has been linked to different molecular mechanisms that include (Figure 2C): (i) mutations in the gene encoding the azole target enzyme lanosterol 14α-demethylase (*ERG11*), with resulting overexpression, and reduced azole binding, which also results in the reduction in or loss of affinity with azoles, preventing azole binding; (ii) alterations in the ergosterol biosynthetic pathway, caused by loss-of-function point mutations in *ERG3*, leading to a depletion of ergosterol and to the accumulation of 14α-methyl fecosterol, which is less damaging to cell membranes, thus enabling continued growth in the presence of azoles; and (iii) the upregulation of multidrug efflux pumps *CDR1* and *CDR2* (*Candida* drug resistance) and *MDR1* (multidrug resistance) genes that transport the drug out of the cells [117,118]. The analysis of serial isolates from individual patients has revealed that acquired azole resistance commonly relies on multiple and often-combined molecular mechanisms [119].

Similarly to *C. albicans*, *C. parapsilosis* harbors several genes that have been found to be involved in resistance development. For example, Mrr1p (multidrug resistance regulator 1) is a zinc cluster transcription factor that controls *MDR1* expression [120]. Several authors have demonstrated that gain-of-function mutations in the *MRR1* gene, which render the transcription factor constitutively active, are responsible for the upregulation of the *MDR1* efflux pump and thus play a central role in the development of drug resistance [121–124]. The hyperactivation of the Tac1 (transcriptional activator of *CDR* genes 1) transcription factor is also conferred by gain-of-function mutations that consequently promote the overexpression of *CDR1* and *CDR2* genes [125,126]. Recently, researchers described a new azole resistance mechanism in *Candida*, particularly among *C. parapsilosis* isolates, involving another Cdr1-like gene, the *CDR1B* (CPAR2_304370). Expression of a GOF mutation in the *MRR1* gene impacts the fluconazole susceptibility in *C. parapsilosis* through *CDR1B* overexpression [114,127]. *CDR1* (CLUG_03113) expression in *Candida lusitaniae* is also shown to be regulated by GOF mutation in *MRR1* [128]. In addition, several pieces of evidence point to another mechanism involved in *C. parapsilosis* antifungal resistance: allele copy number variation. Our group observed an increase in the *CDR1B* copy number, resulting in *CDR1B* overexpression and a consequent reduction in fluconazole susceptibility [114]. The copy number variation mechanism has not only been associated with the drug fluconazole but

also with miltefosine, a drug recently approved by the FDA for the treatment of invasive candidiasis [129].

Upc2 (Sterol uptake control protein 2), another member of the zinc cluster transcription factor family, is a key regulator of ergosterol metabolism that controls the expression of the azole target *ERG11* gene [130–132]. Gain-of-function mutations in *UPC2* lead to the increased *ERG11* expression, contributing to fluconazole resistance in this species [133–135]. As with *UPC2*, the transcription factor Ndt80 also modulates the expression of several ergosterol metabolism genes [132,136]. Moreover, Chen et al. (2004) demonstrated the involvement of this regulatory factor in azole tolerance by controlling the expression of the *CDR1* gene in *C. albicans* [137].

Alterations in the ergosterol biosynthetic pathway, including mutations in the *ERG11* gene or its overexpression, have also been linked to azole resistance [138]. The amino acid Y132F substitution in *ERG11* is frequently reported among *Candida* spp., including *C. parapsilosis* [113,139–142]. The persistence of *C. parapsilosis* isolates harboring the Y132F mutation in clinical settings has been associated with outbreaks of infections in hospitals, with fatal consequences [115,116,143].

5. Final Remarks

Candida parapsilosis is a predominant species within NACs that is responsible for invasive candidosis in low-birth-weight neonates, transplant recipients, critical care patients, and those receiving parenteral nutrition. The high prevalence of *C. parapsilosis* is also promoted by its well-documented ability to persist and thrive in the hospital environments for long periods. Its remarkable ability to adhere to abiotic surfaces, such as catheters, and to form biofilms constitutes a gateway to systemic colonization. The extensive use of antifungals, both prophylactically and therapeutically, is also recognized as a major cause of worldwide antifungal resistance in this pathogen.

In light of the above, there can be no doubt that further comprehensive research efforts addressing the epidemiology, pathogenic attributes, antimicrobial susceptibility profile, and genetic resistance mechanisms of *Candida parapsilosis* will contribute to improved treatments for and the prevention of infections, leading to improved patient outcomes and lower burdens upon healthcare systems.

Author Contributions: Writing—original draft, J.B.; Writing—review and editing, J.B., I.M.M. and A.G.R. All authors have read and agreed to the published version of the manuscript.

Data Availability Statement: All data are publicly available.

Conflicts of Interest: The authors declare no conflict of interest.

References

1. Bongomin, F.; Gago, S.; Oladele, R.O.; Denning, D.W. Global and Multi-National Prevalence of Fungal Diseases-Estimate Precision. *J. Fungi* **2017**, *3*, 57. [CrossRef]
2. Strollo, S.; Lionakis, M.S.; Adjemian, J.; Steiner, C.A.; Prevots, D.R. Epidemiology of Hospitalizations Associated with Invasive Candidiasis, United States, 2002-2012(1). *Emerg. Infect. Dis.* **2016**, *23*, 7–13. [CrossRef]
3. Pappas, P.G.; Lionakis, M.S.; Arendrup, M.C.; Ostrosky-Zeichner, L.; Kullberg, B.J. Invasive candidiasis. *Nat. Rev. Dis. Primers* **2018**, *4*, 18026. [CrossRef]
4. McCarty, T.P.; White, C.M.; Pappas, P.G. Candidemia and Invasive Candidiasis. *Infect. Dis. Clin. N. Am.* **2021**, *35*, 389–413. [CrossRef]
5. Guinea, J. Global trends in the distribution of Candida species causing candidemia. *Clin. Microbiol. Infect.* **2014**, *20* (Suppl. S6), 5–10. [CrossRef]
6. Koehler, P.; Stecher, M.; Cornely, O.A.; Koehler, D.; Vehreschild, M.; Bohlius, J.; Wisplinghoff, H.; Vehreschild, J.J. Morbidity and mortality of candidaemia in Europe: An epidemiologic meta-analysis. *Clin. Microbiol. Infect.* **2019**, *25*, 1200–1212. [CrossRef]
7. Ashford, B.K. Certain conditions of the gastrointestinal tract in Puerto Rico and their relation to tropical sprue. *Am. J. Trop. Med. Hyg.* **1928**, *8*, 507–538. [CrossRef]

8. Tavanti, A.; Davidson, A.D.; Gow, N.A.; Maiden, M.C.; Odds, F.C. Candida orthopsilosis and Candida metapsilosis spp. nov. to replace Candida parapsilosis groups II and III. *J. Clin. Microbiol.* **2005**, *43*, 284–292. [CrossRef]
9. van Asbeck, E.C.; Clemons, K.V.; Stevens, D.A. Candida parapsilosis: A review of its epidemiology, pathogenesis, clinical aspects, typing and antimicrobial susceptibility. *Crit. Rev. Microbiol.* **2009**, *35*, 283–309. [CrossRef]
10. Bonassoli, L.A.; Bertoli, M.; Svidzinski, T.I. High frequency of Candida parapsilosis on the hands of healthy hosts. *J. Hosp. Infect.* **2005**, *59*, 159–162. [CrossRef]
11. van Asbeck, E.C.; Huang, Y.C.; Markham, A.N.; Clemons, K.V.; Stevens, D.A. Candida parapsilosis fungemia in neonates: Genotyping results suggest healthcare workers hands as source, and review of published studies. *Mycopathologia* **2007**, *164*, 287–293. [CrossRef]
12. Levin, A.S.; Costa, S.F.; Mussi, N.S.; Basso, M.; Sinto, S.I.; Machado, C.; Geiger, D.C.; Villares, M.C.; Schreiber, A.Z.; Barone, A.A.; et al. Candida parapsilosis fungemia associated with implantable and semi-implantable central venous catheters and the hands of healthcare workers. *Diagn. Microbiol. Infect. Dis.* **1998**, *30*, 243–249. [CrossRef]
13. Trofa, D.; Gacser, A.; Nosanchuk, J.D. Candida parapsilosis, an emerging fungal pathogen. *Clin. Microbiol. Rev.* **2008**, *21*, 606–625. [CrossRef]
14. Ramage, G.; Martinez, J.P.; Lopez-Ribot, J.L. Candida biofilms on implanted biomaterials: A clinically significant problem. *FEMS Yeast Res.* **2006**, *6*, 979–986. [CrossRef]
15. Nemeth, T.; Toth, A.; Szenzenstein, J.; Horvath, P.; Nosanchuk, J.D.; Grozer, Z.; Toth, R.; Papp, C.; Hamari, Z.; Vagvolgyi, C.; et al. Characterization of virulence properties in the C. parapsilosis sensu lato species. *PLoS ONE* **2013**, *8*, e68704. [CrossRef]
16. Cuellar-Cruz, M.; Lopez-Romero, E.; Villagomez-Castro, J.C.; Ruiz-Baca, E. Candida species: New insights into biofilm formation. *Future Microbiol.* **2012**, *7*, 755–771. [CrossRef]
17. Pammi, M.; Holland, L.; Butler, G.; Gacser, A.; Bliss, J.M. Candida parapsilosis is a Significant Neonatal Pathogen: A Systematic Review and Meta-Analysis. *Pediatr. Infect. Dis. J.* **2013**, *32*, e206–e216. [CrossRef]
18. Nucci, M.; Queiroz-Telles, F.; Alvarado-Matute, T.; Tiraboschi, I.N.; Cortes, J.; Zurita, J.; Guzman-Blanco, M.; Santolaya, M.E.; Thompson, L.; Sifuentes-Osornio, J.; et al. Epidemiology of Candidemia in Latin America: A Laboratory-Based Survey. *PLoS ONE* **2013**, *8*, e59373. [CrossRef]
19. Rodriguez, L.; Bustamante, B.; Huaroto, L.; Agurto, C.; Illescas, R.; Ramirez, R.; Diaz, A.; Hidalgo, J. A multi-centric Study of Candida bloodstream infection in Lima-Callao, Peru: Species distribution, antifungal resistance and clinical outcomes. *PLoS ONE* **2017**, *12*, e0175172. [CrossRef]
20. Faria-Ramos, I.; Neves-Maia, J.; Ricardo, E.; Santos-Antunes, J.; Silva, A.T.; Costa-de-Oliveira, S.; Canton, E.; Rodrigues, A.G.; Pina-Vaz, C. Species distribution and in vitro antifungal susceptibility profiles of yeast isolates from invasive infections during a Portuguese multicenter survey. *Eur. J. Clin. Microbiol. Infect. Dis.* **2014**, *33*, 2241–2247. [CrossRef]
21. Guinea, J.; Zaragoza, Ó.; Escribano, P.; Martín-Mazuelos, E.; Pemán, J.; Sánchez-Reus, F.; Cuenca-Estrella, M. Molecular Identification and Antifungal Susceptibility of Yeast Isolates Causing Fungemia Collected in a Population-Based Study in Spain in 2010 and 2011. *Antimicrob. Agents Chemother.* **2014**, *58*, 1529–1537. [CrossRef]
22. Tedeschi, S.; Tumietto, F.; Giannella, M.; Bartoletti, M.; Cristini, F.; Cioni, G.; Ambretti, S.; Carretto, E.; Sambri, V.; Sarti, M.; et al. Epidemiology and outcome of candidemia in internal medicine wards: A regional study in Italy. *Eur. J. Intern. Med.* **2016**, *34*, 39–44. [CrossRef]
23. Vogiatzi, L.; Ilia, S.; Sideri, G.; Vagelakoudi, E.; Vassilopoulou, M.; Sdougka, M.; Briassoulis, G.; Papadatos, I.; Kalabalikis, P.; Sianidou, L.; et al. Invasive candidiasis in pediatric intensive care in Greece: A nationwide study. *Intensive Care Med.* **2013**, *39*, 2188–2195. [CrossRef]
24. Arendrup, M.C.; Bruun, B.; Christensen, J.J.; Fuursted, K.; Johansen, H.K.; Kjældgaard, P.; Knudsen, J.D.; Kristensen, L.; Møller, J.; Nielsen, L.; et al. National Surveillance of Fungemia in Denmark (2004 to 2009). *J. Clin. Microbiol.* **2011**, *49*, 325–334. [CrossRef]
25. Ericsson, J.; Chryssanthou, E.; Klingspor, L.; Johansson, A.G.; Ljungman, P.; Svensson, E.; Sjolin, J. Candidaemia in Sweden: A nationwide prospective observational survey. *Clin. Microbiol. Infect.* **2013**, *19*, E218–E221. [CrossRef]
26. Chalmers, C.; Gaur, S.; Chew, J.; Wright, T.; Kumar, A.; Mathur, S.; Wan, W.Y.; Gould, I.M.; Leanord, A.; Bal, A.M. Epidemiology and management of candidaemia–a retrospective, multicentre study in five hospitals in the UK. *Mycoses* **2011**, *54*, e795–e800. [CrossRef]
27. Toda, M.; Williams, S.R.; Berkow, E.L.; Farley, M.M.; Harrison, L.H.; Bonner, L.; Marceaux, K.M.; Hollick, R.; Zhang, A.Y.; Schaffner, W.; et al. Population-Based Active Surveillance for Culture-Confirmed Candidemia—Four Sites, United States, 2012–2016. *MMWR Surveill. Summ.* **2019**, *68*, 1–15. [CrossRef]
28. Ting, J.Y.; Roberts, A.; Synnes, A.; Canning, R.; Bodani, J.; Monterossa, L.; Shah, P.S.; Canadian Neonatal Network, I. Invasive Fungal Infections in Neonates in Canada: Epidemiology and Outcomes. *Pediatr. Infect. Dis. J.* **2018**, *37*, 1154–1159. [CrossRef]
29. Tsay, S.V.; Mu, Y.; Williams, S.; Epson, E.; Nadle, J.; Bamberg, W.M.; Barter, D.M.; Johnston, H.L.; Farley, M.M.; Harb, S.; et al. Burden of Candidemia in the United States, 2017. *Clin. Infect. Dis.* **2020**, *71*, e449–e453. [CrossRef]
30. Pfaller, M.A.; Diekema, D.J.; Turnidge, J.D.; Castanheira, M.; Jones, R.N. Twenty Years of the SENTRY Antifungal Surveillance Program: Results for Candida Species From 1997–2016. *Open Forum Infect. Dis.* **2019**, *6*, S79–S94. [CrossRef]
31. Kakeya, H.; Yamada, K.; Kaneko, Y.; Yanagihara, K.; Tateda, K.; Maesaki, S.; Takesue, Y.; Tomono, K.; Kadota, J.I.; Kaku, M.; et al. National Trends in the Distribution of Candida Species Causing Candidemia in Japan from 2003 to 2014. *Med. Mycol. J.* **2018**, *59*, E19–E22. [CrossRef] [PubMed]

32. Xiao, M.; Chen, S.C.; Kong, F.; Xu, X.L.; Yan, L.; Kong, H.S.; Fan, X.; Hou, X.; Cheng, J.W.; Zhou, M.L.; et al. Distribution and Antifungal Susceptibility of Candida Species Causing Candidemia in China: An Update From the CHIF-NET Study. *J. Infect. Dis.* **2020**, *221*, S139–S147. [CrossRef] [PubMed]
33. Rajni, E.; Chaudhary, P.; Garg, V.K.; Sharma, R.; Malik, M. A complete clinico-epidemiological and microbiological profile of candidemia cases in a tertiary-care hospital in Western India. *Antimicrob. Steward. Healthc. Epidemiol.* **2022**, *2*, e37. [CrossRef] [PubMed]
34. Chapman, B.; Slavin, M.; Marriott, D.; Halliday, C.; Kidd, S.; Arthur, I.; Bak, N.; Heath, C.H.; Kennedy, K.; Morrissey, C.O.; et al. Changing epidemiology of candidaemia in Australia. *J. Antimicrob. Chemother.* **2017**, *72*, 1103–1108. [CrossRef]
35. Neji, S.; Hadrich, I.; Trabelsi, H.; Abbes, S.; Cheikhrouhou, F.; Sellami, H.; Makni, F.; Ayadi, A. Virulence factors, antifungal susceptibility and molecular mechanisms of azole resistance among Candida parapsilosis complex isolates recovered from clinical specimens. *J. Biomed. Sci.* **2017**, *24*, 67. [CrossRef]
36. Németh, T.M.; Gacser, A.; Nosanchuk, J.D. Candida psilosis complex. In *Reference Module in Life Sciences*; Roitberg, B.D., Ed.; Elsevier: Amsterdam, The Netherlands, 2018. [CrossRef]
37. Skrzypek, M.S.; Binkley, J.; Binkley, G.; Miyasato, S.R.; Simison, M.; Sherlock, G. The Candida Genome Database (CGD): Incorporation of Assembly 22, systematic identifiers and visualization of high throughput sequencing data. *Nucleic Acids Res.* **2017**, *45*, D592–D596. [CrossRef]
38. Butler, G.; Rasmussen, M.D.; Lin, M.F.; Santos, M.A.; Sakthikumar, S.; Munro, C.A.; Rheinbay, E.; Grabherr, M.; Forche, A.; Reedy, J.L.; et al. Evolution of pathogenicity and sexual reproduction in eight Candida genomes. *Nature* **2009**, *459*, 657–662. [CrossRef]
39. Laffey, S.F.; Butler, G. Phenotype switching affects biofilm formation by Candida parapsilosis. *Microbiology* **2005**, *151*, 1073–1081. [CrossRef]
40. Cavalheiro, M.; Teixeira, M.C. Candida Biofilms: Threats, Challenges, and Promising Strategies. *Front. Med.* **2018**, *5*, 28. [CrossRef]
41. Silva-Dias, A.; Miranda, I.M.; Branco, J.; Monteiro-Soares, M.; Pina-Vaz, C.; Rodrigues, A.G. Adhesion, biofilm formation, cell surface hydrophobicity, and antifungal planktonic susceptibility: Relationship among *Candida* spp. *Front. Microbiol.* **2015**, *6*, 205. [CrossRef]
42. Silva, S.; Negri, M.; Henriques, M.; Oliveira, R.; Williams, D.W.; Azeredo, J. Adherence and biofilm formation of non-Candida albicans Candida species. *Trends Microbiol.* **2011**, *19*, 241–247. [CrossRef] [PubMed]
43. Chandra, J.; Patel, J.D.; Li, J.; Zhou, G.; Mukherjee, P.K.; McCormick, T.S.; Anderson, J.M.; Ghannoum, M.A. Modification of surface properties of biomaterials influences the ability of Candida albicans to form biofilms. *Appl. Environ. Microbiol.* **2005**, *71*, 8795–8801. [CrossRef] [PubMed]
44. de Groot, P.W.; Bader, O.; de Boer, A.D.; Weig, M.; Chauhan, N. Adhesins in human fungal pathogens: Glue with plenty of stick. *Eukaryot. Cell* **2013**, *12*, 470–481. [CrossRef] [PubMed]
45. Modrzewska, B.; Kurnatowski, P. Adherence of Candida sp. to host tissues and cells as one of its pathogenicity features. *Ann. Parasitol.* **2015**, *61*, 3–9.
46. Nobile, C.J.; Andes, D.R.; Nett, J.E.; Smith, F.J.; Yue, F.; Phan, Q.T.; Edwards, J.E.; Filler, S.G.; Mitchell, A.P. Critical role of Bcr1-dependent adhesins in C. albicans biofilm formation in vitro and in vivo. *PLoS Pathog.* **2006**, *2*, e63. [CrossRef] [PubMed]
47. Bertini, A.; Zoppo, M.; Lombardi, L.; Rizzato, C.; De Carolis, E.; Vella, A.; Torelli, R.; Sanguinetti, M.; Tavanti, A. Targeted gene disruption in Candida parapsilosis demonstrates a role for CPAR2_404800 in adhesion to a biotic surface and in a murine model of ascending urinary tract infection. *Virulence* **2016**, *7*, 85–97. [CrossRef] [PubMed]
48. Neale, M.N.; Glass, K.A.; Longley, S.J.; Kim, D.J.; Laforce-Nesbitt, S.S.; Wortzel, J.D.; Shaw, S.K.; Bliss, J.M. Role of the Inducible Adhesin CpAls7 in Binding of Candida parapsilosis to the Extracellular Matrix under Fluid Shear. *Infect. Immun.* **2018**, *86*, e00892-17. [CrossRef]
49. Czechowicz, P.; Nowicka, J.; Gosciniak, G. Virulence Factors of Candida spp. and Host Immune Response Important in the Pathogenesis of Vulvovaginal Candidiasis. *Int. J. Mol. Sci.* **2022**, *23*, 5895. [CrossRef]
50. Ruchel, R.; Boning, B.; Borg, M. Characterization of a secretory proteinase of Candida parapsilosis and evidence for the absence of the enzyme during infection in vitro. *Infect. Immun.* **1986**, *53*, 411–419. [CrossRef]
51. Horvath, P.; Nosanchuk, J.D.; Hamari, Z.; Vagvolgyi, C.; Gacser, A. The identification of gene duplication and the role of secreted aspartyl proteinase 1 in Candida parapsilosis virulence. *J. Infect. Dis.* **2012**, *205*, 923–933. [CrossRef]
52. Dagdeviren, M.; Cerikcioglu, N.; Karavus, M. Acid proteinase, phospholipase and adherence properties of Candida parapsilosis strains isolated from clinical specimens of hospitalised patients. *Mycoses* **2005**, *48*, 321–326. [CrossRef] [PubMed]
53. Tosun, I.; Akyuz, Z.; Guler, N.C.; Gulmez, D.; Bayramoglu, G.; Kaklikkaya, N.; Arikan-Akdagli, S.; Aydin, F. Distribution, virulence attributes and antifungal susceptibility patterns of Candida parapsilosis complex strains isolated from clinical samples. *Med. Mycol.* **2013**, *51*, 483–492. [CrossRef] [PubMed]
54. Gacser, A.; Trofa, D.; Schafer, W.; Nosanchuk, J.D. Targeted gene deletion in Candida parapsilosis demonstrates the role of secreted lipase in virulence. *J. Clin. Investig.* **2007**, *117*, 3049–3058. [CrossRef]
55. Trofa, D.; Agovino, M.; Stehr, F.; Schafer, W.; Rykunov, D.; Fiser, A.; Hamari, Z.; Nosanchuk, J.D.; Gacser, A. Acetylsalicylic acid (aspirin) reduces damage to reconstituted human tissues infected with Candida species by inhibiting extracellular fungal lipases. *Microbes. Infect.* **2009**, *11*, 1131–1139. [CrossRef]

141

56. Ghannoum, M.A. Potential role of phospholipases in virulence and fungal pathogenesis. *Clin. Microbiol. Rev.* **2000**, *13*, 122–143. [CrossRef]
57. Mukherjee, P.K.; Chandra, J. Candida biofilm resistance. *Drug Resist. Updat.* **2004**, *7*, 301–309. [CrossRef]
58. Chandra, J.; Mukherjee, P.K. Candida Biofilms: Development, Architecture, and Resistance. *Microbiol. Spectr.* **2015**, *3*. [CrossRef]
59. Douglas, L.J. Candida biofilms and their role in infection. *Trends Microbiol.* **2003**, *11*, 30–36. [CrossRef]
60. Estivill, D.; Arias, A.; Torres-Lana, A.; Carrillo-Munoz, A.J.; Arevalo, M.P. Biofilm formation by five species of Candida on three clinical materials. *J. Microbiol. Methods* **2011**, *86*, 238–242. [CrossRef]
61. Shin, J.H.; Kee, S.J.; Shin, M.G.; Kim, S.H.; Shin, D.H.; Lee, S.K.; Suh, S.P.; Ryang, D.W. Biofilm production by isolates of Candida species recovered from nonneutropenic patients: Comparison of bloodstream isolates with isolates from other sources. *J. Clin. Microbiol.* **2002**, *40*, 1244–1248. [CrossRef]
62. Branchini, M.L.; Pfaller, M.A.; Rhine-Chalberg, J.; Frempong, T.; Isenberg, H.D. Genotypic variation and slime production among blood and catheter isolates of Candida parapsilosis. *J. Clin. Microbiol.* **1994**, *32*, 452–456. [CrossRef]
63. Silva, S.; Henriques, M.; Martins, A.; Oliveira, R.; Williams, D.; Azeredo, J. Biofilms of non-Candida albicans Candida species: Quantification, structure and matrix composition. *Med. Mycol.* **2009**, *47*, 681–689. [CrossRef]
64. Kuhn, D.M.; Chandra, J.; Mukherjee, P.K.; Ghannoum, M.A. Comparison of biofilms formed by Candida albicans and Candida parapsilosis on bioprosthetic surfaces. *Infect. Immun.* **2002**, *70*, 878–888. [CrossRef]
65. Mitchell, K.F.; Zarnowski, R.; Sanchez, H.; Edward, J.A.; Reinicke, E.L.; Nett, J.E.; Mitchell, A.P.; Andes, D.R. Community participation in biofilm matrix assembly and function. *Proc. Natl. Acad. Sci. USA* **2015**, *112*, 4092–4097. [CrossRef]
66. Silva, S.; Rodrigues, C.F.; Araujo, D.; Rodrigues, M.E.; Henriques, M. Candida Species Biofilms' Antifungal Resistance. *J. Fungi* **2017**, *3*, 8. [CrossRef]
67. Uppuluri, P.; Chaturvedi, A.K.; Srinivasan, A.; Banerjee, M.; Ramasubramaniam, A.K.; Kohler, J.R.; Kadosh, D.; Lopez-Ribot, J.L. Dispersion as an important step in the Candida albicans biofilm developmental cycle. *PLoS Pathog.* **2010**, *6*, e1000828. [CrossRef]
68. Holland, L.M.; Schroder, M.S.; Turner, S.A.; Taff, H.; Andes, D.; Grozer, Z.; Gacser, A.; Ames, L.; Haynes, K.; Higgins, D.G.; et al. Comparative phenotypic analysis of the major fungal pathogens Candida parapsilosis and Candida albicans. *PLoS Pathog.* **2014**, *10*, e1004365. [CrossRef]
69. Nobile, C.J.; Fox, E.P.; Nett, J.E.; Sorrells, T.R.; Mitrovich, Q.M.; Hernday, A.D.; Tuch, B.B.; Andes, D.R.; Johnson, A.D. A recently evolved transcriptional network controls biofilm development in Candida albicans. *Cell* **2012**, *148*, 126–138. [CrossRef]
70. Branco, J.; Martins-Cruz, C.; Rodrigues, L.; Silva, R.M.; Araujo-Gomes, N.; Goncalves, T.; Miranda, I.M.; Rodrigues, A.G. The transcription factor Ndt80 is a repressor of Candida parapsilosis virulence attributes. *Virulence* **2021**, *12*, 601–614. [CrossRef]
71. Ding, C.; Vidanes, G.M.; Maguire, S.L.; Guida, A.; Synnott, J.M.; Andes, D.R.; Butler, G. Conserved and divergent roles of Bcr1 and CFEM proteins in Candida parapsilosis and Candida albicans. *PLoS ONE* **2011**, *6*, e28151. [CrossRef]
72. Denning, D.W.; Hope, W.W. Therapy for fungal diseases: Opportunities and priorities. *Trends Microbiol.* **2010**, *18*, 195–204. [CrossRef] [PubMed]
73. Ben-Ami, R.; Kontoyiannis, D.P. Resistance to Antifungal Drugs. *Infect. Dis. Clin. N. Am.* **2021**, *35*, 279–311. [CrossRef] [PubMed]
74. Carolus, H.; Pierson, S.; Lagrou, K.; Van Dijck, P. Amphotericin B and Other Polyenes-Discovery, Clinical Use, Mode of Action and Drug Resistance. *J. Fungi* **2020**, *6*, 321. [CrossRef] [PubMed]
75. Fanos, V.; Cataldi, L. Amphotericin B-induced nephrotoxicity: A review. *J. Chemother.* **2000**, *12*, 463–470. [CrossRef]
76. Groll, A.H.; Rijnders, B.J.A.; Walsh, T.J.; Adler-Moore, J.; Lewis, R.E.; Bruggemann, R.J.M. Clinical Pharmacokinetics, Pharmacodynamics, Safety and Efficacy of Liposomal Amphotericin B. *Clin. Infect. Dis.* **2019**, *68*, S260–S274. [CrossRef]
77. Lockhart, S.R.; Iqbal, N.; Cleveland, A.A.; Farley, M.M.; Harrison, L.H.; Bolden, C.B.; Baughman, W.; Stein, B.; Hollick, R.; Park, B.J.; et al. Species identification and antifungal susceptibility testing of Candida bloodstream isolates from population-based surveillance studies in two U.S. cities from 2008 to 2011. *J. Clin. Microbiol.* **2012**, *50*, 3435–3442. [CrossRef]
78. Yamin, D.; Akanmu, M.H.; Al Mutair, A.; Alhumaid, S.; Rabaan, A.A.; Hajissa, K. Global Prevalence of Antifungal-Resistant Candida parapsilosis: A Systematic Review and Meta-Analysis. *Trop. Med. Infect. Dis.* **2022**, *7*, 188. [CrossRef]
79. Chowdhary, A.; Prakash, A.; Sharma, C.; Kordalewska, M.; Kumar, A.; Sarma, S.; Tarai, B.; Singh, A.; Upadhyaya, G.; Upadhyay, S.; et al. A multicentre study of antifungal susceptibility patterns among 350 Candida auris isolates (2009-17) in India: Role of the ERG11 and FKS1 genes in azole and echinocandin resistance. *J. Antimicrob. Chemother.* **2018**, *73*, 891–899. [CrossRef]
80. Martel, C.M.; Parker, J.E.; Bader, O.; Weig, M.; Gross, U.; Warrilow, A.G.; Kelly, D.E.; Kelly, S.L. A clinical isolate of Candida albicans with mutations in ERG11 (encoding sterol 14alpha-demethylase) and ERG5 (encoding C22 desaturase) is cross resistant to azoles and amphotericin B. *Antimicrob. Agents Chemother.* **2010**, *54*, 3578–3583. [CrossRef]
81. Young, L.Y.; Hull, C.M.; Heitman, J. Disruption of ergosterol biosynthesis confers resistance to amphotericin B in Candida lusitaniae. *Antimicrob. Agents Chemother.* **2003**, *47*, 2717–2724. [CrossRef]
82. Perlin, D.S. Echinocandin Resistance in Candida. *Clin. Infect. Dis.* **2015**, *61* (Suppl. S6), S612–S617. [CrossRef] [PubMed]
83. Sokol-Anderson, M.; Sligh, J.E., Jr.; Elberg, S.; Brajtburg, J.; Kobayashi, G.S.; Medoff, G. Role of cell defense against oxidative damage in the resistance of Candida albicans to the killing effect of amphotericin B. *Antimicrob. Agents Chemother.* **1988**, *32*, 702–705. [CrossRef] [PubMed]
84. Kristanc, L.; Bozic, B.; Jokhadar, S.Z.; Dolenc, M.S.; Gomiscek, G. The pore-forming action of polyenes: From model membranes to living organisms. *Biochim. Biophys. Acta Biomembr.* **2019**, *1861*, 418–430. [CrossRef] [PubMed]

85. Cowen, L.E.; Lindquist, S. Hsp90 potentiates the rapid evolution of new traits: Drug resistance in diverse fungi. *Science* **2005**, *309*, 2185–2189. [CrossRef]

86. Denning, D.W. Echinocandin antifungal drugs. *Lancet* **2003**, *362*, 1142–1151. [CrossRef]

87. Pappas, P.G.; Kauffman, C.A.; Andes, D.R.; Clancy, C.J.; Marr, K.A.; Ostrosky-Zeichner, L.; Reboli, A.C.; Schuster, M.G.; Vazquez, J.A.; Walsh, T.J.; et al. Clinical Practice Guideline for the Management of Candidiasis: 2016 Update by the Infectious Diseases Society of America. *Clin. Infect. Dis.* **2016**, *62*, e1–e50. [CrossRef]

88. Chen, S.A.; Slavin, M.; Sorrell, T. Echinocandin Antifungal Drugs in Fungal Infections. *Drugs* **2011**, *71*, 11–41. [CrossRef]

89. Beyda, N.D.; Lewis, R.E.; Garey, K.W. Echinocandin Resistance in Candida Species: Mechanisms of Reduced Susceptibility and Therapeutic Approaches. *Ann. Pharmacother.* **2012**, *46*, 1086–1096. [CrossRef]

90. Pfaller, M.A.; Diekema, D.J.; Andes, D.; Arendrup, M.C.; Brown, S.D.; Lockhart, S.R.; Motyl, M.; Perlin, D.S. Clinical breakpoints for the echinocandins and Candida revisited: Integration of molecular, clinical, and microbiological data to arrive at species-specific interpretive criteria. *Drug Resist. Updat.* **2011**, *14*, 164–176. [CrossRef]

91. Douglas, C.M.; D'Ippolito, J.A.; Shei, G.J.; Meinz, M.; Onishi, J.; Marrinan, J.A.; Li, W.; Abruzzo, G.K.; Flattery, A.; Bartizal, K.; et al. Identification of the FKS1 gene of Candida albicans as the essential target of 1,3-beta-D-glucan synthase inhibitors. *Antimicrob. Agents Chemother.* **1997**, *41*, 2471–2479. [CrossRef]

92. Bachmann, S.P.; VandeWalle, K.; Ramage, G.; Patterson, T.F.; Wickes, B.L.; Graybill, J.R.; López-Ribot, J.L. In Vitro Activity of Caspofungin against Candida albicans Biofilms. *Antimicrob. Agents Chemother.* **2002**, *46*, 3591–3596. [CrossRef] [PubMed]

93. Perlin, D.S. Current perspectives on echinocandin class drugs. *Future Microbiol.* **2011**, *6*, 441–457. [CrossRef] [PubMed]

94. Ostrosky-Zeichner, L.; Rex, J.H.; Pappas, P.G.; Hamill, R.J.; Larsen, R.A.; Horowitz, H.W.; Powderly, W.G.; Hyslop, N.; Kauffman, C.A.; Cleary, J.; et al. Antifungal Susceptibility Survey of 2,000 Bloodstream Candida Isolates in the United States. *Antimicrob. Agents Chemother.* **2003**, *47*, 3149–3154. [CrossRef] [PubMed]

95. Perlin, D.S. Resistance to echinocandin-class antifungal drugs. *Drug Resist. Updat.* **2007**, *10*, 121–130. [CrossRef] [PubMed]

96. Garcia-Effron, G.; Canton, E.; Pemán, J.; Dilger, A.; Romá, E.; Perlin, D.S. Epidemiology and echinocandin susceptibility of Candida parapsilosis sensu lato species isolated from bloodstream infections at a Spanish university hospital. *J. Antimicrob. Chemother.* **2012**, *67*, 2739–2748. [CrossRef]

97. Siopi, M.; Papadopoulos, A.; Spiliopoulou, A.; Paliogianni, F.; Abou-Chakra, N.; Arendrup, M.C.; Damoulari, C.; Tsioulos, G.; Giannitsioti, E.; Frantzeskaki, F.; et al. Pan-Echinocandin Resistant C. parapsilosis Harboring an F652S Fks1 Alteration in a Patient with Prolonged Echinocandin Therapy. *J. Fungi* **2022**, *8*, 931. [CrossRef]

98. Ning, Y.; Xiao, M.; Perlin, D.S.; Zhao, Y.; Lu, M.; Li, Y.; Luo, Z.; Dai, R.; Li, S.; Xu, J.; et al. Decreased echinocandin susceptibility in Candida parapsilosis causing candidemia and emergence of a pan-echinocandin resistant case in China. *Emerg. Microbes Infect.* **2023**, *12*, 2153086. [CrossRef]

99. Singh, S.D.; Robbins, N.; Zaas, A.K.; Schell, W.A.; Perfect, J.R.; Cowen, L.E. Hsp90 governs echinocandin resistance in the pathogenic yeast Candida albicans via calcineurin. *PLoS Pathog.* **2009**, *5*, e1000532. [CrossRef]

100. Munro, C.A.; Selvaggini, S.; De Bruijn, I.; Walker, L.; Lenardon, M.D.; Gerssen, B.; Milne, S.; Brown, A.J.P.; Gow, N.A.R. The PKC, HOG and Ca2+ signalling pathways co-ordinately regulate chitin synthesis in Candida albicans. *Mol. Microbiol.* **2007**, *63*, 1399–1413. [CrossRef]

101. Lee, K.K.; Maccallum, D.M.; Jacobsen, M.D.; Walker, L.A.; Odds, F.C.; Gow, N.A.; Munro, C.A. Elevated cell wall chitin in Candida albicans confers echinocandin resistance in vivo. *Antimicrob. Agents Chemother.* **2012**, *56*, 208–217. [CrossRef]

102. Park, S.; Kelly, R.; Kahn, J.N.; Robles, J.; Hsu, M.-J.; Register, E.; Li, W.; Vyas, V.; Fan, H.; Abruzzo, G.; et al. Specific Substitutions in the Echinocandin Target Fks1p Account for Reduced Susceptibility of Rare Laboratory and Clinical Candida sp. Isolates. *Antimicrob. Agents Chemother.* **2005**, *49*, 3264–3273. [CrossRef] [PubMed]

103. Katiyar, S.; Pfaller, M.; Edlind, T. Candida albicans and Candida glabrata Clinical Isolates Exhibiting Reduced Echinocandin Susceptibility. *Antimicrob. Agents Chemother.* **2006**, *50*, 2892–2894. [CrossRef]

104. Garcia-Effron, G.; Kontoyiannis, D.P.; Lewis, R.E.; Perlin, D.S. Caspofungin-Resistant Candida tropicalis Strains Causing Breakthrough Fungemia in Patients at High Risk for Hematologic Malignancies. *Antimicrob. Agents Chemother.* **2008**, *52*, 4181–4183. [CrossRef] [PubMed]

105. Pfaller, M.A.; Messer, S.A.; Woosley, L.N.; Jones, R.N.; Castanheira, M. Echinocandin and Triazole Antifungal Susceptibility Profiles for Clinical Opportunistic Yeast and Mold Isolates Collected from 2010 to 2011: Application of New CLSI Clinical Breakpoints and Epidemiological Cutoff Values for Characterization of Geographic and Temporal Trends of Antifungal Resistance. *J. Clin. Microbiol.* **2013**, *51*, 2571–2581. [CrossRef] [PubMed]

106. Garcia-Effron, G.; Katiyar, S.K.; Park, S.; Edlind, T.D.; Perlin, D.S. A Naturally Occurring Proline-to-Alanine Amino Acid Change in Fks1p in Candida parapsilosis, Candida orthopsilosis, and Candida metapsilosis Accounts for Reduced Echinocandin Susceptibility. *Antimicrob. Agents Chemother.* **2008**, *52*, 2305–2312. [CrossRef]

107. Robbins, N.; Caplan, T.; Cowen, L.E. Molecular Evolution of Antifungal Drug Resistance. *Annu. Rev. Microbiol.* **2017**, *71*, 753–775. [CrossRef]

108. Odds, F.C.; Brown, A.J.P.; Gow, N.A.R. Antifungal agents: Mechanisms of action. *Trends Microbiol.* **2003**, *11*, 272–279. [CrossRef] [PubMed]

109. Cowen, L.E.; Sanglard, D.; Howard, S.J.; Rogers, P.D.; Perlin, D.S. Mechanisms of Antifungal Drug Resistance. *Cold Spring Harb. Perspect. Med.* **2014**, *5*, a019752. [CrossRef]

110. Xiao, L.; Madison, V.; Chau, A.S.; Loebenberg, D.; Palermo, R.E.; McNicholas, P.M. Three-Dimensional Models of Wild-Type and Mutated Forms of Cytochrome P450 14α-Sterol Demethylases from Aspergillus fumigatus and Candida albicans Provide Insights into Posaconazole Binding. *Antimicrob. Agents Chemother.* **2004**, *48*, 568–574. [CrossRef]

111. Akins, R.A. An update on antifungal targets and mechanisms of resistance in Candida albicans. *Med. Mycol.* **2005**, *43*, 285–318. [CrossRef]

112. Xie, J.L.; Polvi, E.J.; Shekhar-Guturja, T.; Cowen, L.E. Elucidating drug resistance in human fungal pathogens. *Future Microbiol.* **2014**, *9*, 523–542. [CrossRef] [PubMed]

113. Magobo, R.E.; Lockhart, S.R.; Govender, N.P. Fluconazole-resistant Candida parapsilosis strains with a Y132F substitution in the ERG11 gene causing invasive infections in a neonatal unit, South Africa. *Mycoses* **2020**, *63*, 471–477. [CrossRef]

114. Branco, J.; Ryan, A.P.; Silva, A.P.; Butler, G.; Miranda, I.M.; Rodrigues, A.G. Clinical azole cross-resistance in Candida parapsilosis is related to a novel MRR1 gain-of-function mutation. *Clin. Microbiol. Infect.* **2022**, *28*, 1655. [CrossRef] [PubMed]

115. Martini, C.; Torelli, R.; de Groot, T.; De Carolis, E.; Morandotti, G.A.; De Angelis, G.; Posteraro, B.; Meis, J.F.; Sanguinetti, M. Prevalence and Clonal Distribution of Azole-Resistant Candida parapsilosis Isolates Causing Bloodstream Infections in a Large Italian Hospital. *Front. Cell Infect. Microbiol.* **2020**, *10*, 232. [CrossRef] [PubMed]

116. Fekkar, A.; Blaize, M.; Bougle, A.; Normand, A.C.; Raoelina, A.; Kornblum, D.; Kamus, L.; Piarroux, R.; Imbert, S. Hospital outbreak of fluconazole-resistant Candida parapsilosis: Arguments for clonal transmission and long-term persistence. *Antimicrob. Agents Chemother.* **2021**, *65*, e02036-20. [CrossRef]

117. Sanglard, D.; Odds, F.C. Resistance of Candida species to antifungal agents: Molecular mechanisms and clinical consequences. *Lancet Infect. Dis.* **2002**, *2*, 73–85. [CrossRef]

118. Pfaller, M.A. Antifungal Drug Resistance: Mechanisms, Epidemiology, and Consequences for Treatment. *Am. J. Med.* **2012**, *125*, S3–S13. [CrossRef]

119. Morio, F.; Pagniez, F.; Besse, M.; Gay-andrieu, F.; Miegeville, M.; Le Pape, P. Deciphering azole resistance mechanisms with a focus on transcription factor-encoding genes TAC1, MRR1 and UPC2 in a set of fluconazole-resistant clinical isolates of Candida albicans. *Int. J. Antimicrob. Agents* **2013**, *42*, 410–415. [CrossRef]

120. Morschhäuser, J.; Barker, K.S.; Liu, T.T.; Blaß-Warmuth, J.; Homayouni, R.; Rogers, P.D. The Transcription Factor Mrr1p Controls Expression of the *MDR1* Efflux Pump and Mediates Multidrug Resistance in *Candida albicans*. *PLoS Pathog.* **2007**, *3*, e164. [CrossRef]

121. Dunkel, N.; Blaß, J.; Rogers, P.D.; Morschhäuser, J. Mutations in the multi-drug resistance regulator MRR1, followed by loss of heterozygosity, are the main cause of MDR1 overexpression in fluconazole-resistant Candida albicans strains. *Mol. Microbiol.* **2008**, *69*, 827–840. [CrossRef]

122. Schubert, S.; Rogers, P.D.; Morschhäuser, J. Gain-of-Function Mutations in the Transcription Factor MRR1 Are Responsible for Overexpression of the MDR1 Efflux Pump in Fluconazole-Resistant Candida dubliniensis Strains. *Antimicrob. Agents Chemother.* **2008**, *52*, 4274–4280. [CrossRef] [PubMed]

123. Branco, J.; Silva, A.P.; Silva, R.M.; Silva-Dias, A.; Pina-Vaz, C.; Butler, G.; Rodrigues, A.G.; Miranda, I.M. Fluconazole and Voriconazole Resistance in Candida parapsilosis Is Conferred by Gain-of-Function Mutations in MRR1 Transcription Factor Gene. *Antimicrob. Agents Chemother.* **2015**, *59*, 6629–6633. [CrossRef] [PubMed]

124. Papp, C.; Bohner, F.; Kocsis, K.; Varga, M.; Szekeres, A.; Bodai, L.; Willis, J.R.; Gabaldon, T.; Toth, R.; Nosanchuk, J.D.; et al. Triazole Evolution of Candida parapsilosis Results in Cross-Resistance to Other Antifungal Drugs, Influences Stress Responses, and Alters Virulence in an Antifungal Drug-Dependent Manner. *mSphere* **2020**, *5*, e00821-20. [CrossRef] [PubMed]

125. Coste, A.T.; Karababa, M.; Ischer, F.; Bille, J.; Sanglard, D. TAC1, transcriptional activator of CDR genes, is a new transcription factor involved in the regulation of Candida albicans ABC transporters CDR1 and CDR2. *Eukaryot. Cell* **2004**, *3*, 1639–1652. [CrossRef] [PubMed]

126. Berkow, E.L.; Manigaba, K.; Parker, J.E.; Barker, K.S.; Kelly, S.L.; Rogers, P.D. Multidrug Transporters and Alterations in Sterol Biosynthesis Contribute to Azole Antifungal Resistance in Candida parapsilosis. *Antimicrob. Agents Chemother.* **2015**, *59*, 5942–5950. [CrossRef] [PubMed]

127. Doorley, L.A.; Rybak, J.M.; Berkow, E.L.; Zhang, Q.; Morschhauser, J.; Rogers, P.D. Candida parapsilosis Mdr1B and Cdr1B Are Drivers of Mrr1-Mediated Clinical Fluconazole Resistance. *Antimicrob. Agents Chemother.* **2022**, *66*, e0028922. [CrossRef] [PubMed]

128. Borgeat, V.; Brandalise, D.; Grenouillet, F.; Sanglard, D. Participation of the ABC Transporter CDR1 in Azole Resistance of Candida lusitaniae. *J. Fungi* **2021**, *7*, 760. [CrossRef]

129. Bergin, S.A.; Zhao, F.; Ryan, A.P.; Muller, C.A.; Nieduszynski, C.A.; Zhai, B.; Rolling, T.; Hohl, T.M.; Morio, F.; Scully, J.; et al. Systematic Analysis of Copy Number Variations in the Pathogenic Yeast Candida parapsilosis Identifies a Gene Amplification in RTA3 That is Associated with Drug Resistance. *mBio* **2022**, *13*, e0177722. [CrossRef]

130. Silver, P.M.; Oliver, B.G.; White, T.C. Role of Candida albicans Transcription Factor Upc2p in Drug Resistance and Sterol Metabolism. *Eukaryot. Cell* **2004**, *3*, 1391–1397. [CrossRef]

131. Schubert, S.; Barker, K.S.; Znaidi, S.; Schneider, S.; Dierolf, F.; Dunkel, N.; Aïd, M.; Boucher, G.; Rogers, P.D.; Raymond, M.; et al. Regulation of Efflux Pump Expression and Drug Resistance by the Transcription Factors Mrr1, Upc2, and Cap1 in Candida albicans. *Antimicrob. Agents Chemother.* **2011**, *55*, 2212–2223. [CrossRef]

132. Branco, J.; Ola, M.; Silva, R.M.; Fonseca, E.; Gomes, N.C.; Martins-Cruz, C.; Silva, A.P.; Silva-Dias, A.; Pina-Vaz, C.; Erraught, C.; et al. Impact of ERG3 mutations and expression of ergosterol genes controlled by UPC2 and NDT80 in Candida parapsilosis azole resistance. *Clin. Microbiol. Infect.* **2017**, *23*, 575. [CrossRef] [PubMed]

133. Heilmann, C.J.; Schneider, S.; Barker, K.S.; Rogers, P.D.; Morschhäuser, J. An A643T Mutation in the Transcription Factor Upc2p Causes Constitutive ERG11 Upregulation and Increased Fluconazole Resistance in Candida albicans. *Antimicrob. Agents Chemother.* **2010**, *54*, 353–359. [CrossRef] [PubMed]

134. Flowers, S.A.; Barker, K.S.; Berkow, E.L.; Toner, G.; Chadwick, S.G.; Gygax, S.E.; Morschhäuser, J.; Rogers, P.D. Gain-of-Function Mutations in UPC2 Are a Frequent Cause of ERG11 Upregulation in Azole-Resistant Clinical Isolates of Candida albicans. *Eukaryot. Cell* **2012**, *11*, 1289–1299. [CrossRef] [PubMed]

135. Dunkel, N.; Liu, T.T.; Barker, K.S.; Homayouni, R.; Morschhäuser, J.; Rogers, P.D. A Gain-of-Function Mutation in the Transcription Factor Upc2p Causes Upregulation of Ergosterol Biosynthesis Genes and Increased Fluconazole Resistance in a Clinical Candida albicans Isolate. *Eukaryot. Cell* **2008**, *7*, 1180–1190. [CrossRef] [PubMed]

136. Sellam, A.; Tebbji, F.; Nantel, A. Role of Ndt80p in Sterol Metabolism Regulation and Azole Resistance in Candida albicans. *Eukaryot. Cell* **2009**, *8*, 1174–1183. [CrossRef]

137. Chen, C.-G.; Yang, Y.-L.; Shih, H.-I.; Su, C.-L.; Lo, H.-J. CaNdt80 Is Involved in Drug Resistance in Candida albicans by Regulating CDR1. *Antimicrob. Agents Chemother.* **2004**, *48*, 4505–4512. [CrossRef]

138. Pristov, K.E.; Ghannoum, M.A. Resistance of Candida to azoles and echinocandins worldwide. *Clin. Microbiol. Infect.* **2019**, *25*, 792–798. [CrossRef]

139. Morio, F.; Loge, C.; Besse, B.; Hennequin, C.; Le Pape, P. Screening for amino acid substitutions in the Candida albicans Erg11 protein of azole-susceptible and azole-resistant clinical isolates: New substitutions and a review of the literature. *Diagn. Microbiol. Infect. Dis.* **2010**, *66*, 373–384. [CrossRef]

140. Vandeputte, P.; Larcher, G.; Berges, T.; Renier, G.; Chabasse, D.; Bouchara, J.P. Mechanisms of azole resistance in a clinical isolate of Candida tropicalis. *Antimicrob. Agents Chemother.* **2005**, *49*, 4608–4615. [CrossRef]

141. Healey, K.R.; Kordalewska, M.; Jimenez Ortigosa, C.; Singh, A.; Berrio, I.; Chowdhary, A.; Perlin, D.S. Limited ERG11 Mutations Identified in Isolates of Candida auris Directly Contribute to Reduced Azole Susceptibility. *Antimicrob. Agents Chemother.* **2018**, *62*, e01427-18. [CrossRef]

142. Singh, A.; Singh, P.K.; de Groot, T.; Kumar, A.; Mathur, P.; Tarai, B.; Sachdeva, N.; Upadhyaya, G.; Sarma, S.; Meis, J.F.; et al. Emergence of clonal fluconazole-resistant Candida parapsilosis clinical isolates in a multicentre laboratory-based surveillance study in India. *J. Antimicrob. Chemother.* **2019**, *74*, 1260–1268. [CrossRef] [PubMed]

143. Arastehfar, A.; Daneshnia, F.; Hilmioglu-Polat, S.; Fang, W.; Yasar, M.; Polat, F.; Metin, D.Y.; Rigole, P.; Coenye, T.; Ilkit, M.; et al. First Report of Candidemia Clonal Outbreak Caused by Emerging Fluconazole-Resistant Candida parapsilosis Isolates Harboring Y132F and/or Y132F+K143R in Turkey. *Antimicrob. Agents Chemother.* **2020**, *64*, e01001-20. [CrossRef] [PubMed]

145

Paper II

Antifungal susceptibility profile characterization of *Candida parapsilosis* species complex:

a Portuguese analysis

Original article

Antifungal susceptibility profile characterization of *Candida parapsilosis* species complex: a Portuguese analysis

Joana Branco[a,b], Cláudia Martins-Cruz[a], Teresa Gonçalves[c], Isabel M. Miranda[d,#,*,†] and Acácio Gonçalves Rodrigues[a,b,†]

[a]Division of Microbiology, Department of Pathology, Faculty of Medicine, University of Porto, Porto, Portugal.

[b]Center for Health Technology and Services Research – CINTESIS@RISE, Faculty of Medicine, University of Porto, Porto, Portugal.

[c]Center for Neurosciences and Cell Biology – CNC.IBILI, Faculty of Medicine, University of Coimbra, Coimbra, Portugal.

[d]Cardiovascular Research & Development Centre – UnIC@RISE, Faculty of Medicine, University of Porto, Porto, Portugal.

Running title: *Candida parapsilosis* complex analysis

[#]Address correspondence to Isabel M. Miranda, imiranda@med.up.pt

[*]Present address: Alameda Prof. Hernâni Monteiro, 4200-319 Porto, Portugal

[†]These authors share the last authorship.

Number of words: 3729

Number of figures/tables: 2

ABSTRACT

Among a clinical isolate collection of *Candida parapsilosis*, we conducted the analysis and characterization of the antifungal susceptibility profiles to azole drugs. From a total of 281 isolates, 88.97% were identified as *C. parapsilosis*, 6.05% as *Candida metapsilosis,* and 4.98% as *Candida orthopsilosis*. Resistant phenotype to fluconazole (FLC) was the most prevalent in *C. parapsilosis* (10.4%), 3.6% exhibited cross-resistance to voriconazole (VRC), and 1.2% of non-wild type profile to posaconazole (PSC). Among cryptic species, one strain of *C. orthopsilosis* and the other of *C. metapsilosis* displayed a non-wild type phenotype to FLC/VRC and VRC, respectively.

Focusing on the twenty-six *C. parapsilosis* FLC resistant strains, the expression of azole resistance genes like *CDR1*, *MDR1,* and *ERG11* was quantified by RT-qPCR. *MDR1* was upregulated in 81% of resistant strains, while Erg11 and Cdr1 overexpression were detected in 30.7% and 26.9%, respectively. Gene sequencing revealed several amino acid substitutions in *CDR1*, *MDR1*, and *ERG11*, and the transcription factor Mrr1p.

Our data confirm that *C. parapsilosis* remains the main etiologic agent among the *psilosis* complex. However, the emergence of *C. metapsilosis* was noticed once its prevalence has duplicated in comparison to our previous studies. An increase of non-susceptible strains was observed mainly associated with Mdr1 efflux pump overexpression, in particular found in *C. parapsilosis* fluconazole resistance.

Keywords:

INTRODUCTION

Worldwide it is estimated that fungal diseases, ranging from allergic syndromes to life-threatening invasive diseases, afflict over a billion people and cause 1.5 million deaths (1). Invasive fungal infections caused by *Candida* species are widely associated with high rates of severe illness and up to 30% of deaths in the health-care environment. Just in USA, prolonged hospitalizations due to candidaemia results in an attributable health cost of US $46,684 per patient (2, 3).

Surveillance programs of healthcare-associated pathogens are essential sources of information necessary for those developing prevention measures. The continuous monitoring of pathogens incidence and antimicrobial resistance patterns are also crucial to elucidate species distribution trends, track the emergence of resistance, monitor changes in underlying conditions and predisposing risk factors, and assess trends in antifungal treatment and outcomes (4).

Etiologically, *Candida albicans* is the most common *Candida* spp. linked with healthcare-associated invasive infections globally. However, an increasing number of infections by non-*albicans Candida* species (NACs) such as *C. glabrata*, *C. parapsilosis*, *C. tropicalis*, *C. krusei,* and *C. auris*, have been registered (5). Pfaller *et al*. (6) accounted for more than 50% of all invasive candidiasis due to NACs in 62.5% of North American hospitals.

Candida parapsilosis is an important pathogen worldwide, particularly among immunocompromised individuals and patients requiring prolonged use of a central venous catheter or other indwelling devices, mostly due to its notorious capacity to adhere and develop biofilm at the surface of intravascular devices (7, 8). Additionally, it is predominantly found in pediatric care units, being responsible for a third of neonatal *Candida* infections, with a mortality rate of approximately 10% (9). Notably, *Candida parapsilosis* is the second most commonly isolated *Candida* species in Asia, in Southern European regions, and Latin American countries, even outranking *C. albicans* in Venezuela and Colombia (10-12). *C. parapsilosis* is part of the *psilosis* complex, also including *C. orthopsilosis* and *C. metapsilosis* (13). These two cryptic

149

species are also opportunistic pathogens, associated with local and systemic diseases. Like *C. parapsilosis* its frequency and distribution differ according to geographical areas (14, 15).

Despite the continuous research for new therapeutic strategies, limited options in terms of antifungal drugs for the treatment of candidiasis are available; resuming to four classes of antifungal drugs: azoles, echinocandins, polyenes, and nucleoside analogs (16). Azoles are the most widely used drugs for the treatment of C*andida* invasive infections (17). They bind to and inhibit the activity of the enzyme lanosterol 14α-demethylase (encoded by Erg11p in yeasts), a key enzyme in the ergosterol biosynthetic pathway (18, 19).

The emergence of antifungal resistance in *Candida* species poses a major challenge to treatment. To date, *Candida* spp. azole resistance has been linked to different molecular mechanisms that include: i) mutations in the gene encoding the azole target enzyme, lanosterol 14α-demethylase (*ERG11*), reducing or impairing binding of azoles to its target; ii) *ERG11* overexpression, diluting fluconazole action; iii) alterations in the ergosterol biosynthetic pathway due to loss of function point mutations in the *ERG3* gene; despite the ergosterol depletion and the accumulation 14α-methyl fecosterol, the latter is less damaging to cell membranes and allows the continued growth even in the presence of azoles; and iv) upregulation of multidrug efflux pumps (*CDR1*, *CDR2,* and *MDR1* genes) that transport the drug out of the cells (20, 21).

Hereby, we characterize the antifungal susceptibility pattern to fluconazole (FLC), voriconazole (VRC), and posaconazole (PSC) of a large number of *C. parapsilosis* complex clinical isolates; in addition, we explore the molecular mechanisms involved in *C. parapsilosis* fluconazole resistance, by evaluating the *CDR1*, *MDR1* and *ERG11* gene expressions. Additionally, the coding sequences of the previous genes and their transcription regulators *TAC1*, *MRR1,* and *UPC2* were sequenced.

MATERIALS AND METHODS

Candida parapsilosis strains

All the strains of *Candida parapsilosis* complex (*n* = 281) assessed in this study were made

available from the fungal collection of the Microbiology Laboratory of the Faculty of Medicine

of the University of Porto (n = 210) and the Clinical Yeast Collection of the University of Coimbra

(CYCUC) (n = 71). They had been previously obtained from patients admitted at Centro

Hospitalar e Universitário de São João, Porto, Portugal, and Hospital dos Covões, Coimbra,

Portugal, isolated from several sources - respiratory tract, urine, central venous catheter, blood,

and skin - during years 2013 to 2016.

Until testing, all strains were stored in YPD broth medium (1% Bacto Yeast Extract, 2% Bacto

Peptone, 2% D-(+)-Glucose) with 40% glycerol at −80°C. For each experiment, the

microorganisms were sub-cultured twice on the recommended medium to assess the purity of

the culture and its viability.

Species complex differentiation

C. parapsilosis strains were initially identified by VITEK 2 YST cards from bioMérieux (Marcy

l'Etoile, France). To differentiate strains among *Candida parapsilosis* complex, restriction

fragment length polymorphism (RFLP) analysis of the *SADH* gene was carried out as described

by Tavanti *et al.* (13). Briefly, the amplification of the *SADH* gene fragment (716 bp) was

performed followed by *BanI* restriction pattern analysis.

Antifungal susceptibility testing

C. parapsilosis, C. orthopsilosis and *C. metapsilosis* strains were characterized regarding the

antifungal susceptibility profile to azoles, namely, FLC (Pfizer, New York, NY, USA), VRC (Pfizer)

and PSC (Schering-Plough, Kenilworth, NJ, USA) accordingly to the broth dilution method of

Clinical and Laboratory Standards Institute (CLSI) M27 protocol guidelines (22).

C. parapsilosis minimal inhibitory concentration (MIC) was registered after 48 h and the susceptibility breakpoints for FLC and VRC were those described in CLSI M60-Ed2 (23). For FLC, the susceptibility MIC was ≤ 2 μg mL^{-1}, the MIC for susceptible-dose dependent (SDD) was 4 μg mL^{-1}, and the MIC for resistance was ≥ 8 μg mL^{-1}. For VRC, the susceptibility MIC was ≤ 0.12 μg mL^{-1}, the MIC for intermediate (I) was 0.25 to 0.5 μg mL^{-1} and the MIC for resistance was ≥ 1 μg mL^{-1}.

For the cryptic species, *C. orthopsilosis* and *C. metapsilosis*, epidemiological cutoff values (ECVs) were also registered after 48 h and analyzed as recommended by CLSI M59-Ed3 (24). For *C. orthopsilosis*, fluconazole and voriconazole ECV of ≤ 2 μg mL^{-1} and ≤ 0.125 μg mL^{-1} were considered as a wild type (WT) phenotype, respectively. For *C. metapsilosis*, fluconazole and voriconazole ECV of ≤ 4 μg mL^{-1} and ≤ 0.06 μg mL^{-1} were considered as a wild type phenotype, respectively.

Real time-quantitative PCR

In *C. parapsilosis* fluconazole resistant strains molecular mechanisms were investigated via *CDR1* (CPAR2_405290)*, MDR1* (CPAR2_301760) and *ERG11* (CPAR2_303740) gene expressions (Table 1), quantified by RT-qPCR, as described by Branco *et al* (25) with adaptations. Briefly, yeast cells were collected after growing in YPD broth medium at 30ºC until reaching an OD$_{600}$ ranging between 0.6 and 0.8. Afterwards, total RNA was extracted with RNeasy Plus Mini Kit (Qiagen), being the concentration and quality controls measured using Nanodrop equipment (Eppendorf). The RNA samples, with A$_{260}$/A$_{280}$ ratios ranging from 1.8 to 2.2 and no signs of degradation after electrophoresis, were used. First-strand cDNA was synthesized using the SensiFAST cDNA Synthesis Kit (Bioline), following the manufacturer´s instructions. cDNA was used in three replicates per strain for each gene expression experiment, performed with the SensiFAST SYBR Hi-ROX Kit (Bioline), 3-step cycling, according to the manufacturer's instructions. RT-qPCR was carried out in a StepOnePlus™ Real-Time PCR System. The constitutively *ACT1* gene signal was

used as a reference for normalizing the relative expression levels of analyzed genes, detailed in Table 1. StepOnePlus™ Software v2.3 8 (Applied Biosystems) was used to determine the dissociation curve and threshold cycle (Ct). The $2^{-\Delta\Delta CT}$ method was used to calculate changes in gene expression among clinical strains.

Gene sequencing

Candida parapsilosis fluconazole resistant strains overexpressing the *CDR1, MDR1* and *ERG11* genes were submitted to an analysis of its encoding sequences. The transcription factors *TAC1* (CPAR2_303510), *MRR1* (CPAR2_807270) and *UPC2* (CPAR2_CPAR2_207280) were also sequenced. All above-mentioned genes were amplified by PCR using the primers listed in Table 1. For genomic DNA extraction, DNeasy Plant Mini Kit (Qiagen) was used as the manufacturer's instructions. PCR products were amplified using NZYProof DNA polymerase (NZYTech) and sequenced in a company, with sanger sequencing methodology. The sequences were analyzed using DNA Sequence Assembler v4 (2013), Heracle BioSoft and compared to the reference strain *C. parapsilosis* CDC317.

RESULTS

Candida parapsilosis complex differentiation

The entire collection, a total of two hundred and eighteen one strains identified within *C. parapsilosis* complex, was tested for *SADH* gene restriction profile. As described by Tavanti *et al.* (13), *C. parapsilosis* contains one *BanI* restriction site at position 196, *C. orthopsilosis* has no restriction site, while *C. metapsilosis* possesses three *BanI* restriction sites at 96, 469, and 529 positions. The amplified fragments of *C. orthopsilosis*, were sequenced to exclude a point mutation in the restriction site of *C. parapsilosis*.

We identified 88.97% (n = 250) as *Candida parapsilosis sensu stricto*, 4.98% (n = 14) as *Candida orthopsilosis* and 6.05% (n = 17) as *C. metapsilosis*.

Azoles susceptibility profile

Azole susceptibility testing was performed in accordance with CLSI guidelines (Supplementary Table S1). We characterized 83.2% of *C. parapsilosis* as susceptible to FLC and 86% as susceptible to VRC (Figure 7). Susceptible-dose dependent (SDD) strains to FLC and with an intermediate (I) phenotype to VRC was found to be 6.40% and 10.8%, respectively; a resistant phenotype to FLC and VRC was detected in 10.4% and 3.2%, respectively. All strains VRC resistant were also resistant to FLC. Relatively to PSC, 98.8% of *C. parapsilosis* strains correspond to a wild type phenotype and 1.2% to a non-wild type profile.

From the fourteen *C. orthopsilosis* strains, thirteen correspond to a wild type phenotype to FLC and VRC; one strain (Co14) exhibits a non-wild type phenotype to FLC (32 µg mL^{-1}) and VRC (0.25 µg mL^{-1}) (Supplementary Table S2).

All *C. metapsilosis* strains revealed an ECV of ≤ 4 µg mL^{-1} to FLC and ≤ 0.06 µg mL^{-1} to VRC, corresponding to a wild type phenotype. An exception was observed in strain Cm09 that corresponded to a non-wild type phenotype, since the VRC ECV was 0.125 µg mL^{-1} (Supplementary Table S3).

All *C. orthopsilosis* and *C. metapsilosis* strains exhibited a wild type phenotype to PSC.

Expression of Cdr1, Mdr1 and Erg11 in *C. parapsilosis* fluconazole resistant strains

The expression of genes *CDR1, MDR1 and ERG11* was quantified by RT-qPCR in the twenty-six *C. parapsilosis* FLC resistant strains. The analysis was performed by comparison to the relative expression average of eight *C. parapsilosis* strains, randomly selected from the collection, displaying FLC and VRC susceptible and PSC wild-type phenotypes. We defined overexpression as a 2-fold increase in gene expression.

Resistance to FLC emerged mainly due to an increase in the capacity of fungal cells to expel fluconazole (19/26) from the inside of the cell to the extracellular environment. This was achieved mostly by the upregulation of *MDR1* gene (21/26), whose expression in these strains vary from 3 to 2393-fold increase comparatively to the control group. Concomitantly with *MDR1* expression, *CDR1* gene was also overexpressed in 5 of the 26 strains assessed, exhibiting relatively low values compared to MDR1 gene expressions, ranging from 2 up to 4-fold increase comparatively to the control group.

Together with azole extrusion, *ERG11* overexpression was clearly a mechanism of FLC response in 2 of the strains, Cp100 and D196, displaying an up regulation of 10,5 and 39-fold respectively. Mild levels of *ERG11* gene expression, around 2-fold increase were also detected in other 5 strains (Cp85, D203, D211, D222, D223).

Interestingly, in 4 of the 26 strains, expression of the genes screened was not different from the one of the control group suggesting that the mechanism associated with FLC resistance is not *ERG11* overexpression or efflux pumps activity.

Sequencing of overexpressed genes and their corresponding transcription factors

In the *C. parapsilosis* fluconazole resistant strains with *CDR1*, *MDR1* and *ERG11* genes overexpressed, we searched for single-nucleotide polymorphisms (SNPs) within its encoding sequences and in its respective regulators *TAC1*, *MRR1* and *UPC2*.

Among the eight strains overexpressing *CDR1* gene we did not detect any nucleotide alteration. The same happened for its transcription factor Tac1p, excepting strain D158, in which a heterozygous L877P (T2630C) substitution was found.

Among the twenty-one *MDR1*-overexpressing strains, mutations leading to amino acid substitutions in Mdr1p were detected in six strains: amino acid substitution I396V (A1186G) in strains D154 and D162; heterozygous I396V (A1186G) alteration in strains D150, D151, D158 and D159. In the *MRR1* nucleotide sequence, it was found the homozygous amino acid substitutions

R405K (G1214A) and G604R (G1810A) in strains Cp37 and Cp141, respectively. A heterozygous D615G (A1844G) alteration was detected in the strains D150, D151 and D154. In the remaining fifteen strains, no gene nucleotide alterations were found.

Since Erg11p is the fluconazole target, all fluconazole resistant strains (n = 26) were screened for polymorphisms in this gene. Among the nineteen resistant strains which did not have Erg11p overexpressed, we found the Y132F amino acid substitution in heterozygosity in four cases. Other SNP G1193T leading to R398I amino acid alteration were found in ten of such resistant strains. We did not identify any alteration in ERG11 gene sequence in the other seven *C. parapsilosis* resistant strains.

Among seven cases exhibiting *ERG11* overexpressing, strains Cp100, D196 and D223 did not reveal any alteration in its encoding sequence; the Y132F heterozygous alteration was detected in strains, Cp85, D221 and D222; the R398I substitution was detected in strain D203. The Erg11p transcription factor, *UPC2* was also analyzed in the eight resistant strains overexpressing the fluconazole target and no alteration was found in their nucleotide sequences.

DISCUSSION

The continuous monitoring of the most relevant healthcare-associated pathogens is crucial for the implementation of preventive measures of infection control, culminating in a better outcome to the patients.

Since 2005, when Tavanti *et al*. (13) confirmed a *C. parapsilosis* complex of three distinct species, namely *C. parapsilosis sensu stricto*, *C. orthopsilosis* and *C. metapsilosis*, several surveillance studies reported its distinct prevalence rates, virulence potential and *in vitro* antifungal susceptibility profiles (14, 26).

While the global prevalence of *C. parapsilosis sensu stricto* ranks within the complex, the incidence of *C. orthopsilosis* and *C. metapsilosis* can vary in different geographical regions (27-

29). The higher prevalence in the hospital environment of *C. parapsilosis* could be linked to a myriad of virulence attributes, compared to *C. orthopsilosis* and *C. metapsilosis* (14).

In 2009 (30) we reported an incidence of 2.3% and 2.9% of *C. orthopsilosis* and *C. metapsilosis*, respectively, while *C. parapsilosis* accounted for 91.4% of the total *C. parapsilosis* complex isolates. In 2014 (31) we observed a decrease in the prevalence of *C. parapsilosis* (89.09%) and an increase of the cryptic species, *C. orthopsilosis* (7.27%) and *C. metapsilosis* (3.64%). Interestingly, in the present study, using a set of unrelated strains that had been recovered at 2 university hospitals, between years 2013-2016, we found 88.97% of *C. parapsilosis*, 4.98% of *C. orthopsilosis* and 6.05% of *C. metapsilosis*. These values might suggest a trend of *C. orthopsilosis* and *C. metapsilosis* species increase in proportion to *C. parapsilosis*, however such conclusion cannot be taken once these strains belong to a collection and no epidemiological study was carried out.

Similarly to our results, Guo *et al*. (32), in a fifteen-year retrospective study conducted in Eastern China, describe a distribution of *C. parapsilosis* and *C. orthopsilosis* of 86.3% and 5.5%, respectively; a higher incidence of 8.1% of *C. metapsilosis* was observed.

In a six-year multicenter study from Iran, a higher percentage of *C. parapsilosis* (94.5%) and a similar value of *C. orthopsilosis* (5.3 %) was reported, in comparation to our study. Surprisingly, C. *metapsilosis* comprised only 0.17% of all *C. parapsilosis* species complex isolates in such study (26).

The antifungal susceptibility profile of *C. parapsilosis* complex has been increasingly studied, as the incidence of the *psilosis* complex prevalence has been raising continuously. Worldwide, the azoles susceptible phenotype of *C. parapsilosis* isolates remains high (89.1–91.6%) (33). However, azole resistance has progressively increased over time with geographic variations. Recent studies reported rates of *C. parapsilosis* FLC resistant or susceptible-dose dependent phenotypes of 15% in Europe and 3.6% in North America (33). In a multicenter study in China, a rate of 6% of *C. parapsilosis* complex isolates were found to be resistant/non-wild type to azoles

(34). Another study from Eastern China describes *C. orthopsilosis* and *C. metapsilosis* bloodstream isolates to be susceptible or wild type to azole drugs (of about 92.3 – 100% to FLC and VRC) (32).

According to our results, the susceptible phenotype or wild type remains the most prevalent phenotype ranging from 83.2% for FLC to 98.80% for PSC among *C. parapsilosis*. The highest values of resistance were found for FLC (10.4%) and VRC (3.2%). However, these susceptibility profiles are not directly comparable with those described by us in 2014 study, once meanwhile fluconazole breakpoint were changed. Interestingly, VRC resistance was found in 3.2% of the *C. parapsilosis* strains, while no resistance was registered in 2014.

The majority (80,8%) of the *C. parapsilosis* fluconazole resistant strains exhibit *MDR1* overexpression, what makes this path the most prevalent azole mechanism among our strain collection. We detected several point mutations in *MDR1* (I396V, in heterozygosity) and *MRR1* (R405K and G604R, in homozygosity; D615G in heterozygosity) genes, which possibly are responsible for the Mdr1p overexpression. Also, the Tac1p mutation L877P was observed in heterozygosity in strain D158. However, it is crucial to confirm whether the described mutations are, in fact, connected with resistance to fluconazole using molecular approaches.

In the last decade several studies aimed to unveil the molecular mechanisms involved in *C. parapsilosis* azole resistance. Berkow *et al*. (35) demonstrated that overexpression of *CDR1* and *MDR1* drug transporters can contribute directly to azole resistance of *C. parapsilosis* through activating mutations in the genes encoding their respective transcriptional factors. Grossman *et al*. 2015 (36), using *C. parapsilosis* isolates from a U.S. surveillance system demonstrated that *ERG11* mutations are a frequent cause of fluconazole resistance in this species and that *MRR1* mutations could also be involved. They also detected R405K mutation in Mrr1p, however an association with fluconazole resistance was not establish since this alteration is present in susceptible, SDD and resistant isolates.

In the present study, in strains with *MDR1* gene activation, we analyzed whether *CDR1* and

ERG11 genes were overexpressed. Interestingly, simultaneous *MDR1*, *CDR1* and *ERG11*

overexpression was observed in three isolates. *ERG11* upregulation was detected in eight *C.*

parapsilosis strains, which displayed also efflux pump gene overexpression (*MDR1* and/or

CDR1). We identified Y132F, in heterozygosity, and R398I mutations in several fluconazole

resistant strains overexpressing *ERG11*. Y132F is the most described mutation in *ERG11* gene

and it is only detected in resistant isolates, being directly involved it in ergosterol biosynthesis

alterations. R398I mutation, has been considered a compensatory mutation and is not

considered to cause azole resistance on its own (33, 37).

It has been considered that single *ERG11* overexpression by itself is an uncommon resistance

mechanism among *C. parapsilosis* isolates; it is usually the detection of a combination of

molecular mechanisms, involving sterol and efflux pump gene alterations that confers such a

resistant profile (14, 33).

AUTHOR CONTRIBUTIONS

JB and IMM conceived and designed the experiments;

JB, CMC and IMM perform the experiments;

JB, CMC, IMM and AGR analyzed the data;

IMM and AGR contributed with reagents and material;

JB, IMM drafted the manuscript. All authors reviewed the manuscript.

LEGEND

Figure 1. Gene expression associated with *C. parapsilosis* fluconazole resistance. Relative expression levels of *CDR1*, *MDR1* and *ERG11* genes in *C. parapsilosis* fluconazole resistant strains. The experiences were performed in triplicate and compared with an average of eight *C. parapsilosis* susceptible/wild type strains. We assumed 2-fold as an increase in gene expression. The represented values are the mean value ± standard error. Strains were grouped according to their MIC to FLC.

REFERENCES

1. Bongomin F, Gago S, Oladele RO, Denning DW. 2017. Global and Multi-National Prevalence of Fungal Diseases-Estimate Precision. J Fungi (Basel) 3.
2. McCarty TP, White CM, Pappas PG. 2021. Candidemia and Invasive Candidiasis. Infect Dis Clin North Am 35:389-413.
3. Strollo S, Lionakis MS, Adjemian J, Steiner CA, Prevots DR. 2016. Epidemiology of Hospitalizations Associated with Invasive Candidiasis, United States, 2002-2012(1). Emerg Infect Dis 23:7-13.
4. Toda M, Williams SR, Berkow EL, Farley MM, Harrison LH, Bonner L, Marceaux KM, Hollick R, Zhang AY, Schaffner W, Lockhart SR, Jackson BR, Vallabhaneni S. 2019. Population-Based Active Surveillance for Culture-Confirmed Candidemia - Four Sites, United States, 2012-2016. MMWR Surveill Summ 68:1-15.
5. Koehler P, Stecher M, Cornely OA, Koehler D, Vehreschild M, Bohlius J, Wisplinghoff H, Vehreschild JJ. 2019. Morbidity and mortality of candidaemia in Europe: an epidemiologic meta-analysis. Clin Microbiol Infect 25:1200-1212.
6. Pfaller MA, Andes DR, Diekema DJ, Horn DL, Reboli AC, Rotstein C, Franks B, Azie NE. 2014. Epidemiology and outcomes of invasive candidiasis due to non-albicans species of Candida in 2,496 patients: data from the Prospective Antifungal Therapy (PATH) registry 2004-2008. PLoS One 9:e101510.
7. Trofa D, Gácser A, Nosanchuk JD. 2008. Candida parapsilosis, an Emerging Fungal Pathogen. Clinical Microbiology Reviews 21:606-625.
8. Krcmery V, Barnes AJ. Non-albicans Candida spp. causing fungaemia: pathogenicity and antifungal resistance. Journal of Hospital Infection 50:243-260.
9. Pammi M, Holland L, Butler G, Gacser A, Bliss JM. 2013. Candida parapsilosis is a Significant Neonatal Pathogen: A Systematic Review and Meta-Analysis. The Pediatric infectious disease journal 32:e206-e216.
10. Nucci M, Queiroz-Telles F, Alvarado-Matute T, Tiraboschi IN, Cortes J, Zurita J, Guzman-Blanco M, Santolaya ME, Thompson L, Sifuentes-Osornio J, Echevarria JI, Colombo AL, on behalf of the Latin American Invasive Mycosis N. 2013. Epidemiology of Candidemia in Latin America: A Laboratory-Based Survey. PLoS ONE 8:e59373.
11. Toth R, Nosek J, Mora-Montes HM, Gabaldon T, Bliss JM, Nosanchuk JD, Turner SA, Butler G, Vagvolgyi C, Gacser A. 2019. Candida parapsilosis: from Genes to the Bedside. Clin Microbiol Rev 32.
12. Guinea J. 2014. Global trends in the distribution of Candida species causing candidemia. Clin Microbiol Infect 20 Suppl 6:5-10.
13. Tavanti A, Davidson AD, Gow NA, Maiden MC, Odds FC. 2005. Candida orthopsilosis and Candida metapsilosis spp. nov. to replace Candida parapsilosis groups II and III. J Clin Microbiol 43:284-92.
14. Neji S, Hadrich I, Trabelsi H, Abbes S, Cheikhrouhou F, Sellami H, Makni F, Ayadi A. 2017. Virulence factors, antifungal susceptibility and molecular mechanisms of azole resistance among Candida parapsilosis complex isolates recovered from clinical specimens. J Biomed Sci 24:67.
15. Németh TM GA, Nosanchuk JD. 2018. Candida psilosis complex. *In* Elsevier SD, CA (ed), In Reference module in life sciences doi:10.1016/b978-0-12-809633-8.20709-7.
16. Denning DW, Hope WW. Therapy for fungal diseases: opportunities and priorities. Trends in Microbiology 18:195-204.
17. Vallabhaneni S, Baggs J, Tsay S, Srinivasan AR, Jernigan JA, Jackson BR. 2018. Trends in antifungal use in US hospitals, 2006-12. J Antimicrob Chemother 73:2867-2875.
18. Cowen LE, Sanglard D, Howard SJ, Rogers PD, Perlin DS. 2014. Mechanisms of Antifungal Drug Resistance. Cold Spring Harbor Perspectives in Medicine doi:10.1101/cshperspect.a019752.

19. Odds FC, Brown AJP, Gow NAR. Antifungal agents: mechanisms of action. Trends in Microbiology 11:272-279.

20. Sanglard D, Odds FC. Resistance of Candida species to antifungal agents: molecular mechanisms and clinical consequences. The Lancet Infectious Diseases 2:73-85.

21. Pfaller MA. 2012. Antifungal drug resistance: mechanisms, epidemiology, and consequences for treatment. Am J Med 125:S3-13.

22. CLSI. 2017. Reference Method for Broth Dilution Antifungal Susceptibility Testing of Yeasts, 4th ed. CLSI standard M27. Wayne, PA: Clinical Laboratory Standards Institute.

23. CLSI. 2020. Performance Standards for Antifungal Susceptibility Testing of Yeasts, 2nd ed. CLSI supplement M60. Wayne, PA: Clinical Laboratory Standards Institute.

24. CLSI. 2020. Epidemiological Cutoff Values for Antifungal Susceptibility Testing, 3rd ed. CLSI supplement M59. Wayne, PA: Clinical Laboratory Standards Institute.

25. Branco J, Ola M, Silva RM, Fonseca E, Gomes NC, Martins-Cruz C, Silva AP, Silva-Dias A, Pina-Vaz C, Erraught C, Brennan L, Rodrigues AG, Butler G, Miranda IM. 2017. Impact of ERG3 mutations and expression of ergosterol genes controlled by UPC2 and NDT80 in Candida parapsilosis azole resistance. Clin Microbiol Infect 23:575 e1-575 e8.

26. Arastehfar A, Khodavaisy S, Daneshnia F, Najafzadeh MJ, Mahmoudi S, Charsizadeh A, Salehi MR, Zarrinfar H, Raeisabadi A, Dolatabadi S, Zare Shahrabadi Z, Zomorodian K, Pan W, Hagen F, Boekhout T. 2019. Molecular Identification, Genotypic Diversity, Antifungal Susceptibility, and Clinical Outcomes of Infections Caused by Clinically Underrated Yeasts, Candida orthopsilosis, and Candida metapsilosis: An Iranian Multicenter Study (2014-2019). Front Cell Infect Microbiol 9:264.

27. Tosun I, Akyuz Z, Guler NC, Gulmez D, Bayramoglu G, Kaklikkaya N, Arikan-Akdagli S, Aydin F. 2013. Distribution, virulence attributes and antifungal susceptibility patterns of Candida parapsilosis complex strains isolated from clinical samples. Med Mycol 51:483-92.

28. Canton E, Peman J, Quindos G, Eraso E, Miranda-Zapico I, Alvarez M, Merino P, Campos-Herrero I, Marco F, de la Pedrosa EG, Yague G, Guna R, Rubio C, Miranda C, Pazos C, Velasco D, Group FS. 2011. Prospective multicenter study of the epidemiology, molecular identification, and antifungal susceptibility of Candida parapsilosis, Candida orthopsilosis, and Candida metapsilosis isolated from patients with candidemia. Antimicrob Agents Chemother 55:5590-6.

29. Pfaller MA, Diekema DJ, Turnidge JD, Castanheira M, Jones RN. 2019. Twenty Years of the SENTRY Antifungal Surveillance Program: Results for Candida Species From 1997-2016. Open Forum Infect Dis 6:S79-S94.

30. Silva AP, Miranda IM, Lisboa C, Pina-Vaz C, Rodrigues AG. 2009. Prevalence, distribution, and antifungal susceptibility profiles of Candida parapsilosis, C. orthopsilosis, and C. metapsilosis in a tertiary care hospital. J Clin Microbiol 47:2392-7.

31. Faria-Ramos I, Neves-Maia J, Ricardo E, Santos-Antunes J, Silva AT, Costa-de-Oliveira S, Canton E, Rodrigues AG, Pina-Vaz C. 2014. Species distribution and in vitro antifungal susceptibility profiles of yeast isolates from invasive infections during a Portuguese multicenter survey. Eur J Clin Microbiol Infect Dis 33:2241-7.

32. Guo J, Zhang M, Qiao D, Shen H, Wang L, Wang D, Li L, Liu Y, Lu H, Wang C, Ding H, Zhou S, Zhou W, Wei Y, Zhang H, Xi W, Zheng Y, Wang Y, Tang R, Zeng L, Xu H, Wu W. 2021. Prevalence and Antifungal Susceptibility of Candida parapsilosis Species Complex in Eastern China: A 15-Year Retrospective Study by ECIFIG. Front Microbiol 12:644000.

33. Castanheira M, Deshpande LM, Messer SA, Rhomberg PR, Pfaller MA. 2020. Analysis of global antifungal surveillance results reveals predominance of Erg11 Y132F alteration among azole-resistant Candida parapsilosis and Candida tropicalis and country-specific isolate dissemination. Int J Antimicrob Agents 55:105799.

34. Xiao M, Chen SC, Kong F, Xu XL, Yan L, Kong HS, Fan X, Hou X, Cheng JW, Zhou ML, Li Y, Yu SY, Huang JJ, Zhang G, Yang Y, Zhang JJ, Duan SM, Kang W, Wang H, Xu YC. 2020.

Distribution and Antifungal Susceptibility of Candida Species Causing Candidemia in China: An Update From the CHIF-NET Study. J Infect Dis 221:S139-S147.

35. Berkow EL, Manigaba K, Parker JE, Barker KS, Kelly SL, Rogers PD. 2015. Multidrug Transporters and Alterations in Sterol Biosynthesis Contribute to Azole Antifungal Resistance in Candida parapsilosis. Antimicrob Agents Chemother 59:5942-50.

36. Grossman NT, Pham CD, Cleveland AA, Lockhart SR. 2015. Molecular mechanisms of fluconazole resistance in Candida parapsilosis isolates from a U.S. surveillance system. Antimicrob Agents Chemother 59:1030-7.

37. Magobo RE, Lockhart SR, Govender NP. 2020. Fluconazole-resistant Candida parapsilosis strains with a Y132F substitution in the ERG11 gene causing invasive infections in a neonatal unit, South Africa. Mycoses 63:471-477.

Table 1. Primers used in this study.

Primer name	Primer sequence (5` to 3`)
RT-qPCR	
CPACT1_F2	TTGATGAAGATTTTGTCCGAA
CPACT1_R2	GATGATTGTGATGAGGTTTGC
CPCDR1_F	TCAGAGGTGTTTCAGGTGGT
CPCDR1_R	GGCAATCAATGGTGTGGTAT
CPMDR1_F1	CATCCCCATTGCTATTGTTG
CPMDR1_R1	CACCTGAAGTTGTCGTTGC
CPERG11_F2	GACCGCATTGACTACCGAT
CPERG11_R2	ACGCCACTTTTCTGTTTCTTC
Gene Amplification/Sequencing	
CPERG11_F1	GCTACTAACTTTCCCTACCTTCG
CPERG11_R1	GTGAGTCAACAAAGAAGACAATC
CPUPC2_F1	GGTAAACCATCCTCAGAGTGAGA
CPUPC2_F	ATTGGAGTGTGGGTATCTTCAT
CPUPC2_F2	CACAATCAGGGCAGCAGCAG
CPUPC2_R1	CCCATTGAGCATATTATCCAGC
CPMRR1_UP_F	CTACTGATATGCCTGACGCCAC
CPMRR1_DOWN_R	GCTTTCTTGTTTTCAATAAGAGAGA
CPMRR1_F2 A	CCCTTTCTTCCGCAGATTTC
CPMRR1_F2 B	CCTTACTTGAACGAAATGGAG
CPMRR_F3	GAAGATGGCGATGAT
CPMRR1_R2 A	CGTTGTAAAGATGGCGTGGT
CPMDR1_F2	GCAACAAAACCCCATCTCA
CPMDR1_R2	GCACGAAAGGGTCAAAGG
CPMDR1_F3	TTTGGAACTTGCCCTTGTC
CPCDR1_F4	ATAACCCATTTCCAACTTTT
CPCDR1_R4	CTGAGCACATACGGCATC
CPCDR1_F	TCAGAGGTGTTTCAGGTGGT
CPCDR1_F2	CGGTTTTTCTTTTATTGGCTCA
CPCDR1_F3	ACTCGTCATTCCAAAGGTCG
CPTAC1_F	GGTCAATAGGCGAAGGAAA
CPTAC1_R	CAAAATGGTTATCAAATGTCAA
CPTAC1_F1	TCGTGATGGAGTTGGTCG

Figure 1
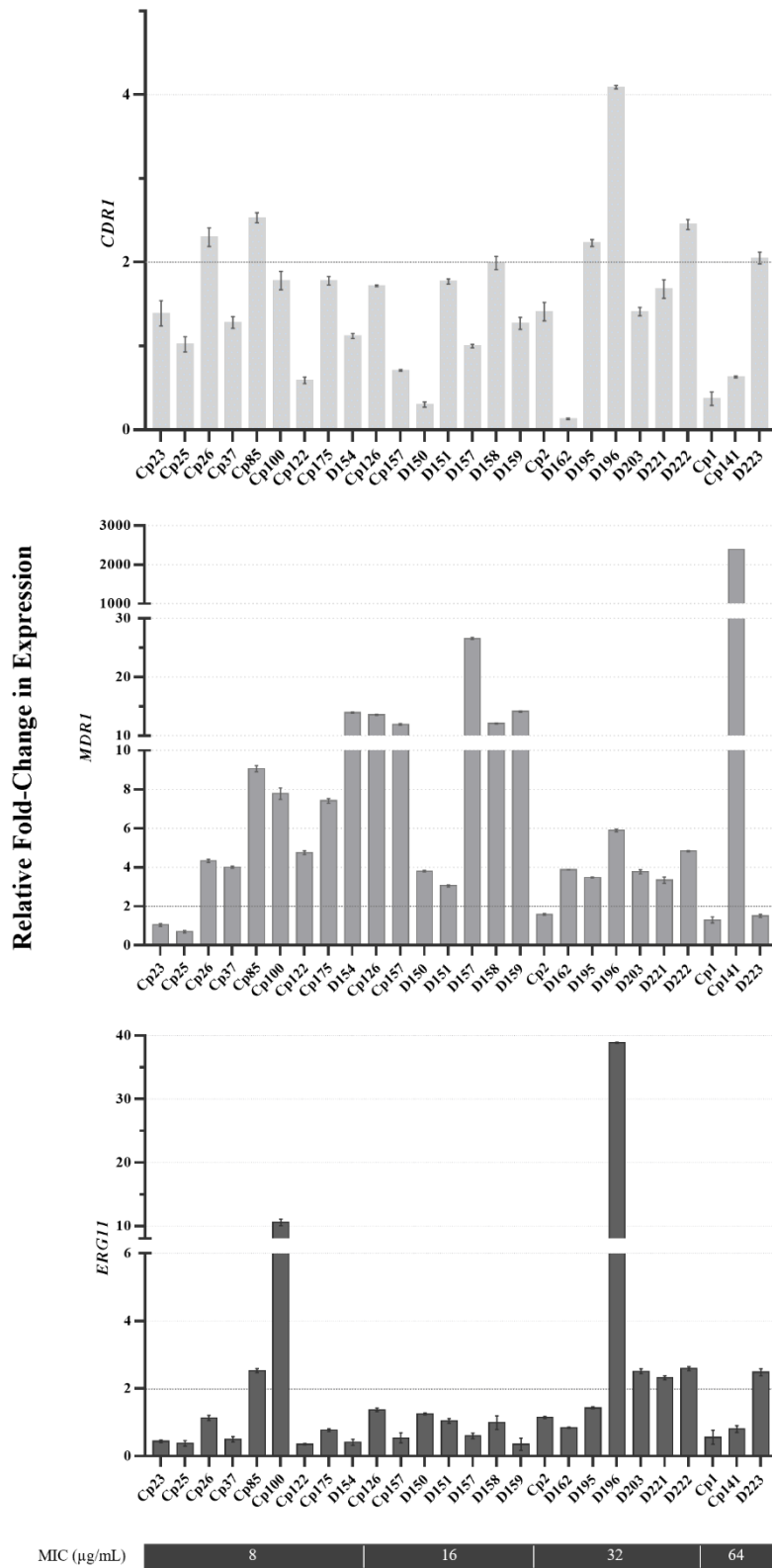
Paper III

Clinical azole cross-resistance in *Candida parapsilosis* is related to a novel *MRR1* gain-of-function mutation

Contents lists available at ScienceDirect

Clinical Microbiology and Infection

CMI
CLINICAL
MICROBIOLOGY
AND INFECTION
ESCMID

Research Note

Clinical azole cross-resistance in *Candida parapsilosis* is related to a novel *MRR1* gain-of-function mutation

Joana Branco [1,2], Adam P. Ryan [3], Ana Pinto e Silva [1,2], Geraldine Butler [3], Isabel M. Miranda [4,*,†], Acácio G. Rodrigues [1,2,†]

[1] Division of Microbiology, Department of Pathology, Faculty of Medicine, University of Porto, Porto, Portugal
[2] Center for Health Technology and Services Research — CINTESIS@RISE, Faculty of Medicine, University of Porto, Porto, Portugal
[3] School of Biomolecular and Biomedical Science, Conway Institute, University College Dublin, Belfield, Dublin, Ireland
[4] Cardiovascular Research and Development Centre — UnIC@RISE, Faculty of Medicine, University of Porto, Porto, Portugal

ARTICLE INFO

ABSTRACT

Objectives: Hereby, we describe the molecular mechanisms underlying the acquisition of azole resistance by a *Candida parapsilosis* isolate following fluconazole treatment due to candiduria.
Methods: A set of three consecutive *C. parapsilosis* isolates were recovered from the urine samples of a patient with candiduria. Whole-genome sequencing and antifungal susceptibility assays were performed. The expression of *MRR1*, *MDR1*, *ERG11* and *CDR1B* (CPAR2_304370) was quantified by RT-qPCR.
Results: The initial isolate CPS-A was susceptible to all three azoles tested (fluconazole, voriconazole and posaconazole); isolate CPS-B, collected after the second cycle of treatment, exhibited a susceptible-dose—dependent phenotype to fluconazole and isolate CPS-C, recovered after the third cycle, exhibited a cross-resistance profile to fluconazole and voriconazole. Whole-genome sequencing revealed a putative resistance mechanism in isolate CPS-C, associated with a G1810A nucleotide substitution, leading to a G604R change in the Mrr1p transcription factor. Introducing this mutation into the susceptible CPS-A isolate ($MRR1_R$) resulted in resistance to fluconazole and voriconazole, as well as up-regulation of *MRR1* and *MDR1*. Interestingly, the susceptible-dose—dependent phenotype exhibited by isolate CPS-B was associated with an increased copy number of the *CDR1B* gene. The expression of *CDR1B* was increased in both isolates CPS-B and CPS-C and in the $MRR1_R$ strain, harbouring the gain-of-function mutation.
Conclusions: Our results describe clinical azole cross-resistance acquisition in *C. parapsilosis* due to a G1810A (G604R) gain-of-function mutation, resulting in *MRR1* hyperactivation and consequently, *MDR1* efflux pump overexpression. We also associated amplification of the *CDR1B* gene with decreased fluconazole susceptibility and showed that it is a putative target of the *MRR1* gain-of-function mutation.
Joana Branco, Clin Microbiol Infect 2022;28:1655.e5—1655.e8

Introduction

Candida species are responsible for approximately 10—15% of urinary tract infections (UTIs) in tertiary care hospitals and specialized medical centres [1]. *Candida albicans* is the most common causative species, accounting for 50—70% of total *Candida*

isolates, followed by *C. glabrata*, *C. tropicalis* and *C. parapsilosis* [2,3]. *C. parapsilosis* is estimated to be responsible for 1—7% of *Candida* UTIs, especially among neonates, and is often associated with systemic infection [3].

According to the Infectious Diseases Society of America (IDSA) guidelines, fluconazole is strongly recommended for the treatment of UTIs [4]. The widespread use of azoles has contributed to the emergence of *Candida* spp. resistant isolates, including *C. parapsilosis* [5]. The persistence of these isolates in clinical settings has been associated with hospital-associated outbreaks with fatal outcomes [6].

* Corresponding author: Isabel M. Miranda, Cardiovascular Research and Development Centre — UnIC@RISE, Faculty of Medicine, University of Porto, Alameda Prof. Hernâni Monteiro, 4200-319 Porto, Portugal.
E-mail address: imiranda@med.up.pt (I.M. Miranda).
† Isabel Miranda and Acácio Rodrigues share last authorship.

J. Branco et al. / Clinical Microbiology and Infection 28 (2022) 1655.e5–1655.e8

In the past decades, the molecular mechanisms underlying azole resistance in *C. parapsilosis* isolates have been scrutinized. The most common mechanism involves the up-regulation of the two main classes of multidrug efflux transporters, the ATP-binding cassette (Cdr1) and the major facilitator superfamily (Mdr1), thus increasing the efflux of azoles by the fungal cell. Alterations in the ergosterol biosynthetic pathway, including mutations in the *ERG11* gene or its overexpression, have also been linked to azole resistance in *C. parapsilosis* [7].

We describe a case of *in vivo* acquisition of crossed azole resistance in *C. parapsilosis*, based on the analysis of three consecutive isolates obtained following fluconazole treatment in a patient diagnosed with candiduria.

Methods

Isolate identification, genome sequencing and antifungal susceptibility

During fluconazole treatment, a set of three consecutive isolates (CPS-A, CPS-B and CPS-C) were obtained from urine cultures (Fig. S1). *C. parapsilosis sensu stricto* isolates were identified using matrix-assisted laser desorption/ionization time-of-flight mass spectrometry (MALDI-TOF MS, VITEK MS, BioMerieux). Afterwards, whole-genome sequencing and antifungal susceptibility testing to fluconazole, voriconazole and posaconazole of all isolates were performed (Supplementary Material).

Editing MRR1 and RT-qPCR

The mutation found in the *MRR1* gene was confirmed as a gain-of-function (GOF) mutation by expressing the gene in the susceptible isolate CPS-A resulting in a change in azole susceptibility phenotype (Fig. S2 and Table S1). The expressions of *MRR1*, *MDR1*, *ERG11* and *CDR1B* (CPAR2_304370) were quantified by RT-qPCR. All protocols are detailed in the Supplementary Material.

Results

In vivo azole resistance acquisition

The antifungal susceptibility profile revealed that the initial isolate, CPS-A, was susceptible to fluconazole, voriconazole and posaconazole. The second isolate, CPS-B, obtained after two cycles of fluconazole treatment, had a susceptible-dose−dependent phenotype and the final isolate, CPS-C, was resistant to fluconazole and voriconazole (Table 1).

Isolates' relationship and genomic changes associated with a decrease in azole susceptibility

The phylogenetic analysis of the three isolates sequences in combination with unrelated *C. parapsilosis* isolates revealed very

Table 1
MICs and susceptibility phenotypes of *Candida parapsilosis* strains

Strain	MIC (μg/mL) | phenotype		
	Fluconazole	Voriconazole	Posaconazole
CPS-A	1 | S	0.03 | S	0.25 | WT
CPS-B	4 | SDD	0.06 | S	0.06 | WT
CPS-C	64 | R	1 | R	0.125 | WT
mrr1ΔΔ	1 | S	0.03 | S	0.03 | WT
MRR1$_{RI}$	32 | R	1 | R	0.03 | WT

R, resistant; S, susceptible; SDD, susceptible-dose dependent; WT, wild type.

few differences between the genomes, suggesting that all three isolates were very closely related and highly likely descended from the same parent isolate (Fig. S3).

(Sorting Intolerant from Tolerant (SIFT) analysis identified several variants among isolates CPS-B and CPS-C (Table S2). A homozygous variant in CPS-C resulted in a nucleotide substitution, from guanine to adenine in the 1810 position (G1810A), leading to a change from glycine to arginine (G604R) in the Mrr1p polypeptide chain (CPAR2_807270).

Because no obvious single-nucleotide polymorphisms or indels to explain the reduced susceptibility were identified in CPS-B, we searched for changes in gene or chromosome copy number (Table S3). Most copy number variations with respect to the reference genome were shared with CSP-A. However, CPAR2_304370 had approximately 15 copies in CPS-B compared with 4 copies found in CPS-A and CPS-C. CPAR2_304370 is a member of the *CDR1* multidrug transporters, recently named *CDR1B* in *C. parapsilosis* [8]. The increase in the copy number of *CDR1B* in CPS-B was correlated with an increase in the expression of approximately 9.5-fold of *CDR1B* in comparison to isolate CPS-A (Fig. 1). Notably, the expression of *CDR1B* was also increased (10.5-fold) in the CPS-C isolate, independently of the gene copy number.

G1810A is a GOF mutation in the MRR1 gene

The deletion of the *MRR1* gene in isolate CPS-A (*mrr1ΔΔ*) did not change its azole susceptibility profile. In contrast, the G1810A nucleotide mutation in *MRR1*$_{RI}$ resulted in resistance to fluconazole and voriconazole, with MICs of 32 and 1 μg/mL, respectively (Table 1).

To determine how the *MRR1* GOF mutation (G1810A) resulted in increased azole resistance, we quantified the expression of *MRR1* and *MDR1*. In CPS-C, expressions were up-regulated by 35-fold and 260-fold, respectively, compared with CPS-A (Fig. 1). Introducing the mutated *MRR1* gene in the *mrr1ΔΔ* clone resulted in an up-regulation of *MRR1* and *MDR1* gene expression by approximately 30-fold and 220-fold, respectively. The expression of *MRR1* and *MDR1* in isolate CPS-B was identical to that in the initial susceptible isolate.

CDR1B expression in the *MRR1*$_{RI}$ strain was 3.5-fold up-regulated compared with isolate CPS-A and 3-fold overexpressed relatively to the *mrr1ΔΔ* strain.

The expression of *ERG11* decreased by approximately 40−60% in isolates CPS-B and CPS-C, respectively, compared with the initial isolate CPS-A. A similar reduction (40%) in *ERG11* gene expression was detected in the *MRR1*$_{RI}$ strain.

Discussion

The emergence of *C. parapsilosis* as one of the most prevalent fungal infections raises questions about the mechanisms underlying antifungal resistance. The up-regulation of *ERG11* expression has been described as a strategy to overcome the fluconazole effect in clinical resistant isolates of *C. parapsilosis* [9]. Conversely, our results show a reduction in *ERG11* expression following prolonged fluconazole exposure, accordingly to what was previously found in an azole induction assay [10].

In *C. parapsilosis*, the efficient efflux of azoles can result from the up-regulation of transporter pumps encoded by *MDR1* and *CDR1*, either by GOF mutations in the nucleotide sequence of these transporters or the transcription factor *MRR1* [9,11,12]. We show that azole resistance exhibited by isolate CPS-C following fluconazole exposure results from the GOF mutation (G604R) in the Mrr1p, upregulating its own expression and its effector, the *MDR1* efflux
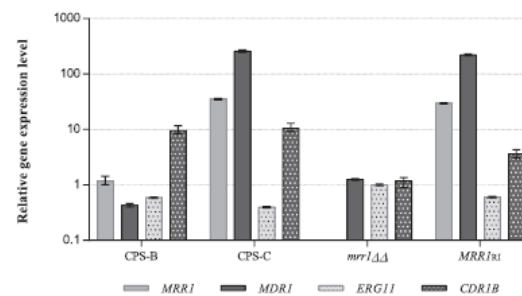
168

Fig. 1. Gene expression associated with *Candida parapsilosis* resistance. Relative expression levels of *MRR1*, *MDR1*, *ERG11* and *CDR1B* in isolates CPS-B and CPS-C and in the transformants, *mrr1ΔΔ* and *MRR1*ᵣᵢ strains, compared with isolate CPS-A. The expression level values represent the mean value ± standard error.

pump. The overexpression of *CDR1* efflux pumps can be caused by GOF mutations [9]. We did not identify any alterations in the sequence of *CDR1*. However, a significant copy number variation of the *CDR1B* gene was detected in isolate CPS-B, a susceptible-dose-dependent profile to fluconazole. In *C. albicans*, changes in the copy number of *ERG11*, *MRR1* and *TAC1* impact the fluconazole resistance, and copy number variations potentiate the emergence of drug-resistant point mutations [13,14]. Independently from increased copy number, the overexpression of *CDR1B* in the resistant isolate CPS-C and in *MRR1*ᵣᵢ clone, expressing the GOF *MRR1* allele, was observed. This strongly suggests that the expression of the *CDR1B* gene is regulated by the *MRR1* transcription factor, as suggested by Doorley et al. [8]. Interestingly, the *CDR1* (CLUG_03113) expression in *C. lusitaniae* was also shown to be regulated by GOF mutation in *MRR1* [15]. Our results show that the expression of *CDR1* impacts azole susceptibility of *C. parapsilosis*, driven by a GOF mutation in Mrr1 (CSP–C) or by increased copy number (CSP–B).

To the best of our knowledge, this is the first study to characterize a step-by-step azole resistance acquired during fluconazole treatment of a candiduria case by *C. parapsilosis*. Both fluconazole exposure of a candiduria selected for the increased copy number of the *CDR1B* and the emergence of a GOF (G604R) mutation in *MRR1* resulted in increased expression of *CDR1B*. Furthermore, the GOF mutation in *MRR1* triggers *MDR1* up-regulation. Our results strongly suggest that *MRR1* regulates the expression of *CDR1B*, which independently from *MDR1*, can impair susceptibility to azoles.

Author contributions

JB, IMM, and GB conceived and designed the experiments; JB, APR, and IMM performed the experiments; JB, APS, APR, GB, IMM, and AGR analysed the data; GB, IMM, and AGR contributed with reagents and material; JB, APR, GB, and IMM drafted the manuscript. All authors reviewed the manuscript.

Transparency declaration

This study was supported by FEDER (Programa Operacional Factores de Competitividade – COMPETE) and FCT (Fundação para a Ciência e Tecnologia), within the project PTDC/DTP-EPI/1660/2012 'Surveillance of *Candida parapsilosis* antifungal resistance'. JB is supported by an FCT grant SFRH/BD/135883/2018. This manuscript

Acknowledgements

Appendix A. Supplementary data

Supplementary data to this article can be found online at https://doi.org/10.1016/j.cmi.2022.08.014.

References

[1] Sobel JD, Fisher JF, Kauffman CA, Newman CA. Candida urinary tract infections-epidemiology. Clin Infect Dis 2011;52:S433–6. https://doi.org/10.1093/cid/cir109.
[2] Gajdács M, Dóczi I, Ábrók M, Lázár A, Burián K. Epidemiology of candiduria and Candida urinary tract infections in inpatients and outpatients: results from a 10-year retrospective survey. Cent Eur J Urol 2019;72:209–14. https://doi.org/10.5173/ceju.2019.1909.
[3] Kauffman CA. Candiduria. Clin Infect Dis 2005;41:S371–6. https://doi.org/10.1086/430918.
[4] Pappas PG, Kauffman CA, Andes DR, Clancy CJ, Marr KA, Ostrosky-Zeichner L, et al. Clinical practice guideline for the management of candidiasis: 2016 update by the infectious Diseases society of America. Clin Infect Dis 2016;62: e1–50. https://doi.org/10.1093/cid/civ933.
[5] Fisher MC, Alastruey-Izquierdo A, Berman J, Bicanic T, Bignell EM, Bowyer P, et al. Tackling the emerging threat of antifungal resistance to human health. Nat Rev Microbiol 2022;20:557–71. https://doi.org/10.1038/s41579-022-00720-1.
[6] Fekkar A, Blaize M, Bouglé A, Normand AC, Raoelina A, Kornblum D, et al. Hospital outbreak of fluconazole-resistant Candida parapsilosis: arguments for clonal transmission and long-term persistence. Antimicrob Agents Chemother 2021;65:e02036-20. https://doi.org/10.1128/AAC.02036-20.
[7] Tóth R, Nosek J, Mora-Montes HM, Gabaldon T, Bliss JM, Nosanchuk JD, et al. Candida parapsilosis: from genes to the bedside. Clin Microbiol Rev 2019;32: e00111–8. https://doi.org/10.1128/CMR.00111-18.

J. Branco et al. / Clinical Microbiology and Infection 28 (2022) 1655.e5—1655.e8

[8] Doorley LA, Rybak JM, Berkow EL, Zhang Q, Morschhäuser J, Rogers PD. *Candida parapsilosis* Mdr1B and Cdr1B are drivers of Mrr 1-mediated clinical fluconazole resistance. Antimicrob Agents Chemother 2022;66:e0028922. https://doi.org/10.1128/aac.00289-22.

[9] Berkow EL, Manigaba K, Parker JE, Barker KS, Kelly SL, Rogers PD. Multidrug transporters and alterations in sterol biosynthesis contribute to azole antifungal resistance in *Candida parapsilosis*. Antimicrob Agents Chemother 2015;59:5942—50. https://doi.org/10.1128/AAC.01358-15.

[10] Silva AP, Miranda IM, Guida A, Synnott J, Rocha R, Silva R, et al. Transcriptional profiling of azole-resistant *Candida parapsilosis* strains. Antimicrob Agents Chemother 2011;55:3546—56. https://doi.org/10.1128/AAC.01127-10.

[11] Branco J, Silva AP, Silva RM, Silva-Dias A, Pina-Vaz C, Butler G, et al. Fluconazole and voriconazole resistance in *Candida parapsilosis* is conferred by gain-of-function mutations in MRR1 transcription factor gene. Antimicrob Agents Chemother 2015;59:6629—33. https://doi.org/10.1128/AAC.00842-15.

[12] Grossman NT, Pham CD, Cleveland AA, Lockhart SR. Molecular mechanisms of fluconazole resistance in *Candida parapsilosis* isolates from a U.S. surveillance system. Antimicrob Agents Chemother 2015;59:1030—7. https://doi.org/10.1128/AAC.04613-14.

[13] Todd RT, Selmecki A. Expandable and reversible copy number amplification drives rapid adaptation to antifungal drugs. Elife 2020;9:e58349. https://doi.org/10.7554/eLife.58349.

[14] Selmecki A, Gerami-Nejad M, Paulson C, Forche A, Berman J. An isochromosome confers drug resistance in vivo by amplification of two genes, ERG11 and TAC1. Mol Microbiol 2008;68:624—41. https://doi.org/10.1111/j.1365-2958.2008.06176.x.

[15] Borgeat V, Brandalise D, Grenouillet F, Sanglard D. Participation of the ABC transporter CDR1 in azole resistance of *Candida lusitaniae*. J Fungi (Basel) 2021;7:760. https://doi.org/10.3390/jof7090760.

Paper IV

The transcription factor Ndt80 is a repressor of *Candida parapsilosis* virulence attributes

Taylor & Francis
Taylor & Francis Group

RESEARCH PAPER

OPEN ACCESS | Check for updates

The transcription factor Ndt80 is a repressor of Candida parapsilosis virulence attributes

Joana Branco[a,b], Cláudia Martins-Cruz[a], Lisa Rodrigues[c,d], Raquel M. Silva[e], Nuno Araújo-Gomes[a], Teresa Gonçalves[c,d], Isabel M. Miranda[f], and Acácio G. Rodrigues[a,b]

[a]Division of Microbiology, Department of Pathology, Faculty of Medicine, University of Porto, Porto, Portugal; [b]CINTESIS - Center for Health Technology and Services Research, Faculty of Medicine, University of Porto, Porto, Portugal; [c]CNC - Centre for Neuroscience and Cell Biology, University of Coimbra, Coimbra, Portugal; [d]FMUC - Faculty of Medicine, University of Coimbra, Coimbra, Portugal; [e]Faculdade De Medicina Dentária, CIIS - Centro De Investigação Interdisciplinar Em Saúde, Universidade Católica Portuguesa, Viseu, Portugal; [f]Cardiovascular R&D Centre, Faculty of Medicine, University of Porto, Porto, Portugal

ABSTRACT

Candida parapsilosis is an emergent opportunistic yeast among hospital settings that affects mainly neonates and immunocompromised patients. Its most remarkable virulence traits are the ability to adhere to prosthetic materials, as well as the formation of biofilm on abiotic surfaces. The Ndt80 transcription factor was identified as one of the regulators of biofilm formation by *C. parapsilosis*; however, its function in this process was not yet clarified. By knocking out *NDT80* (*CPAR2-213640*) gene, or even just one single copy of the gene, we observed substantial alterations of virulence attributes, including morphogenetic changes, adhesion and biofilm growth profiles. Both *ndt80Δ* and *ndt80ΔΔ* mutants changed colony and cell morphologies from smooth, yeast-shaped to crepe and pseudohyphal elongated forms, exhibiting promoted adherence to polystyrene microspheres and notably, forming a higher amount of biofilm compared to wild-type strain. Interestingly, we identified transcription factors Ume6, Cph2, Cwh41, Ace2, Bcr1, protein kinase Mkc1 and adhesin Als7 to be under Ndt80 negative regulation, partially explaining the phenotypes displayed by the *ndt80ΔΔ* mutant. Furthermore, *ndt80ΔΔ* pseudohyphae adhered more rapidly and were more resistant to murine macrophage attack, becoming deleterious to such cells after phagocytosis. Unexpectedly, our findings provide the first evidence for a direct role of Ndt80 as a repressor of *C. parapsilosis* virulence attributes. This finding shows that *C. parapsilosis* Ndt80 functionally diverges from its homolog in the close related fungal pathogen *C. albicans*.

Introduction

Candida parapsilosis is a ubiquitous yeast, often recovered from domestic animals, soil, and marine environments, but is also a commensal of the human skin. Among hospital settings, this species is considered a major opportunistic pathogen involved in invasive fungal infections [1,2]. Its incidence has dramatically increased, being the second most common *Candida* species isolated from blood cultures in Latin America, Asia, and Southern Europe countries [3–8]. *C. parapsilosis* is of particular concern among susceptible populations, comprising low birth weight neonates, immunocompromised individuals, and patients requiring prolonged use of indwelling devices such as central venous catheters [1,9]. Besides its ability to grow and persist in the hospital environment surfaces, *C. parapsilosis* stands out for its capacity to adhere to the abiotic surface of implanted devices, later involving biofilm formation [1,10,11]. In fact, adhesion and formation of biofilm are intimately related with *C. parapsilosis* virulence and are critical for its involvement in hospital outbreaks [2].

Biofilm is an organized community comprised of a dense network of microbial cells embedded in an extracellular matrix of polymers, which clinically restricts drug access and the immune response [12,13]. The ability of fungal cells to adhere to host tissues or medical indwelling devices, as well as cell-cell binding are required for biofilm development and for infection proliferation [14–16]. In contrast to *C. albicans*, *C. parapsilosis* does not form true hyphae and, therefore, its biofilm only involves yeast and pseudohyphal forms [17,18]. To identify putative *C. parapsilosis* biofilm regulators, more than 100

transcription factors were knocked-out and mutants were assessed for biofilm formation ability [19]. Previously identified as biofilm regulators in *C. albicans*, Bcr1, Efg1 and Ace2 were also directly implicated in biofilm development in *C. parapsilosis* [16,19–22], together with the transcription factor Gzf3, whose involvement in biofilm formation seems to be restricted to *C. parapsilosis* [19]. In this large-scale screen of *C. parapsilosis* biofilm defective mutants, *NDT80* was firstly pointed as a putative biofilm regulator, in analogy with *C. albicans* biofilm regulation network. However, in the case of *C. parapsilosis*, *NDT80* role was undisclosed due to marked growth defects exhibited by *ndt80* mutant [19]. In *C. albicans*, Ndt80 was first described as a key modulator of azole drug sensitivity, being involved in the control of ergosterol biosynthesis [23] and activation of the efflux pump Cdr1 [24]. We firstly identified *C. parapsilosis* Ndt80 ortholog to be a transcription factor upregulated following azole resistance acquisition [25]. Later, we showed that *ndt80* mutant exhibits increased susceptibility to azoles and that, together with Upc2 transcription factor, also regulates the expression of various genes of ergosterol biosynthetic pathway, namely *ERG25*, *ERG6*, *ERG2*, *ERG3* and *ERG4* [26].

In this study, we address the role of Ndt80 in *C. parapsilosis* as a repressor of virulence attribute expression, namely morphogenesis, adhesion, and biofilm formation. Additionally, we explore the morphological phenotypes, its constitutive filamentous growth, and the adhesion profile resulting from *NDT80* knock-out, as well as its interaction with host immune system by assessing macrophage-mediated response.

Methods

Culture conditions

Yeast strains used in this study were routinely grown in YPD broth medium (1% yeast extract, 2% bacto-peptone, 2% glucose) at 30°C with agitation (180 rpm) or on YPD agar plates, following addition of 2% of agar. To recycle the *SAT1* flipper cassette, transformants were incubated in YPM medium (1% yeast extract, 2% peptone, 2% maltose) overnight, with agitation (180 rpm); afterward, approximately 100 cells were plated on YPD plates supplemented with nourseothricin at final concentration of 20 µg ml^{-1}. All *C. parapsilosis* strains were stored in YPD broth with 40% glycerol, at – 80°C.

RAW 264.7 murine macrophages were obtained from the European Collection of Cell Cultures and maintained in DMEM (Sigma-Aldrich) with 10% non-inactivated Fetal Calf Serum (FCS), 10 mM HEPES, 12 mM sodium bicarbonate and 11 mg ml^{-1} sodium pyruvate at 37°C in a humidified atmosphere with 5% CO_2. The culture medium was changed every 2 days, until ~70% of cell confluence was reached. RAW 264.7 cells were resuspended in RPMI 1640 medium (Sigma-Aldrich) supplemented with 10% inactivated FCS, 23.8 mM sodium bicarbonate and 50 mM glucose for the experimental assays (initiated until the cells 15th generation).

Plasmid construction

To knockout *NDT80* gene in *C. parapsilosis* BC014S (wild-type strain) [25], the pNG4 disruption cassette described by Branco *et al.* [26] was used. Briefly, a 478 bp upstream and 460 bp downstream sequences of *NDT80* gene were amplified using CpNDT80up_F and CpNDT80up_R primers (containing recognition sites for *KpnI* and *ApaI*) and CpNDT80down_F and CpNDT80down_R primers (containing recognition sites for *SacII* and *SacI*), respectively, and cloned into the flanking sites of pCD8 plasmid [18]. After restriction with *KpnI* and *SacI*, pNG4 disruption cassette was introduced into the native locus of *NDT80* gene of *C. parapsilosis* BC014S. All primer sequences are listed in Table 1.

C. parapsilosis transformation

Transformation of wild-type strain was performed by electroporation as described by Ding *et al.* [18]. Briefly, an overnight cell culture was diluted in 50 ml of YPD broth medium for an initial OD_{600} of 0.2 and incubated at 30°C until reaching approximately OD_{600} of 2.0. After being pelleted, yeast cells were resuspended in 10 ml of Tris-EDTA buffer (10 mM Tris-HCl, 1 mM EDTA, pH 7.5) containing 10 mM dithiothreitol and incubated at 30°C for 1 h with agitation (100 rpm). Yeast cells were washed twice with 40 ml of cold water plus once with 10 ml 1 M Sorbitol and, subsequently resuspended in 125 µl of this solution. Approximately 1 µg of purified *KpnI-SacI* fragment of pNG4 was added to 50 µl of competent cells. The cell mixture was then transferred to a 1 mm electroporation cuvette. Electroporation shock was performed at 1.25 kV, using a Gene Pulser X-cell Electroporator (Bio-Rad). Afterward, 950 µl of YPD containing 1 M sorbitol was immediately added; the mixture was incubated at 30°C for 4 h with agitation; afterward 100 µl were plated on YPD agar supplemented with

Table 1. Primers used in this study.

Primer name	Primer sequence (5` to 3`)
Construction of deletion cassette	
CpNDT80up_F	GGGGGTACCGGCAATTTTGATTTTTGGGTTC
CpNDT80up_R	GGGGGGCCCGAGGCACCACCAGCAGTAGAGT
CpNDT80down_F	TCCCCGCGGGATGGGAGAAAAAACTGAACCTTG
CpNDT80down_R	CGAGCTCAGATGGCATTGTAGTCAGTAGCATC
PCR Confirmation	
CpNDT80gen_F	GCCTTTTACATCTATCGAAGTCAAACTTG
FLP_R	TTTATGATGGAATGAATGGGATG
RT-qPCR	
CpACT1_F1	TGCTCCAGAAGAACACCCA
CpACT1_R1	CACCTGAATCCAAAACAATACCAGT
CpBCR1_F	TCGCCACCACTACTCG
CpBCR1_R	AAAGGATAATGTTGCTGTGA
CpEFG1_F	GAGCGGAGCAGCAGTT
CpEFG1_R	GAAGCATAAGGTTGTTGGG
CpACE2_F	AACAACAACAACAACCCC
CpACE2_R	ACATCTAAATCCTGCAATCC
CpUME6_F	CTTTTCCCCCGTCTGTA
CpUME6_R	TGCAATGTTTTCTGTTCACT
CpMKC1_F	TCAGAGAATCCAGAACAAAA
CpMKC1_R	ATCCAACAGACCACACG
CpCZF1_F	CCAACAACAAAACTCCAAC
CpCZF1_R	TCTCGACTCACAACATCTCT
CpGZF3_F	GATACATTCAAAGCAGCAAA
CpGZF3_R	GTGGTTATCTTCAGTTCCG
CpCPH2_F	TCCAAAGTGACAAAGCC
CpCPH2_R	GCAATTCTCAAAGCAGG
CpRHR2_F	TTTGTTTGACTGTGACGG
CpRHR2_R	TACGGCATCCATGAGAAG
CpALS3_F	CGCACCAGCAAACTCATCAA
CpALS3_R	CCAATGAACTCGGGGGAAAT
CpALS7_F1	CTTCTGTTGTTGTGTGTCATCCCTG
CpALS7_R1	CACCATCTGTTGAGCCTGTAG
NDT80_F3	CAAAGGGCGGTATGAATGGTA
NDT80_R3	TGGTGTGGATGGTGTGGA
CpCW41_F	TGACGACGACGATGAACGCG
CpCW41_R	TGGTGATGAGCGGGGATA
CpSTP3_F	TCCGCCACGATAAAGCCA
CpSTP3_R	GAATCACCCAGACCACCG
CpOCH1_F	AATGCGATGCCCTTGTTGC
CpOCH1_R	TTGCTTGCCCACTCGTCA

nourseothricin at final concentration of 200 μg ml^{-1}. Transformants were obtained after 24 h of incubation at 30°C.

Adhesion assay

Yeast adhesion was quantified by flow cytometry, as described by Silva-Dias *et al.* [27]. Briefly, yeasts were grown overnight at 30°C in Sabouraud broth medium, with agitation (180 rpm); the culture was centrifuged at 10,000 *g* for 5 min and washed twice with phosphate buffer saline (PBS) (Sigma-Aldrich). A yeast suspension was standardized to 2×10^6 cells ml^{-1} in the same buffer and mixed with 2×10^7 microspheres ml^{-1} of 1 μm uncoated carboxylated highly green fluorescent polystyrene microspheres (Molecular Probes). This mixture was incubated at room temperature for 30 min at 150 rpm. The suspensions were vortexed, and 50,000 events were analyzed using a FACS Calibur flow cytometer (BD Biosciences). Cell adhesion results are expressed as the percentage of cells with microspheres attached, representative of at least three independent experiments, performed in triplicate.

Biofilm formation assays

After overnight growth at 37°C with agitation (180 rpm) in Sabouraud broth medium, yeast cells were collected by centrifugation at 10,000 *g* for 5 min, washed once with PBS and standardized to obtain a suspension of 1×10^6 yeast cells ml^{-1} in RPMI-1640 medium supplemented with L-glutamine and buffered with MOPS acid (Sigma-Aldrich). One ml of such cell suspension was placed in each of a 12-well polystyrene microplate and incubated for 24 and 48 h at 37°C. Following incubation, total biomass was quantified by Crystal Violet (CV) assay, as previously described by Silva-Dias *et al.* [28]. Biofilm mass was calculated from at least three independent experiments, performed in triplicate.

For dry mass assessment, *C. parapsilosis* strains were set up as previously described, except the standardization of the cell suspension, which was diluted to an OD$_{600}$ of 1; afterward, 5 ml were distributed in each well of a 6-well polystyrene plate. After 24 and 48 h of incubation at 37°C, adherent biofilms were washed with PBS, scrapped from the bottom of the wells, and vacuum filtered, as described by Holland, *et al.* [19]. The average of the total biomass was calculated by subtracting the initial weight of the filter to the final weight, determined from three independent experiments, performed in triplicate.

Microscopic imaging

Colony phenotypes were observed and photographed under 20× magnification using a Stereo zoom S9i (Leica Microsystems) dissection microscope, after growth on YPD agar at 30°C, for 72 h. Images of yeast cell morphology were taken with a Zeiss Axioplan microscope, coupled with an AxioVision image acquisition system (Zeiss), after staining with Calcofluor White (Sigma-Aldrich) and mounting on glass slides. Yeast cells were photographed under 1000× magnification, oil immersion.

RNA extraction, cDNA synthesis and RT-qPCR

RNA was extracted as described by Kohrer and Domdey [29]. Concentration and quality of RNA samples were measured using a Nanodrop equipment (Eppendorf). Only samples yielding A$_{280}$/A$_{260}$ ratios ranging from 1.6 to 2.2 and showing no signs of degradation, after electrophoresis, were used in subsequent analyses.

From 100 ng of total RNA, the first-strand cDNA was synthesized using the SensiFAST cDNA Synthesis Kit (Bioline) according to the manufacturer´s instructions. The resulting cDNA was stored at −20°C prior to use for real-time quantitative polymerase chain reaction (RT-qPCR). The genes analyzed were the followed: NDT80 (CPAR2_213640), OCH1 (CPAR2_404930), ALS3 (CPAR2_404770), ALS7 (CPAR2_404800), GZF3 (CPAR2_800210), ALS7 (CPAR2_404800), BCR1 (CPAR2_205990), EFG1 (CPAR2_701620), and the ortho-logues of Candida albicans STP3 (CPAR2_200390), CWH41 (CPAR2_501400), STP3 (CPAR2_200390), MKC1 (CPAR2_800090), CPH2 (CPAR2_603440), RHR2 (CPAR2_503990), ACE2 (CPAR2_204370), CPH2 (CPAR2_603440), UME6 (CPAR2_803820) and CZF1 (CPAR2_501290).

For each real-time quantitative PCR, five replicates per strain were analyzed. All primers used are detailed in Table 1. PCRs were performed using the SensiFAST SYBR Hi-ROX Kit (Bioline) 3-step cycling, according to the manufacturer's instructions, in a PikoReal Real-Time PCR System instrument (Thermo Scientific). ACT1 gene expression was used to normalize the signal obtained for each gene. Data obtained were analyzed with REST software.

Bioinformatic analysis

Sequences from C. parapsilosis CDC317 open reading frames (ORFs) plus 1000 bp upstream and downstream (version s01-m03-r14, from 7 February 2016) were downloaded from the Candida Genome Database (CGD, http://candidagenome.org/). To identify puta-tive Ndt80-regulated genes, a search for the MSE con-sensus motif (gNCRCAAAY) was performed in the promoter regions (1000 bp upstream the start codon). The resulting ORFs containing MSE sequences were grouped according to Gene Ontology (GO) terms using the CGD Gene Ontology Slim Mapper with the default parameters.

Macrophage-yeast interaction assays

Macrophage-yeast interaction assays were carried out as previously described [30]. Briefly, RAW 264.7 macrophage cells were platted in 96-, in 12-well (with 16 mm glass coverslips) or in μ-slide 8 well plates, and incubated for 18 h at 37°C, under a 5% CO2 atmosphere. After this incubation period, yeast cells were added to the macrophages at an MOI (Multiplicity of Infection) of 1:1.

Immunofluorescence and microscopic analysis

Macrophages grown in coverslips were incubated with C. parapsilosis as described below. At the end of each incubation period (10 min, 30 min, 1 h 30 min, 3 h), coverslips were washed twice with ice-cold PBS and fixed with 4% paraformaldehyde in PBS for 15 min at room temperature. After 3 washing steps with PBS, cell membranes were stained with WGA, for 10 min, pro-tected from light. Macrophages were treated with a blocking solution of 10% bovine serum albumin in PBS for 30 min at 37°C. Cells were then incubated overnight, at room temperature, with the primary rab-bit polyclonal antibody against Candida (GTX40096; GeneTex), diluted (1:200) in blocking solution. Coverslips were washed and incubated for 2 h at room temperature with the AlexaFluor 488 donkey anti-rabbit IgG secondary antibody (A21206; Invitrogen). Finally, after a washing step, macrophage cells were incubated with DAPI 0.02% for 10 min at room temperature. Cells were subsequently washed and the coverslips were mounted in glass slides with DAKO mounting medium and kept at −20°C until observation under confocal or fluorescence microscopy. Digital images were captured using a Carl Zeiss LSM 710 Confocal Microscope, using Plan-ApoChromat 40x/63x/1.4 oil objectives; Zen Blue and FiJi software's were used to analyze the images.

Yeast and macrophage viability assays

The yeast cell viability following interaction with RAW 264.7 macrophage cells was assessed by a colony-forming unit (CFU) assay. After 30 min and 3 h of co-incubation, supernatants were collected and plated on YPD agar, to count non-internalized or non-adhered yeast cells. The remaining adhered RAW 264.7 macro-phages were scraped and lysed with 0.5% Triton X-100. This cell suspension, representing the amount of yeast cells internalized was plated on YPD agar, using serial dilutions. Following 3 days of incubation, at 30°C, the number of yeast colonies per ml was calculated.

For macrophage viability assay, after 30 min and 3 h of co-incubation, viable, and death macrophage cells were calculated using a hemocytometer, after staining with Trypan Blue (T8154; Sigma-Aldrich).

Live cell imaging assays

For live cell imaging assays, culture media without phenol-red was used and macrophage cell membranes were stained with Wheat Germ Agglutinin, Tetramethylrhodamine conjugate (WGA, W849; Molecular Probes). Image acquisitions were conducted during at least 45 min, using a confocal Cell Observer Spinning Disk microscope (Zeiss), equipped with an

LCI PlanNeofluar 63x/1.3 glycerol objective; Zen Blue software was used to analyze the time-lapse videos obtained.

Statistical analysis

Statistical analysis of results of adhesion, biofilm and infection assays was performed using one-way ANOVA followed by a Dunnett post hoc test. Differences were considered statistically significant for a p-value <0.05. Significant differences were marked with an asterisk character (*), in which *p < 0.05, **p < 0.01, ***p < 0.001. All results are presented as mean ± standard deviation, of at least three independent experiments.

Results

Deleting NDT80 transcription factor gene triggers morphogenesis

To gain insight into the role of Ndt80 in C. parapsilosis virulence attribute expression, two independent lineages lacking one (ndt80Δ – NG2 strain) or both (ndt80ΔΔ – EF16 strain) copies of NDT80 were generated from C. parapsilosis strain BC014S (wild-type strain) [25]. Deletion was carried out using a gene-specific disruption cassette (pNG4) based on the recyclable nourseothricin-resistant marker as previously described [18]. The introduction of pNG4 into theNDT80 locus of the wild-type strain, generated NG1 clone, which after cassette recycling, resulted in the NG2 strain. To delete the second copy of NDT80 gene, a second round of integration/recycling were performed, generating EF15 and EF16 clones, respectively. Gene knockout was confirmed by PCR (Figure 1 (a) and (b)).

Deletion of NDT80 had a major effect upon colony and yeast cell morphology (Figure 2(a) and (b)). The parental strain and the ndt80Δ haploid mutant grow as smooth-white and creaky-opaque colonies, respectively, whereas colonies from ndt80ΔΔ diploid mutant display a crepe phenotype. Wild-type and haploid cells are yeast-shaped cells; in contrast, the ndt80ΔΔ cell population is mostly composed of elongated cells and pseudohyphae.

Deleting NDT80 increases adhesion and biofilm formation ability

The yeast to pseudohyphae transition was observed along with the formation of fungal cell aggregates, typical of enhanced cell to cell adhesion. The ndt80Δ

and ndt80ΔΔ mutants flocculate in liquid medium, suggesting that Ndt80 negatively affects the cell-cell adhesion process (Figure 3(a)). The ability of C. parapsilosis to adhere to polystyrene microspheres, representative of abiotic surfaces, was quantified using a flow cytometric adhesion assay, as described previously [27]. Compared to wild-type, manipulated strains displayed a significant increase of about 2-fold in adhesion ability (Figure 3(b)).

Filamentous growth and adhesion displayed by ndt80ΔΔ mutant are two known enhancers of biofilm formation. We assessed wild-type and mutants strains regarding the ability to form biofilm, using two independent methods, Cristal Violet (CV) staining [28] and dry weight [19]. C. parapsilosis lacking one or both copies of NDT80 gene exhibits enhanced capacity to form biofilm compared to wild-type strain (Figure 3(c) and (d)). Differences were statistically significant when using both methodologies. Nevertheless, comparatively to ndt80Δ mutant, ndt80ΔΔ mutant had lower biofilm biomass, a result statistically significant when using CV staining for biofilm quantification.

Ndt80 regulates the expression of adhesion-, morphology- and biofilm-related genes

A set of transcription factor genes, namely Czf1, Ume6, Gzf3, Cph2, Efg1, Bcr1, Ace2, additional regulators like Stp3, Cwh41, Och1, Rhr2, one protein kinase (Mkc1) and also adhesins Als-like (Als7, Als3), were identified by several authors [19,31,32] as regulators of morphology transition, and as effectors in adhesion and biofilm formation by C. parapsilosis. In an attempt to identified Ndt80 targets involved in triggering virulence factors, we quantified the expression of the above-mentioned genes by RT-qPCR (Figure 4).

Relatively to adhesin-like genes, the expression of ALS7 in ndt80Δ and ndt80ΔΔ mutants was upregulated 210- and 180-fold, respectively, compared to wild-type. In contrast, ALS3 gene expression was not changed significantly among the studied mutant strains. The expression of UME6 was upregulated, approximately, 5-fold in the ndt80Δ haploid mutant and a 13-fold in the ndt80ΔΔ diploid mutant, compared to the wild-type. MKC1 expression was also upregulated 2.8-fold and 36-fold in haploid and diploid mutants, respectively, comparatively to the wild-type. CPH2 gene exhibited a 1.2-fold upregulation in ndt80Δ mutant and of approximately 4-fold increased expression in ndt80ΔΔ mutant, in comparison to the wild-type.

ACE2, CWH41 and OCH1 genes displayed similar expression values of approximately 3-fold, 2-fold, and 1.2-fold, respectively, in the haploid and diploid
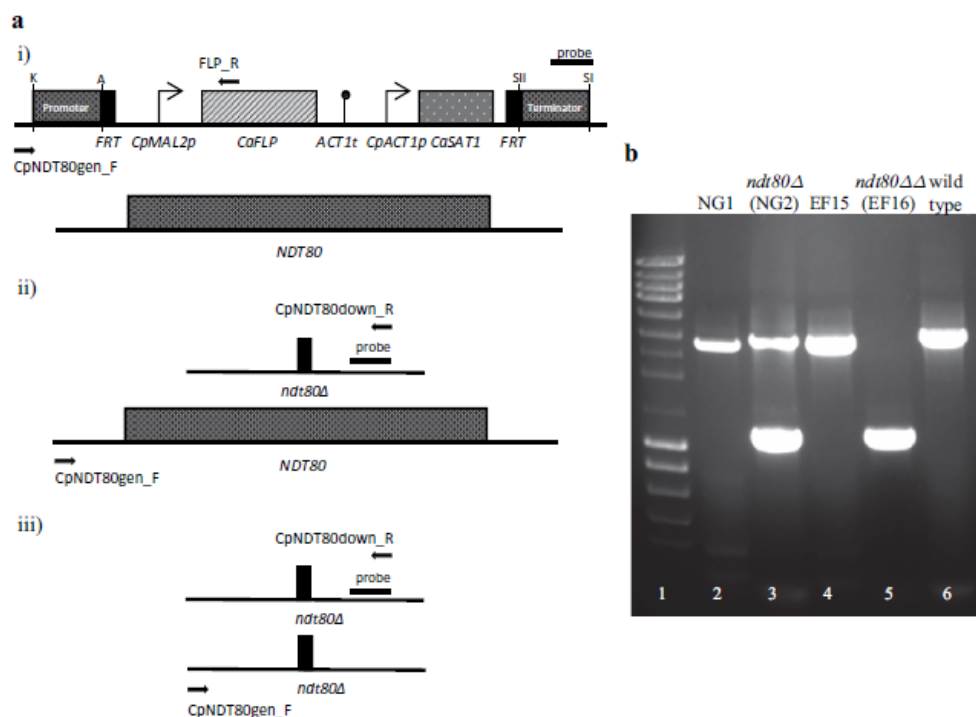
Figure 1. Deletion of *NDT80* transcription factor gene in *C. parapsilosis*. Gene knockout was confirmed by PCR. Genomic integration of *NDT80* disruption cassette in the wild-type strain was confirmed using the following pairs of primers CpNDT80gen_F and FLP_R (a, i), which amplified a 2.9 kb fragment (b, NG1 strain, lane 2). The recycling of the disruption cassette was confirmed using primers CpNDT80gen_F and CpNDT80down_R (a, ii), originating a 3.1 kb (second copy of *NDT80* gene) and 1.2 kb PCR products (disruption of the first copy) (b, NG2 strain, lane 3). Disruption of the second allele in strain NG2 was confirmed following the same strategy, using the primers: CpNDT80gen_F and FLP_R (a, i), which amplified a 2.9 kb fragment that corresponds to the second integration of *NDT80* disruption cassette (b, EF15 strain, lane 4) and CpNDT80gen_F and CpNDT80down_R (A, iii), amplifying a 1.2 kb PCR product, indicating a successful recycling of the cassette (b, EF16 strain, lane 5). Wild-type strain was used as PCR control of CpNDT80gen_F and CpNDT80down_R pair primers, amplifying a 3.1 kb fragment (b, lane 6). Lane 1 represents the molecular size marker (NZYDNA Ladder III, NZYTech).

mutants. *BCR1* gene was 1.5 and 1.7-fold upregulated in *ndt80Δ* and *ndt80ΔΔ* mutants in comparison to wild-type. The expression of *STP3* was increased approximately 1.8-fold in *ndt80Δ* mutant but remained unchanged in *ndt80ΔΔ* mutant. In contrast, *EFG1*, *GZF3* and *RHR2* were downregulated in *ndt80ΔΔ* mutant comparatively to the wild-type; *ndt80Δ* mutant exhibited a slight upregulation of expression of such genes (of about 1.1-, 1.4-, and 2.6- fold, respectively). *CZF1* gene was progressively downregulated following sequential *NDT80* gene copy deletion, by approximately 30% and 70%, respectively.

As expected, no *NDT80* transcript was observed in the null strain. Interestingly, the expression of *NDT80* in *ndt80Δ* mutant was 1.6-fold up-regulated. Since *NDT80* gene has in its promoter region the MSE binding sequence, we could hypothesize that to cope with one copy gene deletion, Ndt80 up-regulates itself expression, as described in *S. cerevisiae* and *A. nidulans* [33,34].

Identification of putative *NDT80*-regulated genes

Ndt80 was found to bind to the middle sporulation element (MSE) (5'-CACAAA-3') in the target gene promoter region [35] of *C. albicans* and *S. cerevisiae* ORFeomes [22,23]. The putative colony transition, adhesion- and biofilm-related genes mentioned above were analyzed for the presence of MSE motifs using the NCBI blast tool. As some of the promoter regions bound by biofilm regulators are larger than the normal [22,35], the considered sequence was approximately 1
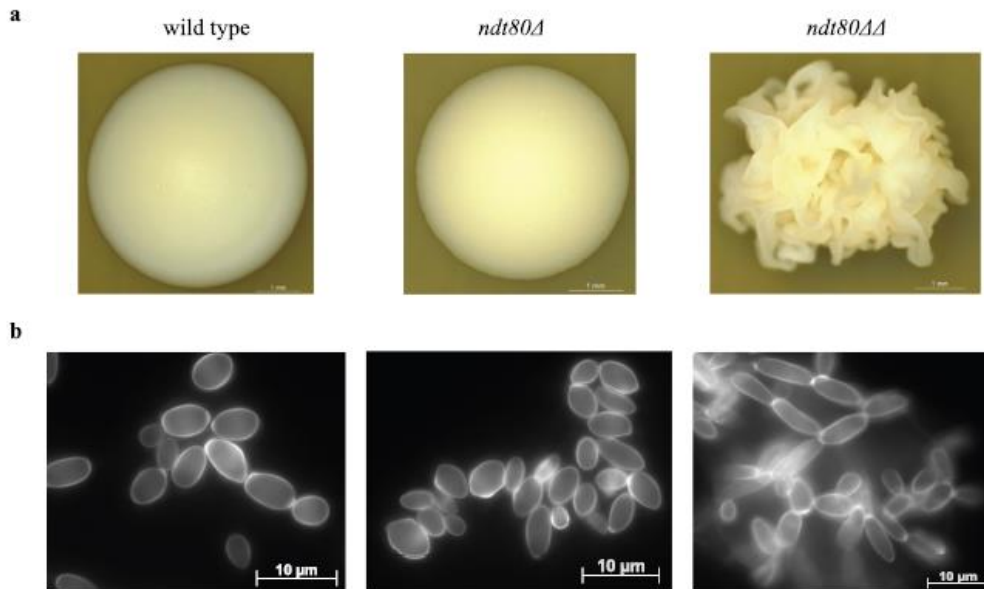
a

| wild type | ndt80Δ | ndt80ΔΔ |

b

Figure 2. *NDT80* deletion triggers morphogenesis changes in *C. parapsilosis*. (a) Colony morphology of wild-type, *ndt80Δ* and *ndt80ΔΔ* strains. Yeasts were grown at 30°C for 2 days and colonies photographed under 20× magnification. Smooth colonies were found in wild-type strain; *ndt80Δ* mutant displays creaky-opaque colonies, while only crepe phenotype colonies were observed in the *ndt80ΔΔ* mutant strain. (b) Cell morphology of wild-type, *ndt80Δ* and *ndt80ΔΔ* strains. Staining of wild-type and *ndt80Δ* cells with calcofluor white revealed a cell population mainly composed by yeasts; in contrast, *ndt80ΔΔ* mutant shows a mixture of elongated cells and pseudohyphae. Cells were visualized under fluorescence microscopy and photographed under 1000× magnification, oil immersion.
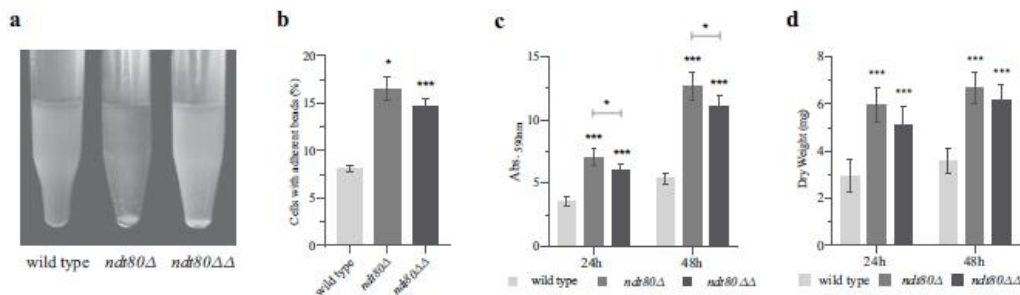
Figure 3. Deletion of *NDT80* increases adherence and biofilm formation ability. (a) Images of wild-type, *ndt80Δ* and *ndt80ΔΔ* strains grown in liquid media; the mutants strains exhibit a strong flocculation (cell-cell adhesion) phenotype. (b) Percentage of yeast cells with adherent beads. *ndt80Δ* and *ndt8ΔΔ* mutants exhibited significantly higher adhesion ability than wild-type. The ability to form biofilm was quantified by (c) Cristal Violet (CV) staining and (d) dry weight, following 24 and 48 h of growth; in both assays, a significant increase of biofilm formation by *ndt80Δ* and *ndt8ΔΔ* mutants compared to the parental strain was observed. CV staining revealed a statistical decrease in biofilm formation between *ndt80Δ* and *ndt8ΔΔ* mutants, at both time points. $*p < 0.05$, $**p < 0.01$ and $***p < 0.001$ wild-type vs *ndt80Δ* and *ndt8ΔΔ* mutants, or both groups.

kb upstream of the start codon. All genes assessed for their expression (Figure 4) contain putative MSE recognition sites, being identified in promoter regions.

Attaching to such results, we further expanded the search for MSE consensus sequences in the complete *C. parapsilosis* ORFeome. This analysis allowed the
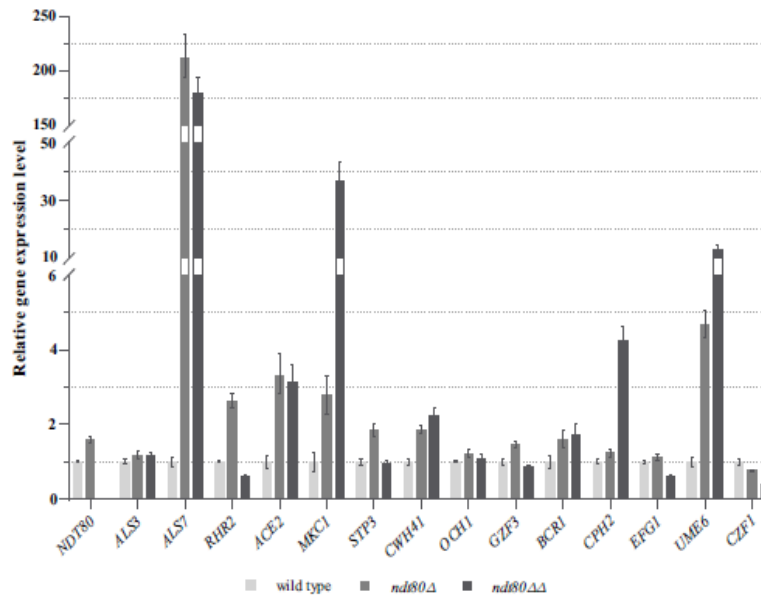
Figure 4. Putative targets of Ndt80 transcription factor. Relative expression levels of *NDT80, ALS7, ALS3, CZF1, UME6, GZF3, CPH2, EFG1, BCR1, ACE2, STP3, CWH41, OCH1, RHR2* and *MKC1* genes in *ndt80Δ* and *ndt8ΔΔ* strains compared with wild-type strain. *ACT1* was used as a normalizer gene. Expression values represent the mean value and ± standard deviation of five independent experiments.

retrieval of 417 ORFs containing MSE motifs in their promoters. These were mapped to GO terms and grouped according to Biological Process, Molecular Function or Cellular Component (Figure 5). Results showed that most ORFs with MSE elements (with over 10% and excluding the unknowns) belong to cell transport regulation, organelle organization, response to stress/chemical and RNA metabolic processes. Also, these ORFs are mostly related with enzymes with hydrolase or transferase activity which in addition to the cytoplasm and nucleus, many are located in cell membranes and mitochondria (Figure 5).

C. parapsilosis strains lacking *NDT80* are more resistant to macrophage attack and impair macrophage viability

The capacity of fungal cells to resist to macrophage-mediated killing contributes to its pathogenicity [36–38]. We conducted a phagocytic assay using the murine macrophage cell line RAW264.7 in order to determine the impact resulting from *NDT80* deletion upon phagocytic cells response. The interaction between macrophages and *C. parapsilosis* cells begins as early as 10 min (Figure 6(a)). However,

while *C. parapsilosis* wild-type cells hardly interact, at the same time point a higher number of *ndt80ΔΔ* cells are attached to macrophages with clear signs of internalization, as indicated by the tridimensional green staining fading (Figure 6(a)); the *ndt80Δ* cells showed a intermediate behavior. Clearly, mutant strains exhibited a more effective adherence and internalization profile soon after 27 min of co-culturing (Movie S1), while this process is more lagging for the wild-type macrophage interaction; after 30 min of interaction, most of the *C. parapsilosis* cells were outside of the macrophages, adherent or not (Figure 6(b), i). Following 3 h of interaction, wild-type and both mutant strains were mostly internalized; notably, the number of *ndt80ΔΔ* mutant cells inside macrophages was statistically higher versus the two other cell types (Figure 6(b), ii).

Macrophage viability decreased along the assay (Figure 6(c), i and ii). Macrophage challenge with *ndt80ΔΔ* mutant cells, caused a significant reduction of the number of viable macrophages soon after 30 min (Figure 6(c), i). Following 3 h of co-culture, an increase of lysed macrophages was observed with all the strains assessed; however,
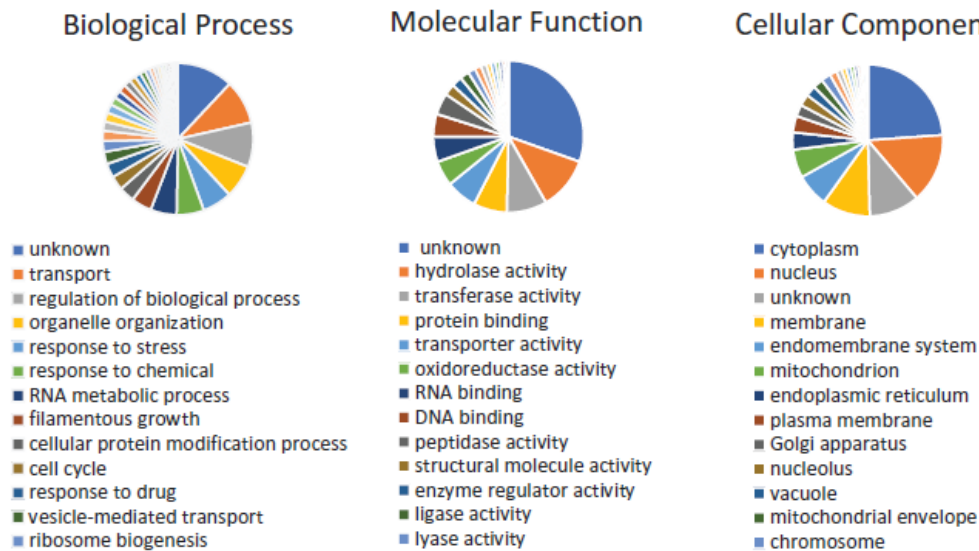
Figure 5. GO analysis of *Candida parapsilosis* genes putatively regulated by the Ndt80 transcription factor. ORFs containing MSE elements are grouped according to Biological Process, Molecular Function and Cellular Component.

this result was statistically significant in the case of *ndt80ΔΔ* strain (Figure 6(c), ii).

Discussion

While molecular mechanisms are well characterized in *C. albicans*, several studies addressing the regulatory networks of non-*albicans* species, like *C. glabrata* and *C. parapsilosis*, demonstrate a significant difference in the evolutionary adaptation of such yeasts to the human host [19,39]. Although the available knowledge regarding the expression of *C. parapsilosis* virulence attributes is still somewhat limited, this species displays many biological features that are presumed to be directly related to its environmental colonization and pathogenicity, such as enhanced adherence and biofilm development on abiotic surfaces.

Adhesion, morphogenetic variations and biofilm formation are virulence attributes clearly depicted for *C. albicans* [40,41] and are intimately related to each other. Filamentous growth is closely related to the expression of surface proteins, such as Als1, Als3 and the hyphal-specific protein, Hwp1. In turn, these proteins play relevant roles in cell-cell and cell-surface adhesion and are required for biofilm formation as contact mediators that promote further biomass accumulation and enhance biofilm resilience [14,15]. Ndt80 was identified as one of the many regulators of

filamentous growth by binding to promoters of genes encoding cell wall components (e.g. *ALS3* and *HWP1*), being required for their normal expression [42]. Thus, deletion of *NDT80* reduces *C. albicans* virulence *in vivo*, by blocking yeast to hyphal transition, as well as the expression of genes involved in the filamentous transcriptional program [42].

Surprisingly, and opposing to what was described for *C. albicans*, the disruption of *C. parapsilosis NDT80* gene triggers two noticeable phenotypic changes: morphogenesis in a spontaneous and constitutive manner (Figure 2), and prompted adhesion, both cell to cell and to abiotic surfaces, but also to murine macrophages (Figure 3 and Figure 6, respectively). Despite the scarce knowledge on *C. parapsilosis* adhesion mediators, we demonstrate that *ndt80* mutants adhesion is conferred by *ALS7* (CPAR2_404800), whose expression is extraordinary increased. This adhesin was previously identified as a mediator of *C. parapsilosis* adhesion to human buccal epithelial cells [31]. Although only 0.5% of the ORFs related with cell adhesion contain putative recognition sites for Ndt80, *ALS7* and *ALS3* are included in this group.

According to our findings Ndt80 can have a dual role in yeast to pseudohyphae transition: on one hand, by impairing the expression of *UME6* and *CPH2*, described as inducers of yeast to pseudohyphae transition [19]; on the other hand, by acting as an
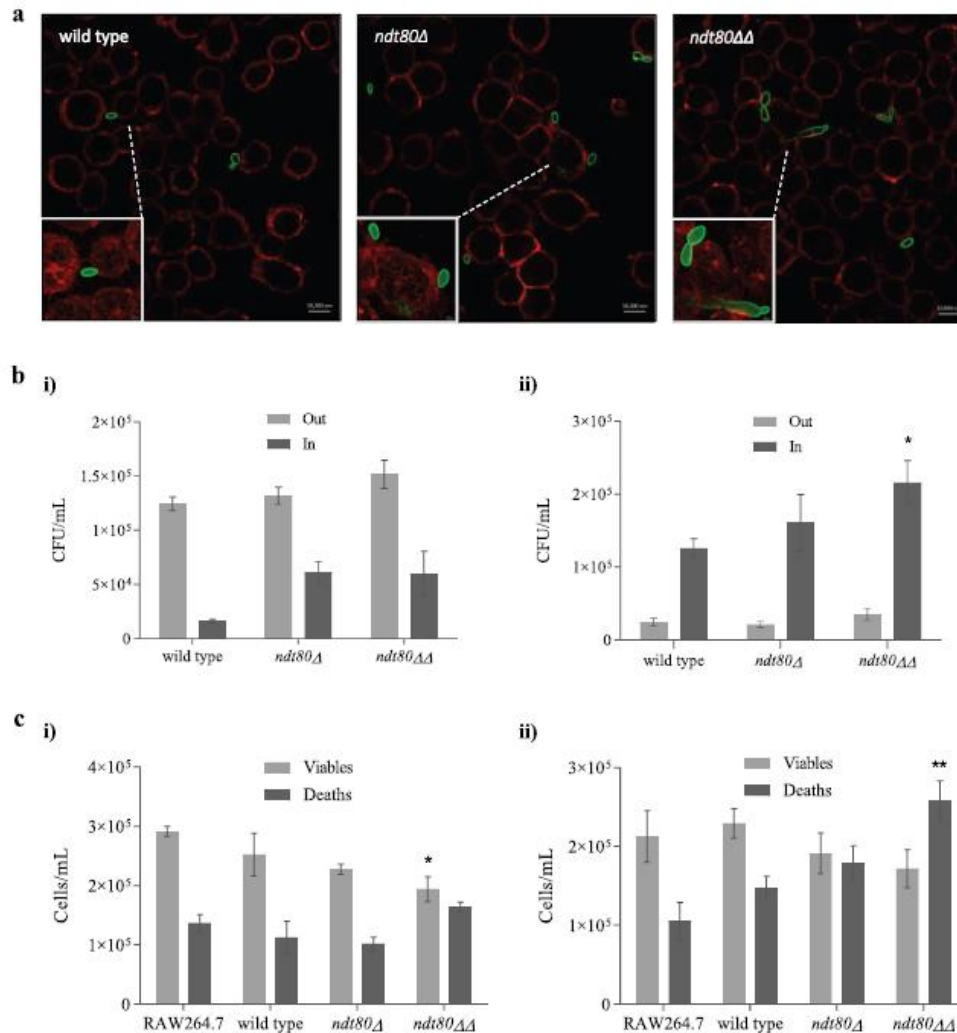
Figure 6. Interaction of *C. parapsilosis NDT80* deletion strains with RAW264.7 macrophage cells. (a) Representative confocal microscopy images of RAW264.7 macrophages and wild-type, *ndt80Δ* and *ndt80ΔΔ* strains after 10 min of interaction at MOI of 1:1; scale bar represents 10 μm. Cells are distinguished through their different fluorescence staining with WGA (red macrophages) and Alexa Fluor 488 labeled anti-Candida antibody (green yeasts). Small boxes correspond to fluorescent projection details, highlighting mutant yeasts more adherent and internalized by macrophages ("tridimensional" images with fading green staining as indicator of phagocytosis and inclusion inside macrophages), when compared with wild-type. (b) Viable *C. parapsilosis* counts after i) 30 min and ii) 3 h interaction with macrophages at MOI of 1:1. Viable counts were performed using a CFU assay of co-culture supernatants (yeasts not internalized or adherent) and of lysed macrophage cells (phagocyted/internalized yeasts). (c) Viable and dead macrophage counts after i) 30 min and ii) 3 h interaction with *C. parapsilosis* strains at MOI of 1:1. Macrophage counts were performed after Trypan Blue exclusion test of cell viability. *p < 0.05 and **p < 0.01 wild-type or RAW264.7 macrophages control groups.

activator of Czf1 and Efg1 [19,35], two known transcription factors regulating phenotypic switching and filamentous growth in *C. albicans*. Other genes like *OCH1*, the orthologs of *C. albicans CWH41* and *STP3*

are also involved in *C. parapsilosis* phenotypic switching, as positive and negative regulators, respectively [32,36]. We found that Ndt80 has no impact upon the expression of *OCH1* and the ortholog of *C. albicans*

STP3; interestingly, the ortholog *C. albicans CWH41* expression doubles in *ndt80ΔΔ* mutant, suggesting that this gene could be a target for Ndt80, which putatively represses the expression of this pseudohyphae formation factor.

Ndt80 is also part of a network of six transcription factors (Bcr1, Efg1, Tec1, Rob1, Bgr1, and Ndt80) responsible for the regulation of *C. albicans* biofilm development [22]. In this species, *NDT80* deletion significantly compromises biofilm formation either *in vitro* or *in vivo* models [22]. Conversely, we found that deletion of *C. parapsilosis NDT80* gene promotes biofilm growth *in vitro*, suggesting that this transcription factor is acting as a repressor of genes involved in such process. Other biofilm regulators, acting as repressors and activators in a circuit system were already previously identified in *C. albicans* and *C. parapsilosis* [19]. Efg1, Bcr1, and Ace2 play similar roles regarding biofilm development in both species, while Cph2, Czf1, Gzf3, and Ume6 have major roles just in *C. parapsilosis* [19]. In *C. parapsilosis*, deletion of *CZF1*, *GZF3*, *UME6*, and *CPH2* was associated with a reduced biofilm formation ability. Although Ndt80 was not identified as a component of *C. parapsilosis* regulatory network due to the inherent growth defects [19], we analyzed the promoter sequences of all the biofilm transcription factors described by Holland *et al.* [19] for the presence of Ndt80 MSE motifs and identified putative recognition sites in all of the genes tested. The gene expression profile analysis of *ndt80ΔΔ* mutant revealed an approximately 36-fold, 13-fold, 4-fold and 3-fold upregulation of *MKC1*, *UME6*, *CPH2* and *ACE2*, respectively, while other genes also described to be required for biofilm formation, such as *GZF3* and *CZF1*, were demonstrated to be downregulated. These findings strongly suggest the role of Ndt80 as a negative regulator of *MKC1*, *UME6*, *CPH2* and *ACE2* expression and as an activator of *GZF3* and *CZF1* expression. Thus, in Ndt80 absence, and despite *GZF3* and *CZF1* genes exhibiting a reduced expression, the upregulation of *MKC1*, *UME6*, *CPH2* and *ACE2* genes occurs and biofilm development is promoted (Figure 4). *RHR2* was also considered to be involved in biofilm development by *C. parapsilosis*, as its expression was increased during biofilm formation [19]. Nevertheless, in *ndt80ΔΔ* mutant characterized by enhanced biofilm production, *RHR2* gene is downregulated probably denoting the lack of Ndt80 regulation as an activator.

The virulence-related phenotypes exhibited by *ndt80ΔΔ* mutant led us to explore its interaction with immune system cells. The ability to switch from yeast to a filamentous form is a key factor that allows successful phagocytosis evasion of *C. albicans* [43]. In the case of *C. parapsilosis*, several studies have elucidated distinct virulence traits of this species that could modulate the mechanism by which phagocytosis and the immune response proceed [44–46]. We found, in our *in vitro* infection assays a prompter interaction of both mutants with the macrophage cells in comparison to the wild-type strain. This finding is also in accordance with results obtained with the adhesion assays to abiotic surfaces and to other yeast cells.

Toth *et al.* [37] using other host cell models (J774.1 murine macrophage cell line and human peripheral blood mononuclear cells) described that the length of *C. parapsilosis* pseudohyphae did not correlate with the engulfment time. In our assays, after 3 h of coculturing, only the *ndt80ΔΔ* mutant induced a significantly increase of macrophage killing with concomitant higher yeast viability, while neither the wild-type nor the *ndt80Δ* mutant promoted significant damage of the macrophage cells. These results show that the phenotype prompted by *NDT80* knockout results in a more virulent *C. parapsilosis* strains, more resistant to macrophage attack, associated with a decrease of macrophage cytoplasmic membrane integrity and a concomitant increase of macrophage cell death. Virulence features are not exclusively related to the constitutive pseudohyphal form; notably, the promoted expression of *ALS7* and *MKC1* transcripts (factors essential to cell wall integrity and remodeling) [47,48] provides a strong evidence of alterations of cell wall concerning composition and architecture in the *ndt80ΔΔ* mutant, with impact upon adhesion and recognition by immune system cells [49].

In fungi, *NDT80*-like genes recognize the conserved DNA-binding domain motif, MSE, through an Ig fold. As other members of the Ig-fold family of transcription factors, such as p53 or NFAR from mammals, *NDT80*-like genes share a similar regulation mechanism [50]. However, the number and attributable functions of *NDT80*-like genes are divergent among fungal species and even within species [34]. These disparities range from *NDT80* absence, as seen in *Schizosaccharomyces pombe*, to a family of six members, as seen in *Fusarium oxysporum*. While in *Saccharomyces cerevisiae*, *NDT80* single gene functions as a master regulator of meiosis process and sporulation [51], in other fungal species possessing several paralogous of *NDT80*-like genes the unraveling of its function and regulation mechanism is laborious and far from being obtained. NdtA and XprG are two of the Ndt80-like proteins in the filamentous fungal species *Aspergillus nidulans*. The former has a high homology with Ndt80 and like in *S. cerevisiae*, it is crucial for sexual reproduction. The later, under carbon starvation, regulates positively fungal response by

controlling its extracellular proteases, mycotoxin, and penicillin expression, which could result in autolysis, hyphal fragmentation and ultimately in cell death [52]. *Neurospora crassa* possesses three Ndt80-like proteins, Vib-1, Ncu04729 and Fsd-1. Vib1, closely related to XprG, is an activator of extracellular protease production and is also associated with apoptosis [53]; Fsd1 (more similar to NdtA) together with Vib-1, is involved in the female sexual structure formation, but no one is required for meiosis. So far, NCU04729 gene deletion has no effect upon phenotype, which impairs the understanding of its function. In the CTG clade, *C. albicans* has three *NDT80*-like DNA-binding domain genes, *NDT80, RON1* and *REP1* [54]. These Ndt80-like transcription factors seem to be functionally independent from each other. Rep1 was found to be a regulator of the drug efflux pump *MDR1* and is required for yeast growth on presence of N-acetylglucosamine (GlcNAc) and galactose. Ron1 is associated with GlcNAc regulation signaling.

Notably, Ndt80 was identified as a morphogenesis and biofilm regulator, in *C. albicans* and *C. parapsilosis*, although it diverged to opposite functional roles. Our study highlights the importance of Ndt80 on the complex regulation of *C. parapsilosis* virulence attributes, as a major repressor.

Acknowledgments

Disclosure statement

The authors declare no competing financial interests.

Funding

References

[1] Trofa D, Gacser A, Nosanchuk JD. Candida parapsilosis, an emerging fungal pathogen. Clin Microbiol Rev. 2008;21:606–625.

[2] van Asbeck EC, Clemons KV, Stevens DA. Candida parapsilosis: a review of its epidemiology, pathogenesis, clinical aspects, typing and antimicrobial susceptibility. Crit Rev Microbiol. 2009;35:283–309.

[3] Costa-de-Oliveira S, Pina-Vaz C, Mendonca D, et al. A first Portuguese epidemiological survey of fungaemia in a university hospital. Eur J Clin Microbiol Infect Dis. 2008;27:365–374.

[4] Silva AP, Miranda IM, Lisboa C, et al. Prevalence, distribution, and antifungal susceptibility profiles of Candida parapsilosis, C. orthopsilosis, and C. metapsilosis in a tertiary care hospital. J Clin Microbiol. 2009;47:2392–2397.

[5] Pratikaki M, Platsouka E, Sotiropoulou C, et al. Epidemiology, risk factors for and outcome of candidaemia among non-neutropenic patients in a Greek intensive care unit. Mycoses. 2011;54:154–161.

[6] Nucci M, Queiroz-Telles F, Alvarado-Matute T, et al., Latin American Invasive Mycosis N. Epidemiology of candidemia in Latin America: a laboratory-based survey. PLoS One. 2013;8:e59373.

[7] Guinea J, Zaragoza O, Escribano P, et al., Candipop Project G-G, Reipi. Molecular identification and antifungal susceptibility of yeast isolates causing fungemia collected in a population-based study in Spain in 2010 and 2011. Antimicrob Agents Chemother. 2014;58:1529–1537.

[8] Hirai Y, Asahata S, Ainoda Y, et al. Nosocomial Candida parapsilosis candidaemia: risk factors, antifungal susceptibility and outcome. J Hosp Infect. 2014;87:54–58.

[9] Pammi M, Holland L, Butler G, et al. Candida parapsilosis is a significant neonatal pathogen: a systematic review and meta-analysis. Pediatr Infect Dis J. 2013;32:e206–16.

[10] Pfaller MA, Diekema DJ. Epidemiology of invasive candidiasis: a persistent public health problem. Clin Microbiol Rev. 2007;20:133–163.

[11] Cuellar-Cruz M, Lopez-Romero E, Villagomez-Castro JC, et al. Candida species: new insights into biofilm formation. Future Microbiol. 2012;7:755–771.

[12] Donlan RM, Costerton JW. Biofilms: survival mechanisms of clinically relevant microorganisms. Clin Microbiol Rev. 2002;15:167–193.

[13] Perlin DS, Shor E, Zhao Y. Update on antifungal drug resistance. Curr Clin Microbiol Rep. 2015;2:84–95.

[14] Nobile CJ, Schneider HA, Nett JE, et al. Complementary adhesin function in C. albicans biofilm formation. Curr Biol. 2008;18:1017–1024.

[15] Fox EP, Nobile CJ. A sticky situation: untangling the transcriptional network controlling biofilm development in Candida albicans. Transcription. 2012;3:315–322.

[16] Pannanusorn S, Ramirez-Zavala B, Lunsdorf H, et al. Characterization of biofilm formation and the role of BCR1 in clinical isolates of Candida parapsilosis. Eukaryot Cell. 2014;13:438–451.

[17] Kuhn DM, Chandra J, Mukherjee PK, et al. Comparison of biofilms formed by Candida albicans and Candida parapsilosis on bioprosthetic surfaces. Infect Immun. 2002;70:878–888.

[18] Ding C, Butler G. Development of a gene knockout system in Candida parapsilosis reveals a conserved role for BCR1 in biofilm formation. Eukaryot Cell. 2007;6:1310–1319.

[19] Holland LM, Schroder MS, Turner SA, et al. Comparative phenotypic analysis of the major fungal pathogens Candida parapsilosis and Candida albicans. PLoS Pathog. 2014;10:e1004365.

[20] Ramage G, VandeWalle K, Lopez-Ribot JL, et al. The filamentation pathway controlled by the Efg1 regulator protein is required for normal biofilm formation and development in Candida albicans. FEMS Microbiol Lett. 2002;214:95–100.

[21] Finkel JS, Xu W, Huang D, et al. Portrait of Candida albicans adherence regulators. PLoS Pathog. 2012;8: e1002525.

[22] Nobile CJ, Fox EP, Nett JE, et al. A recently evolved transcriptional network controls biofilm development in Candida albicans. Cell. 2012;148:126–138.

[23] Sellam A, Tebbji F, Nantel A. Role of Ndt80p in sterol metabolism regulation and azole resistance in Candida albicans. Eukaryot Cell. 2009;8:1174–1183.

[24] Chen CG, Yang YL, Shih HI, et al. CaNdt80 is involved in drug resistance in Candida albicans by regulating CDR1. Antimicrob Agents Chemother. 2004;48:4505–4512.

[25] Silva AP, Miranda IM, Guida A, et al. Transcriptional profiling of azole-resistant Candida parapsilosis strains. Antimicrob Agents Chemother. 2011;55:3546–3556.

[26] Branco J, Ola M, Silva RM, et al. Impact of ERG3 mutations and expression of ergosterol genes controlled by UPC2 and NDT80 in Candida parapsilosis azole resistance. Clin Microbiol Infect. 2017;23:575 e1– 575 e8.

[27] Silva-Dias A, Miranda IM, Rocha R, et al. A novel flow cytometric protocol for assessment of yeast cell adhesion. Cytometry A. 2012;81:265–270.

[28] Silva-Dias A, Miranda IM, Branco J, et al. Adhesion, biofilm formation, cell surface hydrophobicity, and antifungal planktonic susceptibility: relationship among Candida spp. Front Microbiol. 2015;6:205.

[29] Kohrer K, Domdey H. Preparation of high molecular weight RNA. Methods Enzymol. 1991;194:398–405.

[30] Almeida MC, Antunes D, Silva BMA, et al. Early interaction of alternaria infectoria conidia with macrophages. Mycopathologia. 2019;184:383–392.

[31] Bertini A, Zoppo M, Lombardi L, et al. Targeted gene disruption in Candida parapsilosis demonstrates a role for CPAR2_404800 in adhesion to a biotic surface and in a murine model of ascending urinary tract infection. Virulence. 2016;7:85–97.

[32] Toth R, Cabral V, Thuer E, et al. Investigation of Candida parapsilosis virulence regulatory factors during host-pathogen interaction. Sci Rep. 2018;8:1346.

[33] Pak J, Segall J. Regulation of the premiddle and middle phases of expression of the NDT80 gene during sporulation of Saccharomyces cerevisiae. Mol Cell Biol. 2002;22:6417–6429.

[34] Katz ME, Cooper S 2015. Extreme diversity in the regulation of Ndt80-like transcription factors in fungi. G3 (Bethesda) 5:2783–2792.

[35] Connolly LA, Riccombeni A, Grozer Z, et al. The APSES transcription factor Efg1 is a global regulator that controls morphogenesis and biofilm formation in Candida parapsilosis. Mol Microbiol. 2013;90:36–53.

[36] Toth R, Nosek J, Mora-Montes HM, et al. Candida parapsilosis: from genes to the bedside. Clin Microbiol Rev. 2019;32:e00111-18.

[37] Toth R, Toth A, Papp C, et al. Kinetic studies of Candida parapsilosis phagocytosis by macrophages and detection of intracellular survival mechanisms. Front Microbiol. 2014;5:633.

[38] Nemeth T, Toth A, Szenzenstein J, et al. Characterization of virulence properties in the C. parapsilosis sensu lato species. PLoS One. 2013;8: e68704.

[39] Galocha M, Pais P, Cavalheiro M, et al. Divergent approaches to virulence in C. albicans and C. glabrata: two sides of the same coin. Int J Mol Sci. 2019;20:2345.

[40] Naglik JR, Challacombe SJ, Hube B. Candida albicans secreted aspartyl proteinases in virulence and pathogenesis. Microbiol Mol Biol Rev. 2003;67: 400–428. table of contents.

[41] Polke M, Hube B, Jacobsen ID. Candida survival strategies. Adv Appl Microbiol. 2015;91:139–235.

[42] Sellam A, Askew C, Epp E, et al. Role of transcription factor CaNdt80p in cell separation, hyphal growth, and virulence in Candida albicans. Eukaryot Cell. 2010;9:634–644.

[43] Tavanti A, Campa D, Bertozzi A, et al. Candida albicans isolates with different genomic backgrounds display a differential response to macrophage infection. Microbes Infect. 2006;8:791–800.

[44] Toth A, Zajta E, Csonka K, et al. Specific pathways mediating inflammasome activation by Candida parapsilosis. Sci Rep. 2017;7:43129.

[45] Singh DK, Nemeth T, Papp A, et al. 2019. Functional characterization of secreted aspartyl proteases in candida parapsilosis. mSphere 4.

[46] Bliss JM. Candida parapsilosis: an emerging pathogen developing its own identity. Virulence. 2015;6:109–111.

[47] Neale MN, Glass KA, Longley SJ, et al. Role of the inducible adhesin CpAls7 in binding of candida parapsilosis to the extracellular matrix under fluid shear. Infect Immun. 2018;86:e00892-17.

[48] Navarro-Garcia F, Alonso-Monge R, Rico H, et al. A role for the MAP kinase gene MKC1 in cell wall construction and morphological transitions in Candida albicans. Microbiology. 1998;144(Pt 2):411–424.

[49] Chen T, Jackson JW, Tams RN, et al. Exposure of Candida albicans (1,3)-glucan is promoted by activation of the Cek1 pathway. PLoS Genet. 2019;15: e1007892.

[50] Fingerman IM, Sutphen K, Montano SP, et al. Characterization of critical interactions between Ndt80 and MSE DNA defining a novel family of Ig-fold transcription factors. Nucleic Acids Res. 2004;32:2947–2956.

[51] Chen X, Gaglione R, Leong T, et al. Mek1 coordinates meiotic progression with DNA break repair by directly

phosphorylating and inhibiting the yeast pachytene exit regulator Ndt80. PLoS Genet. 2018;14:e1007832.

[52] Katz ME, Braunberger K, Yi G, et al. 2013. A p53-like transcription factor similar to Ndt80 controls the response to nutrient stress in the filamentous fungus, Aspergillus nidulans. F1000Res 2: 72.

[53] Hutchison EA, Glass NL. Meiotic regulators Ndt80 and ime2 have different roles in Saccharomyces and Neurospora. Genetics. 2010;185:1271–1282.

[54] Min K, Biermann A, Hogan DA, et al. 2018. Genetic analysis of NDT80 family transcription factors in candida albicans using new CRISPR-Cas9 approaches. mSphere 3.

185